Structure/Function Analysis of the Essential Protein Rad4^{TopBP1} in *S. pombe*

A thesis submitted to the University of Sussex

for the degree of Doctor of Philosophy

by

Su-Jiun Lin

October 2010

Declaration

I hereby declare that this thesis has not been submitted, either in the same or different form, to this or any other University for a degree.

Signed:

Su-Jiun Lin

Acknowledgements

I am thankful to Tony Carr for giving me the opportunity to pursue my PhD in his laboratory at the Genome Damage and stability Centre in the University of Sussex.

I especially appreciate Valerie Garcia for supervising me since I was totally new for this field at the time when I started my PhD project. Also, Valerie Garcia put a lot of efforts for critically reading and correcting my manuscript of PhD dissertation. Besides, I want to thank Stephanie Schalbetter, Shih-Chieh Chiang, and Takashi Morishita for helping with my writing.

Thanks to Adam Watson, Cong Liu, Izumi Miyabe, Jo Murray, Ken'ichi Mizuno, Takashi Morishita, and Yasukazu Daigaku and other members in Tony Carr's laboratory who gave me suggestions with my experiments during my PhD. Thanks to Cong Liu and Landi Guo who helped me when I first came here and gave me conveniences for the accommodation during my writing.

Lastly, I appreciate my grateful parents who have always given me support during the time I studied abroad.

University of Sussex

Su-Jiun Lin **DPhil Thesis**

Structure/Function Analysis of the Essential Protein Rad4^{TopBP1} in *S. pombe*

Summary

Rad4^{TopBP1}, a multiple BRCT domain protein, is essential for initiation of replication and participates in checkpoint responses following genotoxic treatment during the S and G2 phases of the cell cycle. Rad4 interacts with several proteins that are involved in initiation of DNA replication (*i.e.* Sld2) or activation of Chk1 and/or Cds1 checkpoint kinases (*i.e.* Rad9, Crb2, and Rad3). However, it remained unclear how Rad4 and its homologues are regulated to coordinate these diverse functions. This PhD project presents a comprehensive structure/function analysis of the fission yeast Rad4^{TopBP1}.

In order to obtain separation of function mutants of Rad4, a hydroxylamine random mutagenesis genetic screen was performed. However, we were not able to separate a checkpoint activation function from replicative function. Rad4 being phosphorylated in a Cdc2-dependent manner, the role of Rad4 phosphorylation by Cdc2 was investigated. A mutant strain containing multiple mutations at Rad4 Cdc2 consensus phosphorylation sites does not exhibit significant sensitivity to DNA damage or HU. In addition, Rad4 Cdc2 phosphorylation sites do not play a role in DNA re-replication. There is no significant phenotypic effect observed after DNA damage in *S. pombe* strains expressing a Rad4 protein deleted for a putative domain (RXL motif) interaction with cyclin, or harboring mutations in putative sumoylation motifs, or C-terminus truncation.

In higher eukaryotes, TopBP1 binds and activates the ATR-ATRIP complex via an ATR-activating domain (AAD) in order to activate a checkpoint function. We identified a potential AAD in C-terminal of Rad4 in *S. pombe*. I show that Rad4 physically associates with Rad3 *in vitro* in an AAD-dependent manner. *S. pombe* strains mutated in the AAD show a slight sensitivity to DNA damage and HU. The *rad4 AAD* mutants do not completely prevent Rad3-mediated G2/M checkpoint activation after DNA damage. The sensitivity in a *rad4 AAD* mutant increases when damage occurs in S-phase, when histone H2A phosphorylation is defective. I established an artificial checkpoint induction system in the absence of exogenous lesions by targeting checkpoint proteins onto chromatin in *S. pombe*. Interestingly, Rad4 AAD is essential for checkpoint activation in this system. Because this checkpoint activation is independent of ssDNA-RPA formation, the data suggest that the AAD plays a role in chromatin-mediated checkpoint maintenance/amplification. Altogether, this pathway seems to play an important role in S-phase when DSBs resection is limited.

List of contents

List of figures and tables

Chapter 5 Role of Rad4^{TopBP1} ATR-activating domain in a LacI/LacO artificial checkpoint induction system

Chapter 6 Screen for separation-of-function *rad4* alleles by hydroxylamine random mutagenesis using the RMCE system

Chapter 7 Final discussion

Chapter 1 General Introduction

The fission yeast *Schizosaccharomyces pombe* (abbreviated as *S. pombe*) diverged from budding yeast *Saccharomyces cerevisiae* (abbreviated as *S. cerevisiae*) approximately 1100 million years ago (Oliva et al., 2005). It is a popular model organism widely used for studying basic mechanisms of eukaryotic cells such as cell cycle, DNA repair and the DNA damage checkpoint pathway because of its short generation time (between 2~4 hours), genetic tractability, easy molecular manipulation and small genome size. In addition, the whole genome sequence was made available in 2002 (Wood et al., 2002), providing a stimulus in using *S. pombe* as a model organism to study the biological function of proteins. *S. pombe* was mainly used in this project to perform a structure/function analysis of Rad4^{TopBP1}.

1.1 The *S. pombe* life cycle

The *S. pombe* cell cycle, like any higher eukaryotes, is divided into four sequential phases, G1, S (synthesis), G2, and M (mitosis) (Fig.1-1). Cells duplicate chromosomes accurately during S phase and DNA content become 2C. Subsequently, the chromosomes segregate, the nucleus divides (mitosis) and the cell divides (cytokinesis). Cells transit into G1 and enter S phase before the cells complete cytokinesis. G1 and G2 are known as “Gap” phases between M-S phase and S-M phase. *S. pombe* Cdc2/CDK1, a cyclin-dependent kinase (CDK), functions at a time in late G1 phase, known as “START” in yeast, to commit cells to a new round of cell division (Russell and Nurse, 1986). In addition, Cdc2/CDK1 functions at a time in late G2 phase to initiate mitosis and cell division (Russell and Nurse, 1986). Cdc2 phosphorylation on residue

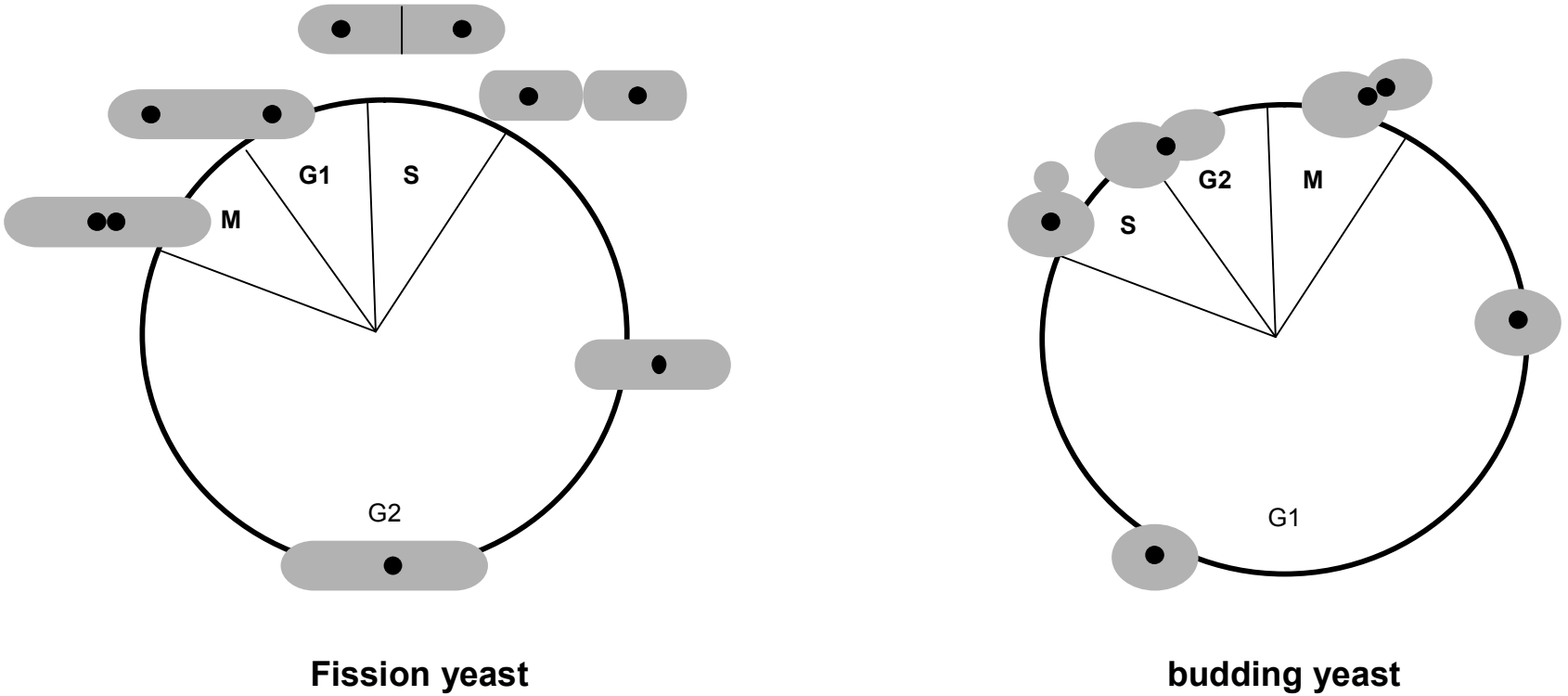

Figure 1-1- The cell cycle in the fission yeast and budding yeast

Both the fission yeast and budding yeast cell cycle have four sequential phases: G1, S, G2, and M phases. The fission yeast has a typical cell cycle with a long G2 phase which spans 70% of cell cycle and S, G1, and M phase are relatively short in a exponential growing population. Unlike fission yeast, budding yeast cells has relatively long G1 phase in a cell cycle.

tyrosine-15 (Y15) by Weel and Mik1 kinases, leads to its inactivation, while dephosphorylation of Y15 by Cdc25 leads to Cdc2 activation (see 1.2.5) (Boddy et al., 1998; O'Connell et al., 1997; O'Connell et al., 2000). *S. pombe* spends 70% of the cell cycle in G2 (Forsburg, 2003). G1, S, and M phases are relatively short, spanning 10% the of cell cycle (Forsburg, 2003).

The coordination of cell cycle progression is driven by different CDK complexes triggered by association of Cdk with cyclins. Cdc2 is known to be the only CDK controlling the transitions of the cell cycle in *S. pombe* and its homologous in *S. cerevisiae* is Cdc28 (Forsburg and Nurse, 1991; Moser and Russell, 2000). Although the protein level of Cdc2 is constant throughout the cell cycle, its activity oscillates (Moser and Russell, 2000). Cdc2 kinase is activated during G1, is relatively low in S phase, and peaks at G2/M phase to trigger cell cycle machinery for entry into mitosis (Moser and Russell, 2000). Cdc2 activity is important for both the G1/S and G2/M transitions and is regulated by its association with four different cyclins Cig1, Cig2, Puc1 and Cdc13, in which Cig2 is the primary S-phase-promoting cyclin and Cdc13 is required for onset of mitosis (Booher et al., 1989; Mondesert et al., 1996).

1.2 The DNA checkpoint pathway

To ensure the maintenance of genome integrity, cells have developed a variety of cellular responses such as DNA repair and the DNA damage checkpoint pathway (DNA-integrity checkpoint) that respond to internal stress or exposure to DNA damaging agents. In response to DNA damage, the DNA damage checkpoint is activated, allowing cells to delay cell cycle progression to provide time to repair the damaged chromosomes. When the damaged chromosomes have been repaired, the

checkpoint arrest signal is extinguished, therefore, allowing cells re-enter the cell cycle, *i*.e., continuing mitosis or S phase. If the DNA checkpoint is defective, it results in genome instability and can lead to cell death, severe disease or cancer in metazoan cells.

1.2.1 Sensor checkpoint proteins

Both hATM/spTel1/scTel1 (ataxia-telangiectasia mutated) and hATR/spRad3/scMec1 (ATM and Rad3-related) kinases are members of the phosphoinositide 3-kinase (PI3K)-related protein kinase (PIKK) family and play roles in the primary DNA damage detection event of the DNA damage checkpoint pathway. These protein kinases phosphorylate target substrates on consensus SQ/TQ sites. For clarity I will use sp to stand for *S. pombe*, sc to stand for *S. cerevisiae*, h to stand for human, and x to stand for *Xenopus*. These prefixes will be used in the following parts (see Table 1-2).

hATR and hATM are involved in different signaling checkpoint pathways since they recognize different DNA structures; single-strand DNA (ssDNA) associated with replication protein A (RPA), and double-strand breaks (DSBs) ends, respectively (Cimprich and Cortez, 2008; Shiotani and Zou, 2009). Therefore, ATR and ATM respond to different types of DNA damage. ATR is more important for the response to DNA lesions that result from UV-irradiation and also for agents that inhibit replication directly, such as the ribonucleotide reductase (RNR) inhibitor hydroxyurea (HU). ATR activation leads to Chk1 activation. ATM is the primary player in response to ionizing radiation (IR) and its activation leads to phosphorylation and activation of Chk2. Although ATR and ATM play a role in distinct signaling pathways, recent studies demonstrated that there is crosstalk between the ATR and ATM signaling pathways (Cimprich and Cortez, 2008; Stiff et al., 2006). For example, when IR occurs in S and G2 phase of cell cycle, ATM regulates the generation of IR-induced ssDNA-RPA, which

	Homo Sapiens	Fission yeast	Budding yeast
PI3Kinase family	ATR	Rad3	Mec1
	ATM	Tel1	Tel1
PI3Kinase binding partner	ATRIP	Rad26	Ddc2
Checkpoint clamp	Rad9	Rad9	Ddc1
	Hus1	Hus1	Mec3
	Rad1	Rad1	Rad17
Checkpoint clamp loader	Rad17	Rad17	Rad24
Mediator protein	53BP1, MDC1, BRCA1	Crb2	Rad9
	Claspin	Mrc1	Mrc1
Other BRCT domain protein	TopBP1	Rad4/Cut5	Dpb11
Effector kinase	Chk1	Chk1	Chk1
	Chk2	Cds1	Rad53
MRX complex	Mre11	Rad32	Mre11
	Rad50	Rad50	Rad50
	Nbs1	Nbs1	Xrs2

Table 1-2- DNA damage checkpoint proteins orthologues in different species (adapted from Lambert and Carr 2005).

results in ATR recruitment and subsequently Chk1 phosphorylation (Jazayeri et al., 2006). When cells are deficient for ATM, ATR is required for Chk2 phosphorylation checkpoint signaling in response to IR (Wang et al., 2006).

The ataxia-telangiectasia (A-T) patients are hypersensitive to IR, and have a predisposition to cancer which is caused by mutations in the *ATM* gene (Lavin and Shiloh, 1997). A-T cells exhibit approximately four times more sensitivity to IR than other human cells but A-T cells have a normal response to UV irradiation. In the absence of ATM function cells are unable to arrest at the G1/S or G2/M boundaries, and are able to arrest DNA synthesis after IR. ATM is present as a homodimer in unirradiated cells, and ATM kinase is stimulated by the introduction of double-strand breaks (DSBs) which causes the dissociation of the homodimer to ATM monomers and this conformational change in the ATM protein leads the ATM kinase to autophosphorylate at serine 1981 (Kastan and Bartek, 2004). When a DSB occurs, it is primarily detected by the direct interaction of the DNA ends with the DNA repair complex, hMre11/spRad32/scMre11, Rad50, and hNbs1/spNbs1/scXrs2 (MR(X)N complex) (Pardo et al., 2009) . Besides a role in DSB repair (see in 1.3), MR(X)N is essential for recruitment of activated ATM to sites of DSBs in order to facilitate the phosphorylation of ATM substrates via its kinase domain, such as Chk2 (Paull and Lee, 2005). Studies in human cells showed that Nbs1 C-terminal interacts with a region of ATM N-terminal containing of HEAT repeats (Fig.1-3), and this interaction is specifically required for ATM recruitment to sites of DSBs (Falck et al., 2005). The lysine 3016, located within the highly conserved FATC domain at the C-terminus of ATM, is targeted for ATM acetylation by Tip60 histone acetyltransferase and this acetylation is required for ATM autophosphorylation and the subsequent phosphorylation of ATM substrates (Sun et al., 2007). All PIKKs share a similar domain

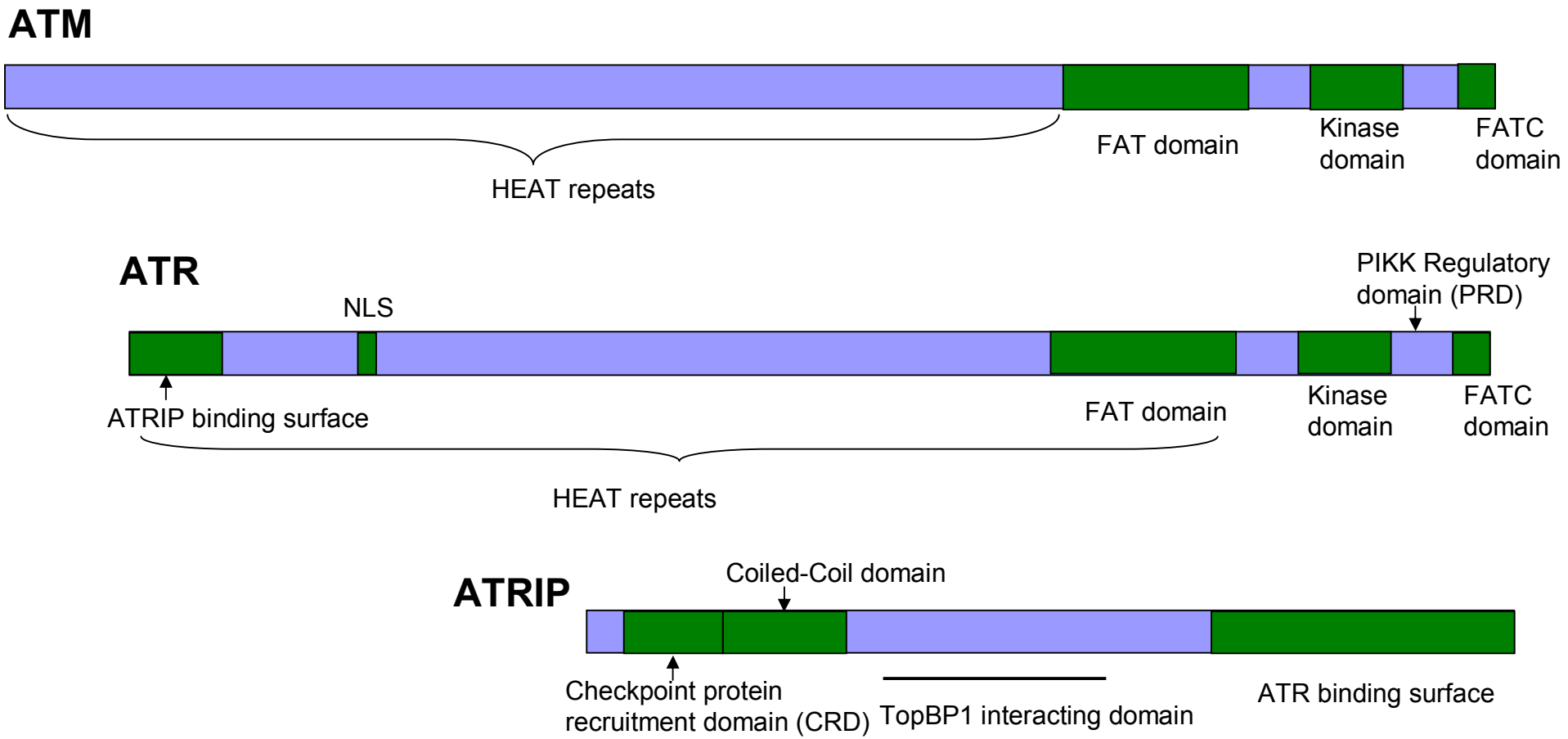

Figure 1-3- Structure of ATM, ATR and ATRIP in mammals

The detail of domains in ATM, ATR and ATRIP are described in the text. (adapted from Ball, Myers et al. 2005; Falck, J., J. Coates, et al. 2005; Cimprich and Cortez 2008; Mordes, Glick et al. 2008)

architecture (Fig.1-3), and ATM and ATR both contain N-terminal HEAT repeats and a kinase domain flanked by FAT and FATC domains. Therefore, it might be expected that the mechanisms that control their regulation would be similar. There is some evidence, for example, that ATM and ATR localize to sites of DNA damage via their interaction with Nbs1 and ATR-interacting protein (ATRIP), respectively; ATM and ATR are regulated to phosphorylate their substrates by a protein activator MR(X)N and TopBP1 (see 1.6.3.2), respectively.

ATR exists as a complex with ATRIP in mammalian cells via association of ATR N-terminus HEAT repeats with the C-terminus of the ATR binding surface of ATRIP (Fig.1-3) (Ball et al., 2005; Chen et al., 2007b; Cortez et al., 2001). Similarly, Mec1 interacts with Ddc2 in *S. cerevisiae* (Paciotti et al., 2000). ATR-ATRIP/Mec1-Ddc2 complex is recruited to damage sites through interaction between the checkpoint protein recruitment domain (CRD) of ATRIP/Ddc2 and RPA (Ball et al., 2007; Ball et al., 2005; Zou and Elledge, 2003). The FAT domain of ATR is predicted to fold into an extended α-helical HEAT repeats structure (Cimprich and Cortez, 2008). The ATR PIKK Regulatory domain (PRD) located between the kinase domain and FATC domain is poorly conserved among PIKKs but highly conserved within orthologues in different organisms (Cimprich and Cortez, 2008). The PRD regulates TopBP1-dependent ATR kinase activity and this domain is essential for cell viability but does not affect basal ATR kinase activity (for detail see 1.6.3.2) (Mordes et al., 2008a). The basal ATR kinase activity is regulated by the ATR FATC domain (Mordes et al., 2008a). Interestingly, the ATR FATC domain was reported to be able to substitute for the ATM FATC domain, suggesting that the FATC domains of ATR and ATM are functionally equivalent (Jiang et al., 2006). In contrast, Mordes, Glick et al. (2008), showed that replacement of the ATR FATC domain with the ATM FATC domain could not elicit the phosphorylation of

an ATR substrate. Oligomerization of ATRIP through its coiled-coil domain is important for stable association of the ATR-ATRIP complex and is also essential for ATR-mediated checkpoint signaling (Ball and Cortez, 2005). ATR is required in checkpoint activation in response to ssDNA formed at replication forks (see below) which induce Chk1 activation (Petermann and Caldecott, 2006; Zou and Elledge, 2003). For example, when a progressing replication fork encounters a lesion, the replication fork stalls while the helicase continues to unwind the DNA, generating large sections of ssDNA associated with RPA (ssDNA-RPA) at the fork. The ssDNA-RPA complex is recognized by ATR-ATRIP, which results in the stabilization of the replication fork, the blocking cell cycle progression, and the blocking of the firing of late origins through activating the intra-S phase checkpoint (Paulsen and Cimprich, 2007). This is a Chk1-mediated ATR pathway that is also known as the DNA replication checkpoint.

Deletion of *tel1* in yeast has little effect on checkpoint responses (O'Connell et al., 2000). Rad3/Mec1 in both *S. pombe* and *S. cerevisiae* appears to be more important than Tel1 in the DNA damage checkpoint response to DSBs, which is a striking difference from the requirement for ATM in mammalian cells (Melo and Toczyski, 2002). While in higher eukaryotes ATR is activated principally in response to replication stress, budding yeast Mec1 and fission yeast Rad3 play a central role in both the DNA damage checkpoint and the DNA replication checkpoint. Like ATR/Mec1 in mammals and *S. cerevisiae*, Rad3 exists as a complex with Rad26 in *S. pombe* (Edwards et al., 1999). Rad26 recruitment to the site of damage occurs in a Rad3-dependent manner after DNA damage. Rad26 is phosphorylated at this point by Rad3 but this phosphorylation is independent of other checkpoint proteins, including Rad17 and Rad1-Rad9-Hus1 complex (Edwards et al., 1999; O'Connell et al., 2000). Similarly, phosphorylation of Ddc2, the budding yeast counterpart of Rad26, is dependent on Mec1 and is

independent of other known checkpoint factors: Rad17, Rad24, Mec3, Ddc1, Rad9, and Rad53 (Paciotti et al., 2000). This has led to the idea that ATR/ATRIP and its homologues can detect ssDNA (*i.e.* DNA damage) independently from other checkpoint proteins.

1.2.2 Checkpoint clamp and clamp loader

ATR-ATRIP recruitment to damaged sites is not sufficient for full ATR activation. Complete activation of ATR-dependent checkpoint pathway requires at least another two groups of proteins, the checkpoint clamp loading factor (CCL) hRad17/scRad24/ spRad17, which interacts with replication factor C (Rfc2-5) and the heterotrimeric checkpoint sliding clamp complex Rad9-Rad1-Hus1 (9-1-1) complex (Table 1-2).

The 9-1-1 complex is conserved in eukaryotes and exhibits structural similarity to proliferating cell nuclear antigen (PCNA) (O'Connell et al., 2000). In *S. pombe* Rad9 phosphorylation on threonine 412 (S/T Q) by Rad3 occurs during unperturbed S phase or in response to DNA damage and this C-terminus Rad9 phosphorylation is required for recruitment of Rad4/TopBP1, possibly to sites of DNA damage, when cells are challenged with IR, when cells are arrested in S phase with HU, or during unperturbed S phase (Furuya et al., 2004). Rad4 recruitment occurs via Rad9 C-terminal interaction with the Rad4 C-terminus, including BRCT domain 3 and 4 (Furuya et al., 2004). Furthermore, an interaction between Rad4 and Rad3 occurs in a Rad9 T412 phosphorylation-dependent manner. This mechanism of Rad4/TopBP1 juxtaposition with Rad3-Rad26/ATR-ATRIP complex via Rad9 C-terminal phosphorylation is conserved in higher eukaryotes (see 1.6.3.1) (Delacroix et al., 2007; Lee et al., 2007; St Onge et al., 2003). Unlike *S. pombe*, mammalian Rad9 phosphorylation at serine 387, which regulates hRad9 interaction with TopBP1, is constitutive rather than

damage-induced. The extent of S387 phosphorylation did not change significantly following replication perturbation or DNA damage (St Onge et al., 2003).

hRad17 and RFC function as sensor proteins since RPA-coated ssDNA is required for recruitment of hRad17 to the damaged site, and hRad17 is required for recruitment of the 9-1-1 to 5'-ss/ds DNA junctions (Majka et al., 2006a; Yang and Zou, 2006; Zou et al., 2002). 9-1-1 complex with hRad17-Rfc2-5 are recruited at sites of DNA damage independently of ATR-ATRIP (Zou et al., 2002). Similarly in *S. cerevisiae* and *S. pombe*, 9-1-1 complex along with scRad24/spRad17-Rfc2-5 are recruited to sites of DNA damage independently of the Mec1-Ddc2/Rad3-Rad26 complex (Carr, 2002; Melo et al., 2001).

1.2.3 Mediator proteins and checkpoint effector kinases

The mediator proteins appear to function as a bridge required to transduce the checkpoint signal from upstream sensor proteins hATR/spRad3/scMec1 or hATM/ spTel1/scTel1 kinase to the downstream effector kinase Chk1 or hChk2/spCds1/scRad53. These two effector kinases are responsible for two distinct checkpoint pathways: the DNA damage checkpoint pathway and the replication checkpoint pathway.

Checkpoint effector kinase

In *S. pombe*, there is a clear distinct function for the effector kinases: the Chk1 dependent G2/M DNA damage checkpoint is activated following DNA damage leading to a G2-cell cycle delay (Walworth and Bernards, 1996). The Cds1 dependent replication checkpoint is activated following replication block by HU or DNA damage occurring in S phase, such as an alkylating agent of MMS (methyl methanesulfonate). It

results in a slow down of DNA replication, which is defined as the "intra-S checkpoint" as well as preventing mitosis while cells remain in S phase (S-M checkpoint) (Lambert and Carr, 2005). DNA damage fails to activate Chk1 phosphorylation when it occurs in HU-arrested cells (Brondello et al., 1999). However, Cds1 and Chk1 may have redundant roles in the S/M checkpoint. Chk1 is activated in response to DNA damage in S phase and replication block by HU in the absence of *cds1*. The *chk1-d cds1-d* double mutant is as deficient in response to HU as *rad3-d* and *rad26-d* mutants (Lindsay et al., 1998). In *S. cerevisiae*, Chk1 and Rad53 are both activated following DNA damage and Rad53 is activated following replication arrest. In contrast to the yeasts, the roles of hChk1 and hChk2 in mammals seem to be shuffled. hChk1 and hChk2 are both activated following DNA damage while hChk1 is activated following replication arrest in mammals (Rhind and Russell, 2000) (see Fig.1-4).

The mediator proteins

Mediator proteins transduction of the DNA-damage signal

In *S. pombe*, Crb2, also known as Rhp9, is responsible for transducing the signal to spChk1 in response to DNA damage, while Mrc1 (mediator of the replication checkpoint 1) is responsible for transmission the signal to spCds1 in response to DNA replication stress (see below) (Tanaka and Russell, 2004). Both Chk1 and Cds1 phosphorylation occur in a Rad3-dependent manner (Lindsay et al., 1998; Martinho et al., 1998; Walworth and Bernards, 1996).

The mediator proteins Crb2 in *S. pombe*, Rad9 in *S. cerevisiae* and 53BP1 (p53-binding protein 1) in mammals are grouped mainly by function since their sequences are poorly conserved outside of the homology regions containing Tudor domains and BRCT

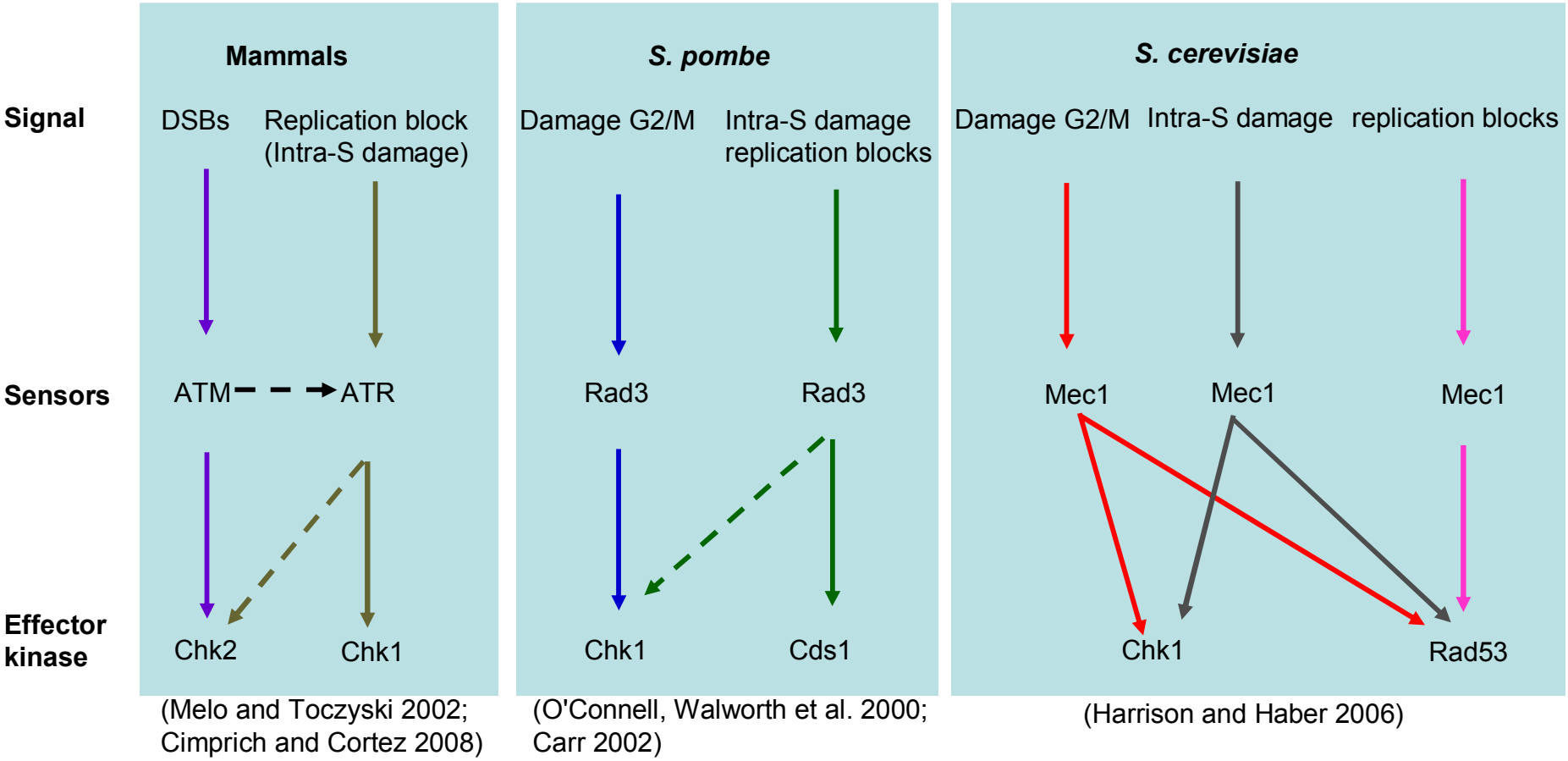

Figure 1-4- Checkpoint pathway in eukaryotes

Comparison of checkpoint signaling pathways in eukaryotes (mammals, *S. pombe*, and *S. cerevisiae*). A checkpoint signal arising from replication block refers to the inhibition of DNA replication, *i.e.*, HU and Aphidocolin. Intra-S phase damage refer to DNA damage induced during S phase.

domains (Fig.1-5). The BRCT domain was first identified in BRCA1 (breast cancer type-1 susceptibility protein); the main function of BRCT domain is to bind to phosphorylated proteins (Rodriguez et al., 2003; Yu et al., 2003). Mammalian MDC1 (mediator of DNA-damage checkpoint 1) and BRCA1 also contain protein-protein interaction domains such as the forkhead-associated (FHA) domain and the BRCT domain and it is believed they function as mediator proteins. In *S. pombe*, the two Crb2 BRCT domains bind phospho-H2A which recruits Crb2 to the sites of DNA damage, allowing Chk1 phosphorylation (Kilkenny et al., 2008). Similarly, *S. cerevisiae* Rad9 binds to phospho-H2A which is required for Rad53 phosphorylation, however, this mechanism in *S. cerevisiae* is more pronounced during G1 than in G2/M-arrested cells (Hammet et al., 2007). In addition, h53BP1/spCrb2/ scRad9 is also targeted to sites of DSBs via its Tudor domains, which recognize histone methylation (Huyen et al., 2004; Sanders et al., 2004; Toh et al., 2006). But, neither histone phosphorylation nor histone methylation significantly affect cells sensitivity to DNA damaging agents in *S. pombe* (Du et al., 2006). Interestingly, Crb2 is recruited to HO-induced DSBs in a Crb2-threonine 215 phosphorylation-dependent manner in the absence of histone phosphorylation and histone methylation (Du et al., 2006). This leads to the conclusion that Crb2 recruitment to sites of DNA damage occurs via two parallel pathways: histone modification and Crb2 phosphorylation at T215; in the absence of the histone modification-dependent recruitment pathway, the role of T215 phosphorylation in response to DNA damage (see below) becomes essential for recruitment of Crb2 to sites of DNA damage.

Both spCrb2 and scRad9 are phosphorylated by CDK in normal unperturbed cell cycle (Esashi and Yanagida, 1999; Vialard et al., 1998). Crb2 is phosphorylated at T215 by Cdc2 kinase and this phosphorylation is a prerequisite for its subsequent

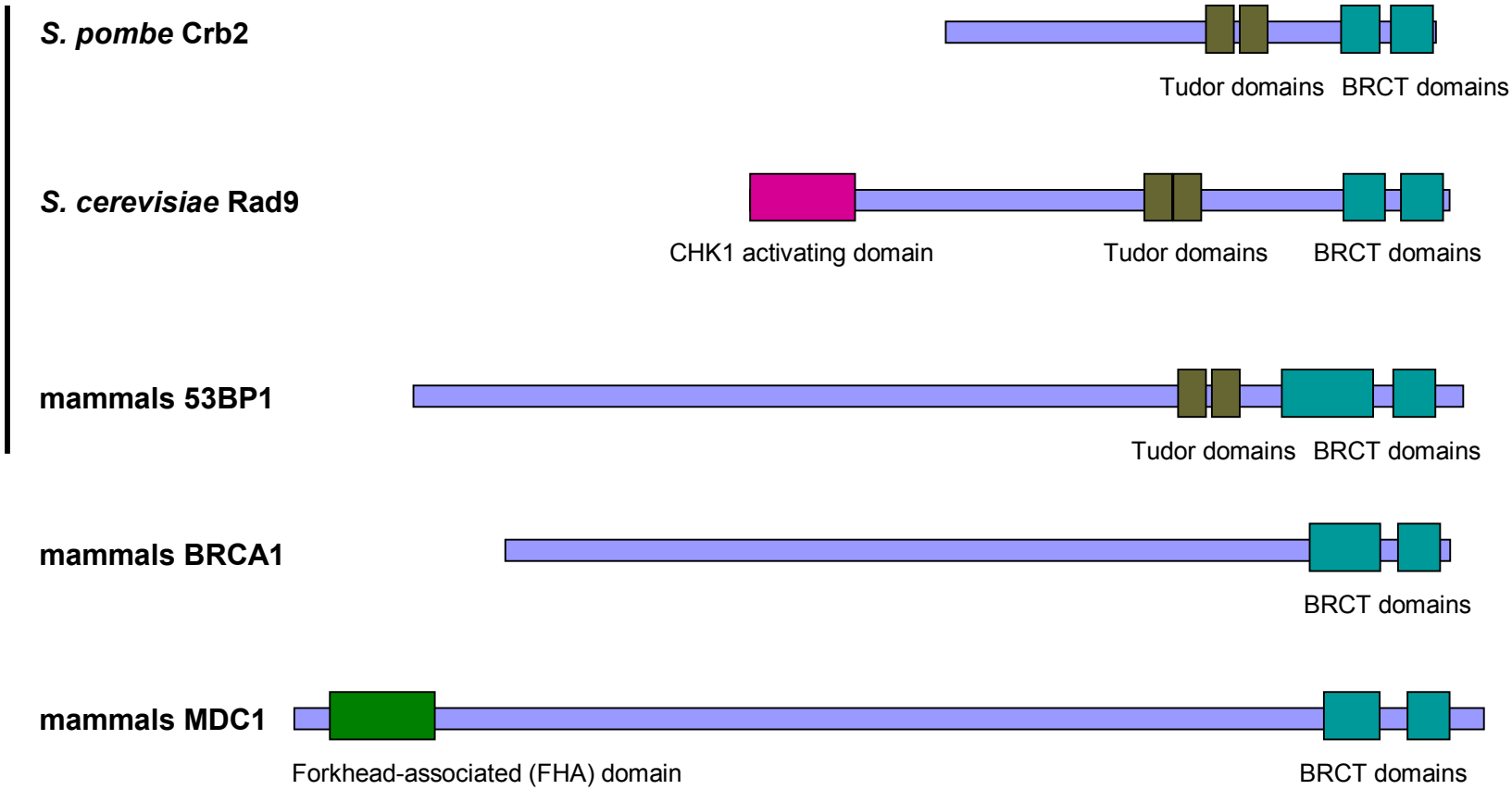

Figure 1-5- Structure of the mediator proteins Crb2 in *S. pombe*, Rad9 in *S. cerevisiae,* 53BP1, BRCA1 and MDC1 in mammals

The main structural feature of Crb2, Rad9, 53BP1 is Tudor domains and BRCT domains, indicated as colored boxes. Other mediator proteins in mammals are BRCA1 and MDC1, containing BRCT domains but no Tudor domains. (Du, Nakamura et al. 2006 ;FitzGerald, Grenon et al. 2009)

Rad3-dependent hyperphosphorylation after DNA damage (Esashi and Yanagida, 1999). Crb2 phosphorylation at T215 was reported to be essential for cells to reenter the cell cycle after checkpoint activation because *S. pombe crb2-T215A* mutant fail to reduce the amount of phosphorylated Chk1, leading to permanent checkpoint arrest of damage cells (Esashi and Yanagida, 1999). These data could not be reproduced in Caspari et al 2002. In addition, Crb2 phosphorylation at T215 is also implicated in the repair process (Caspari et al., 2002).

Crb2 regulates the DNA damage checkpoint response through temporal and dynamic association with Rad3, Rad4 and Chk1 (Mochida et al., 2004; Saka et al., 1997). The Crb2-Chk1 interaction is regulated by Rad3 and this interaction increases after DNA damage. Crb2-Rad4 association also increases after DNA damage (Mochida et al., 2004). Two-hybrid studies have identified an interaction between Chk1 and Rad4 BRCT domain 3 and 4 (Saka et al., 1997). Crb2 and Chk1 are phosphorylated in a Rad3-dependent manner; besides, Chk1 phosphorylation requires Crb2 phosphorylation by Rad3 (Mochida et al., 2004; Nakamura et al., 2004; Saka et al., 1997). Thus, Crb2, Rad4, and Chk1 may form a checkpoint sensor transmitting checkpoint signaling to arrest the cell cycle.

In *S. cerevisiae*, Rad9 is phosphorylated in a Mec1-dependent manner after DNA damage (Emili, 1998; Vialard et al., 1998). In response to DNA damage, the phosphorylation of TQ/SQ sites in Rad9 by Mec1 promotes its interaction with Rad53 mediated by interaction with two FHA domains of Rad53, which leads to Rad53 phosphorylation by Mec1 (Blankley and Lydall, 2004; Schwartz et al., 2002; Sweeney et al., 2005). However, DNA damage-induced Rad9 phosphorylation at TQ/SQ sites are not essential for the regulation of scChk1 phosphorylation by Rad9 (Schwartz et al.,

2002). The Rad9 Chk1 activation domain (CAD) is specifically important for phosphorylation and activation of the scChk1 kinase but not for phosphorylation and activation of Rad53 (Blankley and Lydall, 2004). scRad9 has been identified to interact with scChk1 in two-hybrid assays and this interaction is required for Chk1 phosphorylation after DNA damage (Melo and Toczyski, 2002). Taken together, data suggest that the functionally independent domain within the Rad9 mediates between upstream Mec1 kinase and two parallel downstream Rad53 and scChk1 kinase signaling pathways independently.

Mediator proteins transduction of the replication-stress signal

Although *S. cerevisiae* Rad9 is required for scChk1 and Rad53 kinases activation in response to DNA damage, it has no role in responding to DNA replication stress in wild-type cells. Mediator of the replication checkpoint (Mrc1) is known to be required for Rad53 activation during replication stress (Alcasabas et al., 2001). Mrc1 is phosphorylated in a Mec1-dependent and Rad53-independent manner, suggesting Mrc1's function lies between Mec1 and Rad53 in the checkpoint signaling pathway (Melo and Toczyski, 2002). *mrc1* mutants exhibit a significant delay in the timing of Rad53 activation when replication is blocked (Alcasabas et al., 2001). It is thought that in the absence of an immediate response via Mrc1, DNA replication stress causes DNA damage in *mrc1* mutants, which alternatively activates scRad9 and subsequently activates Rad53. Consistently, in the absence of Rad9, *mrc1* mutants show no activation of Rad53 (Alcasabas et al., 2001). These data suggest that scRad9 and scMrc1 act as mediator proteins redundantly for Rad53 activation. Similarly, Crb2 in *S. pombe* is required for Chk1 activation in response to DNA damage, and Mrc1 is known to be required for Cds1 activation when replication is blocked (Tanaka and Russell, 2001). Mrc1 has been identified to associate with the FHA domain of Cds1 in two-hybrid

assays and this interaction facilitates recruiting Cds1 to Rad3-Rad26 (Tanaka and Russell, 2004). In addition, the Mrc1-Cds1 interaction is required for Cds1 activation by Rad3 kinase (Tanaka and Russell, 2004). Tanaka and Russell 2001 showed that *S. pombe* cells in the absence of Mrc1 protein were completely defective for Cds1 activation in response to HU. However, *S. pombe* cells lacking Mrc1 protein activate Chk1 in a Crb2-dependent manner in response to DNA replication stress (Tanaka and Russell, 2001). Thus, unlike *S. cerevisiae*, *S. pombe* Chk1 and Cds1 kinases each appear to have a specific adaptor protein dedicated to kinase activation. The Mrc1 homologue in vertebrates is Claspin. Claspin is phosphorylated after DNA damage and this phosphorylation is required for xCHK1-Claspin interaction (Kumagai and Dunphy, 2000). Immunodepletion of Claspin from *Xenopus* egg extracts abolish xCHK1 phosphorylation and activation and depleted extracts are unable to block mitosis in response to replication stress, suggesting that Claspin mediates xCHK1 activation by xATR in response to replication block in *Xenopus* (Guo et al., 2000; Kumagai and Dunphy, 2000).

hTopBP1/scDpb11 are orthologues of Rad4 in *S. pombe*, and they share conserved BRCT repeat structure (see 1.6). hTopBP1/spRad4/scDpb11 is known to be required for the initiation of DNA replication and to be essential for checkpoint activation. They are considered to be mediator proteins since the BRCT repeats have been demonstrated to play a role as a scaffold in Rad3-mediated checkpoint activation (for detail see 1.6.3.1 and 1.6.3.2), besides their function in protein-protein interactions (*i.e.* spCrb2-Rad4, spRad9-Rad4, spChk1-Rad4, spSld2-Rad4).

Taken together, the published literature suggests a model of checkpoint signaling in *S. pombe* is presented in Fig.1-6 (Carr, 2002; Furuya et al., 2004; Lambert and Carr, 2005;

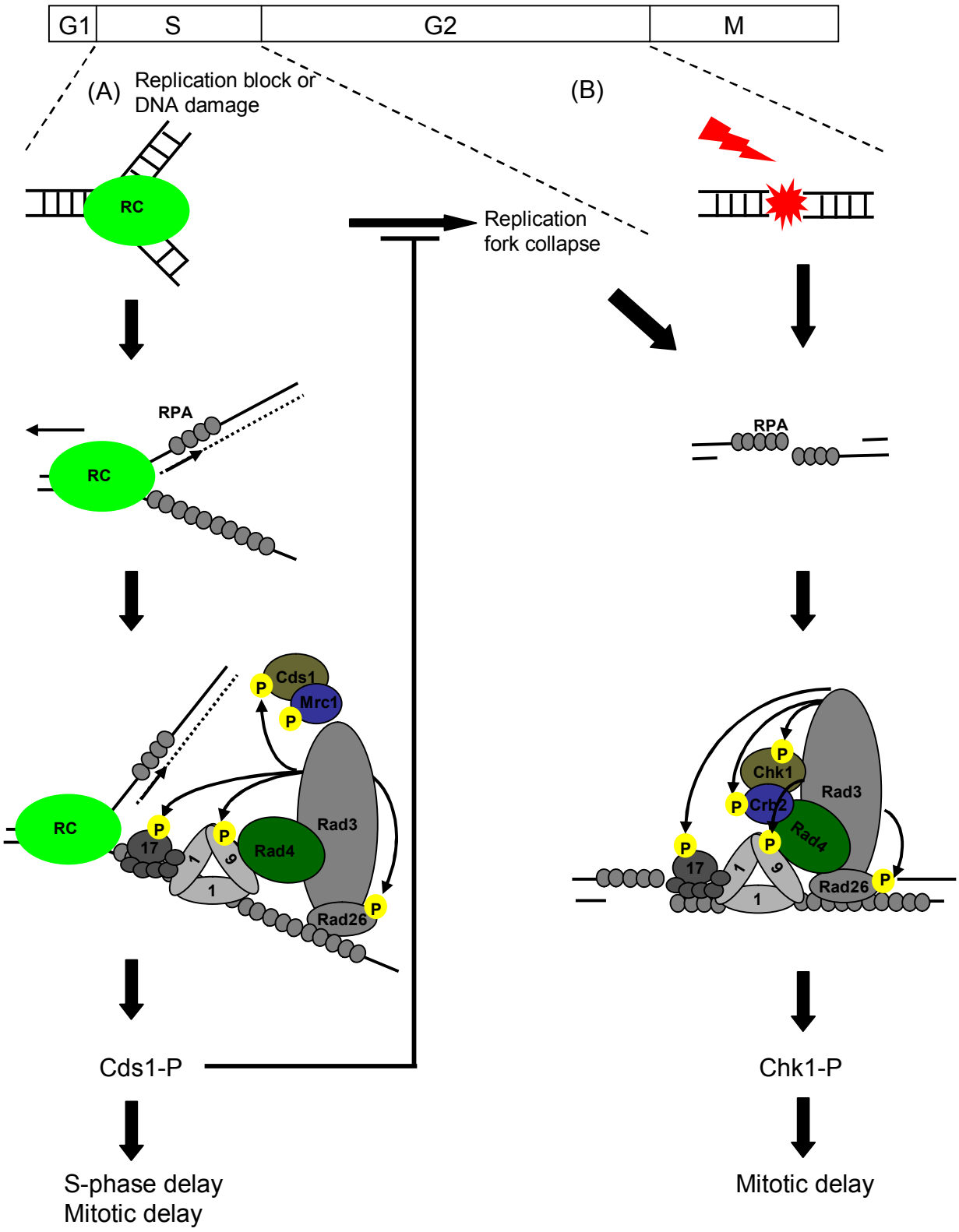

Figure 1-6- Model of the checkpoint pathway in *S. pombe*

The pathway of the replication checkpoint (A) and the DNA damage checkpoint (B) are shown and the details are in the text. (adapted from O'Connell, Walworth et al. 2000; Carr 2002)

O'Connell et al., 2000). Rad9 phosphorylation occurs in a Rad3-dependent manner and is a prerequisite for Rad9-Rad4 association during normal S phase. When DNA replication fork is stalled by nucleotide depletion (HU) or UV-light (Fig.1-6A), Rad3-Rad26 complex and 9-1-1 complex with Rad17-Rfc2-5 assemble independently to the replication complex (RC). Rad3 phosphorylates Mrc1, which associates with the FHA domain of Cds1, and Mrc1 recruits Cds1 into proximity with Rad3. Subsequently, Cds1 kinase is phosphorylated by Rad3. This prevents the firing of new origins, stabilization of activated replication fork, and delay of mitotic entry (Lambert and Carr, 2005; Tanaka and Russell, 2004). However, if the DNA replication checkpoint (S/M phase checkpoint/intra-S phase checkpoint) is deficient (in absence of *cds1*), it results in replication fork collapse (Lambert and Carr, 2005). Collapsed replication forks are then recognized as DNA damage.

When DNA damage occurs during G2 phase or is present as cells exit S phase into G2 phase (Fig.1-6B), DSBs or collapsed replication forks are processed to generate ssDNA, and this is coated with RPA. Rad3-Rad26 complex is recruited to sites of DNA damage via Rad26 CRD interaction with RPA. The 9-1-1 complex is recruited by Rad17-Rfc2-5 independently of Rad3-Rad26. Furthermore, C-terminus Rad9 phosphorylation by Rad3 then promotes the formation of Rad4-Rad9 complex and subsequently Rad4-Rad3 complex. Crb2 is recruited to sites of DNA damage via its BRCT domain interaction with phospho-histone and via its Tudor domain interaction with methylated histone. In addition Crb2 interacts with the first two BRCT domains of Rad4 (Saka et al., 1997), Crb2 recruits Chk1 into the proximity of Rad3. Both Crb2 and Chk1 are phosphorylated in a Rad3-dependent manner. Subsequently, Chk1 kinase is activated, leading to mitotic delay.

1.2.4 Checkpoint maintenance

Checkpoint mediator proteins play a role in transducing the checkpoint signal from hATR/spRad3/scMec1 or hATM/spTel1/scTel1 kinase to Chk1 or hChk2/spCds1/scRad53 kinase. In addition, checkpoint mediator proteins MDC1, 53BP1 and BRCA1 in mammalian cells and Crb2 in *S. pombe* are involved in amplification or maintenance of checkpoint signals (Du et al., 2003; Du et al., 2006; Nakamura et al., 2004; van Attikum and Gasser, 2009).

MDC1 acts an early regulator of DNA damage response (DDR) factors. MDC1's BRCT domain binds directly to phosphorylated H2AX, also referred to as γ-H2AX, and its FHA domain binds directly to ATM and Nbs1 (Lou et al., 2006). Through these interactions, MDC1 accumulates ATM and MRN (Mre11-Rad50-Nbs1) near the sites of damage and further enhance the ATM-dependent γ-H2AX surrounding DNA breaks in order to amplify DNA damage signaling (Lou et al., 2006; Stucki et al., 2005). H2AX is phosphorylated along the laser path when DSBs are introduced into mammalian cells are by using a laser-dissecting microscope. Both Nbs1 and 53BP1 distribute along the laser path in wild-type or MDC-/- cells. Unlike in wild-type cells, Nbs1 and 53BP1 foci do not remain along the laser path in MDC-/- cells after several hours (Lou et al., 2006). In addition to the failure of retention of Nbs1 and 53BP1 near sites of damage, MDC-/- cells are defective in phosphorylation of ATM substrates, Chk1 and Chk2 (Lou et al., 2006).

In *S. pombe*, H2A phosphorylation (γ-H2A) is dependent on Rad3/Tel1 and is required for Crb2 foci formation (Nakamura et al., 2004). H2A phosphorylation mutant (H2A-AQE mutant) shows a near abrogation in both Crb2 and Chk1 phosphorylation after low dose IR, and a premature release from cell cycle arrest in response to

Bleomycin (Nakamura et al., 2004). The concept of maintenance of checkpoint signaling is also supported by the fact that damaged-induced Crb2 foci co-localize with Rad22 at sites of DSBs, suggesting that Crb2 persists at sites of damage until damaged DNA is repaired (Du et al., 2003). γ-H2A modulates checkpoint and DNA repair via recruitment of Crb2 to sites of DNA damage and this function correlates with mammalian studies showing that γ-H2AX regulates the recruitment of BRCT domains-containing proteins, such as MDC1, 53BP1 and the repair protein Nbs1. While initiation of damage-induced Crb2 foci formation does not require *rad3*, *rad26*, *chk1*, *rad1*, *rad17*, and *rad9*, the persistent localization of Crb2 at site of damaged is Rad proteins-dependent including *rad3*, *rad26*, *rad1*, *rad17*, and *rad9* (Du et al., 2003).

1.2.5 Cell cycle arrest

Cell cycle progression has been well characterized in fission yeast. The Chk1 kinase dependent G2/M DNA damage checkpoint and the Cds1 kinase dependent S/M replication checkpoint mediate cell cycle arrest through inactivation of Cdc2, by maintaining Y15 phosphorylation of Cdc2. Dephosphorylation of Y15 by Cdc25 leads to Cdc2 activation which commits cells to mitosis (Fig.1-7) (Boddy et al., 1998; O'Connell et al., 1997; O'Connell et al., 2000). Both Chk1 and Cds1 arrest the cell cycle by phosphorylating Cdc25, which promotes its binding to 14-3-3 proteins and also inhibits the phosphatase activity of Cdc25 (Furnari et al., 1999; Zeng et al., 1998). The association of 14-3-3 and Cdc25 contribute to nuclear exclusion of Cdc25 (Zeng and Piwnica-Worms, 1999). Cdc25 stays in both the cytoplasm and nucleus during G2 phase of cell cycle and the amount of Cdc25 in the nucleus appears to increase in the late G2 phase just before mitosis (Lopez-Girona et al., 1999).

Furthermore, Chk1 and Cds1 up-regulate Weel and/or Mik1 tyrosine kinase which

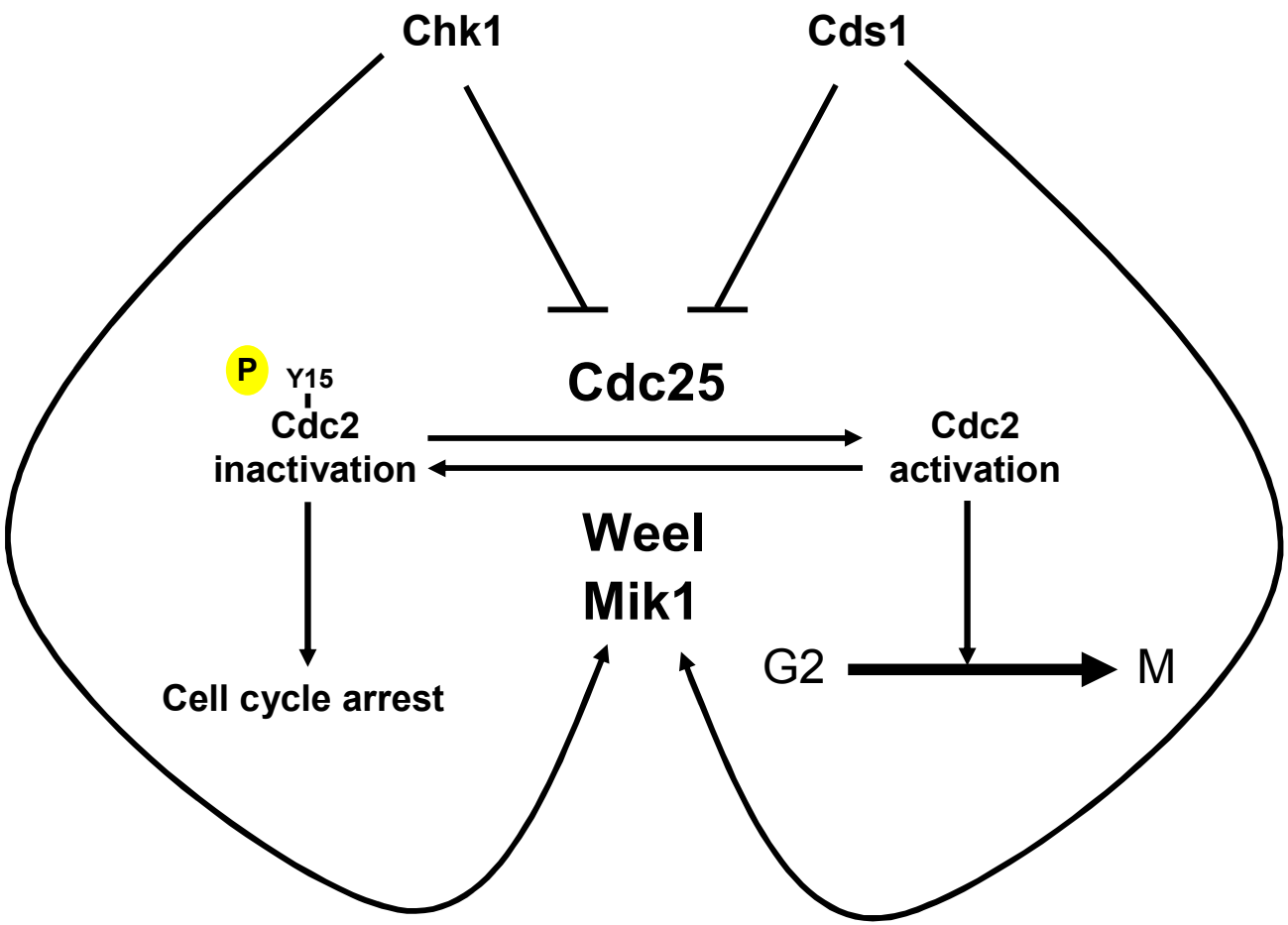

Figure 1-7- Cdc2 regulates cell cycle progression in fission yeast

Chk1 and Cds1 mediate cell cycle arrest through phosphorylation of Cdc25 to inhibit its phosphatase activity and phosphorylation of weel link to activate their kinase activity. Cdc2 phosphorylation on residue Y15 by Weel and Mik1 leads to its inactivation. Dephosphorylation of Y15 by Cdc25 leads to Cdc2 activation. Active Cdc2 is required for mitotic delay.

phosphorylate Y15 of Cdc2 and therefore inactivate Cdc2. Weel is phosphorylated by Chk1 and/or Cds1 and Y15 phosphorylation of Cdc2 is maintained in order to prevent cells entering mitosis (Boddy et al., 1998; O'Connell et al., 1997). Mik1 is able to phosphorylate Y15 of Cdc2 and it is accumulated when HU treatment induces Cds1 kinase activation in *S. pombe* cells (Boddy et al., 1998); Mik1 also plays an overlapping function with Weel in G2 damage checkpoint but Mik1 seems to play a minor role in G2 control in the presence of Weel (O'Connell et al., 1997).

1.2.6 Checkpoint recovery

Cells turn off checkpoint signaling and re-enter the cell cycle in a process termed "checkpoint recovery" (Calonge and O'Connell, 2008; Harrison and Haber, 2006). In *S. pombe*, the PP1-family phosphatase Dis2 was shown to control the timing of release from G2 DNA damage checkpoint via de-phosphorylation of Chk1 (Chk1 inactivation). Importantly, Dis2 does not affect the phosphorylation or function of Rad checkpoint proteins upstream of Chk1 in the checkpoint signaling pathway, including Rad3 and Rad9 (den Elzen et al., 2004; den Elzen and O'Connell, 2004). In mammals, overexpression of PPM1D abrogates the checkpoint response; siRNA to PPMD1 results in enhanced Chk1 phosphorylation after UV-irradiation. Thus, PPM1D is required for Chk1 inactivation in human cells (Calonge and O'Connell, 2008). γ-H2AX reaches a maximal level within 1-2 h after damage, and steadily decreases in correlation with kinetics of DNA repair (Paull et al., 2000; Rios-Doria et al., 2006). This led to the hypothesis that de-phosphorylation of γ-H2AX also influenced termination of checkpoint signaling as DNA repair is completed. In *S. cerevisiae*, a histone H2A phosphatase complex (HTP-C), composed of Pph3, Psy2, and Yb1046w, has been shown to de-phosphorylate γ-H2AX *in vitro* and *in vivo* and cells lacking any subunits cause persistent γ-H2AX foci formation in irradiated cells (Harrison and Haber, 2006).

Furthermore, cells lacking Pph3 present a defect in recovery from checkpoint arrest and Rad53 persist activation (Keogh et al., 2006). The PP2C-family phosphatase Ptc2 and Ptc3 were also shown to bind and inactivate Rad53 in order to promote checkpoint recovery (Leroy et al., 2003).

1.3 DNA repair pathways

In response to DNA damage, cells trigger checkpoint signaling in order to arrest the cell cycle progression and also activate repair pathways, *i.e.*, base excision repair (BER), nucleotide excision repair (NER), mismatch repair (MMR), nonhomologous end-joining (NHEJ) and homologous recombination (HR) to maintain the genome stability. An extra pathway (UVER) for excision of UV photoproducts in addition to NER exists in *S. pombe* and is in agreement with *S. pombe* NER-defective cells being not as sensitive as *S. cerevisiae* in response to ultra-violet radiation (McCready et al., 2000).

In general, there are two types of DNA breaks: DSBs and single-strand breaks (SSB). DSBs are especially harmful lesions to the cells and can induce cell death (Czornak et al., 2008; Khanna and Jackson, 2001). Approximately 10 DSBs per cell cycle arise spontaneously in human cells, most of them during replication when replication fork encounter a lesion, *i.e.*, endogenous metabolism product of cellular respiration such as ROS (reactive oxygen species). Such encounters can lead to the replication fork collapse (Raji and Hartsuiker, 2006). Recently, the endonuclease Mus81 has been shown to be involved in cleaving stalled replication forks and thus generating DSBs in order to re-start DNA replication (Hanada et al., 2007). Despite DSBs arising in cells endogenously, DSBs can also arise from exogenous sources, when cells are exposed to DNA damaging agents including IR, UV light, or Camptothecin (CPT) (Wan et al.,

1999). IR cause a wide spectrum of DNA damage, including DSBs, SSBs and base damages; UV light creates replication blocking lesions; CPT, an inhibitor of topoisomerase I, traps topoisomerase I after a single-strand of DNA has been cleaved and prevented re-ligation of that strand. CPT stabilizes the topoisomerase I-DNA intermediate and when a DNA replication fork collides with a CPT-topoisomerase I-DNA complex, it results in the generation of a double-stranded DNA break.

In eukaryotic cells, nonhomologous end-joining (NHEJ) and homologous recombination (HR) are two primary mechanisms to repair DSBs. NHEJ and HR will be the focus of the next paragraph. During HR, the broken ends are repaired using homologous chromosome or sister chromatid in the genome as template, therefore, HR is classified as an error-free pathway; NHEJ is responsible for the ligation of two DSBs-ends and may require gap-filling prior to ligation, therefore, NHEJ is often classified as an error-prone pathway, since it can often result in DNA insertion or deletion at the sites of DSBs (Pardo et al., 2009). NHEJ and HR are important for DSB repair in mammals, whereas HR is the primary DSB repair mechanism in yeast. However, the contribution of NHEJ or HR for DSB repair varies during the cell cycle. In yeast while NHEJ is more efficient than HR in G1, HR is favored in G2 because sister chromatids are available as DNA templates (Humpal et al., 2009; Raji and Hartsuiker, 2006).

The MR(X)N complex, formed by hMre11/spRad32/scMre11, Rad50, and hNbs1/spNbs1/scXrs2, is involved in the early response to DSBs (Fig.1-8A). During NHEJ, MR(X)N complex functions in bridging the two broken DNA ends in mammals and *S. cerevisiae* (de Jager et al., 2001; Lobachev et al., 2004). In *S. cerevisiae*, two MRX complexes bind to each side of DSB ends and interact through the Zn-hook

Figure 1-8- DSB repair by NHEJ and HR pathways in *S.cerevisiae*

MR(X)N is recruited DSBs in the early response (A).
NHEJ: DSB ends are further stabilized by ku70/80 (B). The ligase complex is recruited and two DSB ends can be aligned and ligated (C, D).
HR: when DSB ends are tethered by MR(X)N, DSB ends are resected by MR(X)N and other nucleases (E). RPA binds the single-strand DNA generated by resection (F). RPA-coated single-strand DNA is replaced by Rad51-filament. Formation is promoted by with Rad52, Rad55-Rad57, Rad54 (G). Rad51-filament search homology template (gray line) and strand invasion results in the formation of a D-loop (H). While a double HJ is formed, it can be resolved either HJ resolution or HJ dissolution which will be described in figure 1-9. (adapted from Pardo, Gomez-Gonzalez et al. 2009)

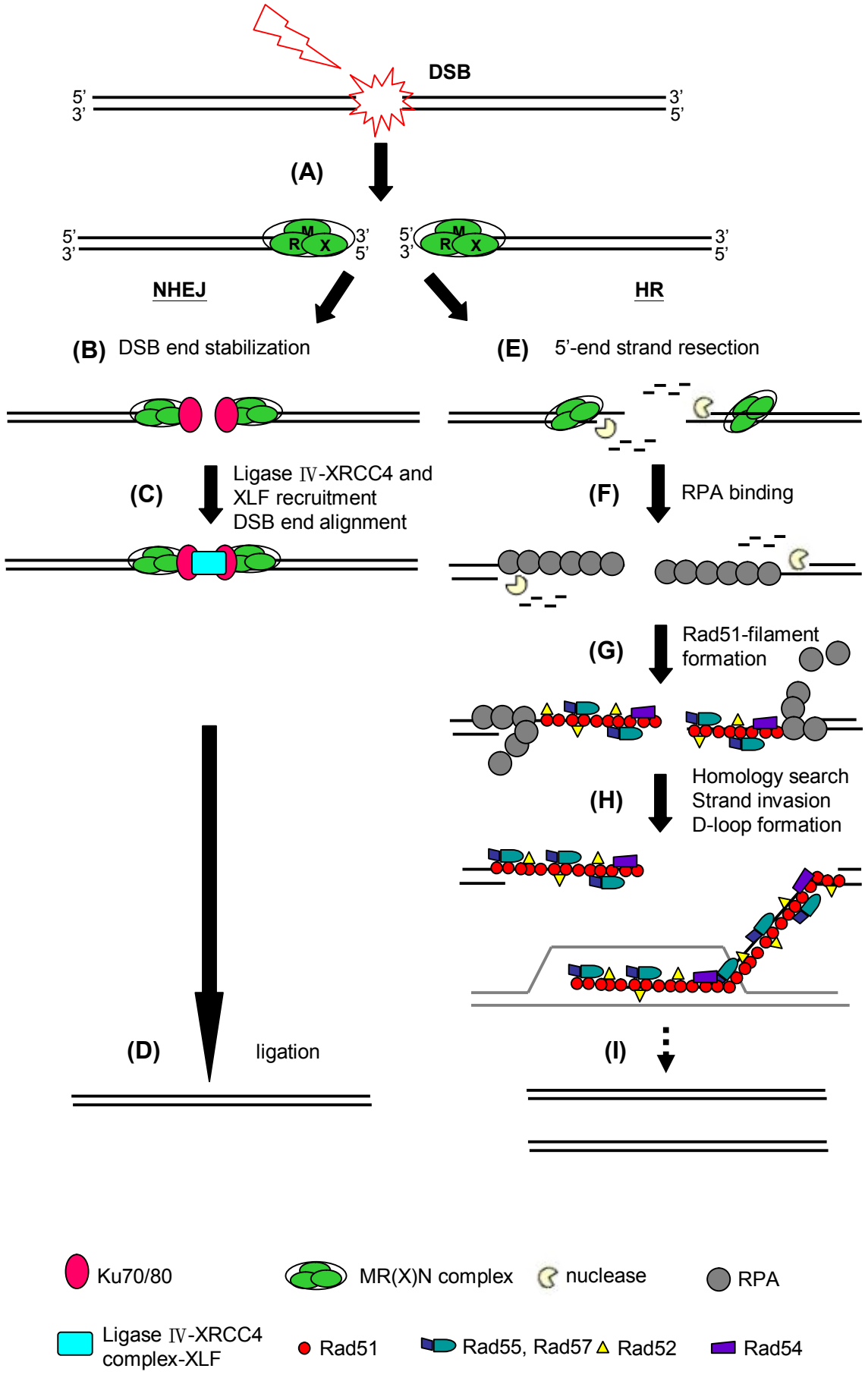
DSB
5'
3'
3'
5'
(A)
M
R
X
NHEJ
HR
(B) DSB end stabilization
(E) 5'-end strand resection
(C)
Ligase Ⅳ-XRCC4 and
XLF recruitment
DSB end alignment
(F) RPA binding
(G) Rad51-filament
formation
(H) Homology search
Strand invasion
D-loop formation
(D) ligation
(I)
Ku70/80
MR(X)N complex
nuclease
RPA
Ligase Ⅳ-XRCC4
complex-XLF
Rad51
Rad55, Rad57
Rad52
Rad54

domain of Rad50. In *S. pombe*, however, the MRN does not apparently affect DSB repair by NHEJ; NHEJ is not impaired in cells lacking Rad50 or Rad32 (Manolis et al., 2001). MR(X)N complex also functions in the initiation of the HR pathway by processing DSBs ends to a single-strand DNA (see below) (Pardo et al., 2009; Raji and Hartsuiker, 2006).

1.3.1 Nonhomologous end-joining (NHEJ)

Three protein complexes are involved in the NHEJ mechanism and they are MR(X)N, Ku/DNA-PK, DNA Ligase Ⅳ-XRCC4 complex. Ku70 and Ku80 form a heterodimeric complex essential for NHEJ. In mammalian cells Ku70/Ku80 form a complex with DNA-dependent protein kinase catalytic subunit (DNA-PKcs), whose catalytic subunit DNA-PK is also required for NHEJ (Gottlieb and Jackson, 1993; Pardo et al., 2009). The Ku70/Ku80 complex is recruited to DSBs ends (Uematsu et al., 2007; Walker et al., 2001) and protects DSB ends from degradation (Lee et al., 1998) by preventing 5'-end resection (Fig.1-8B). DSBs ends often lose 5' phosphataes and 3' hydroxyls or other problems at the break ends. Therefore, several enzymes, *i.e.*, nucleases, polymerases etc, might need to process DSB ends prior to ligation. For example, mammalian polynucleotide kinase (PNK) is recruited via its interaction with XRCC4 and this enzyme corrects both modifications at 5' and 3' break ends to generate ligatable 5' phosphataes and 3' hydroxyls. DNA nucleases may be needed for removing damaged bases or mismatches and polymerases may be needed for single-stranded gap filling, allowing end pairing (Pardo et al., 2009). The consequence of this processing often causes DNA insertion or deletion at the DSBs site. The last step of NHEJ relies on DNA Ligase Ⅳ-XRCC4 complex and XLF to ligate two DSBs-ends together (Fig.1-8C.D).

1.3.2 Homologous recombination (HR)

Classical HR includes three successive steps: first, DNA 5'-end resection; second, strand invasion and strand exchange; third, resolution of recombination intermediates. Mre11, hCtIP/spCtp1/scSae2, and hEXO1/spExo1/scExo1 are all involved in the initiation step of HR, DNA 5'-end resection (Fig.1-8E) generating 3' single-stranded DNA (ss-DNA) coated with RPA (Fig.1-8F). hRad52/spRad22/scRad52 promotes Rad51 binding to 3' ss-DNA by displacing RPA and Rad51 wraps around ssDNA to form a nucleoprotein filament (Fig.1-8G) (Song and Sung, 2000; Sung, 1997a). Rad55-Rad57 heterodimers and Rad54 mediate Rad51 nucleoprotein filament assembly (Fig.1-8G). Rad55-Rad57 and Rad54 not only promote Rad51 loading but also stimulate homology search and subsequent strand exchange (Fig.1-8H) (Heyer et al., 2006; Sung, 1997b). Szostak and coworkers (Szostak et al., 1983) have proposed a double-strand break repair (DSBR) model where a double Holliday junction (HJ) is formed during the process of DSBs-repair by HR, that can either be resolved or dissolved (Fig.1-9A.B). Resolution of HJ intermediates results in gene conversion associated with or without a crossover. Dissolution of HJ only results in non-crossover recombinants. Rqh1, a helicase in *S. pombe*, has been proposed to be involved in non-recombinogenic resolution of HJ (Doe et al., 2000), and is homologous to BLM in mammalian cells. BLM and Topoisomerase III α are together involved in dissolution of HJ, preventing crossover recombinants formation (Seki et al., 2006; Wu and Hickson, 2003). In fission yeast, Mus81-Eme1 is responsible for HJ cleavage and formation of gene conversion associated with a crossover (Osman et al., 2003).

1.4 Chromatin modification

DNA in eukaryotic cells is packaged into a high level of organization into chromatin.

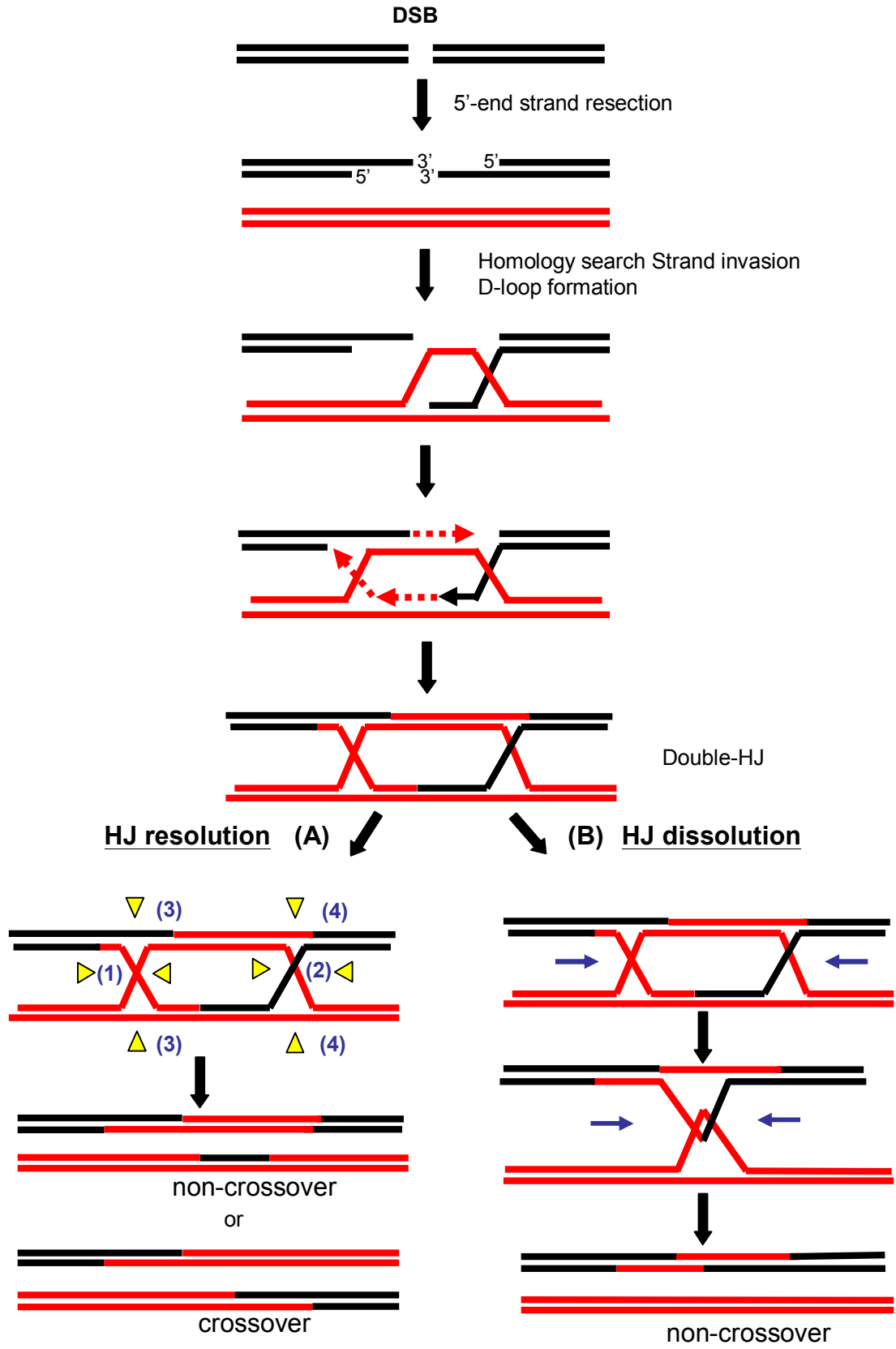

Figure 1-9- HJ resolution and HJ dissolution

A double HJ formed during HR can be processed by two ways: (A) HJ resolution and (B) HJ dissolution. **HJ resolution**: for example, the cleavage at (1)+(2) produces a non-crossover; the cleavage at (1)+(4) produces a crossover. **HJ dissolution**: HJ branch can migrate and strand decatenation produce non-crossover recombinants (adapted from Pardo, Gomez-Gonzalez et al. 2009)

Chromatin is composed of the nucleosome wrapped around DNA and a linker histone H1 associates the DNA between each nucleosome. One nucleosome contains two copies of each of four core histones: H3, H4, H2A, and H2AB. Histone modifications include histone phosphorylation, methylation, acetylation, ubiquitylation, and sumoylation. Two of these histone modifications, phosphorylation and methylation, have been strongly linked to the DNA damage checkpoint pathway (Humpal et al., 2009) and related to DNA checkpoint maintenance through regulation of localization of mediator proteins to chromatin.

1.4.1 Histone phosphorylation

In the early step of checkpoint response, ATM is recruited to DSBs and not only activates the DNA damage checkpoint pathway and DNA repair, but also ATR/ATM-dependent H2AX phosphorylation (Downs et al., 2000; Nakamura et al., 2004; Ward and Chen, 2001). Serine 139 in the mammalian C-terminal serine-glutamine-glutamate (SQE) motif of the histone variant H2AX, or serine-129 in yeast H2A, is phosphorylated rapidly in response to DNA damage (Downs et al., 2000; Rogakou et al., 1998). The H2A phosphorylation signal in *S. cerevisiae* can spread ~50 kb bp away on the each side of a DSB and up to 1 megabase either side in mammalian cells (Shroff et al., 2004; Srivastava et al., 2008). The response to DSBs induced by IR causes the accumulation of DDR proteins such as MDC1, Nbs1 and BRCA1 in nuclear foci called IR-induced nuclear foci (IRIF) that are thought to be sites of DNA damage. γ-H2AX is required not only for efficient accumulation of BRCT domain containing-proteins e.g., Nbs1, 53BP1, MDC1, BRCA1 into IRIF but also for their retention (Stucki et al., 2005; van Attikum and Gasser, 2009). Moreover, a H2A phosphorylation mutant (H2A-AQE) in *S. pombe* is defective in maintaining both cell cycle arrest in response to Bleomycin and maintaining Chk1 and Crb2 phosphorylation.

Recruitment of Crb2 into IRIF is also defective (see also previous section 1.2.4) (Nakamura et al., 2004). This suggests that γ-H2A functions primarily in checkpoint maintenance.

1.4.2 Histone methylation

Histone methylation is implicated in the DNA damage checkpoint through localization of checkpoint mediator proteins. Examples are spCrb2 and scRad9, whose IRIF formation could be regulated by both histone phosphorylation and methylation (Du et al., 2006; Toh et al., 2006). Lysine 79 methylation (H3-K79^{Me}) by Dot1 methyltransferase in both *S. cerevisiae* and mammalian cells (Giannattasio et al., 2005; Huyen et al., 2004), and H4-K20 methylation by Set9 methyltransferase in *S. pombe* (Sanders et al., 2004) are essential for localization of h53BP1/scRad9/spCrb2. Moreover, in all species histone methylation mediates the recruitment of mediator proteins h53BP1/spCrb2/scRad9 to DSBs via their Tudor domain (Huyen et al., 2004; Wysocki et al., 2005). *S. cerevisiae* cells lacking Dot1 methyltransferase result in a defect in Rad53 phosphorylation following UV and MMS and this is presumably due to the fact that lysine 79 methylation in *S. cerevisiae* is essential for allowing Mec1 to efficiently phosphorylate scRad9 (Giannattasio et al., 2005).

1.5 DNA replication

In eukaryotes, many replication origins are firing at the same time during replication in order for the whole genome to be replicated within a short time, but replication occurs only once per cell cycle following a two-step mechanism. The origin recognition complex (ORC), hCdc6/scCdc6/spCdc18, Cdt1, and the minichromosome maintenance (Mcm2-Mcm7) proteins are first assembled at autonomously replication sequence (ARS)

during late M to G1 phase of the cell cycle to form the pre-replicative complexes (pre-RCs). The inactivate form of pre-RC is activated into pre-initiation complexe (pre-IC) by S-phase cyclin-dependent kinase (S-CDK), and Dbf4-dependent Cdc7 kinase (DDK) (scCDC7/spHsk1) (reviewed in Nishitani and Lygerou, 2002). Subsequently, Cdc45, replication protein A (RPA), and DNA polymerase are loaded onto the replication origins (Fig.1-10).

1.5.1 Pre-replication complex (pre-RC)

ARS acts as the core recognition sequence for the ORC, which binds replication origins throughout the cell cycle in *S. pombe* and *S. cerevisiae* (Bell and Dutta, 2002; Newlon, 1997; Wuarin and Nurse, 1996). ORC, a heteromeric protein with six subunits (Orc1-6), binds directly to replication origins (Fig.1-10A) and is necessary for the subsequent recruitment of scCdc6/spCdc18, Cdt1, and MCM (Fig.1-10B.C). ORC is essential for the initiation of DNA replication and is conserved from yeast to human. spCdc18 assembling with ORC in late M-G1 is essential for the recruitment of MCM complex. spCdt1 associates with C-terminus spCdc18 and cooperates to promote MCM recruitment (Fig.1-10B.C) (Nishitani et al., 2000). Similar to *S. pombe*, scCdc6 plays a crucial role in assembling the pre-RC after ORC complex binding and the interaction scCdc6 with scCdt1 promotes MCM proteins loading at replication origins (Chen et al., 2007a; Duncker et al., 2009). *In vitro* assays performed in *S. cerevisiae* indicated that pre-RCs assembly requires two ATP-dependent steps, one is required for ORC association with replication origin, and the other is required for Cdc6 and MCM recruitment (Seki and Diffley, 2000). In addition, it has been shown that ORC, Cdc6, and MCM proteins assemble at replication origins only under low CDK activity during G1, and pre-RC activation is driven by the increase CDK activity at late G1 (Seki and Diffley, 2000). CDK plays a dual role in triggering initiation and preventing

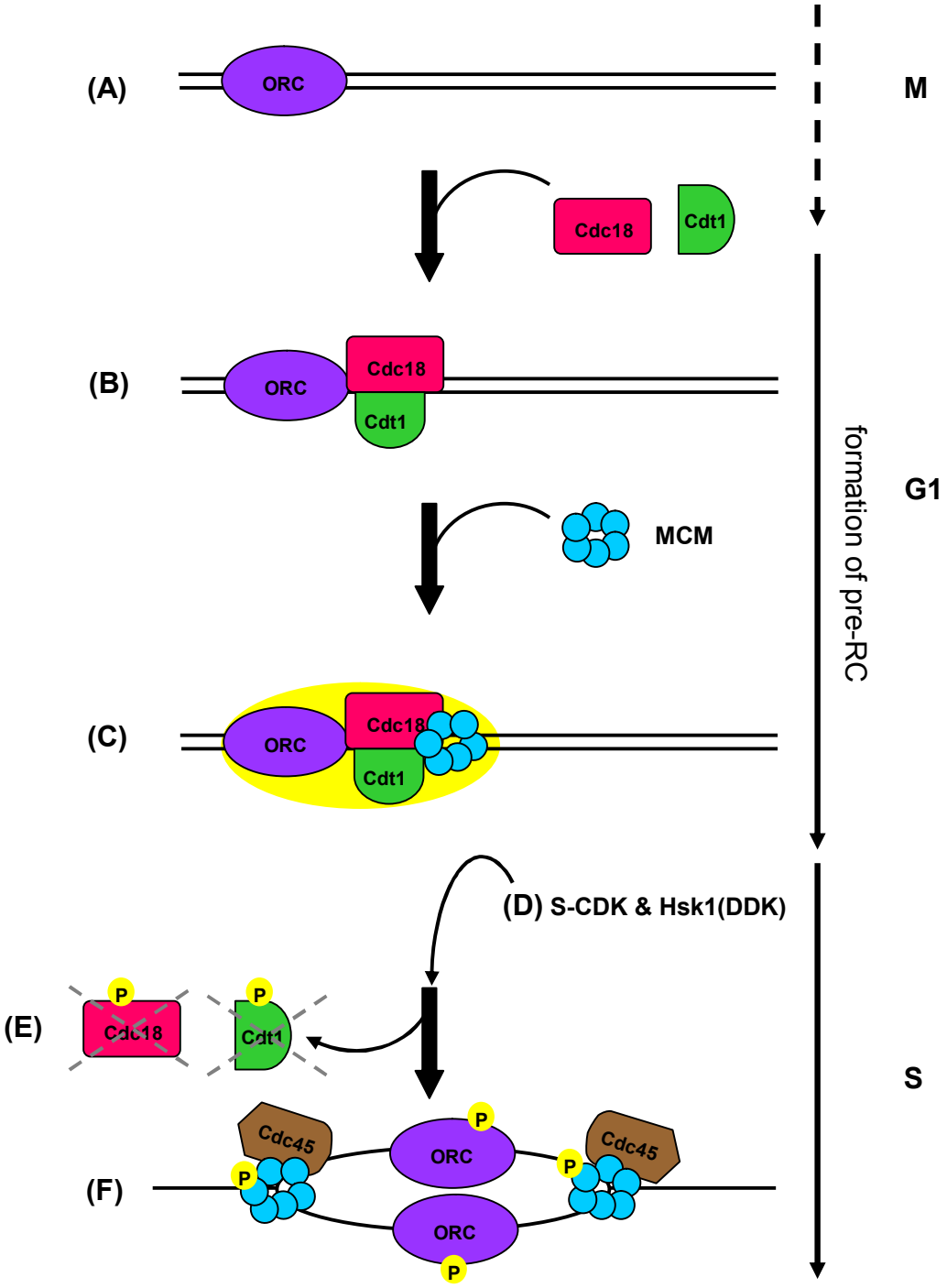

Figure 1-10- Regulation of DNA replication initiation in *S. pombe*

ORC, Cdc18, and Cdt1 recruit MCM onto DNA to form the pre-replicative complex (pre-RC) (A)(B)(C). The pre-RC is activated into a pre-initiation complex (pre-IC) by S-phase cyclin-dependent kinase and Hsk1 (D) to recruit Cdc45 and RPA. As DNA replication is initiated, Cdc18 and Cdt1 are degraded (E), and MCM proteins and Cdc45 move with replication fork (F). (adapted from Newlon 1997; Gopalakrishnan, Simancek et al. 2001)

re-assembly of pre-RC in order to ensure that replication origins are only firing once in a single cell cycle. This process is called replication licensing (see below). Such a CDK-regulated licensing control is conserved from yeast to higher eukaryotes. Only when CDK activity drops at the completion of mitosis, is the block to replication licensing relieved and a new round of replication primed.

1.5.2 Pre-initiation complexes (pre-IC)

The pre-RC is activated into a pre-IC at the onset of S-phase by DDK and S-CDK and additional replication factors are recruited such as, Rad4/Dpb11 (see 1.6.1), Drc1/Sld2, Sld3, GINS, Cdc45, RPA and polymerase ε (Pol ε) and α (Pol α) in order to unwind the origins and initiate DNA replication (Fig.1-10D) (Bell and Dutta, 2002).

spCdc18 becomes highly phosphorylated by Cdc2 during the G1/S phase transition and its phosphorylation causes its inactivation and degradation at the initiation of S phase (Fig.1-10E) (Jallepalli et al., 1997). The protein level of Cdt1 peaks at G1/S and it is also degraded at the initiation of S phase (Fig.1-10E) (Nishitani et al., 2000). Therefore, once firing of replication origins has occurred, degradation of spCdc18 triggered by CDK phosphorylation and degradation of Cdt1 are essential for preventing re-firing of replication origins until the next cell cycle (Yanow et al., 2001). Redundant regulatory mechanisms of re-replication exists in fission yeast: Overexpression of Cdt1 with $Cdc18^{CDK}$ expressing under the control of the $cdc18^{+}$ promoter induces re-replication, but overproduction of Cdt1 alone does not induce re-replication phenotype, indicating that Cdt1 works synergistically with Cdc18 in order to restrict DNA synthesis to once per cell cycle; high levels of $Cdt1^{S382A}$ expression with $Cdc18^{CDK}$ expressing under the control of the $cdc18^{+}$ promoter greatly enhanced re-replication compared to expression of wild-type Cdt1 under the same condition (S382 being a potential CDK

phosphorylation site) (Gopalakrishnan et al., 2001).

DDK and S-CDK are both required for Cdc45 recruitment to chromatin (Zou and Stillman, 2000). DDK is able to phosphorylate MCM proteins and this phosphorylation is thought to enhance MCM interaction with Cdc45 (Masai et al., 2006; Sheu and Stillman, 2006). Mcm4/6/7p was shown to possess DNA helicase activity (Lee and Hurwitz, 2001). MCM proteins and Cdc45 unwind the origins during initiation and elongation of replication, and MCM proteins and Cdc45 move with the progressing replication forks (Fig.1-10F) (Aparicio et al., 1997). The tetrameric GINS complex, composed of Sld5, Psf1, Psf2, and Psf3, plays an essential role in the initiation and elongation steps of DNA replication with MCM and Cdc45 (Gambus et al., 2006; Labib and Gambus, 2007). It is thought that MCM-Cdc45-GINS together form the active replicative helicase. S-CDK positively regulates the formation of Sld2-Dpb11 and Sld3-Dpb11 complexes, required for DNA replication initiation in budding yeast (for detail see 1.6.1) (Zegerman and Diffley, 2007).

1.6 General introduction of Rad4^{TopBP1}/Cut5

S. pombe Rad4^{TopBP1}, *S. cerevisiae* Dpb11, *Xenopus* Xcut5, Drosophila Mus101 and human DNA topoisomerase II binding protein1 (TopBP1) are homologous proteins whose structure and function in initiation of DNA replication and DNA replication and DNA damage checkpoints are conserved throughout eukaryotic organisms (Garcia et al., 2005; Makiniemi et al., 2001). Rad4/Cut5 in *S. pombe* was originally identified from two different screens: the *cut5* mutant was identified from temperature-sensitive mutant screen, exhibiting a cell untimely torn (cut) phenotype caused by cells continuing into cytokinesis without nuclear division at restrictive temperature (Hirano et al., 1986).

Rad4 was identified in a radiation sensitive screen. Two *cut5* alleles (*cut5-580* and *cut5-T401*) appear to be UV and IR sensitive at the permissive temperature (Saka and Yanagida, 1993). The *rad4-116* allele confers sensitivity to UV and IR (Duck et al., 1976) and *rad4-116* cells carry the same substitution of T45M with *cut5-580* and *cut5-T401*, but *cut5-T401* carries an additional mutation K62Q. The identity between Cut5 and Rad4 was further shown by gene cloning and sequencing (Fenech et al., 1991).

Structurally, Rad4 and Dpb11 both have four BRCT domains, whereas orthologous in higher eukaryotes contains eight BRCT domains, the additional BRCT domains being associated to different function (Fig.1-11) (Garcia et al., 2005; Hashimoto and Takisawa, 2003; Hashimoto et al., 2006). For example, ATM phosphorylates E2F1 in response to DNA damage and this results in the sixth BRCT-repeat of TopBP1 interacting with phosphorylated E2F1 (Liu et al., 2003). E2F1 is required for the G1/S phase transition, apoptosis, and regulation of the transcription of DNA repair, DNA replication and DNA damage checkpoint genes (Liu et al., 2003; Ren et al., 2002; Stevens and La Thangue, 2004). The interaction with TopBP1 suppresses the E2F1 transcriptional activity in response to DNA damage (Liu et al., 2003).

1.6.1 Role in DNA replication

Rad4^{TopBP1}, Dpb11, XCut5, and TopBP1 are essential for cell viability: besides their function in checkpoint activation (see 1.6.3), they are essential for initiation of DNA replication (Furuya et al., 2004; Garcia et al., 2005; Saka and Yanagida, 1993). In *S. cerevisiae*, the *dpb11-1* thermo-sensitive mutant is deficient in S-phase progression and subsequently cell division occurs with unequal chromosome segregation leading to cell viability loss at the non-permissive temperature, suggesting Dpb11 is essential for DNA

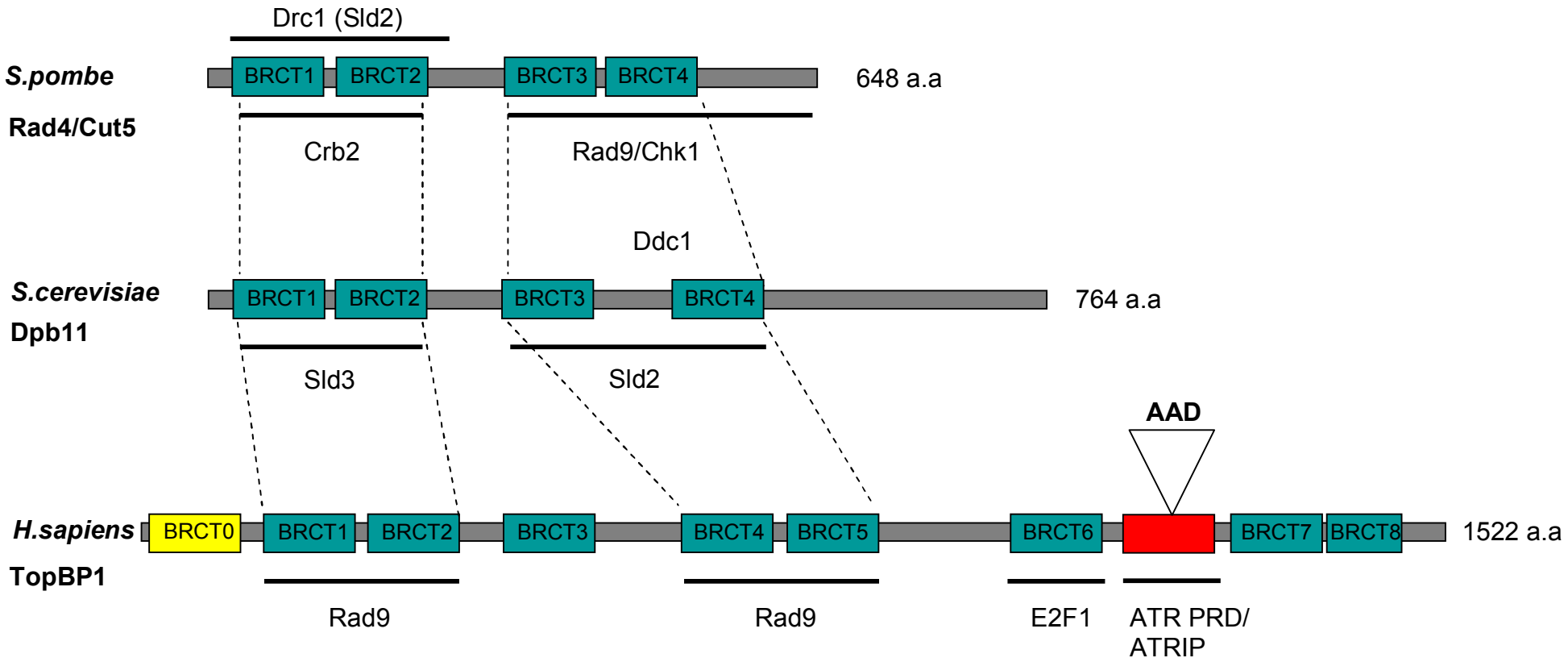

Figure 1-11- Structure of TopBP1 and its orthologous

TopBP1 has multiple BRCT repeats and this structure is conserved throughout eukaryotic organisms. In addition to the eight BRCT domains in TopBP1, BRCT 0 at the extreme N-terminus (represented the yellow box) has been reported. Both *S. cerevisiae* and *S. pombe* contain four BRCT domains. The pair of BRCT domains 1-2 and 3-4 in yeasts (Dpb11 and Rad4) show similarity to the pairs of BRCT domains 1-2 and 4-5 in mammalian TopBP1. Total amino acids in TopBP1 and its homologues are indicated on the right of each protein. The known interaction sites amongst Rad4/Dpb11/TopBP1 are underlined. (adapted from Garcia, Furuya et al. 2005)

replication and intra-S phase checkpoint (Araki et al., 1995). Several replication initiation factors Sld1 (Dpb3, one subunit of Pol ε), Sld2/Drc1, Sld3, Sld4 (Cdc45), and Sld5 (one component of the GINS complex) have been identified to have interaction with Dpb11 by isolating synthetic lethal mutations with *dpb11-1* (Kamimura et al., 1998).

Xcut5 depletion experiments demonstrate that Xcut5 is indispensable for chromatin binding of Pol ε, Pol α, and the pre-initiation component Cdc45 (Hashimoto and Takisawa, 2003). In contrast, loading of pre-RC components (*i.e.*, ORC, MCM proteins) are not dependent on Xcut5. This sequence of replication factors binding dependent on $Xcut5^{TopBP1}$ seems to be conserved in yeasts (Dolan et al., 2004; Garcia et al., 2005). Hashimoto and Takisawa demonstrate that the chromatin association of Xcut5 occurs in two distinct modes: S-CDK-independent and S-CDK-dependent. Xcut5 binds weakly to the chromatin in a S-CDK-independent manner but this is sufficient for initiation of DNA replication. The S-CDK functions after Xcut5 binding and before the Cdc45 chromatin binding. Xcut5 chromatin binding is greatly increased in a S-CDK-dependent manner, but this increased amount of binding is dispensable for DNA replication. In *S. cerevisiae*, S-CDK and DDK are required for subsequent loading of Cdc45 and RPA at replication origins, consequent conversion of the pre-RC to pre-IC and the unwinding the replication origins (Zou and Stillman, 2000). Pol ε and Pol α are then recruited to form the initiation complex (IC) (Zou and Stillman, 2000). The loading of the GINS complex and of Dpb11/Rad4 at origins are mutually dependent in both budding and fission yeast (Labib and Gambus, 2007; Yabuuchi et al., 2006).

In *S. cerevisiae*, Sld2 and Sld3 phosphorylation by S-CDK is a prerequisite for their interaction with Dpb11 C-terminal and N-terminal pairs of BRCT-repeats, respectively,

and this is the minimal requirement for DNA replication initiation by S-CDK (Tanaka et al., 2007; Zegerman and Diffley, 2007). Interestingly, DNA replication occurs in the absence of S-CDK when a fusion Sld3-Dpb11 is co-expressed with a phospho-mimicking Sld2 mutant, which bypasses the requirement for Sld3 phosphorylation and the N-terminal BRCT-repeats of Dpb11. Similarly, *S. pombe* Cdc2 promotes DNA replication by regulating Rad4 N-terminus association with Drc1, a homologue of Sld2 (Noguchi et al., 2002).

1.6.2 Role in DNA repair

TopBP1 and its orthologues might be involved in DNA repair. However, whether this role is direct remains unclear. *dpb11-1* in *S. cerevisiae* was found to display sensitivity to MMS and UV light but its G2 DNA damage checkpoint remained intact when *dpb11-1* was exposed to DNA damage in G2 cells, suggesting a repair defect (Wang and Elledge, 2002). Subsequently, Dpb11 was suggested to play a role in the HR repair pathway of MMS-induced DNA damage in collaboration with Ddc1 (Ogiwara et al., 2006). In mammalian cells, Nbs1 is required to recruit TopBP1 into IRIF, and TopBP1-depleted cells display a repair defect (Morishima et al., 2007). Also, ATR-dependent Chk1 phosphorylation is impaired in the absence of Nbs1 function (Stiff et al., 2005). Therefore, it has been proposed that TopBP1 may play a role in transducing the damage checkpoint signal from Nbs1 to ATR and promotes HR repair in response to IR (Morishima et al., 2007). However, there is so far no direct evidence that $Rad4^{TopBP1}$ in *S. pombe* and its homologues in *Xenopus* and Drosophila play a role in DNA repair.

1.6.3 Role in the DNA checkpoint

More recently, several groups studied the role of TopBP1/Rad4/Dpb11 in the

stimulation of ATR-ATRIP/Rad3-Rad26/Mec1-Ddc2 complex in checkpoint signaling in yeasts, *Xenopus*, and mammalian cells. Here, I summarize the recent findings on ATR signaling in four areas: 9-1-1 complex recruits $Rad4^{TopBP1}$ in order to activate Rad3; TopBP1 directly activates ATR via its ATR-activating domain (AAD); TopBP1-dependent ATR activation occurs in an ATRIP/Ddc2-dependent manner; Rad9/Ddc1 can activate Mec1 independently of Dpb11.

1.6.3.1 The 9-1-1 complex recruits $Rad4^{TopBP1}$ in order to activate Rad3

The C-terminal T412/S423 phosphorylation of Rad9 by Rad3 occurs in unperturbed S phase, and this phosphorylation is required for Rad4-Rad9 and Rad4-Rad3 interaction and, subsequently, Chk1 activation following HU treatment or after DNA damage (Furuya et al., 2004). Furthermore, both Rad4 and Crb2 phosphorylation are dependent on Rad9 C-terminal phosphorylation. Similarly in *S. cerevisiae*, phosphorylation of Ddc1 on threonine 602 (SQ/TQ site) by Mec1 is critical for Rad53 activation in response to UV-irradiation (Puddu et al., 2008). Two-hybrid experiments suggest that this phosphorylation promotes Ddc1 association with Dpb11 (Puddu et al., 2008).

In human cells, the C-terminal tail of Rad9 was shown to interact with TopBP1 BRCT domain 4 and 5 by two-hybrid assays and co-immunoprecipitation (Makiniemi et al., 2001). More recently, TopBP1 BRCT domain 1 and 2 have been shown to interact with Rad9 (see below). Unlike scDdc1 T602 and spRad9 T412, hRad9 S387 in mammals is constitutively phosphorylated rather than damage-induced and a co-immunoprecipitation experiment indicates that phosphorylation of this specific residue is essential for hRad9 association with TopBP1 (St Onge et al., 2003). hRad9 C-terminal tail has multiple phosphorylation sites and Chk1 phosphorylation induced by HU or UV was abrogated by mutating all of the phosphorylation sites (Rad9-9A)

(Roos-Mattjus et al., 2003). Furthermore, analysis of "add-back" mutant revealed that HU-induced Chk1 phosphorylation was abrogated in Rad9-/- chicken DT40 cells expressing Rad9-9A; while phosphorylation of S387 restored Chk1 phosphorylation nearly as well as wild-type Rad9 (Delacroix et al., 2007). Phosphorylation of Rad9 on S387 is essential for Rad9 interaction with TopBP1 BRCT domain 1 and 2 (Delacroix et al., 2007). This is in contrast to an observation made by Makiniemi, Hillukkala et al, who showed this interaction is via TopBP1 BRCT domain 4 and 5. While TopBP1-Rad9 fusion can not elicit HU-induced Chk1 phosphorylation in Rad17-/- DT40 cells, this Chk1 phosphorylation was restored by a fusion between PCNA and TopBP1 ATR-activating domain (AAD) (described detail in section 1.6.3.2) or by a fusion between PCNA and Rad9 C-terminal tail, which fusion proteins bypassed the requirement for Rad17 to localize TopBP1 or Rad9 on chromatin in order to induce checkpoint activation. Altogether, these results suggest that the function of Rad9 and Rad17 is to localize TopBP1 at stalled replication fork, and this occurs via Rad9 C-terminal tail phosphorylation which promotes a TopBP1-Rad9 interaction in order to trigger Chk1 activation (Delacroix et al., 2007; Furuya et al., 2004).

hRad9 S387 is highly conserved in eukaryotes and corresponds to serine 373 of Xrad9 (Lee et al., 2007). In *Xenopus*, the Xrad9 C-terminus interaction with Xcut5 requires Xrad9 phosphorylation on S373 (Lee et al., 2007). Xchk1 phosphorylation in Xcut5-depleted egg extracts following replication block by aphidicolin or DSBs-induced checkpoint by $(dA)_{70}$-$(dT)_{70}$ oligonucleotides is restored by the recombinant full-length Xcut5 but not by recombinant Xcut5 protein truncated of BRCT domain 1 and 2 or truncated of the AAD, suggesting that Xcut5 BRCT domain 1 and 2, and the AAD, are essential for Xatr-mediated Xchk1 activation (Lee et al., 2007).

Taken together, a role of Rad9 in the ATR-mediated checkpoint signaling via its association with TopBP1, allowing colocalization with ATR-ATRIP is conserved within *S. cerevisiae*, *S. pombe*, *Xenopus*, and mammals. This function is performed via BRCT repeats 3 and 4 of Dpb11/Rad4 in both *S. cerevisiae* (Wang and Elledge, 2002) and *S. pombe* (Furuya et al., 2004), via BRCT repeats 1 and 2 in *Xenopus* (Lee et al., 2007) (Fig.1-11). A discrepancy exists in the literature as to whether mammalian Rad9 associates with TopBP1 via BRCT repeats 1 and 2 or 4 and 5 (Fig.1-11).

1.6.3.2 TopBP1 directly activates ATR via its ATR-activating domain (AAD)

In *S. pombe*, the *rad4-116* thermo-sensitive mutant retains almost identical viability as wild-type cells at 32°C but is deficient for the replication checkpoint resulting in the failure of mitotic arrest in response to HU at 32℃ (McFarlane et al., 1997). This indicates that the role of $Rad4^{TopBP1}$ in DNA replication can be separated from DNA replication checkpoint function. Similarly to *S. pombe* with a separation-of-function, the group of W. Matthew Michael find a region of Xcut5 in *Xenopus*, named as Mini, truncated right after BRCT domain 5, that can separate functions of DNA replication from Xchk1 activation for Xcut5 (Yan et al., 2006). *Xenopus* egg extracts immunodepleted of Xcut5 have neither replication function nor aphidicolin-induced Xchk1 activation. Addition of recombinant full-length Xcut5 rescues both functions. Interestingly, addition of recombinant “Mini” rescues the replication defect but not Xchk1 activation defect, suggesting that Xchk1 phosphorylation requires the Xcut5 C-terminus (Yan et al., 2006). Consistently, Xcut5 functions in DNA replication and checkpoint activation were shown to be regulated independently via the Xcut5 N-terminus and C-terminus, respectively; Xcut5 N-terminal fragment includes BRCT domain 1~5 and C-terminal fragment includes BRCT domain 6~8 (Hashimoto et al., 2006). Recombinant N-terminus Xcut5 restores the replication defect of Xcut5-depleted

extract while Xcut5 C-terminus alone does not. Conversely, C-terminus Xcut5 restore Xchk1 phosphorylation defect inducible by $(dA)_{70}$-$(dT)_{70}$ oligonucleotides in Xcut5-depleted extract, while N-terminus Xcut5 alone does not.

Furthermore, Xcut5 phosphorylation on serine 1131 (SQ/TQ site), embedded in the ATR-activating domain, is essential for checkpoint activation. When supplemented with Xcut5-S1131A mutant protein in Xcut5 depleted extracts, Xchk1 phosphorylation is not elicited in the presence of $(dA)_{70}$-$(dT)_{70}$ oligonucleotides or aphidicolin. When supplemented with recombinant Xcut5 carrying S1131E (phospho-mimetic), Xchk1 phosphorylation is elicited (Hashimoto et al., 2006). Interestingly, incubation of recombinant Xchk1 and Xatr with Xcut5 carrying S1131A does not induce Xchk1 phosphorylation but this is induced by recombinant Xcut5 carrying S1131E. This suggests Xcut5 has a direct role in ATR activation (Hashimoto et al., 2006). Xatm regulates phosphorylation Xcut5 on S1131 in response to DSBs, but not in response to DNA replication stress and this phosphorylation is critical for Xcut5 association with Xatr-Xatrip and for Xchk1 phosphorylation (Yoo et al., 2007).

In agreement with findings mentioned above, William G. Dunphy's group showed that in addition to Xcut5 directly activating Xatr, mammalian TopBp1 has this conserved function (Kumagai et al., 2006). The **A**TR-**a**ctivating **d**omain (AAD) in *Xenopus* Xcut5-(972-1279) or mammalian TopBP1-(978-1192), located between BRCT domain 6 and 7, directly triggers ATR activation and phosphorylation of downstream targets by ATR, *i.e.*, Mcm2, Chk1 (Kumagai et al., 2006). Firstly, Xatr kinase activity was increased in an Xcut5 dose-dependent manner upon recombinant Xcut5 incubation with the Xatr-Xatrip complex isolated from *Xenopus* egg extracts. Secondly, a fragment of (972-1279) ≈ 300 amino acids of Xcut5, or 978-1192 of hTopBP1, can activate ATR

kinase *in vitro*. Moreover, this region of Xcut5 (972-1279) interacts with Xatr. Thirdly, Xatr kinase activity is abrogated by deleting a highly conserved segment (WDDP) from Xcut5 AAD or by mutating W1138 to arginine (W1138R) in the WDDP motif. Expressing hTopBP1 (978-1286) with a point mutation W1145R, analogous to the W1138R mutant of Xcut5, in human cells fails to stimulate Mcm2 phosphorylation as detected by immunofluorescence. All these experiments were performed *in vitro* without replication inhibitor, DNA damage or DNA substrates. Finally, the AAD in recombinant Xcut5 was shown to be required for the checkpoint-induced ATR-mediated Xchk1 activation in response to aphidicolin (replication block) after adding and sperm DNA to Xcut5-immunodepleted extracts.

TopBP1-dependent ATR kinase activity during Chk1 kinase signaling is strongly stimulated by damaged DNA under a physiologically relevant reaction condition (a high ionic strength condition: 85mM high salt condition) (Choi et al., 2007). Furthermore, TopBP1 C-terminus, including the AAD and BRCT domain 7 and 8, was shown to preferentially bind to damaged DNA and was sufficient to mediate damaged DNA-dependent ATR activation in a manner similar to full-length TopBP1 (Choi et al., 2009).

Interestingly, in mammalian cells, the AAD of TopBP1 interacts with ATR PRD (Mordes et al., 2008a). A mutation (K2589E) in PRD decreased ATR association with TopBP1 but not with ATRIP in a pull-down assay. Importantly, K2589E mutation separated basal ATR kinase activity from TopBP1-induced ATR kinase activity. The K2589E mutation results in markedly decreased ATR activation mediated by TopBP1, but it does not affect the basal activity of ATR kinase (in the absence of TopBP1) (Mordes et al., 2008a). Surprisingly, this specific residue is critical for human cell

viability because expressing ATR PRD-K2589E does not rescue ATR-/- cell line lethality (Mordes et al., 2008a).

The architecture of the TopBP1 C-terminus, including the AAD, is conserved in vertebrate cells but lacks obvious sequence similarity with Dpb11/Rad4 in both budding yeast and fission yeast. However, *in vitro*, *S. cerevisiae* Dpb11 can directly activate Mec1 kinase activity and trigger phosphorylation of the Mec1 target, Rad53. This event is abrogated when the Dpb11 C-terminus is truncated (Navadgi-Patil and Burgers, 2008). Furthermore, overexpression of Dpb11 can partially suppress the HU-sensitivity of *ddc2-top*, a mutant disrupting Ddc2/ATRIP association with Dpb11 (discussed further in 1.6.3.3) (Mordes et al., 2008a). *ddc2-top* sensitivity to HU could not be suppressed by overexpression of Dpb11-1 (Mordes et al., 2008b). Because both *dpb11-1* and *ddc2-top* have a S-phase checkpoint defect (Araki et al., 1995; Mordes et al., 2008a), this suppression could be due to an interaction between C-terminal Dpb11 and Ddc2. In agreement with Burgers et al, *in vitro*, recombinant Dpb11-(571-764), the C-terminus tail of Dpb11, was shown to associate with Mec1-Ddc2 complex, and this association is required to stimulate Mec1 kinase activity (Mordes et al., 2008b). *In vitro*, Mec1 activation by Dpb11 C-terminal tail was reduced efficiently by mutating Dpb11 T731 (SQ/TQ site) to alanine, and was partially restored by T731E mutant. *In vivo*, overexpression of Dpb11-T731A could not suppress the HU-sensitivity of *ddc2-top* mutant. Altogether (Mordes et al., 2008b), this suggests that phosphorylation of Dpb11 on T731 by Mec1 is critical for Mec1-Ddc2 activation.

1.6.3.3 TopBP1-dependent ATR activation occurs in a ATRIP/Ddc2-dependent manner

TopBP1 AAD-dependent ATR activation and TopBP1 AAD association with ATR occur

in an ATRIP-dependent manner in *Xenopus* (Kumagai et al., 2006). Similarly in mammalian cells, TopBP1-dependent ATR activation is further enhanced by overexpression of both ATR and ATRIP compared to overexpression of ATR alone (Mordes et al., 2008a). Mordes, Glick et al. who identified a TopBP1-interacting region of ATRIP by using two-hybrid, defined an ATRIP-top mutant, a substitution mutation in this region of ATRIP (LLSS332AAAA) that nearly abolished ATRIP association with TopBP1 but retained ATRIP association with ATR. By using purified proteins, ATRIP-top caused reduced association of ATR with TopBP1; TopBP1-dependent ATR activation was significantly reduced in the kinase assay (Mordes et al., 2008a). As the TopBP1-interacting region sequence is not conserved in *S. cerevisiae*, the *ddc2-top* mutant was generated according to a structural prediction (Mordes et al., 2008a).

Mordes, Glick et al. made use of the mammalian ATRIP-top and *S. cerevisiae ddc2-top* mutants to study the role of ATRIP/Ddc2 in TopBP1/Dpb11-dependent ATR/Mec1 kinase checkpoint signaling after replication fork stalling or DNA damage *in vivo* (Mordes et al., 2008a). In contrast to cells expressing wild-type ATRIP, mammalian cells expressing ATRIP-top or ATRIP-depleted in the presence of HU for 24 hours are unable to replicate their DNA after HU removal. Viability of cells expressing ATRIP-top or ATRIP-depleted is significantly reduced compared to cells expressing wild-type ATRIP, suggesting the mutant could not recover from replication fork stalling. Also, cells expressing ATRIP-top appeared to have a G2/M checkpoint defect in response to IR. In *S. cerevisiae*, in addition to *ddc2-top* exhibiting significant sensitivity to HU and MMS, *ddc2-top* showed a defect in Rad53 phosphorylation. Consistently, in *S. cerevisiae* studies using a *ddc2-top* mutant, the interaction of Dpb11 with Mec1 and Dpb11-dependent Mec1 kinase activation both occur in a Ddc2-dependent manner *in vitro* (Mordes et al., 2008b). Therefore, the role of ATRIP in regulating

TopBP1-mediated ATR kinase activation seems conserved throughout evolution (Kumagai et al., 2006; Mordes et al., 2008a).

.

The RPA binding domain (RBD) localized in the N-terminus of ATRIP, also named checkpoint protein recruitment domain (CRD), is required for its interaction with RPA to localize ATR-ATRIP to sites of damage, and this function is conserved in mammals and *S. cerevisiae* (Ball et al., 2007). Strikingly, a truncation of ATRIP N-terminus, including the CRD, does not effect ATR activation by TopBP1, suggesting that TopBP1-dependent ATR activation occurs independently of RPA (Ball et al., 2007; Kumagai et al., 2006).

1.6.3.4 Rad9/Ddc1 can activate Mec1 independently of Dpb11

In *S. cerevisiae*, Ddc1 alone can sufficiently activate Mec1 activity in the absence of other 9-1-1 subunits, the Rad24-RFC clamp loader and effector DNA, when assayed under the condition of very low salt concentrations (≤ 40mM NaCl) (Majka et al., 2006b).

Besides a role in recruiting hTopBP1/spRad4/scDpb11 by hRad9/spRad9/scDdc1, Ddc1 also plays a direct role in stimulating Mec1 kinase activity independently of Dpb11. These two functions in Ddc1 have been first separated successfully in *S. cerevisiae* and, importantly, the role of Ddc1 in Mec1 activation varies at the different phases of cell cycle (Navadgi-Patil and Burgers, 2009): the Ddc1 C-terminal tail is critical for G1 phase checkpoint activation of Mec1 whereas Dpb11 is dispensable. In G2 phase, 9-1-1 activates Mec1 by two distinct mechanisms: stimulation of Mec1 kinase activity directly by Ddc1 in a Dpb11-independent manner, and Dpb11 recruitment mediated through Ddc1 phosphorylation on T602 (Dpb11-dependent). These results are also in agreement

with their previous *in vitro* study showing that Dpb11 and the 9-1-1 complex with Rad24-RFC clamp loader could activate Mec1 kinase independently (Navadgi-Patil and Burgers, 2008). Thus in *S. cerevisiae*, the 9-1-1 clamp can directly activate Mec1, but evidence from other organisms is still missing.

1.7 The aims of the project

Rad4^{TopBP1} is known to interact with several proteins that are involved in the DNA replication and checkpoint processes (Fig.1-11) (*i.e.* Sld2/Drc1, Rad9, Crb2, Chk1 and Rad3), to initiate DNA replication or activate the downstream checkpoint protein kinases Chk1 and/or Cds1. However, it remains unclear how Rad4^{TopBP1} and its homologues are regulated to coordinate these distinct functions in the replication initiation and DNA replication and damage checkpoint activation. The purpose of this PhD project is to realize a straightforward but comprehensive structure/function analysis of the fission yeast Rad4^{TopBP1}.

Results of the project are divided into three main parts:

Part I - the role of Rad4^{TopBP1} phosphorylation by the Cdc2^{CDK1} (Chapter 3)

Dr. Valerie Garcia in the laboratory has mapped seven Cdc2/CDK1 phosphorylation sites on Rad4^{TopBP1} by mass-spectrometry. I follow up these findings by investigating whether the function of Rad4^{TopBP1} is regulated by Cdc2/CDK1 phosphorylation *in vivo*.

Part II - functional characterizations of Rad4^{TopBP1} RXL motif (Chapter 3) and ATR-activating domain (Chapter 4, 5)

Rad4^{TopBP1} sequence contains two further motifs of interest in its extreme C-terminal tail, an RXL motif and an ATR-activating domain (AAD).

The RXL motif serve as a docking site for the binding of the CyclinA-CDK kinase complex onto its substrate (K. Fukuchi et al., 2003), and the RXL motif is often necessary for substrate phosphorylation (Loog and Morgan, 2005; Schulman et al., 1998). Dr. Valerie Garcia has shown that Rad4^{TopBP1} interacts with Cdc13, the cyclin B associated with Cdc2. We aimed to investigate whether of Rad4^{TopBP1} interaction with Cdc13 and its phosphorylation by Cdc2 is dependent on the RXL motif.

TopBP1 AAD was first characterized by its role in checkpoint signaling as an ATR activator in *Xenopus* and mammalian cells when we initiated this project; the function was not known in yeasts due to lack of obvious AAD in yeasts. An alignment was kindly provided by Charly Chahwan. Therefore, we aim to create Rad4^{TopBP1} AAD mutant in *S. pombe* cells and study what is the function of Rad4^{TopBP1} AAD in *S. pombe* and whether this function is conserved with higher eukaryotes. However, in the course of this study, recent reports have demonstrated C-terminus of Dpb11 in budding yeast has functional conservation to TopBP1 AAD in higher eukaryotes.

Part III - Rad4^{TopBP1} a separation-of-function mutant screen (Chapter 6)

The purpose of a random mutagenesis screen is to obtain novel and informative mutants in order to overcome the limited knowledge of Rad4 function. In particular, we developed a screen in order to identify separation-of-function mutants between replication checkpoint, DNA damage checkpoint, perhaps DNA repair defect (*i.e.* a DNA damage sensitivity not associated with a checkpoint defect) and the essential function in initiation of DNA replication.

As for part I and II, a classical mutagenesis and genetic approach has been taken; as for part III, a library of random mutants has been created. These classical methods are being

combined with a novel Cre-Lox “Recombination Mediated Cassette Exchange” gene targeting system that has been established by Adam Watson in the laboratory (Watson et al., 2008) (detailed in Chapter 2).

Chapter 2 Materials and Methods

2.1 General Bacterial techniques

2.1.1 *E. coli* media

Luria-Bertani (LB)

10 g/l Bacto tryptone
5 g/l Bacto yeast extract
5 g/l NaCl
1 g/l Glucose

adjust pH to 5.6

LA

LB with 12.5 g/l Difco agar

2.1.2 Transformation

DH5α competent cells were thawed on ice. Competent cells and transformed DNA was mixed and incubated on ice for 20 minutes. The mixture was incubated at 42°C for 45 seconds and immediately incubated on ice for 2 minutes. The mixture was spread onto LA plates supplemented with 100 μg/ml ampicillin. The plates were incubated at 37°C overnight.

2.1.3 DNA purification

Plasmid DNA miniprep, midiprep, maxiprep, gel extraction, and PCR purification were carried out by following the Qiagen kit protocols.

2.1.4 Site-directed mutagenesis

The purpose of site-directed mutagenesis is to introduce either point mutations or deletions. A forward primer containing the mutations was designed around 30 bps in length and a reverse primer was designed complementary to a forward primer. The reaction mixture contained 10 ng of DNA template, 5 µl of 10x Pfu DNA polymerase reaction buffer, 5 µl of 2 mM of dNTPs, 1.5 µl of 10 µM of forward primer and reverse primer, 1 µl of PfuUltra® High-Fidelity DNA Polymerase (STRATAGENE®), and the volume was adjusted with distilled water to have 50 µl in total. The reaction was heated to 95°C for 2 minutes. 20 cycles of 95°C for 1 minute, 55°C for 1 minute and 1 minute/kb of DNA template at 68°C was executed. Subsequently, the PCR reaction was heated at 68°C for another 10 minutes and kept at 4°C.

2.1.5 Polymerase chain reaction (PCR)

The principle of RCR is a tool to amplify a region of fragment by a forward primer and a reverse primer. Several different methods of PCR are available to be applied depending on the purpose of experiments.

<u>*E. coli* colony PCR</u>

A tip of *E.coli* colony was suspended into 10 µl of distilled water and heated at 99.9°C for 10 minutes. The PCR reaction contained 10 µl of the cell mixture, 10 µl of 10x Taq DNA polymerase buffer, 10 µl of 2 mM dNTPs, 1 µl of 100 µM each of forward primer and reverse primer, 1 µl of Taq DNA Precision DNA Polymerase (Thermo Scientific), and the volume was adjusted with distilled water to 100 µl in total. The reaction was heated to 95°C for 3 minutes. 30 cycles of 95°C for 30 seconds, 55°C for 30 seconds and 72°C for 1 minute were executed. Subsequently, the PCR reaction was heated at 72°C for another 10 minutes and kept at 4°C.

PCR for the molecular cloning

PCR reactions were set up in conditions of 3, 4, 5, or 6 µl of 25 mM $MgSO_4$ with 10 ng DNA template, 10 µl of 10x KOD polymerase buffer, 10 µl of 2 mM dNTPs, 1 µl of 100 µM each of forward and reverse primers, 1 µl KOD Hot start DNA polymerase (Novagen®) and the volume was adjusted with distilled water to 50 µl in total. The reaction was heated to 95°C for 3 minutes. 30 cycles of 95°C for 30 seconds, 55°C for 30 seconds and 72°C for 1 minute was executed. Subsequently, the PCR reaction was heated at 72°C for another 10 minutes and kept at 4°C. 5 µl of PCR product were analyzed on the agarose gel to determine most efficient Mg^{2+} concentration and this concentration was applied for further experiments.

Yeast colony PCR

Colony PCR is an easy and less time consuming way to amplify a PCR fragment of genomic DNA but it is difficult to amplify a fragment longer than 500 base pairs. Cells were streaked on YEA plates and incubated at 30°C before the day of proceeding colony PCR. A tip of fresh cells were mixed into 10 µl of distilled water, and heated at 95°C for 10 minutes. The PCR reaction mixture contained 10 µl of the cell mixture, 10 µl of 10x Taq DNA polymerase buffer, 10 µl of 2 mM dNTPs, 1 µl of 100 µmole/l each of forward primer and reverse primer, 1 µl of Taq Precision DNA Polymerase (Fisher Scientific) and the volume was adjusted with distilled water to 100 µl in total. The PCR program was performed similar as above.

2.2 General yeast techniques

2.2.1 *S. pombe* media

Yeast Extract (YE)

5 g/l	BACTO Yeast Extract
30 g/l	Glucose
200 mg/l	Adenine
100 mg/l	each of Argenine, Leucine, Uracil, Histadine

Yeast Extract Agar (YEA)

10 g BACTO Agar to 400 ml YE

YNB (Yeast Nitrogen base without Thiamine Media)

1.9 g/l	Formedium YNB
5 g/l	Ammonium sulphate
20 g/l	Glucose
2 M/l	Sodium hydroxide (NaOH)

Yeast Nitrogen base without Thiamine Agar (YNBA)

10 g BACTO Agar to 400 ml YNB

Extremely Low Nitrogen (ELN)

27.3 g/l	Formedium EMM
50 mg/l	Ammonium chloride
200 mg/l	Adenine
100 mg/l	each of Argenine, Leucine, Uracil, Histadine

add 10 g BACTO Agar to 400 ml volume of ELN

20x EMM2 salts

61.2 g/l	Potassium Hydrogen Phthalate
20 g/l	KCl
21.4 g/l	$MgCl_2 \cdot 6H_2O$
200 mg/l	Na_2SO_4
260 mg/l	$CaCl_2 \cdot 2H_2O$

10000x trace elements

5 g/l	H_3BO_3	
4 g/l	$MnSO_4$	
4 g/l	$Zn\ SO_4 \cdot 7H_2O$	
2 g/l	$FeCl_3 \cdot 6H_2O$	or 300 mg of $Fe_2(SO_4)_3$
1.5 g/l	Na_2MoO_4	
1 g/l	KI	
400 mg/l	$CuSO_4 \cdot 5H_2O$	
10 g/l	Citric Acid	

1000x Vitamins

1 g/l	Pantotenic acid
10 g/l	Nicotinic acid
10 g/l	Inositol
10 mg/l	Biotin

EMM2 (Edinburgh minimal medium)

50 ml/l	20x EMM2 salt
25 ml/l	20% NH_4Cl
25 ml/l	0.4 M Na_2HPO_4
12.5 ml/l	40% Glucose
1 ml/l	1000x Vitamin
100 µl/l	10000x Trace elements

EMM2 Agar

10 g BACTO Agar in 300 ml water, and 100 ml EMM2

2.2.2 *S. pombe* transformation

10 OD (1 OD= 2x 10^7 cells/ml) mid-logarithmically growing cells were used for a single transformation. Cells were harvested by spinning at 3,500 rpm for 5 minutes at RT and washed with 1x LiAc/TE (0.1 M LiAc, 10 mM Tris-HCl, 1 mM EDTA, pH 7.5). Cells were mixed with 2 µl 10 mg/ml carrier DNA (Sonicated Salmon Sperm DNA, STRATAGENE®) and PCR fragment or plasmid DNA and incubated at RT for 20 minutes. Then, 260 µl of 40% PEG-4000/LiAc-TE was added to the cell suspensions and the cell mixture was incubated at 30°C for an hour. 43 µl of Dimethyl sulfoxide (DMSO) was added and heat-shocked at 42°C for 5 minutes. Cells were washed in 1 ml distilled water. Finally, cells were resuspended in 200 µl distilled water and 100 µl of cells were plated on EMM plates supplemented with appropriate amino acids. The plates were incubated at 30°C for 4~5 days to allow colonies formation.

2.2.3 Crossing

Random spore analysis

A loop of fresh h+ and h- strains were mixed with 5 µl sterile water on an ELN plate. The plate was incubated at 25°C for 2~3 days. A loop of the crossed cells was inoculated in 100-fold diluted of Helicase (Helix Pomatia Juice) and incubated at room temperature (RT) rotating overnight. The spore number was counted by using a haemocytometer. The suspension was diluted to 10^4 spores/ml, and 50 µl, 100 µl and 150 µl of the diluted spores were plated onto YEA plates and incubated at an appropriate temperature until the spores germinate and give rise to colonies.

Tetrad analysis

Cells crossed for 2 days on ELN plates were streaked on a YEA plate and incubated at

30°C for 3 hours. The micromanipulator (SINGER INSTRUMENT MSM system) was used to dissect 4 spores from the same asci and they were incubated at an appropriate temperature until the spores germinate and give rise to colonies.

2.2.4 TCA (Trichloro Acetic Acid) protein extracts

5 ODs of mid-logarithmically growing cells were spun down at 3,000 rpm for 5 minutes. The cell pellets were resuspended in 200 µl of 20% TCA and transferred into 2 ml ribolyzer tube. An eppendorf tube cap of glass beads was added to the mixture and incubated on ice for 2 minutes. The cells were lysed 3 times at 6,500 rpm for 30 seconds by Fast Prep™ FP120 (Thermo savant) and incubated on ice for one minute between each ribolyzing step. 400 µl of 5% TCA was added into the ribolyzed mixture. A 1.5 ml greiner tube was put in a 15 ml falcon tube and the ribolyzer tube was punctured with a hole on the bottom and placed on the top of the 1.5 ml greiner tube. Cell suspension was spun at 4,000 rpm for 2 minutes at 4°C and the 1.5 ml greiner tubes were spun at 13,000 rpm for 10 minutes at 4°C. The cell pellets were resuspended in 200 µl of 1x sample buffer and boiled at 95°C for 5 minutes. The protein extract was used to be analyzed by western blot.

2.2.5 Extraction of genomic DNA

Spheroplast buffer (SP1)

1.2 M	Sorbitol
50 mM	Sodium citrate
50 mM	Sodium phosphate
40 mM	EDTA

adjust pH to 5.6 and filter sterilize

Cells at mid-logarithmical phase were grown overnight to late stationary phase. Cells

were spun down at 3,000 rpm for 5 minutes and the cell pellets were resuspended in 1 ml of 1 mg/ml Zymolyase 100T in SP1 and incubated at 37°C for 30 minutes. Cells were mixed with 10% SDS on a slide and check for spheroplast formation under a microscope. Cells were spun down at 3,000 rpm for 5 minutes. Cell pellets were resuspended in 450 µl of 5x TE (5 mM EDTA, 50 mM Tris-HCl pH 8) and 50 µl of 10% SDS, and cell mixture were transferred to eppendorf tubes at RT for 5 minutes. 150 µl of 5 M potassium acetates (pH 5.5) was added to the cell mixture and it was incubated on ice for 10 minutes. Proteins and genomic DNA were separated after centrifugation at 13,000 rpm for 10 minutes at 4°C. The supernatant containing soluble DNA was transferred to fresh tubes, and the equal amount of isopropanol was added to the supernatant. 70% of ethanol was used to clean DNA and the genomic DNA was resuspended in 250 µl of 1x TE.

2.3 General yeast genetic analysis experiments

2.3.1 Spot test

10^7 cells/ml of mid-logarithmically growing cells were taken and 10-fold serial dilutions were made from 10^7 cells/ml to 10^6, 10^5, 10^4, and 10^3 cell/ml. 6 µl of each dilution were spotted onto YEA plates and irradiated with an indicated dose of UV light or YEA plates containing the indicated concentrations of different genotoxic agents such as: HU, CPT, MMS, 4-nitroquinoline 1-oxide (4-NQO). The plates were incubated at appropriate temperature for 2~3 days.

2.3.2 Cell survival analysis after IR

Logarithmically growing cells were diluted serially from 10^7 to 10^6, 10^5, 10^4, and 10^3

cells/ml and irradiated with an indicated dose of IR. Cells were plated on YEA plates and incubated 3~5 days at appropriate temperature. The number of colony was counted using a colony counter.

2.3.3 *S. pombe* cell cycle synchronization in G2 phase

Synchronization by lactose gradient

in 50 ml falcon tubes

% lactose	volume of 30% lactose (ml)	volume of 7% lactose (ml)	Fraction no.
7	0	4	9
10	0.5	3.5	8
13	1	3	7
15	1.5	2.5	6
18.5	2	2	5
21	2.5	1.5	4
24	3	1	3
28	3.5	0.5	2
30	4	0	1

7% and 30% lactose solution were prepared and filter sterilized. 9 fractions of lactose gradients were prepared by mixing 7% and 30% lactose solutions following the table above. 4 ml of 30%, 28%, 24%...7% of lactose gradients were applied into a 50 ml falcon tube. 120 ODs of mid-logarithmically growing cells concentrated in 4 ml YE were applied on to top of the 7% of lactose gradient. The lactose gradients were centrifuged at 1,000 rpm for 8 minutes at RT. G2 cells were taken and checked under a microscope. G2 cells were washed with YE and resuspened in YE for further experiments.

Synchronization by *cdc25-22* blocking and releasing

cdc25-22 (a thermo-sensitive strain) was grown at 25°C (permissive temperature) to a titer of $3x10^6$ cells/ml and the culture was shifted to 36.5°C (restrictive temperature) for 3.5 hours to synchronize cells in the G2 phase of the cell cycle. Cells were released from the G2 phase by cooling down the culture rapidly in ice-cold water until 25°C.

2.3.4 Irradiation of cells by UV light

(A) irradiation on a PVDF membrane filter

2×10^7 cells were collected on a single PVDF membrane filter (0.45 μm, 47 mm diameter, MILLIPORE) to form a monolayer of cells. Cells were exposed to UV light and the PVDF membrane filters with the irradiated cells were transferred to culture tubes in order to recover the cells from the filters.

(B) irradiation on YEA plates

6 ODs of cells were spread evenly on YEA plates. The cells were irradiated with an indicated dose of UV light and recovered from YEA plates by suspending with YE.

(C) irradiation on the Hybond™-ECL™ nitrocellulose membrane

20 ODs of cells were spread evenly on a single Hybond™-ECL™ nitrocellulose membrane (Amersham Biosciences) on top of a square YEA plates. Cells were irradiated with UV light and the membranes were transferred to flasks with YE in order to recover the cells.

2.3.5 Calcofluor and 4',6-diamidino-2-phenylindole (DAPI) staining

Staining solution

50%	Glycerol
50%	PBS
1 µg/ml	DAPI
50 µg/ml	Calcofluor

Stored at 4°C in the dark.

Cells were spun at 3,000 rpm for 1 minute and 5 µl of concentrated cells were placed on a microscope slide. Cells were stained with 3 µl of staining solution. Calcofluor was used to stain the cell wall and septum and DAPI was used to stain nuclear DNA.

2.3.6 Live cell imaging

10 µl of concentrated cells were mounted onto a layer of 1% agarose formed on a glass slide. A cover slip was put on the cell suspension and the cells were observed under a fluorescence microscope.

2.3.7 Fluorescence Activated Cell Sorter (FACS) analysis

1 ml of mid-logarithmically growing cells were spun down and washed once with 500 µl of chilled STOP buffer (PBS+ 0.1% NaN_3) with 50 µl of 0.2 M EDTA. Ice-cold ethanol was added to cells to a final concentration of 70% and cells were stored at 4°C overnight. Cells were washed once and resuspended in 500 µl of 50 mM sodium citrate (pH 7.0). 50 µl of 10 mg/ml RNaseA was added to a final concentration of 1 mg/ml and the cells were incubated at 37°C for 2~3 hours. 20 µl of 1 mg/ml propidium iodide and 1 ml of BD FACSFlow™ were mixed with 200 µl of the cell mixture. The stained cell suspensions were applied to the FACSCalibur™ (Becton Dickinson).

2.4 Biochemical techniques performed in the project

2.4.1 Western blotting

10x Running buffer

0.25 M Tris base
1.92 M Glycine
1% SDS

1x Transfer buffer

25 mM Tris base
192 mM Glycine
20% methanol

The pH value was adjusted to 8.3.

10x PBS (phosphate-buffered saline)

80 g NaCl
2.0 gKCl
14.4 g Na_2HPO_4
2.4 gKH_2PO_4

adjusted pH to 7.4 using 1 N HCl

4x SDS sample buffer: 100 ml

25 ml 1 M Tris-base, pH 6.8
20 ml 100% glycerol
0.4 gBromphenol blue
8 g SDS

1x SDS sample buffer: 12 ml

3 ml 4x sample buffer
3 ml 1 M Tris, pH 8
600 µl β-mercaptoethanol
5.4 ml distilled water

2x SDS sample buffer: 40 ml

10 ml	1 M Tris-HCl pH 6.8
8 ml	100% glycerol
4 ml	β-mercaptoethanol
1 ml	1% Bromophenol blue
1 g	SDS
17 ml	distilled water

Extracts were separated by sodium dodecyl sulfate-polyacrylamide gel electrophresis (SDS-PAGE) using 1x Running buffer and transferred onto Hybond™-ECL™ nitrocellulose membrane (Amersham Biosciences). Transfer was usually carried out at 15 Volts overnight or 0.35 Amp for 90 minutes in cooled 1x transfer buffer. The membrane was blocked with 3% skimmed milk PBST (1x PBS with 0.1% Tween) at RT for an hour or overnight at 4°C. The immunoblots were probed with an appropriate primary antibody. The membrane was washed with PBST twice for 10 minutes at RT. The immunoblot was probed with a secondary antibody for an hour at RT. Then, the membrane was washed with PBST 3 times for 10 minutes at RT. The protein was detected with the Western Lightning® Chemiluminescence Reagent Plus (Perkin Elmer®) and exposed to High performance Chemiluminescence film (GE Healthcare).

Antibodies used in this study:

Antibody	Type	Dilution	Source or supplier
Anti-HA	Mouse monoclonal	1:2000	BabCo
Anti-cMyc	Mouse monoclonal	1:2000	Santa Cruz Biotechnology
Anti-GFP	Mouse monoclonal	1:4000	Roche Diagnostics
Anti-Cds1	Rabbit polyclonal	1:5000	Dr. Howard Lindsay
Anti-Cdc13	Mouse	1:500	Dr. J. Hayles
Anti-Cdc2	Rabbit polyclonal	1:2500	Santa Cruz Biotechnology
Anti-H2A (p-S129)	Rabbit polyclonal	1:2000	Abcam®

Antibody	Type	Dilution	Source or supplier
Anti-Mouse Immunoglobulins HRP	Rabbit polyclonal	1:2000	DakoCytomation
Anti-Rabbit Immunoglobulins HRP	Swine polyclonal	1:2000	DakoCytomation

2.4.2 Southern blotting

Depurination solution: 250mM HCl

Denaturation buffer

87.66 g/l NaCl
20 g/l NaOH

Stored at RT.

Neutralization buffer

87.66 g/l NaCl
60.5 g/l Trizma base

The pH 7.5 adjusting by 1 N HCl. Stored at RT.

Nucleic acid transfer buffer (20x SSC)

88.23 g/l Tris-sodium citrate
175.32 g/l NaCl

pH 7-8 and stored at RT.

Hybridization buffer

0.5 M NaCl
4% (W/V) Blocking reagent (supplied in Amersham™ AlkPhos Direct Labelling Reagents (GE Healthcare))

Stored at -20°C.

Primary wash buffer

2 M	Urea
0.2% (W/V)	SDS
50 mM	Na phosphate, pH 7.0
150 mM	NaCl
1 mM	$MgCl_2$
0.2% (W/V)	Blocking reagent (supplied in Amersham™ AlkPhos Direct Labelling Reagents (GE Healthcare))

It was kept at 4°C.

Secondary wash buffer (20x stock)

121 g/l	Tris base
112 g/l	NaCl

pH 10.0 and stored at 4°C.

Secondary wash buffer (working dilution)

1:20	Secondary wash buffer stock dilution
2 mM	Magnesium

This buffer should be prepared fresh

Purification of *S. pombe* genomic DNA for southern blotting

Genomic DNA was extracted as described in 2.2.5. For southern blotting, the precipitated DNA was resuspended in 500 µl of 5x TE and 10 µl of 10 mg/ml RNase, and incubated at 37°C for 20 minutes. 4 µl of 10% SDS and 20 µl of 10 mg/ml Proteinase K was added to the DNA solution and the DNA mixture was incubated at 55°C for an hour. 500 µl Phenol:Chloroform:Isoamyl alcohol 25:24:1 was mixed with the mixture and then spun down at 13,000 rpm for 5 minutes. The genomic DNA soluble in the upper phase was extracted for second time by 500 µl Chloroform: Isoamyl alcohol. 1/10 volume of 3 M NaAc and 2.5 volume of 90% ethanol were mixed with the

DNA mixture and incubated on ice for 10 minutes. DNA was spun down at 14,000 rpm at 4°C and the DNA pellet was washed with 70% ethanol. The genomic DNA was resuspended in 100 µl of 1x TE.

Digestion of genomic DNA by restriction enzyme

In this study, LacO repeats (~1.2 kb) was obtained from a pPS-8.4 vector (Robinett et al., 1996) digested with restriction enzymes of *BamH*I and *Sal*I.

Electrophoresis

The genomic DNA was separated on an agarose gel with 0.2 µg/ml ethidium bromide.

Southern blotting by vacuum transfer

The VacuGene XL Vacuum Blotting System (GE Healthcare) was used to transfer DNA from an agarose gel to a Hybond-N+ membrane (Amersham Biosciences). A piece of Whatman 3MM paper soaked in distilled water was placed on the tray of the VacuGene XL Vacuum Blotting unit and a wet Hybond-N+ membrane was placed on the top of a Whatman 3MM paper. The air bubbles were avoided in between each layer. Once the VacuGene XL Vacuum Blotting System was settled, the pump was stabilized with the vacuum pressure at 50 mbar. The agarose gel was incubated in Depurination solution, Denaturation buffer, and Neutralization buffer and 30 minutes each. 20x SSC was used for transferring for 3 hours. After blotting, the transferred DNA was fixed on the membrane by UV cross-linking twice.

Labeled probe DNA preparation

The DNA to be labeled (LacO repeat sequences) was diluted to a concentration of 10 ng/µl using the water supplied in the Amersham™ AlkPhos Direct Labelling Reagents

(GE Healthcare) and boiled for 5 minutes. Then, the DNA mixture was immediately incubated on ice for 5 minutes. 10 µl of reaction buffer was mixed with the cooled DNA mixture. Subsequently, 2 µl of labeling reagent and 10 µl of cross-linker solution were added to the mixture of DNA. The labeled probe DNA mixture was incubated at 37°C for 30 minutes and it can be used immediately or kept on ice for up to 2 hours. The labeled probe DNA could be stored for long time in 50% (V/V) glycerol at -20°C.

Hybridization

AlkPhos Direct hybridization buffer was pre-heated to 55°C and the hybridization oven (Jencons-PLS) was warmed up to 55°C. The amount of hybridization buffer should be equivalent to 0.17 ml/cm^2 of blotting membrane. The blotting membrane was placed in the hybridization tube with pre-heated hybridization buffer and hybridized for at least 15 minutes at 55°C in the hybridization oven (pre-hybridization step). 5-10 ng probe DNA (per ml of buffer) was added to the buffer used for the pre-hybridization step, and the blotting membrane was hybridized at 55°C overnight.

Post-hybridization stringency washes

The primary wash buffer was warmed up to 55°C and used for washing the blotting membrane at the 55°C hybridization oven for 10 minutes twice. Then, the blotting membrane was washed with secondary wash buffer for 5 minutes at RT twice.

Signal generation and detection

The membrane was treated with the CDP-Star™ detection reagent (GE Healthcare) and signal was detected by High performance Chemiluminescence film (GE Healthcare).

2.4.3 Cds1 kinase assay

Preparation of protein extract for Cds1 kinase assay

lysis buffer

50 mM	Tris-HCl, pH 7.5
250 mM	NaCl
5 mM	EDTA
0.1%	NP-40
40 mM	β-glycerophosphate
40 mM	sodium orthovanadate (Na_3VO_4)
50 mM	NaF
10 mg/ml	Aminoethylbenzene sulfonyl fluoride hydrochloride (AEBSF)
1 mM	Dithiothreitol (DTT)

1x complete protease inhibitor cocktail (Roche)

Supplemented with 40 mM β-glycerophosphate, 40 mM Na_3VO_4, 50 mM NaF, 10 mg/ml AEBSF, 1 mM DTT, and protease inhibitor cocktail (Roche) just before use

Mid-logarithmically growing cells were washed in ice-cold PBS, and then washed with lysis buffer. Cells were disrupted with glass beads in lysis buffer in a Fast Prep™ FP120 (Thermo savant) at 6500 rpm for 30 seconds 3 times with incubation on ice for 1 minute between each ribolyzing step. The protein extract was cleared by centrifugation at 3000 rpm at 4°C for 2 minutes. Protein extracts can be used immediately for immunoprecipitation or frozen in liquid nitrogen (LN) and stored at -80°C (Lindsay et al., 1998).

Immunoprecipitation of Cds1 and Immunoblotting

1x kinase buffer

10 mM	HEPES, pH 7.5
75 mM	KCl
5 mM	$MgCl_2$
0.5 mM	EDTA
1 mM	DTT (added just before use)

10 mg of total protein extract was diluted in 500 µl with lysis buffer and incubated at 4°C for 2 hours with an anti-Cds1 antibody at a dilution of 1:5000. Immunocomplexes were incubated with 40 µl Dynabeads® protein A sepharose beads rotating at 4°C for an hour. Pellets were washed 3 times with lysis buffer and 3 times in 1x kinase buffer. The samples were subjected to immunoblotting or the Cds1 kinase assay. Samples for western blot were boiled in 30 µl of 1x SDS sample buffer, and separated on 10% [200:1 acrylamide/bis acrylamide] SDS-polyacrylamide gels followed by immunoblotting with an anti-Cds1 antibody.

Cds1 kinase assay

Protein A pellets were washed in lysis buffer 3 times, kinase buffer 3 times, and the beads were resuspended in 10 µl of 1x kinase buffer. 20 µl of bead pellet was incubated with 11 µl of 2x kinase buffer, 0.5 µl of [γ-^{32}P]ATP, 0.2 µl of 10 mM Adenosine 5'-triphosphate (ATP) and 5 µl of 1 mg/ml myelin basic protein (MBP) at 30°C for 15 minutes. The reaction was stopped by adding 7 µl of 4× SDS sample buffer. Samples were separated on 15% SDS-polyacrylamide gel and exposed to film (Hyperfilm, Amersham).

2.4.4 Co-Immunoprecipitation (Co-IP)

TEG buffer (Extraction buffer)

50 mM	Tris-HCl, pH 7.5
10 mM	EDTA
10%	Glycerol
0.1%	NP-40
10 mM	N-ethylmaleimide (NEM)
1 mM	phenyl-methylsulfonyl fluoride, dissolved in ethanol (PMSF, SIGMA®)

1x complete protease inhibitor cocktail (Roche)

NEM, PMSF, and the protease inhibitor cocktail tablets were added just before use

$3x10^8$ of mid-logarithmically growing cells were washed in TEG buffer and suspended in 2 ml TEG buffer. The cell suspension was dropped into LN and the frozen clots (popcorn) were ground by the 6850 freezer mill (Caspari et al., 2000). The cell extract was immediately used for IP or stored at -80°C.

The cell extract was supplemented in 1 ml TEG buffer and cleared by centrifugation at 5,000 rpm for 5 minutes at 4°C. 1.3 ml of 10 mg/ml cell extract was cleared by centrifugation at 14,000 rpm for 10 minutes at 4°C. 50 µl of the supernatant containing soluble proteins was taken and mixed with 50 µl of 2x SDS sample buffer and boiled at 95°C for 5 minutes. It was used to analyze as an input control. 40 µl of Rabbit IgG-coated magnetic beads were washed in TEG buffer 3 times at 4°C for 5 minutes. The cell extract was incubated with the IgG beads at 4°C for 3 hours. The beads were washed 4 times with TEG buffer at 4°C for 3 minutes. The beads were placed on the magnet to remove the buffer, resuspended in 50 µl of 2x SDS sample buffer, and boiled at 95°C for 5 minutes (Furuya et al., 2004).

2.4.5 GST pull down

cDNA of the gene of interest was cloned into a pGEX-KG vector in frame with

glutathione-S-transferase (GST). The fusion protein was expressed in *E. coli* B834 (DE3) strain and purified using glutathione sepharose beads.

Transformation

1 µl of plasmid DNA was mixed with competent cells of *Escherichia coli* B834 (DE3) strain and incubated on ice for 20 minutes. The cells were heat-shocked at 42°C for 2 minutes, and then incubated on ice for 5 minutes. 1 ml LB was added to the cell suspension and incubated at 37°C for an hour. The cells were spun down at 13,000 rpm for 10 seconds, the supernatant was removed and the cell pellet was suspended in the remaining supernatant. The cells were spread onto LA plates containing with 100 µg/ml ampicillin and 34 µg/ml chloramphenicol and incubated at 37°C overnight.

Large-scale purification

A single *E. coli* colony was inoculated in 2 ml LB supplemented with 100 µg/ml ampicillin and 34 µg/ml chloramphenicol and incubated at 37°C overnight. 100 µl of this pre-culture was added into 50 ml LB supplemented with ampicillin and chloramphenicol and incubated overnight. 50 ml pre-culture was added in 500 ml LB supplemented with ampicillin and chloramphenicol and incubated at 37°C for 2 hours (OD_{600}: 0.5~0.7). The culture was supplemented with Isopropyl β-D-thiogalactoside (IPTG) to a final concentration of 5 mM and incubated at 30°C for 4 hours. The cells were harvested by centrifugation at 6,000 rpm for 5 minutes at 4°C. The pellets were resuspended in 10 ml chilled 1x PBS and transferred to a 50 ml falcon tube. To check induction, 100 µl cell suspensions were centrifuged at 6,000 rpm for 5 minutes at 4°C and the cell pellet was resuspended in 500 µl of 1x SDS sample buffer and boiled at 95°C for 5 minutes. It can be analyzed by western blot. The rest of the cell suspensions

were spun down at 4,000 rpm at 4°C for 10 minutes and the cell pellet was frozen in LN and stored at -80°C.

Purification of recombinant GST fusion proteins

NET-N buffer

0.5%	NP-40
20 mM	Tris-HCl, pH 8.0
100 mM	NaCl
1 mM	EDTA
1 mM	PMSF (added just before use)

1x complete protease inhibitor cocktail (Roche) (added just before use)

Washing buffer

1 mM	EDTA
500 mM	NaCl
100 mM	Tris-HCl, pH 8.0

The bacterial cell pellet stored at -80°C was resuspended in 20 ml of NET-N buffer and sonicated with a Ultrasonic Processor sonicator (Jencons scientific) 4 times at 40% for 15 seconds on ice. The cell lysate was centrifuged at 14,000 rpm at 4°C for 10 minutes to remove cell debris and insoluble proteins. The clean cell lysate was transferred to a 50 ml falcon tube and kept on ice. Gluthione sepharose™ 4B beads were spun down at 2,000 rpm for 1 minute and washed twice with 1 ml of NET-N buffer. The beads were resuspended in NET-N buffer supplemented with PMSF and protease inhibitor and 100 µl beads was added to the clean cell lysate. It was incubated at 4°C for 1.5 hours and subsequently washed under the following conditions: 3 times for 5 minutes at 4°C in NET-N buffer supplemented with PMSF and protease inhibitor, once for 5 minutes and twice for 10 minutes in washing buffer, and once for 5 minutes in 1x PBS. Each sample was suspended in 100 µl of 1x PBS and aliquots of 25 µl in eppendorf tubes were

frozen in LN and stored at -80°C.

Pull-down a protein from *S. pombe* that interacts with a GST-fusion protein

Lysis buffer

50 mM	Tris-HCl, pH 8.0
150 mM	NaCl
5 mM	EDTA
10%	Glycerol
0.1%	NP-40
1 mM	DTT (added just before use)
1 mM	PMSF (added just before use)

1x complete protease inhibitor (Roche) (added just before use)

20 OD mid-logarithmically growing yeast cells were washed in lysis buffer once and the cells were lysed in 200 µl lysis buffer by glass beads for 3 times for 30 seconds at 6,500 rpm. The cell extract was clarified by centrifugation at 14,000 rpm at 4°C for 10 minutes. 400 µl lysis buffer was added to the cell extract to a final protein concentration of 0.5 µg/µl. The cell extract was incubated with the purified recombinant GST-fusion protein with glutathione sepharose beads at 4°C for 1.5 hours. The beads were retrieved after washing 3 times in lysis buffer containing 0.1 mM PMSF and then resuspended in 40 µl 1 x sample buffer for western blotting.

2.4.6 Coomassie blue staining

Gel-fixing solution

50% (V/V)	ethanol
10% (V/V)	acetic acid

Gel-washing solution; Destaining solution

50% (V/V)	methanol
10% (V/V)	acetic acid

Staining solution

0.1% (W/V) Coomassie blue R250
20% (V/V) methanol
10% (V/V) acetic acid

After SDS-PAGE, the protein was fixed on the gel in gel-fixing solution for an hour. The gel was rinsed by gel-washing solution and stained in the staining solution for 1~2 hours at RT. Then, the gel was destained in destaining solution overnight. Destaining was stopped as soon as the background staining of the gel became low enough to see the protein bands.

2.5 Integration of mutations in yeast by Cre-Lox recombinase-mediated cassette exchange (RMCE)

To facilitate the rapid creation of multiple mutations in the genomic copy of the *rad4* gene, we took advantage of the novel Cre-Lox recombinase-mediated cassette exchange (RMCE) gene targeting system using LoxP/LoxM3 whereby the entire gene sequence can be replaced (Watson et al., 2008). This system has been established by Adam T. Watson in the laboratory.

The RMCE system can be summarized as below (Fig. 2-1). Because *rad4*$^+$ is an essential gene, the *rad4* open reading frame can not be deleted, thus, *the rad4*$^+$ base-strain (435) was constructed in which *rad4* gene was flanked by the LoxP sequences and the *ura4*$^+$-LoxM3 sequence. A *rad4*$^+$ base-strain was constructed where the LoxP site was 158 bp upstream of the *rad4* start codon and the *ura4*$^+$-LoxM3 sequence was 26 bp downstream of the *rad4* stop codon (constructed by Dr. Valerie Garcia). A pAW8 plasmid expresses the Cre recombinase under an *nmt41* promoter and contains a LEU2

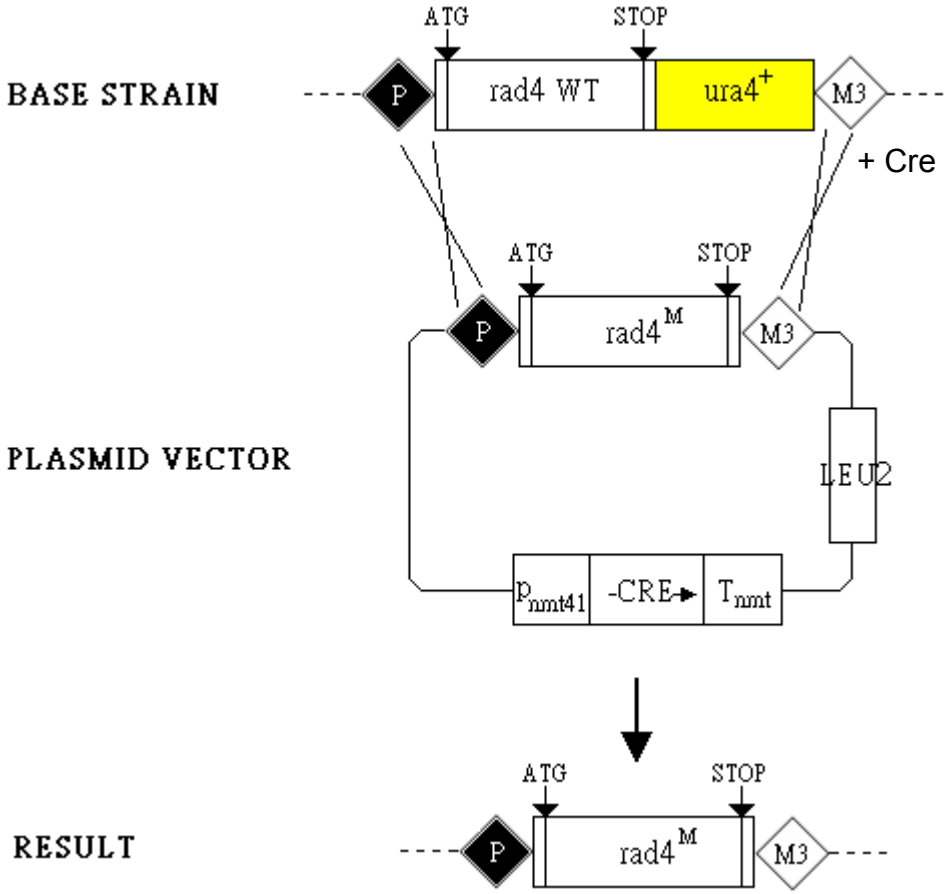

Figure 2-1- Schematic representation of the Cre-Lox recombinase-mediated cassette exchange (RMCE) system
In the *rad4* base strain (435), the LoxP is integrated upstream of *rad4* open reading frame and the ura4-LoxM3 are integrated downstream of *rad4* gene. A plasmid (pSJ25) expresses the Cre recombinase under an *nmt41* promoter and contains a *LEU2* marker, and single or multiple mutations were introduced within the *rad4* gene by standard site-directed mutagenesis PCR. When Cre recombinase is expressed, homologous recombination occurs between the two LoxP sites and the two LoxM3 sites between the base strain and the Cre-expressing plasmid. This results in the replacement of wild-type *rad4* by a mutated version (adapted from Watson, Garcia et al. 2008)

marker. The *rad4* sequence was cloned into pAW8 multiple cloning sites (MCS) flanked by LoxP and LoxM3 for subsequent cassette exchange. The *rad4*$^{+}$ gene was amplified from genomic DNA prepared from 501 cells using a 5' primer (P17) carrying a *Sac*I restriction site and a 3' primer (P18) carrying a *Spe*I restriction site (P17 and P18 primers are described in Watson, Garcia et al. 2008). The product was restricted with *Sac*I and *Spe*I and cloned into *Sac*I/*Spe*I restricted pAW8 and the construct was named pSJ25. pSJ25 was used to introduce single or multiple mutations within the *rad4* gene by standard site-directed mutagenesis PCR. The primers used for introducing the mutations are listed in the appendix A. The resulting plasmids containing mutated *rad4* genes were transformed in *S. pombe* cells of the wild-type *rad4*$^{+}$ base strain (435). When Cre recombinase was expressed under the control of the thiamine-repressible *nmt41* promoter, homologous recombination occurred between the two LoxP sites and the two LoxM3 sites of the plasmid and the *rad4* base strain. LoxP is a 34 bp element which consists of two 13 bp inverted repeats separated by an asymmetric 8 bp spacer. The sequence of LoxM3 differs from the LoxP in the spacer region at several nucleotides (Watson et al., 2008) which prevents recombination between them. Expression of the Cre results in the replacement of the wild-type *rad4* genomic sequence by the mutated *rad4* sequence from the plasmid. The transformants were selected on EMM plates supplemented with adenine plus 15μM thiamine (EMM+ade+thi). The *nmt41* promoter has low basal activity in the presence of thiamine and appears to give expression of Cre recombinase for cassette exchange sufficiently (Watson et al., 2008). After incubation at 30°C for 5~6 days, the transformants were re-streaked to fresh EMM+ade+thi plates. Subsequently, transformants were cultured in YE medium at 30°C for 3 days to saturation in order to select for the cells having lost the plasmid. Cell density was determined and 100 μl of 10^4, 10^5 and 10^6 cells/ml dilutions were plated on YEA plates supplemented with 1 mg/ml of 5-Fluoroorotic Acid

(5-FOA) to select for *ura*$^{-}$ cells (5-FOA resistant cells). Plates were incubated at 30°C until colonies were formed. 5-FOA resistant colonies were streaked on fresh 5-FOA plates to give rise to single colony and the replacement of wild-type *rad4*$^{+}$ by the mutated one was verified by sequencing of the *rad4* locus.

All the *S. pombe rad4* mutant strains described in this thesis were created using the RMCE system. These mutants were further characterized using genetic or biochemical assays.

2.6 Hydroxylamine random mutagenesis

The hydroxylamine hydrochloride (H_3NO-HCl, Fluka) was dissolved in 4.55 ml ice-cold sterile MQ water and 450 µl of 5 M NaOH, and pH value was adjusted to 6.7. The solution was kept on ice until use. 10 µg plasmid pSJ25 was incubated with 500 µl of hydroxylamine solution in an eppendorf tube sealed with parafilm at 37°C for 20 hours. DNA was recovered from the hydroxylamine mixture using the Qiaquick PCR purification kit (Qiagen) and was used to transform in *S. pombe* cells using the RMCE system (detailed in 2.5).

Chapter 3 Role of Rad4^{TopBP1} phosphorylation by Cdc2/CDK1

3.1 Functional characterization of Cdc2 phosphorylation sites

3.1.1 Introduction

In *S. pombe*, a unique cyclin-dependent kinase Cdc2/CDK1 drives the cell cycle progression, and is required for the initiation of DNA replication and progression into and through mitosis (Durkacz et al., 1986). During DNA replication, several DNA replication proteins, such as Drc1, are phosphorylated in a CDK-dependent manner. spDrc1/scSld2 phosphorylation by Cdc2 at the G1-S transition promotes its interaction with spRad4 and this is essential for DNA replication (Noguchi et al., 2002). This regulation appears to be conserved in budding yeast (Masumoto et al., 2002; Tak et al., 2006). Cdc2 phosphorylates spCdc18 which causes its inactivation and its degradation at the G1/S phase transition to ensure replication once per cell cycle in *S. pombe* (see Chapter1 1.5.2) (Jallepalli et al., 1997). Other proteins involved in DNA replication, such as Cdt1, ORC proteins, and Mcm proteins, are also regulated by CDK-dependent phosphorylation (Ishimi et al., 2000; Liu et al., 2004; Nguyen et al., 2001; Vas et al., 2001).

In addition to its function in regulating initiation of DNA replication, CDK activity is also required for checkpoint signaling and repair pathways during DSBs processing. Cdc2 activity has been shown to influence DNA repair of radiation-induced DSBs by homologous recombination during the G2 phase of the cell cycle (Caspari et al., 2002). Firstly, Caspari, Murray et al. 2002 have demonstrated that CDK activity regulates a

processing pathway required for Rad51 focal assembly after IR (IRIF) and that this function is redundant with Rad50 at an early stage of HR, suggesting a role in DSBs resection. Secondly, in response to IR, phosphorylation of Crb2 on T215 by CDK regulates Rqh1 helicase activity required to form hemicatenane by dissolving two HJs. This structure is subsequently resolved by Top3 at a late stage in HR repair (Caspari et al., 2002). In *S. cerevisiae*, Cdc28 has subsequently been shown to be required for efficient 5'→3' resection of DSBs to generate 3' ssDNA, which is necessary for RPA recruitment (Ira et al., 2004). Therefore, CDK activity influences indirectly the initiation of HR through the recruitment of recombination protein Rad51 and Rad52 and the activation of Mec1-dependent DNA damage checkpoints, because ssDNA-RPA is known to be an intermediate recognized by the checkpoint machinery (Barlow and Rothstein, 2009; Ira et al., 2004; Zou and Elledge, 2003). hCtlP/spCtp1/scSae2 is required for ssDNA-RPA formation by resection of DSBs ends and this function is conserved in mammalian cells, budding and fission yeast (Huertas et al., 2008; Huertas and Jackson, 2009; Limbo et al., 2007). CtIP function is regulated by CDK1/Cdc28-dependent phosphorylation of hCtlP/scSae2 in human cells and *S. cerevisiae* (Huertas et al., 2008; Huertas and Jackson, 2009). Although *S. pombe* Ctp1 lacks obvious *cdc2* consensus phosphorylation sites, transcription of $ctp1^{+}$ is cell-cycle regulated and its expression coincides with the onset of DNA replication (Limbo et al., 2007). Therefore, higher eukaryotes and fission yeast have involved in different mechanisms to activate hCtlP/spCtp1 activity in late S/G2 phase when DSBs resection is required for repair by HR.

CDK activity was shown to be required for the initiation and maintenance of checkpoints induced by co-localization of Ddc2-Mec1 and 9-1-1 complex to LacO array in the chromatin (Bonilla et al., 2008). *sc*Rad9 phosphorylation by CDK1/Cdc28 is

required for downstream sensor proteins localization because co-localization of Ddc1 and Ddc2 to chromatin could not elicit Rad53 phosphorylation in a *rad9-18A* mutant (when 18 potential CDK consensus sites are mutated to alanine) (Bonilla et al., 2008). Unlike wild-type cells, *rad9-18A* cells are not phosphorylated in the cell cycle-dependent manner (Bonilla et al., 2008).

Studies carried out by Dr. Valerie Garcia in this laboratory indicate that Rad4 is phosphorylated after treatment with HU (a replication inhibitor) or after treatment with DNA damaging agents (gamma-rays). These phosphorylation events are both dependent upon Rad3, since the Rad4 band shift is completely abolished when the *rad3* locus is deleted (Valerie Garcia, personal communication). Unexpectedly, Rad4 does not contain consensus sites for Rad3 or Tel1-dependent phosphorylation (SQ/TQ sites), but does contain seven consensus sequences for Cdc2/CDK1-dependent phosphorylation (TP/SP sites) although only one (T54) is matching the canonical TP/SPK consensus. In addition, it has been shown that IR-induced Rad4 phosphorylation is substantially reduced when Cdc2/CDK1 activity is ablated *in vivo* by using an analogue-sensitive mutant version of Cdc2/CDK1 (*cdc2as*) (Valerie Garcia, personal communication). *cdc2as* mutation modifies the ATP-binding pocket and *cdc2-as* kinase activity can be inhibited by accommodating a bulky ATP analogue (Dischinger et al., 2008). These data suggest that Rad4 phosphorylation occurs in a Cdc2 kinase-dependent manner. Furthermore, it has been shown that Rad4 interacts with Cdc13, the regulatory subunit (cyclin B) of Cdc2/CDK1, using Tandem affinity purification (TAP) and protein identification by mass spectroscopy. This association occurs when the cells are challenged by HU. The Cdc13-Rad4 association has not been tested in response to IR. Also, only small amounts of Cdc2 interacted with Rad4 by immunoprecipitation *in vivo* and the weak interaction is only detected in response to HU, but not in exponential growing cells (Valerie Garcia,

personal communication). Interestingly, this raises the question whether Rad4 phosphorylation by Cdc2 *in vivo* occurs on the identified Cdc2 consensus sites. If this is the case, what is the function of Rad4 phosphorylation by Cdc2? The recombinant C-terminal moiety of Rad4 (BRCT repeats 3 and 4 and C-terminal tail), when expressed and purified from *E. coli*, is highly phosphorylated by Cdc2/CDK1 *in vitro*. A fragment corresponding to the two N-terminal BRCT repeats is not phosphorylated. *In vitro* Rad4 phosphorylation by Cdc2 was reduced when the C-terminal consensus sites were mutated (Valerie Garcia, personal communication). The Rad4 C-terminus contains five consensus sites (TP/SP) for Cdc2-dependent phosphorylation (T528, S532, T589, S592, and S483), of which 4 (T528, S532, T589, and S592) were found to be phosphorylated by mass-spectrometry. S483 was not phosphorylated in this assay (Fig. 3-1A). The four phosphorylated Cdc2 consensus sites present in Rad4 are distributed in two clusters containing two Cdc2 consensus sites each (T528/S532 and T589/S592). Additionally, 3 amino acids (S556, S558, and S641) not following the Cdc2/CDK1 consensus phosphorylation sequences were phosphorylated *in vitro* by Cdc2 as identified by mass-spectrometry (Fig. 3-1A). Whether T54 and T278 (the Cdc2 consensus sites not present in the C-terminal recombinant fragment used for this assay) are phosphorylated *in vitro* remained to be analyzed. In this part of the project I intended to pursue this work by investigating the function of Rad4 phosphorylation by Cdc2/CDK1 *in vivo*. We hypothesize that the multiple functions of Rad4 in DNA replication initiation, checkpoint and repair could be regulated by Cdc2/CDK1 phosphorylation.

3.1.2 Cdc2 phosphorylation sites in Rad4 are not required for resistance to DNA damage and HU

In order to study the function of Rad4 phosphorylation by Cdc2/CDK1 *in vivo*, codons encoding serine or threonine residue of the *cdc2* consensus phosphorylation sites within

Figure 3-1- Functional analysis of the Rad4 phosphorylation sites by Cdc2 (A) Schematic representation of the Rad4 protein. Cdc2 consensus phosphorylation sites are highlighted in red. 3 amino acids (S556, S558, and S641) not following the Cdc2 consensus phosphorylation sequences are highlighted in green and blue, respectively. T528, S532, S556, S558, T589, S592, and S641 are located at C-terminal tail of Rad4 and were identified to be phosphorylated *in vitro* by Cdc2 by mass spectrometry. Whether T54 and T278 are phosphorylated remained to be analyzed, referring to ND (ND: non-determined). (B) Schematic representation of the Rad4 mutant strains created. Cdc2 consensus phosphorylation sites are highlighted in red. S641 and SNSK are highlighted in blue and green, respectively. Different combination of the Cdc2 consensus sites mutated in Rad4 are denoted with an asterisk. (C) Spot tests of single or combinations of point mutations in several Cdc2 consensus phosphorylation sites of Rad4. 10-fold serial dilutions of $1x10^7$cells/ml were spotted onto YEA plates and exposed to UV or to different genotoxic agents with the indicated doses. The plates were incubated at 30°C for 3 days. “501” and “435” are *rad4*$^+$ and *rad4*$^+$ (RMCE) controls, respectively.

(A)

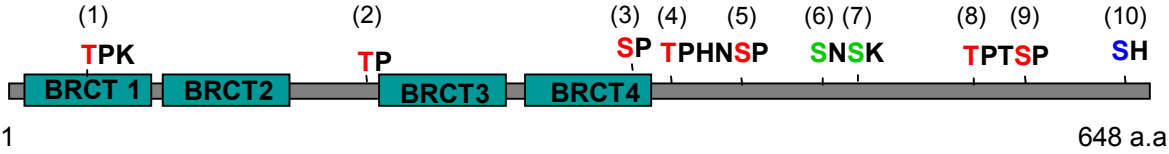

	(1)	(2)	(3)	(4)	(5)	(6)	(7)	(8)	(9)	(10)
residue	T54	T278	S483	T528	S532	S556	S558	T589	S592	S641
CDK consensus	Yes	Yes	Yes	Yes	Yes	No	No	Yes	Yes	No
mass-spectrometry	ND	ND	No	Yes	Yes	Yes	Yes	Yes	Yes	Yes

(B)

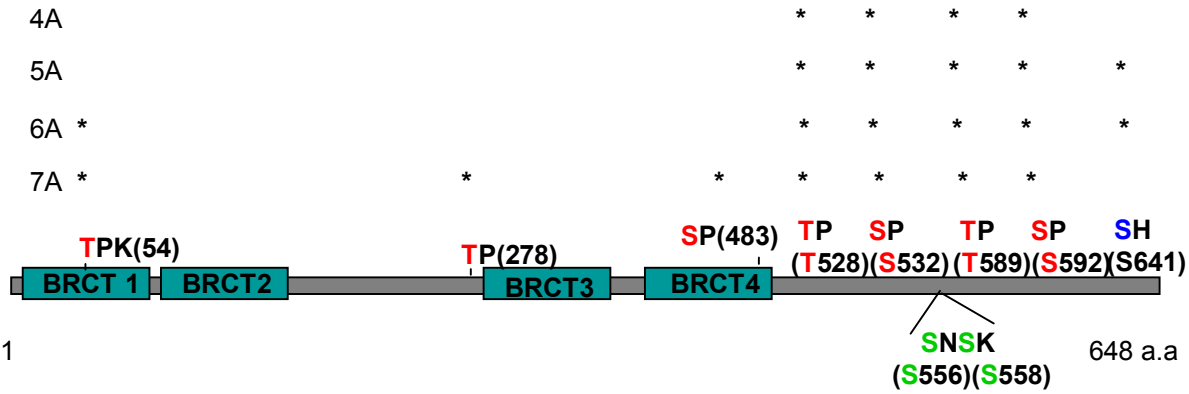

(C)

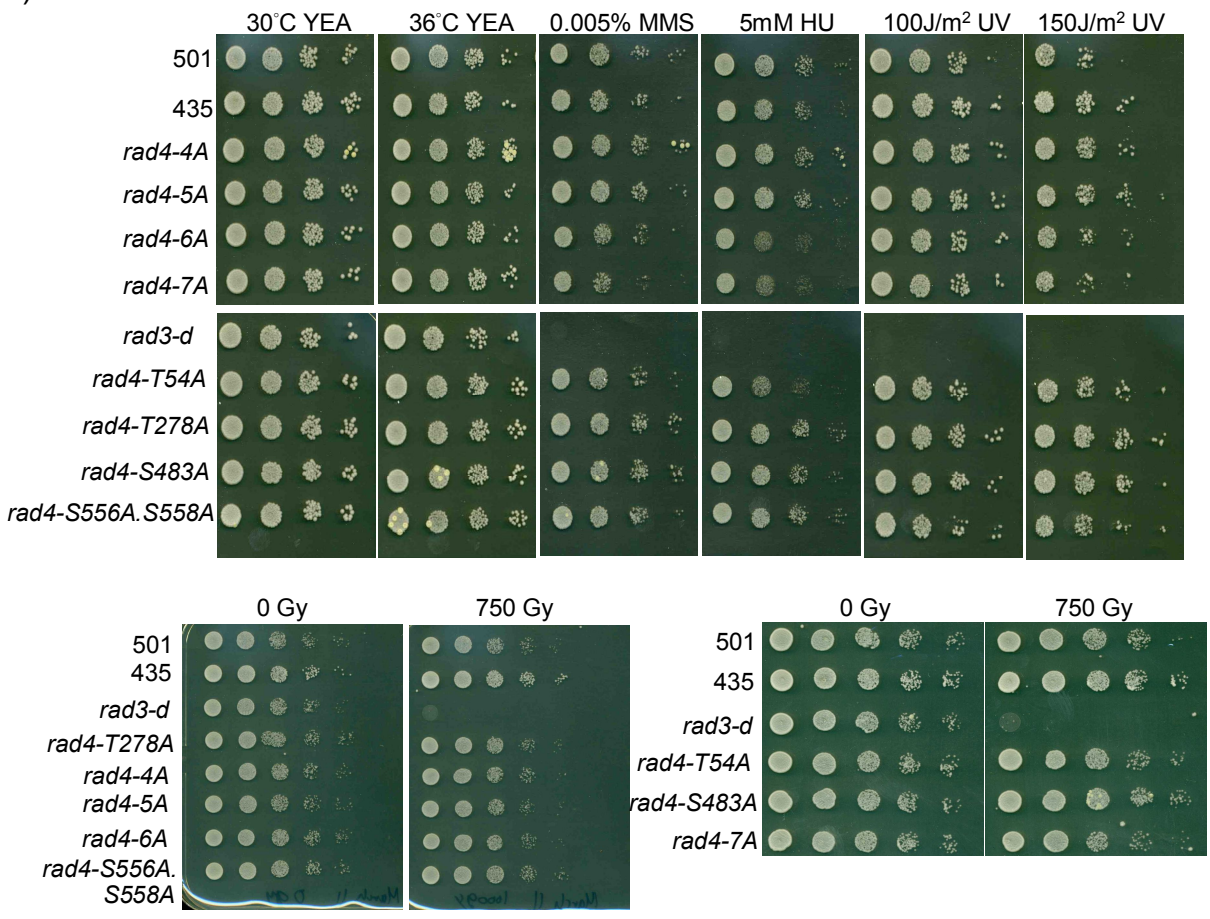

the *rad4* gene were mutated to encode alanine and integrated into the genome using the RMCE system developed in the laboratory (described in detail in Chapter 2). A plasmid (pAW8-loxP-*rad4*$^{+}$-loxM, pSJ25) carrying wild-type *rad4*$^{+}$ gene flanked by a loxP and loxM3 sequences was used to introduce single or various combination of multiple mutations in Cdc2 consensus phosphorylation sites by mutagenesis PCR. The resulting plasmids containing mutated *rad4* genes were transformed in a base strain, named as "435", which contains the Rad4 open reading frame flanked by loxP and loxM3 sequences. The plasmids express the Cre recombinase gene under an *nmt41* promoter. When Cre endonuclease is expressed, homologous recombination occurs between two loxP sites and between two loxM3 sites of a plasmid and the genomic endogenous *rad4*. This results in the replacement of the wild-type *rad4* genomic sequence by the mutated *rad4* sequence from the plasmid (see Fig. 2-1). The resulting mutants are expressed from the endogenous *rad4* promoter.

The function of Rad4 phosphorylation by Cdc2 was investigated by spot test. Single mutation of Cdc2 consensus phosphorylation sites (*rad4-T54A*, *rad4-T278A*, *rad4-S483A)* or different combination, (*rad4-4A*, *rad4-5A*, *rad4-6A*, or *rad4-7A*, carrying different combination of mutations are described as Fig. 3-1B), and the non-consensus mutant *rad4-S556A.S558A* did not show significant sensitivity to UV irradiation, MMS, HU, or IR (Fig. 3-1C). The growth rates in the mutants were not effected at 36°C (Fig. 3-1C). *rad4-T54A*, *rad4-6A*, and *rad4-7A* (Fig. 3-1C) are slightly sensitive to 5mM HU, and show a similar level of sensitivity, suggesting that *rad4-6A* and *rad4-7A* sensitivity is due to T54A, which is located in first BRCT domain (Fig. 3-1B). T54A mutation confers a mild checkpoint defect. T54 has not been shown to be phosphorylated *in vitro* (Valerie Garcia, personal communication).

A glutamate (E) point mutation can mimic constitutive phosphorylation on serine or threonine residues. Four of the *rad4* Cdc2 consensus phosphorylation sites were mutated to glutamate (E) using the RMCE system: *rad4-T528E.S532E* (*rad4-2E*), *rad4-T528E.S532E.T589E* (*rad4-3E*), and *rad4-T528E.S532E.T589E.S592E* (*rad4-4E*) (Fig. 3-2A). The sensitivity to DNA damage and HU was investigated by spot test. None of these "E mutants" show sensitivity to DNA damaging agents or HU (Fig. 3-2B), suggesting that constitutive Cdc2-dependent phosphorylation of Rad4 does not affect Rad4 function in resistance to DNA damage.

3.1.3 Rad4 Cdc2 consensus phosphorylation sites do not play a role in the control of re-replication

scCdc6 phosphorylation by S-CDK activity triggers its degradation by the proteosome at the G1/S boundary (Bell and Dutta, 2002). Similarly in *S. pombe*, Cdc18, a homologue of Cdc6, is phosphorylated by Cdc2 at the G1/S transition and this phosphorylation causes its inactivation and degradation in order to limit the initiation of replication of a single origin to once in a single cell cycle (Bell and Dutta, 2002). However, a re-replication phenotype is not detectable in cells expressing Cdc18 with five mutations in Cdc2 phosphorylation sites ($Cdc18^{CDK}$) when expressed at low level (Gopalakrishnan et al., 2001). Therefore, although inactivation of Cdc18 by Cdc2 is important in *S. pombe*, it is not the only mechanism in limiting the initiation of replication. A redundant mechanism preventing re-initiation of replication was discovered in fission yeast: Overexpression of Cdt1 in a strain where $Cdc18^{CDK}$ is expressed under the control of the $cdc18^{+}$ promoter induces re-replication, but overexpression of Cdt1 alone does not induce re-replication. This indicates that Cdt1 works synergistically with Cdc18 in order to restrict DNA synthesis to once per cell cycle; high levels of $Cdt1^{S382A}$ expression with $Cdc18^{CDK}$ expressed under the control of

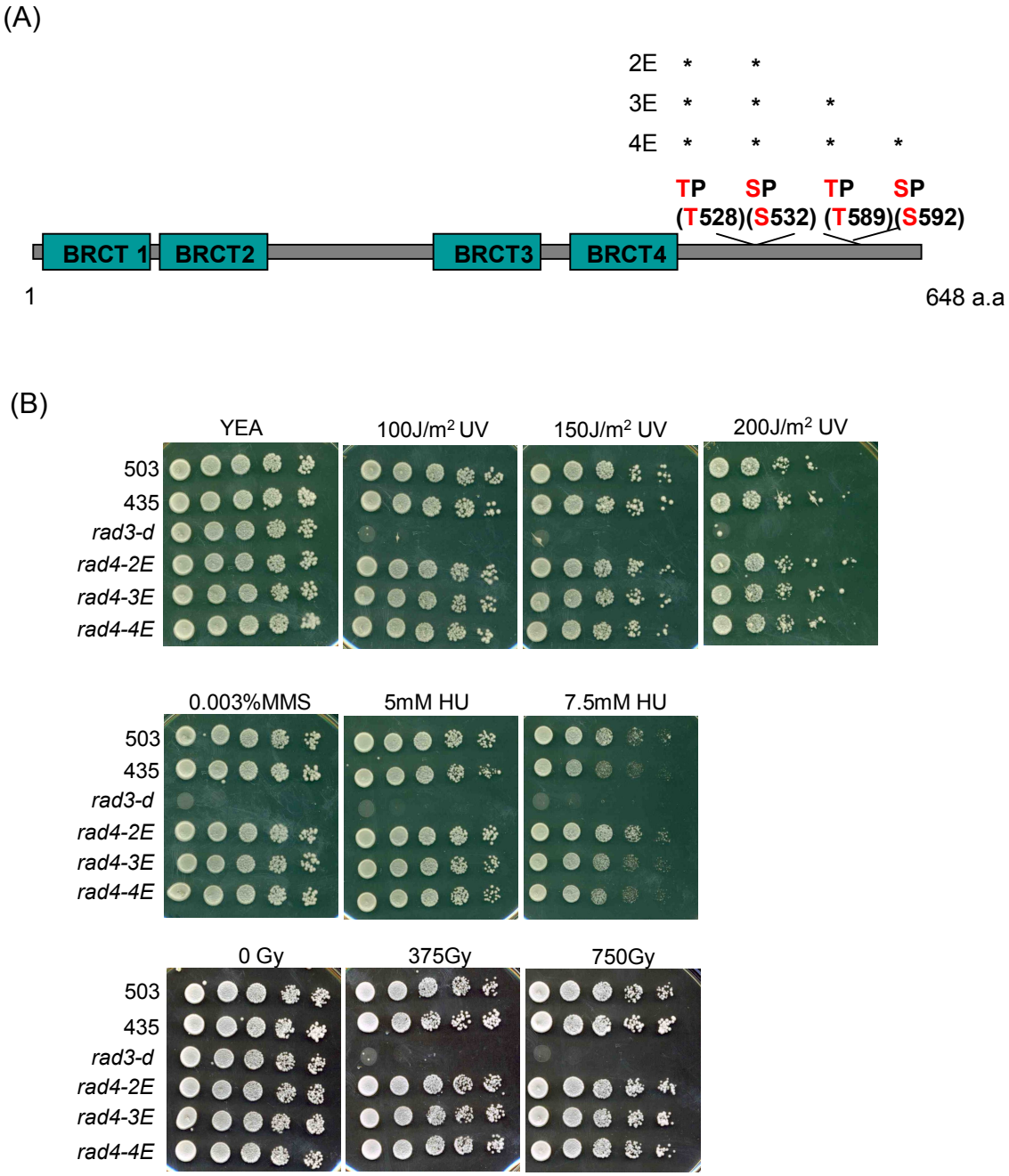

Figure 3-2- Analysis of the Rad4 Cdc2 phosphorylation consensus sites mutated to Glutamic acid
(A) Schematic representation of Rad4 protein. Cdc2 consensus phosphorylation sites mutated to glutamate (E) are highlighted in red. (B) Spot tests of the corresponding mutant strains. 10-fold serial dilutions of $1x10^7$cells/ml were spotted onto YEA plates and exposed to UV or to different genotoxic agents with the indicated doses. The plates were incubated at 30˚C for 3 days. “503” and “435” are *rad4*$^+$ and *rad4*$^+$ (RMCE) Controls, respectively.

the *cdc18*$^{+}$ promoter further enhanced re-replication compared to expression of wild-type Cdt1 under the same conditions (S382 being a potential CDK phosphorylation site) (Gopalakrishnan et al., 2001). Another replication protein spOrp2, a member of the origin recognition complex (ORC), associates with Cdc2 and its phosphorylation is regulated by Cdc2. A mutant containing four mutations in *cdc2* consensus phosphorylation sites (*orp2-4A*) is viable and showed no defect in DNA replication initiation (Vas et al., 2001). However, *orp2-4A* expressed from its endogenous promoter enhanced re-replication induced by overexpression of *cdc18** (*cdc18**: four mutations at Cdc2 phosphorylation sites) (Vas et al., 2001).

Despite the fact that Rad4 interacts with Cdc13/Cdc2 and that Rad4 is phosphorylated by Cdc2 *in vitro* and *in vivo*, *rad4* strains mutated for Cdc2 consensus phosphorylation sites did not show a strong sensitivity to DNA damaging agents or HU. We next investigated whether Rad4 phosphorylation by Cdc2 plays a role in the control of replication initiation, particularly in preventing replication origins firing more than once per cell cycle. The Cdc2 phosphorylation site mutant *rad4-7A* or a wild type *rad4*$^{+}$ strain were crossed to a strain with a stable integrated copy of *cdc18*$^{+}$ under a control of a thiamine-repressible *nmt1* promoter (JLP511, a kind gift of Janet Leatherwood) and were sporulated and dissected. Each individual yeast colony derived from a dissected tetrad was analyzed by PCR (to identify *rad4* mutant) or cell morphology (to identify cells where Cdc18 is under the control of a thiamine-repressible *nmt1* promoter, these cells are elongated even in the presence of thiamine). Therefore, the four strains of interest (wild type, *rad4-7A*, *nmt1-cdc18*$^{+}$, and *rad4-7A nmt1-cdc18*$^{+}$ strains) were derived from a single tetrad.

The experiments needed to be performed within a few days after tetrad dissection

because some level of re-replication is known to occur in a *orp2-4A nmt1-cdc18*$^{+}$ double mutant in the presence of thiamine, due to the leakiness of the *nmt* promoter (Janet Leatherwood, personal communication). In order to determine if *rad4-7A* enhance the re-replication phenotype of *cdc18*$^{+}$ overexpression, cell cycle progression was followed in wild type, *rad4-7A*, *nmt1-cdc18*$^{+}$, and *rad4-7A nmt1-cdc18*$^{+}$ strains, derived from the same tetrad, when *cdc18*$^{+}$ expression was maximal (without thiamine) or partially induced (0.05 μM thiamine). The DNA content was analyzed by fluorescence-activated cell sorter analysis (FACS) immediately after release into media without thiamine (or 0.05 μM thiamine) and 11, 12, 13, 14, and 18 hours after induction. The *rad4-7A* strain displays a cell cycle progression similar to wild-type cells (Fig. 3-3), suggesting the seven putative Cdc2 phosphorylation sites are not required for unperturbed replication; the strain overexpressing Cdc18 shows a re-replication phenotype under both conditions (full or partial induction). However, overexpressing Cdc18 in a *rad4-7A* background does not enhance the re-replication defect (Fig. 3-3).

Since *rad4-7A* is slightly sensitive to HU compared to control cells, the same experiment was performed in the presence of HU in the condition of partial induction (0.05 μM thiamine) in order to determine whether this sensitivity could be due to an intra-S phase checkpoint defect causing a defect in the control of origins firing. The cell culture was split in two after 14 hours of partial induction, and 10mM HU was added to one half (Fig. 3-4A). The DNA content was analyzed by FACS at the onset of induction (T_0), and 12, 14, 16, 18, and 20 hours after partial induction. Both wild-type cells and *rad4-7A* have a very similar FACS profile with or without HU (Fig. 3-4B). The *nmt1-cdc18*$^{+}$ strain and *rad4-7A nmt1-cdc18*$^{+}$ strain showed again a similar re-replication phenotype in the presence of HU (Fig. 3-4B). These results indicate that Rad4 phosphorylation by Cdc2 does not play a significant role in the control of re-replication.

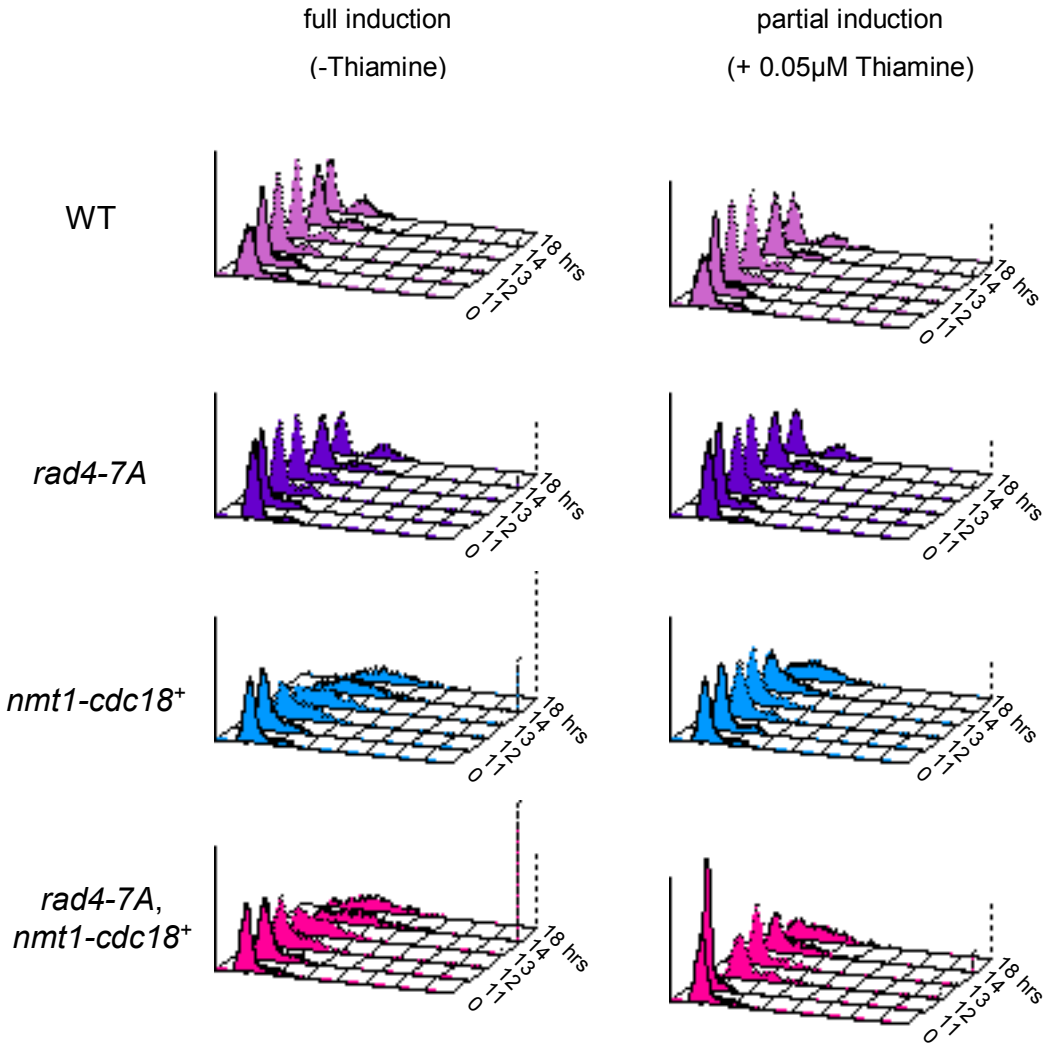

Figure 3-3- Role of Rad4 phosphorylation by Cdc2 function in the control of re-replication

Cell cycle progression of wild-type, *rad4-7A, nmt1-cdc18*$^{+}$, and *rad4-7A nmt1-cdc18*$^{+}$ was followed by FACS when *cdc18*$^{+}$ expression is maximal (full induction) in the absence of thiamine or partial (partial induction) in the presence of 0.05 μM thiamine.

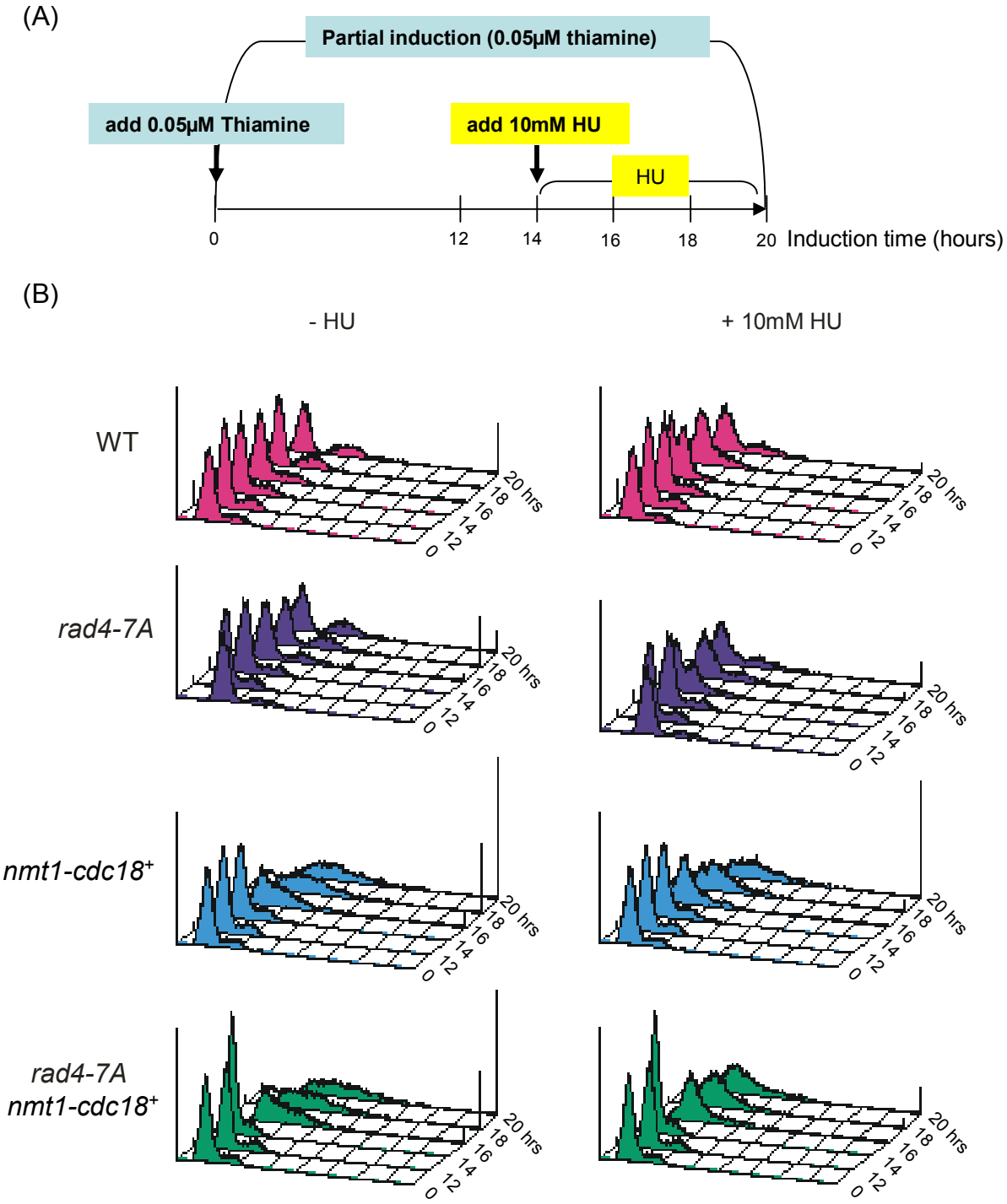

Figure 3-4- Role of Rad4 phosphorylation by Cdc2 in the control of re-replication in the presence of HU
(A) Schematic representation of experimental setup. *nmt41* was partially induced for 20 hours. The cell culture were split into two after 14 hours of partial induction (0.05 μM thiamine), and 10mM HU was added to one half.
(B) Cell cycle progression of wild-type, *rad4-7A, nmt1-cdc18*$^{+}$, and *rad4-7A nmt1-cdc18*$^{+}$ was followed by FACS when *cdc18*$^{+}$ overexpression is partially induced with or without HU.

3.1.4 Rad4 phosphorylation is dependent on the Cdc2 consensus site

The Rad4 bandshift induced by HU and IR is completely abolished in a *rad3-d* background. The IR-induced Rad4 bandshift is reduced in a *cdc2* analog sensitive mutant in the presence of ATP analogue (see Fig. 3-5A) (Valerie Garcia, personal communication). To determine whether the Rad4 Cdc2 consensus sites are phosphorylated in response to DNA damage, antibodies recognizing phosphorylated S528, S532, S589, and S592 were raised in our laboratory. Affinity purified antibody recognized both unphosphorylated and phosphorylated Rad4 peptides with a strong preference for the phosphopeptides. However, affinity purified antibody in combination with the unphosphorylated peptide (in order to titrate the non-phospho specific antibody) specifically recognize peptides phosphorylated on threonine 528, serine 532, threonine 589, and serine 592 (Valerie Garcia, personal communication). Furthermore, the affinity purified antibodies against serine 532 and serine 592 are able to recognize Rad4 phospho-protein in yeast cells extracts.

The phosphorylation state of Rad4 at Cdc2 consensus site S592 was further analyzed using these antibodies (with or without competition by the corresponding unphosphorylated peptide) after treatment with 375 Gy γ-rays or 20mM HU. A slightly stronger signal appeared in wild-type and *rad3-d* cells after treatment with 20mM HU or IR compared to untreated cells (Fig. 3-5B, left panel). This affinity purified antibody in combination with an unphosphorylated peptide recognizes a faint band in the untreated wild-type and *rad3-d* cells (Fig. 3-5B, right panel), suggesting that a low amount of the Rad4 pool is phosphorylated on S592 in the absence of DNA damage.

Rad4 protein forms a bandshift in response to IR or HU-treated during SDS-PAGE and the slower migrating form is considered to be the phosphorylated form of Rad4.

(A)

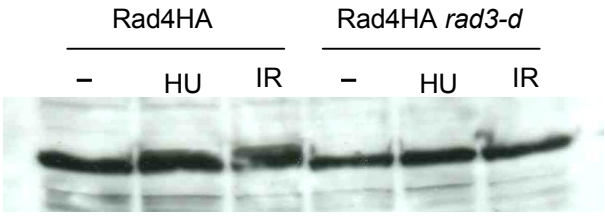

(B)

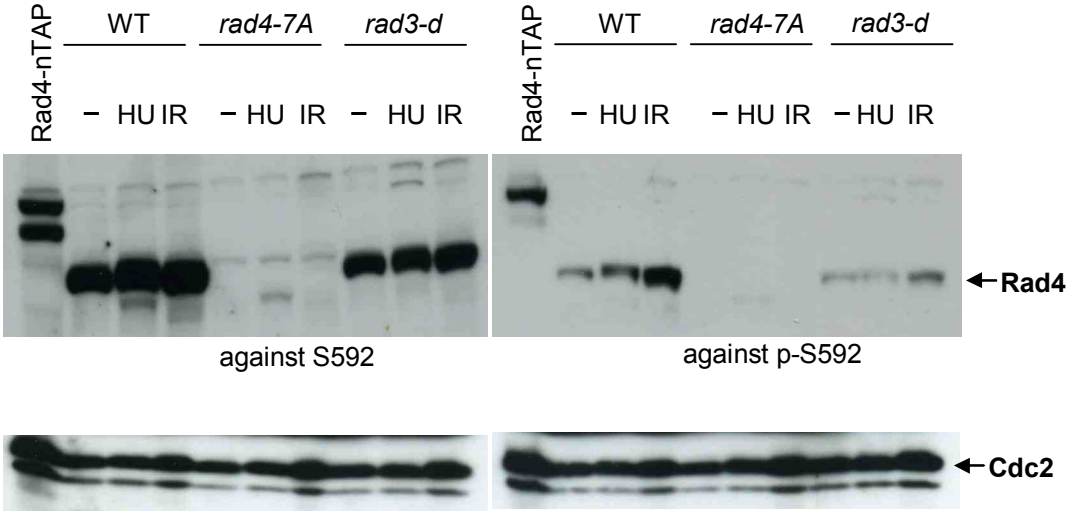

Figure 3-5- Rad4 phosphorylation on S592 in response to IR and HU
(A) Rad4 bandshift induced by HU and IR is completely abolished in a *rad3-d* background (Valerie Garcia, personal communication). (B) Wild-type, *rad4-7A* and *rad3-d* cells were treated with HU (20 mM) for 3.5 hours or IR (375 Gy). The protein extracts were probed with anti-S592 (left panel) either affinity purified (1/1000) or with specificity for the phosphorylated form of S592 (right panel) using a combination of the affinity purified antibody (1/1000) with the corresponding unphosphorylated peptide (50 μg). In parallel, protein extracts of Rad4-nTAP were probed with anti-S592 either affinity purified or affinity purified in combination with unphosphorylated peptide and used as a positive control. Cdc2 was detected as a loading control.

However, this bandshift is difficult to detect and very sensitive to the type of protein preparation or the concentrations acrylamide used during SDS-PAGE. Even though the resolution of Rad4 bandshift in wild-type cells after IR or HU is not clear in Fig. 3-5B, the signal detected using the phospho-specific S592 antibody increased in wild-type cells following IR or HU when compared to untreated cells (Fig. 3-5B, right panel). This suggests that Rad4 is phosphorylated on S592 *in vivo* in response to DNA damage and HU-treated. Interestingly, the DNA damage-dependent Rad4 phosphorylation on S592 is reduced in a *rad3-d* strain (Fig. 3-5B, right panel). Therefore, Rad4 phosphorylation by Rad3 is likely to be a prerequisite for Rad4 phosphorylation by Cdc2 (see discussion in Chapter 7).

3.2 Functional characterization of Rad4 RXL motif and Serine 641

3.2.1 Introduction

In addition to the BRCT domains and Cdc2 consensus phosphorylation sites, Rad4 sequence contains a small motif of interest: an RXL motif is present at the Rad4 C-terminal extremity (Fig. 3-6A). An RXL motif is a very short sequence present in a number (but not all) of cyclin A-CDK2 complex substrates and has been shown to serve as the docking site for binding on the surface of Cyclin A (Brown et al., 2007; Brown et al., 1999; Loog and Morgan, 2005). This interaction is usually critical for CDK-phosphorylation of substrates containing RXL motifs (Schulman et al., 1998). Even though cyclin B binds RXL motifs more weakly than cyclin A (Brown et al., 2007), in budding yeast, phosphorylation of Orc6 by Clb5 (cyclin B type) during S phase is reduced by mutating its RXL motif (Wilmes et al., 2004).

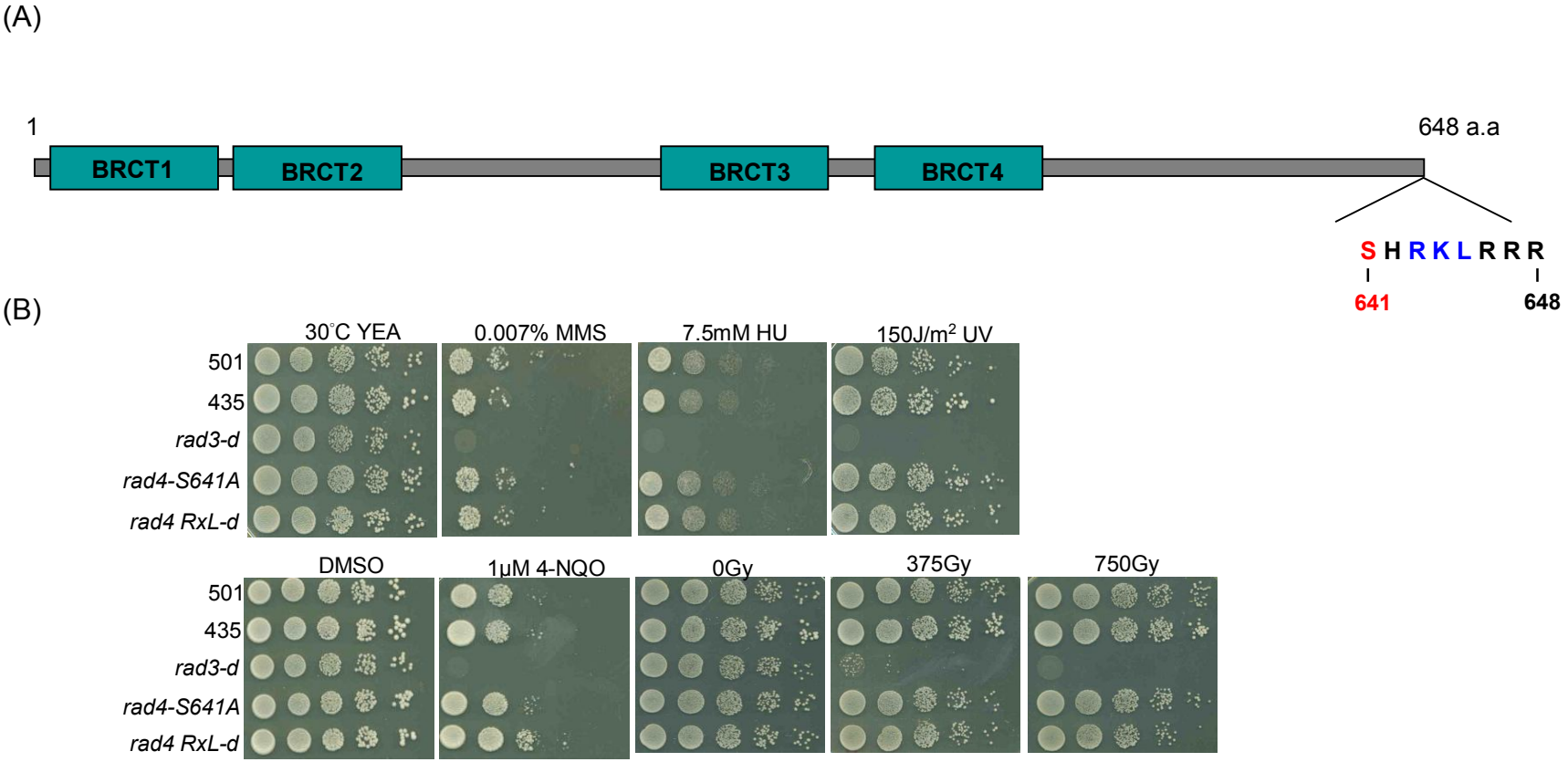

Figure 3-6- Functional analysis of the Rad4 RXL motif.
(A) Schematic representation of the Rad4 protein. S641 was identified to be highly phosphorylated by mass spectrometry is highlighted in red. The RXL motif is highlighted in blue. (B) Spot tests of *rad4 RXL-d* and *rad4-S641A* mutants. 10-fold serial dilutions of 1x10^{7}cells/ml were spotted onto YEA plates and exposed to UV or to different genotoxic agents with the indicated doses. 4-NQO is dissolved in DMSO, therefore, a plate with DMSO is used for the control. The plates were incubated at 30˚C for 3 days. “501” and “435” are *rad4*$^+$ and *rad4*$^+$ (RMCE) controls, respectively.

Interestingly, Rad4 interacts with Cdc13, a B-type cyclin associated with Cdc2 *in vivo* (Valerie Garcia, personal communication) and *in vitro* (see Chapter 4 Fig. 4-7B, middle panel). We hypothesized that this interaction is required for Rad4 phosphorylation by Cdc2 and might be dependent on the RXL motif. The dependency of phosphorylation on the RXL motif in response to DNA damage was investigated using a yeast strain expressing a Rad4 protein under its endogenous promoter in which the RXL motif is deleted. Furthermore, S641, in close proximity to the RXL motif, has been identified to be highly phosphorylated by Cdc2 *in vitro* by mass spectrometry (Fig. 3-6A). We thus proposed that S641 phosphorylation may affect Rad4 interaction with Cdc13. Therefore, a yeast strain expressing a Rad4 protein in which S641 residue is mutated to alanine was created to address this question. *rad4-dRXL* and *rad4-S641A* were both created by using the RMCE system.

3.2.2 Rad4 RXL motif is not required for resistance to DNA damages and HU

The sensitivity to DNA damaging agents (UV, MMS, 4-NQO) or to the replication inhibitor HU was examined by spot test. Both *rad4-dRXL (d(643-645))* and *rad4-S641A* did not show increased sensitivity to these agents when compared to a wild-type control strain (Fig. 3-6B), suggesting that perhaps the Rad4 RXL motif or S641 do not regulate Rad4 interaction with Cdc2/Cdc13 or that this interaction is not required for resistance to DNA damaging agents.

3.2.3 Rad4 interaction with Cdc13 is not dependent on the RXL motif or S641

To determine whether the interaction between Cdc13 and Rad4 is dependent on the RXL motif and/or S641, we performed a GST pull down assay. Recombinant C-terminal Rad4$^{865\sim1947}$ GST proteins; wild type (Valerie Garcia's plasmid collection # 84), *rad4-dRXL* (pSJ23), and *rad4-S641A* (Valerie Garcia's plasmid collection # 109) were

constructed by site-directed mutagenesis and mutant proteins expressed in *Escherichia coli*. GST fusion proteins were incubated with yeast cell extracts and the interaction with Cdc13 was assessed by western blot using an anti-Cdc13 antibody (kind gift from J. Hayles). This experiment confirmed that a specific interaction between Cdc13 and Rad4 is present. However, using *rad4-dRXL* and *rad4-S641A* fusion protein versions, the amount of Cdc13 interacting with Rad4 was similar to that seen with wild type (Fig. 4-7B, middle panel). This suggests that Rad4 RXL motif is not a docking site for binding to Cdc13, and that S641 residue is not involved in regulating this interaction. Intriguingly, Cdc13 seems to be modified *in vitro* when incubated with recombinant C-terminal Rad4 containing S641A.

3.3 Other functional characterization of Rad4 motifs

Rad4 is modified *in vitro* by small ubiquitin-related modifier (SUMO) (Felicity Watts, personal communication) and SUMO modification is known to regulate some biological pathways to maintain genome stability through its influence on DNA repair, DNA replication, and recombination (Ohuchi et al., 2008; Ohuchi et al., 2009). Three potential sumoylation target sites are present in Rad4: K126, K260, and K408 (Fig. 3-7A). In order to assess whether Rad4 sumoylation consensus sites regulate cells resistance to DNA damage, a yeast strain expressing a Rad4 protein from its endogenous promoter in which Rad4 lysine126, lysine260, and lysine408 were all mutated to alanine was constructed by the RMCE system and was investigated by spot-test. The mutant *rad4-K126A.K260A.K408A* did not show any significant sensitivity to DNA damaging agents (UV-irradiation and MMS) or HU when compared to wild type control cells (Fig. 3-7B). Since possible sumoylation can occur on non consensus sites when sumoylation sites are mutated *in vivo* (Felicity Watts, personal communication),

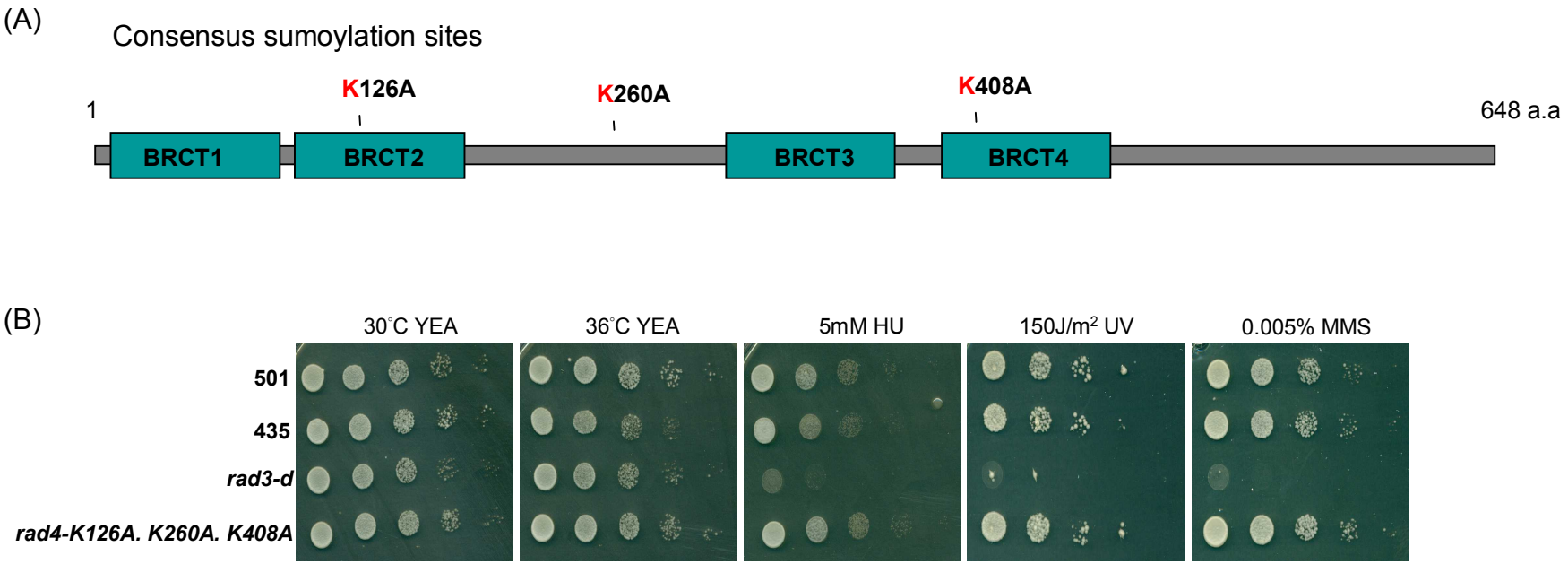

Figure 3-7- Functional analysis of Rad4 sumoylation consensus sites.
(A) Localization of the putative sumoylation sites in Rad4 protein. (B) Spot tests of the Rad4 sumoylation mutant. 10-fold serial dilutions of $1x10^7$cells/ml were spotted onto YEA plates and exposed to UV or to different genotoxic agents with the indicated doses. The plates were incubated at 30˚C for 3 days and one is incubated at 36˚C. “501” and “435” are *rad4*$^+$ and *rad4*$^+$ (RMCE) controls, respectively.

we can not reject the hypothesis that Rad4 is sumoylated *in vivo* and that this regulates its activity.

3.4 Conclusion

In vivo, Rad4 is phosphorylated in response to DNA damage or HU in a Cdc2-dependent manner. *In vitro*, Rad4 is phosphorylated by Cdc2, and the phosphorylation sites were identified by mass spectrometry. Some mutants carrying single or multiple substitutions of Cdc2 phosphorylation sites display only a slight sensitivity to HU and DNA damaging agents. In addition, Rad4 Cdc2 phosphorylation sites do not play a role in the control of DNA re-replication. Interestingly, Rad4 phosphorylation on S592 *in vivo* is highly reduced in a *rad3-d* strain following IR or HU-treated, suggesting that Rad4 phosphorylation by Cdc2 is likely to be dependent on Rad3. The recombinant C-terminus Rad4 where the RXL motif is deleted or S641 is mutated to alanine does not affect the Rad4 interaction with Cdc13 *in vitro*. Besides, there is no phenotypic effect observed after DNA damage or HU in *rad4-dRXL* and *rad4-S641A* mutants.

Chapter 4 Characterization of the Rad4^{TopBP1} ATR-activating domain (AAD)

4.1 Functional characterization of a putative AAD

4.1.1 Introduction

TopBP1 in human and Xcut5 in *Xenopus* have been shown to be required for the activation of ATR kinase activity, and a domain responsible for the activation has been identified and named **AAD**, standing for **A**TR-**a**ctivating **d**omain (Kumagai et al., 2006). The AAD, which resides between BRCT domains VI and VII in human and *Xenopus* TopBP1, is conserved between TopBP1 homologues in vertebrates, including human, chicken, zebrafish and *Xenopus*, but does not appear to be conserved in the yeast orthologues Dpb11 and Rad4/Cut5 (Kumagai et al., 2006). Kumagai, Lee et al., demonstrated that TopBP1 AAD function is conserved in human and *Xenopus*. *In vitro*, both Xcut5 AAD (a fragment of Xcut5 (972-1279) ≈ 300 amino acids) and hTopBP1 AAD (a fragment of hTopBP1 (978-1192)) can activate Xatr-Xatrip. The function in stimulation of ATR activity was narrowed down to a small highly conserved peptide (1138-1141(WDDP)) in the Xcut5 AAD. In addition, a single substitution of an aromatic amino acid to arginine (W1138R) localized within the WDDP peptide completely abolished this Xatr activation function (Kumagai et al., 2006). Similarly, a recombinant fragment corresponding to the hTopBP1 AAD can stimulate ATR kinase to phosphorylate Mcm2 while a recombinant fragment of hTopBP1 AAD with a W1145R mutation (equivalent to a residue W1138 of Xcut5) can not (Kumagai et al., 2006). These observations reveal that the TopBP1/Xcut5 AAD appears to be required for and sufficient for ATR activation *in vitro*. Finally, Xcut5 with an intact AAD, when

incubated in *Xenopus* cell extracts that has been depleted of endogenous Xcut5 can elicit a robust ATR-dependent of Chk1 phosphorylation in response to aphidicolin. On AAD mutated Xcut5, however could not. This indicates that the AAD is a direct activator of ATR kinase and the AAD is required for checkpoint activation in response to replication fork stalling (Kumagai et al., 2006).

Recently, Daniel Mordes and his colleagues have identified an ATRIP-*top* mutant in mammalian cells which retains interaction with ATR but loses an interaction with TopBP1. TopBP1 association with ATR-ATRIP-*top* is significantly reduced compared to that with ATR-ATRIP, and ATRIP-*top* severely reduces TopBP1-dependent stimulation of ATR kinase *in vitro* (Mordes et al., 2008a). *In vivo*, ATRIP-*top* mutant cells exhibit a defect in the recovery from HU-induced replication fork stalling and a defect in cell cycle arrest after IR. Similarly to ATRIP-*top* mutant in mammals, *S. cerevisiae* cells expressing *ddc2-top* (Ddc2 is the *S. cerevisiae* ATRIP homolog) show a very strong sensitivity to HU and MMS and reduced phosphorylation of Rad53, a substrate of Mec1 (Mordes et al., 2008b). Both TopBP1-dependent ATR activation and the interaction of TopBP1 with ATR-ATRIP are dependent on the ATRIP homologs in *S. cerevisiae*, *Xenopus*, and human cells (Kumagai et al., 2006; Mordes et al., 2008a; Mordes et al., 2008b). Taken together, these data indicate that an ATRIP interaction with TopBP1 is a prerequisite for TopBP1-dependent ATR activation in response to DNA lesions.

In *S. pombe*, the Rad4-Rad3 interaction increases after IR or S-phase arrest by HU, suggesting that Rad4-Rad3 forms an active checkpoint complex (Furuya et al., 2004). When we initiated this project, the AAD had just been characterized in vertebrates. In this chapter, we address whether *S. pombe* Rad4 plays an activator role in stimulation of Rad3 equivalent to ATR activation by *Xenopus* Cut5 and human TopBP1. The AAD

itself was reported to not be conserved in yeast (Kumagai et al., 2006), however an alignment of the core of the AAD between yeast species and the hTopBP1 AAD was provided by Charly Chahwan (Fig. 4-1). Interestingly, in all the fungi species used for the alignment, the conserved tryptophan (W1138 in Xcut5 or W1145 in *h*TopBP1) present in higher eukaryotes is replaced with another aromatic amino acid, a tyrosine (Y) (see Fig. 4-1). The putative AAD is localized in the unstructured C-terminal tail of both Rad4 and Dpb11 (Fig. 4-2A).

4.1.2 *rad4-Y599R* and *rad4-AAD* are sensitive to DNA damage

In order to study the function of this putative AAD in *S. pombe* and to determine whether the function of the AAD is conserved with higher eukaryotes, *S. pombe* strains expressing Rad4 with either a deletion of the conserved core of the AAD (*rad4-AAD*, deleted for a small region 595-601 (EHVSYID)) or a substitution of the key aromatic amino acid localized in AAD (*rad4-Y599R*) were created. *rad4-Y599R* and *rad4-AAD* were integrated into the genome using the RMCE system (described in Chapter 2), and are thus expressed from the endogenous *rad4* promoter.

rad4-Y599R and *rad4-AAD* cells grow like wild-type and *rad4*$^{+}$ (RMCE) control cells 501 and 435, respectively (Fig. 4-2B). Sensitivity to DNA damaging agents (UV, MMS, 4-NQO) and to a nucleotide inhibitor (HU) was assessed by spot tests. *rad4-Y599R* and *rad4-AAD* are mildly sensitive to DNA damaging agents and display the same level of sensitivity. Both *rad4-Y599R* and *rad4-AAD* mutant sensitivity is observed at 100 and 150 J/m^2 doses of UV-irradiation, 5 and 7.5 mM HU and 0.007% MMS (Fig. 4-2B). However, their hypersensitivity is not as severe as *rad3-d* cells, suggesting that Rad3 activity is reduced but not completely abolished in response to DNA damage in these mutants. Only a very mild sensitivity to IR in *rad4-Y599R* and *rad4-AAD* mutant

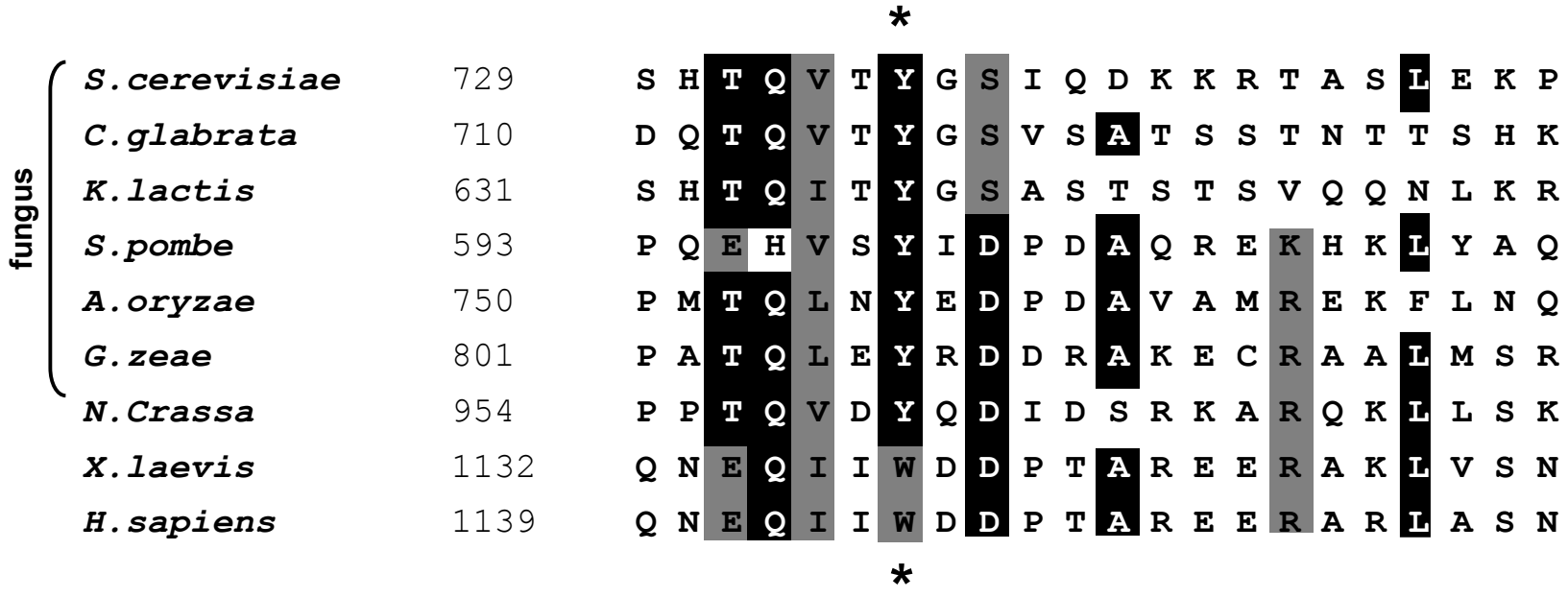

Figure 4-1- Alignment of the TopBP1 ATR-activating domain (AAD)
A substitution of a conserved tryptophan (W1138R in Xcut5 and W1145R in hTopBP1) denoted with an asterisk abolishes ATR activation. Note that this residue is replaced by another aromatic amino acid, a tyrosine, in yeasts. In this work, a deletion of EHVSYID (*rad4-AAD*) and a single amino acid substitution (*rad4-Y599R*) were constructed to study the function of the AAD in *S. pombe*. The black boxes highlight amino acids are identical between 5 or more sequences, and gray boxes are identical between at least 2 sequences.

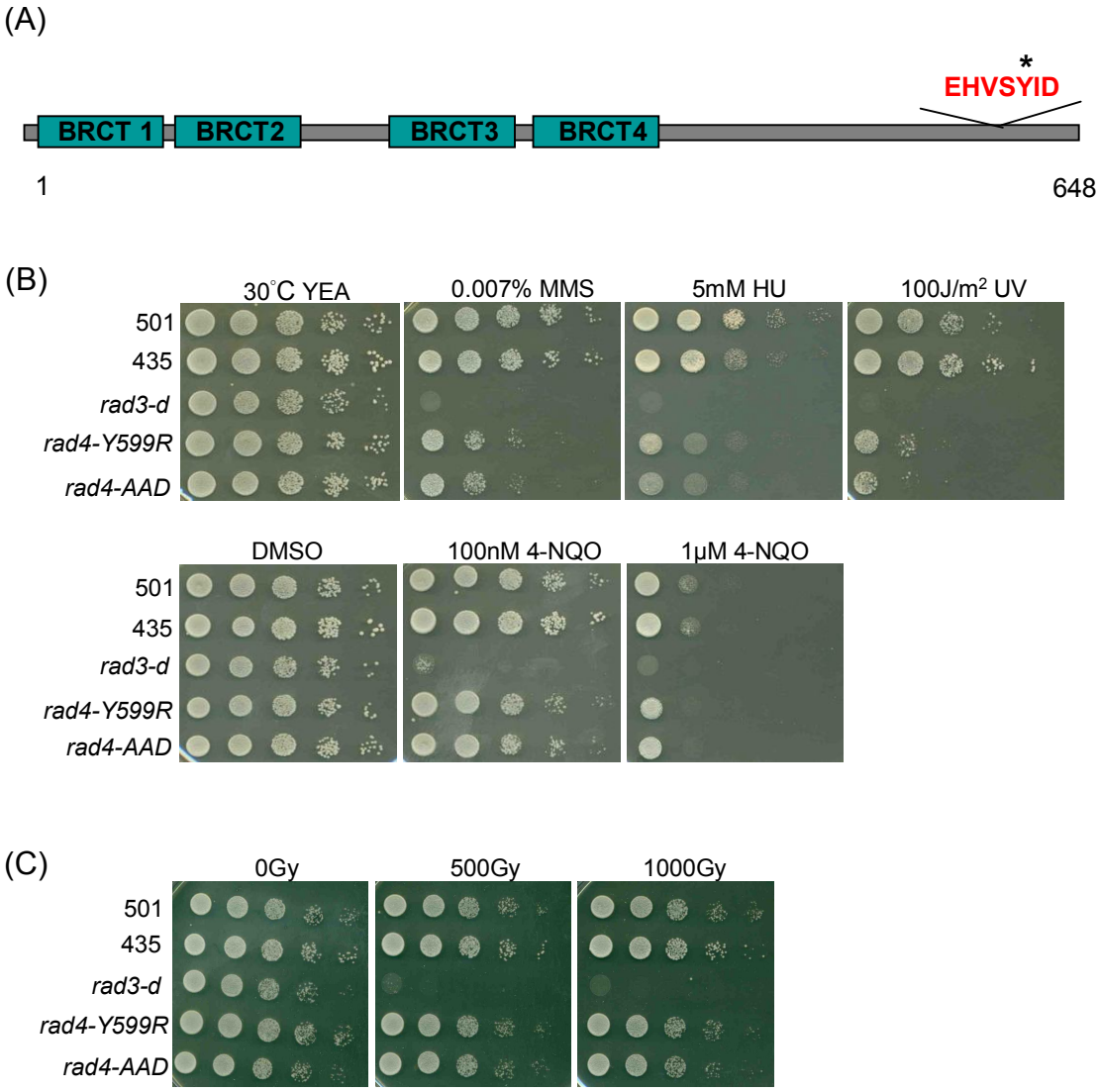

Figure 4-2- Functional analysis of the Rad4 AAD
(A) Schematic representation of Rad4 protein. The core of the AAD motif (EHVSYID) is highlighted in red and the key aromatic amino-acid (Y599) is marked with an asterisk. (B) Spot tests of *rad4-AAD*, *rad4-Y599R*, *rad3-d* and wild-type *rad4*$^{+}$ control cells.10-fold serial dilutions of 1x10^{7} cells/ml were spotted onto YEA plates and exposed to UV, or spotted on YEA plates supplemented with different genotoxic agents at the indicated doses (a plate with DMSO is used for control). The plates were incubated at 30˚C for 3 days. (C) Spot tests of *rad4-Y599R and rad4-AAD.* 10^{7} cells/ml were untreated (0Gy) or irradiated with 500 or 1000 Gy, and a 10-fold serial dilution was spotted onto YEA plates and incubated at 30˚C for 3 days.“501” and “435” are *rad4*$^{+}$ and *rad4*$^{+}$ (RMCE) controls, respectively.

compared to wild-type was detected after irradiation at high doses of 1000 Gy (Fig. 4-2C).

4.1.3 *rad4-Y599R* and *rad4-AAD* have a checkpoint defect in response to UV

To determine whether the sensitivity of *rad4-Y599R* and *rad4-AAD* to UV-irradiation is due to a defect in checkpoint activation, G2-phase cells synchronized by lactose gradient were irradiated with UV, released into rich media and the septation index was scored every 20 minutes after release. *rad4-Y599R* (Fig. 4-3A) and *rad4-AAD* cells (Fig. 4-3B) form septum (*i.e.*, re-enter the cell cycle) earlier than the wild type cells: about 40~60 minutes earlier after cells are exposed to 25 J/m^2 of UV, and 40~80 minutes earlier after cells are exposed to 50 J/m^2 of UV. In other words, both mutants escape from cell cycle arrest earlier than the wild type cells after UV-irradiation, indicating that the checkpoint arrest is partially defective in both mutants in response to UV.

4.1.4 *rad4-Y599R* or *rad4-AAD* sensitivity to UV is epistatic with *cds1-d*

To examine if the checkpoint defect of the *rad4-Y599R* and *rad4-AAD* strains in response to UV-irradiation is due to a defective activation of the G2/M DNA damage checkpoint kinase Chk1 or the replication checkpoint kinase Cds1, or both, we performed an epistasis analysis with either *rad4-Y599R* or *rad4-AAD* strains combined with *chk1-d* or *cds1-d*. In such epistasis experiments, two genes are considered to function in the same DNA damage sensitivity pathway when a double mutant has a similar level of sensitivity to either single mutant in response to DNA damaging agents; two genes are considered to function in different genetic pathways when a double mutant is more sensitive than either single mutant in response to DNA damaging agents. The UV sensitivities of a double mutant *rad4-Y599R cds1-d* or *rad4-AAD cds1-d* appear to be similar to the sensitivity of *cds1-d*, indicating that *rad4-Y599R* and *rad4-AAD* are

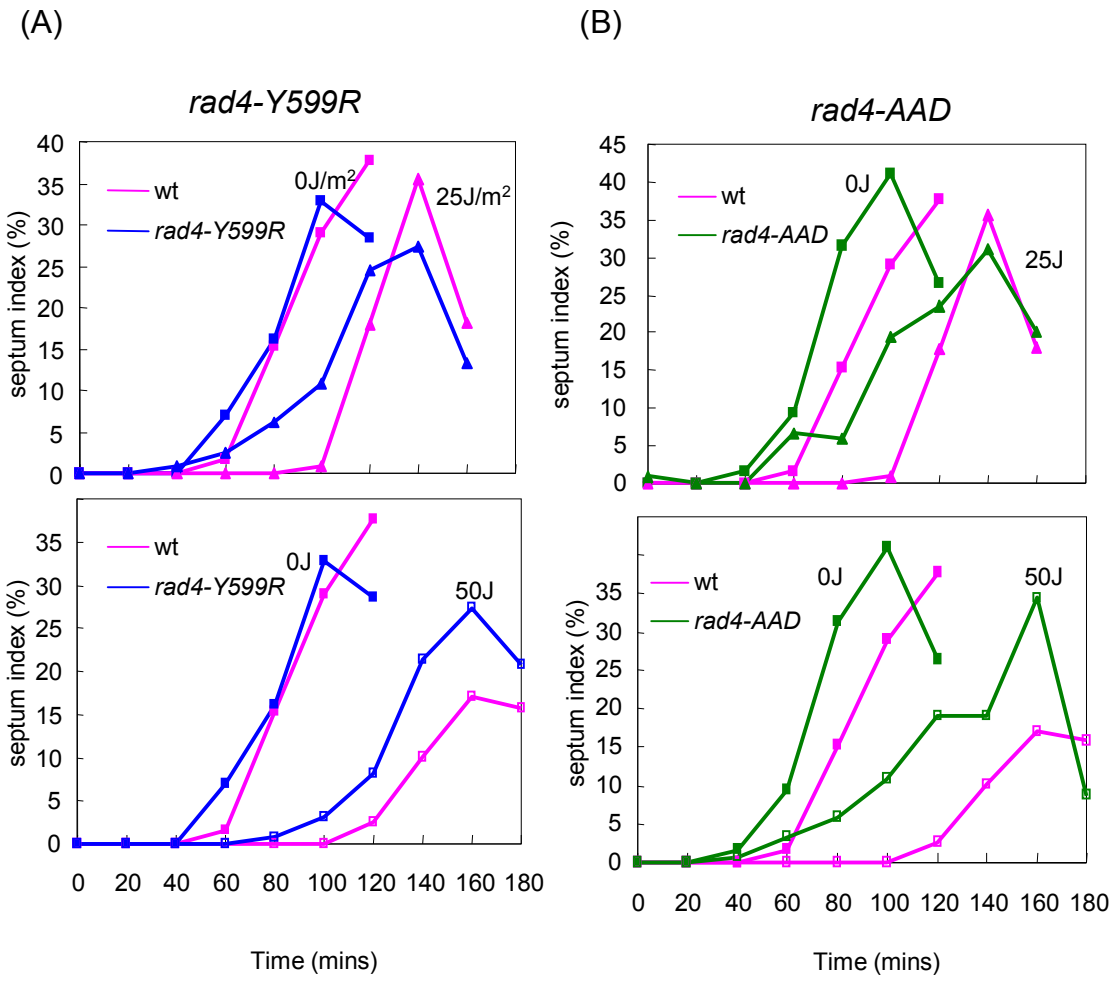

Figure 4-3- Analysis of checkpoint function in *rad4-Y599R* (panel A) and *rad4-AAD* (panel B) mutants in response to UV-irradiation
Cells were synchronized in G2 phase by lactose gradient, collected on filters, exposed to UV and resuspended in YE media. Samples were collected every 20 minutes, fixed with methanol and stained with DAPI and calcofluor. Septation was scored under a fluorescence microscope. (pink lines, control cells; blue lines, *rad4-Y599R;* green lines, *rad4-AAD*).

epistatic with *cds1-d* (Fig. 4-4). Therefore, both *rad4-Y599R* and *rad4-AAD* are considered to affect the same genetic pathway as *cds1-d* in response to UV. In contrast, the double mutants *rad4-Y599R chk1-d* or *rad4-AAD chk1-d* are more sensitive to UV-irradiation than any of the corresponding single mutant. Therefore *rad4-Y599R* and *rad4-AAD* are additive/synergistic with *chk1-d*. Similarly, *rad4-Y599R* and *rad4-AAD* are additive/synergistic with *chk1-d* in response to MMS (Fig. 4-4). The additive or synergistic interaction with Chk1 indicates the AAD participates in a pathway distinct from Chk1 but does not rule out the possibility that Rad4 is also required for Chk1 activation (see below). No informative conclusion could be drawn in response to HU since *cds1-d* shows a high sensitivity to 1mM and 1.5mM of HU while *rad4-Y599R* and *rad4-AAD* sensitivity are very mild (Fig. 4-4).

4.1.5 Rad4 AAD is required for both Cds1 kinase activity and Chk1 phosphorylation in response to UV

To examine further whether the AAD was required for Cds1 activation in response to UV, we performed a Cds1 kinase assay using a *rad4-Y599R* mutant. In this assay, the Cds1 kinase was immunoprecipitated using an anti-Cds1 antibody from the wild-type or *rad4-Y599R* cell extracts immediately after either mock irradiation of cells or after cells were irradiated with 200 J/m^2 of UV. Immunoprecipitated Cds1 was incubated with myelin basic protein (MBP), which is used as a substrate of Cds1 (Lindsay et al., 1998). *rad4-Y599R* cells exhibit a two-fold decrease in the induction level of Cds1 activity after UV-irradiation asynchronous cells when compared to that of wild-type cells (Fig.4-5A.B).

As mentioned before, the additive or synergistic phenotype of *rad4 AAD* mutants with *chk1-d* does not rule out the possibility that Rad4 AAD participates in Chk1 activation.

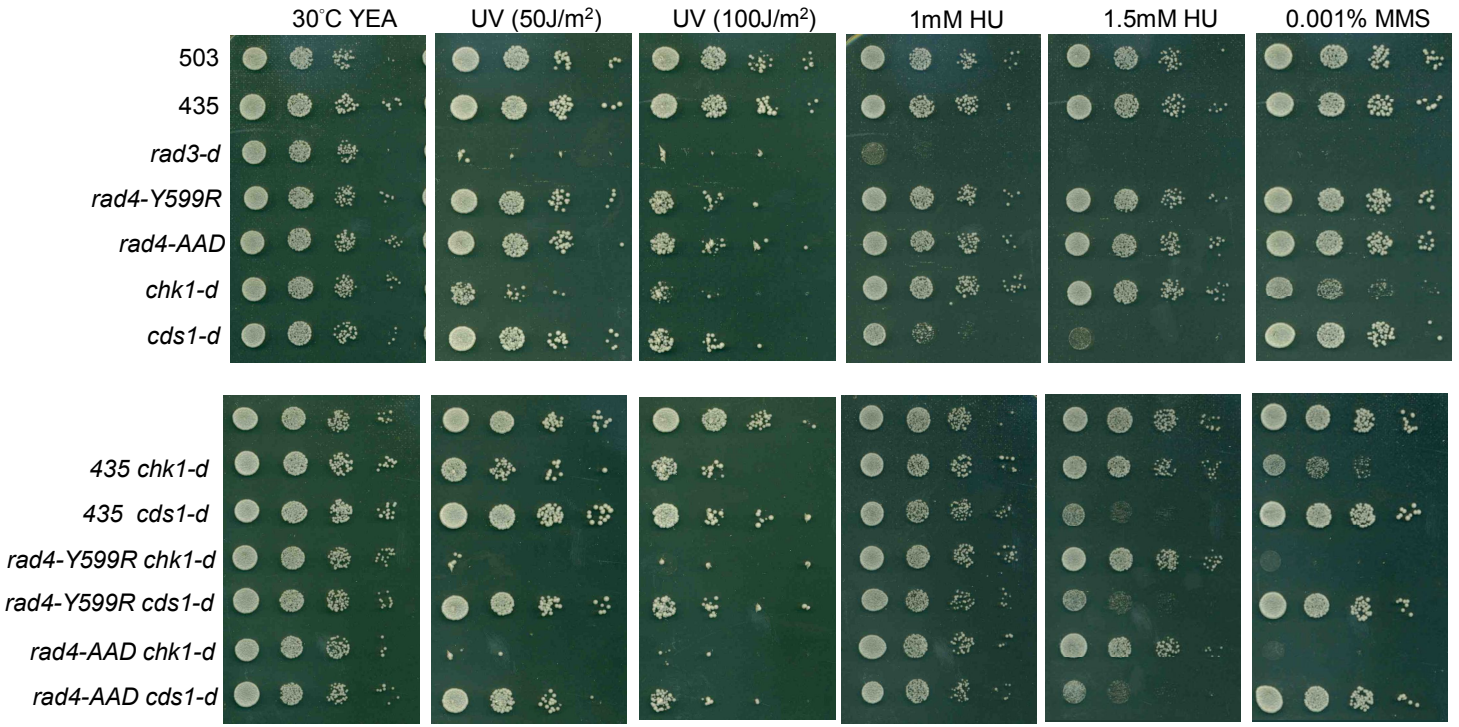

Figure 4-4- Epistasis analysis of *rad4-AAD* or *rad4-Y599R* with *cds1-d* and *chk1-d*
10-fold serial dilutions of 1x10^{7}cells/ml were spotted onto YEA plates and exposed to UV or spotted onto YEA plates supplemented with different genotoxic agents at the indicated doses. The plates were incubated at 30˚C for 3 days. “501” and “435” are *rad4*$^+$ and *rad4*$^+$ (RMCE) controls, respectively.

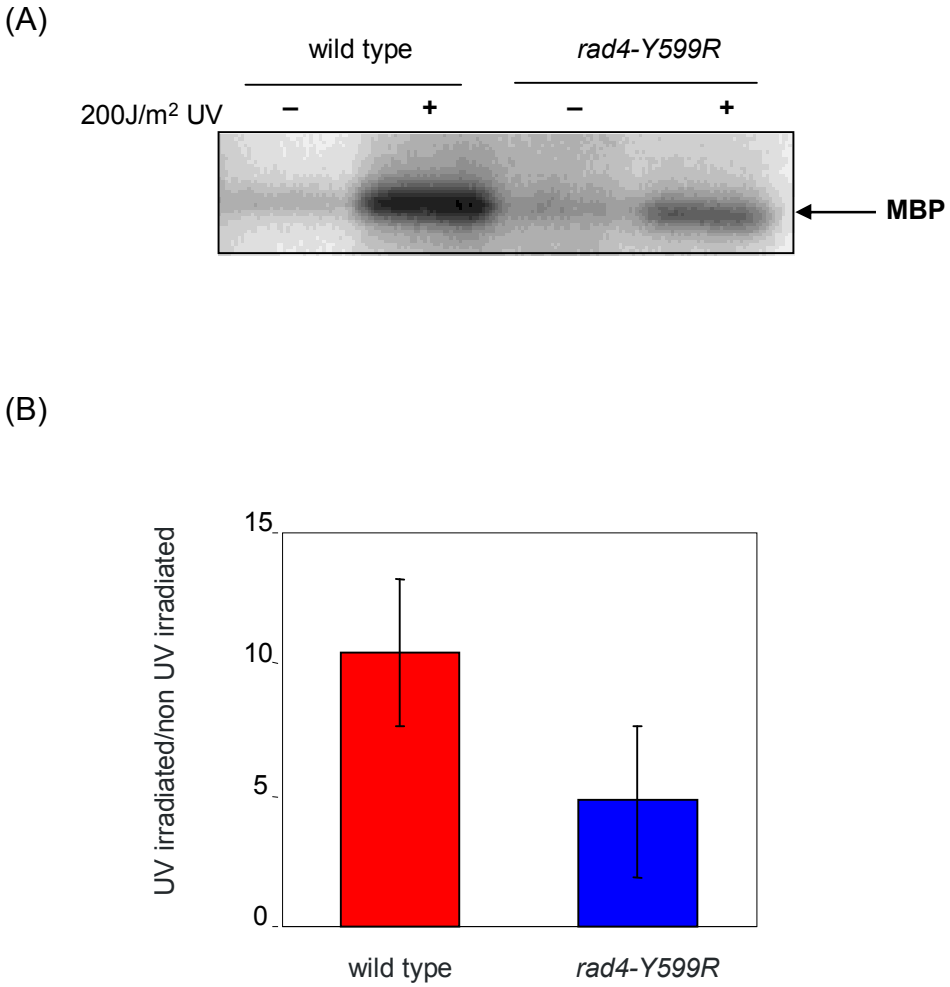

Figure 4-5- Analysis of Cds1 kinase activity and Chk1 phosphorylation after UV-irradiation in the *rad4-Y599R* mutant
(A) *rad4*$^{+}$ (RMCE) control and *rad4-Y599R* cells treated with 200J/m^2 UV or untreated as a control were assayed for Cds1 kinase activity using MBP as a substrate. (B) Cds1 kinase fold induction (UV irradiated/non irradiated) is an average of two individual experiments (quantified with PhosphoImager). (C) *rad4-Y599R Chk1-HA* and *Chk1-HA* were exposed to 10, 25, 50, and 100 J/m^2 UV. The proteins were extracted and phosphorylation of Chk1 was analyzed by western blot. Cdc2 was used as a loading control. * represents the phosphorylation form of Chk1.

rad4 AAD mutants display a G2/M checkpoint defect in response to UV-irradiation performed in G2, indicating that it is indeed partially required for Chk1 function (activation). Chk1 phosphorylation is a marker for DNA damage checkpoint activation (Martinho et al., 1998) and this modification is detectable as a decreased mobility of the Chk1 protein during SDS-PAGE and appears as a bandshift (Walworth and Bernards, 1996). Wild-type and *rad4-Y599R* strains containing HA-tagged *chk1* were generated by genetic crosses and were used to analyze Chk1 phosphorylation in response to UV-irradiation by western blot with an anti-HA antibody. Cells were evenly plated on YEA plates and irradiated with the different indicated doses of UV. Cells were recovered from plates by suspending in fresh YE medium and protein extraction was performed after UV-irradiation or mock irradiation (see Chapter 2 Material and Methods 2.3.4 (B) in detail). Chk1 phosphorylation in wild-type cells is not detectable in the absence of UV-irradiation and the intensity of Chk1 phosphorylation increases with increasing doses of UV-irradiation. In contrast, Chk1 phosphorylation is significantly reduced in *rad4-Y599R* mutant cells in response to 10, 25, 50, or 100 J/m^2 UV-irradiation when compared to wild-type cells (Fig. 4-5C). These results reveal that the Rad4 AAD participates not only in Cds1 kinase activation but also in Chk1 kinase phosphorylation in response to UV-irradiation.

4.1.6 Rad4 AAD is not required for IR-induced G2/M checkpoint activation

To explore further the lack of sensitivity to IR in *rad4 AAD* mutants, G2-phase cells synchronized by lactose gradient were irradiated with various doses of IR or mock irradiated as a control, released into rich media, and cell cycle progression was monitored by scoring the septation index every 20 minutes after irradiation. *rad4-Y599R* cells forms a septum about 20 minutes later than the wild-type control strain in response to 375 Gy of IR and 40 minutes later than the wild-type control strain in response to 500

Gy of IR. Therefore, *rad4-Y599R* G2/M checkpoint is intact in response to IR (Fig. 4-6A). In fact, the DNA damage checkpoint arrest is even slightly prolonged after 500 Gy compared to wild-type cells. This prolonged arrest could be due to a repair defect in response to IR.

To test whether or not Chk1 phosphorylation is affected in *rad4-Y599R* cells after IR, asynchronous cells were irradiated with 12, 25, 50, and 100 Gy or mock irradiated, and a TCA extraction of proteins was performed immediately after irradiation. As expected, Chk1 phosphorylation in *rad4-Y599R* in response to 12, 25, 50, or 100 Gy of IR is similar to wild type, confirming that *rad4-Y599R* mutant is proficient in checkpoint activation in response to IR (Fig. 4-6B).

4.1.7 Rad4 interaction with Rad3 is dependent on the AAD

We next examined if the phenotypes of the *rad4 AAD* mutant is correlated with a defective interaction with Rad3. *In vivo*, an interaction between Rad4 and Rad3 has been shown by co-immunoprecipitation (co-IP) after IR or HU (Furuya et al., 2004). After many attempts to repeat this experiment, the interaction detected was too weak to address whether Rad4 interaction with Rad3 is reduced or abolished in the *rad4 AAD* mutant. A GST-pull down experiment was therefore developed in order to re-address this issue. A plasmid (pGEX-KG) expressing recombinant Rad4 C-terminus ($Rad4^{865\sim1947}$, covering the third and fourth BRCT domains and the Rad4 unstructured C-terminal tail) was previously constructed on the laboratory (Valerie Garcia's plasmid collection # 84) and used to express recombinant Rad4 C-terminal moiety. The same plasmid was modified by site-directed mutagenesis in order to introduce the *rad4* Y599R mutation (pSJ38) (Fig.4-7A). Recombinant Rad4 mutated either for the AAD (*rad4-Y599R*), Serine 641 (*rad4-S641A*) and the RXL motif (*rad4-dRXL*) (described in

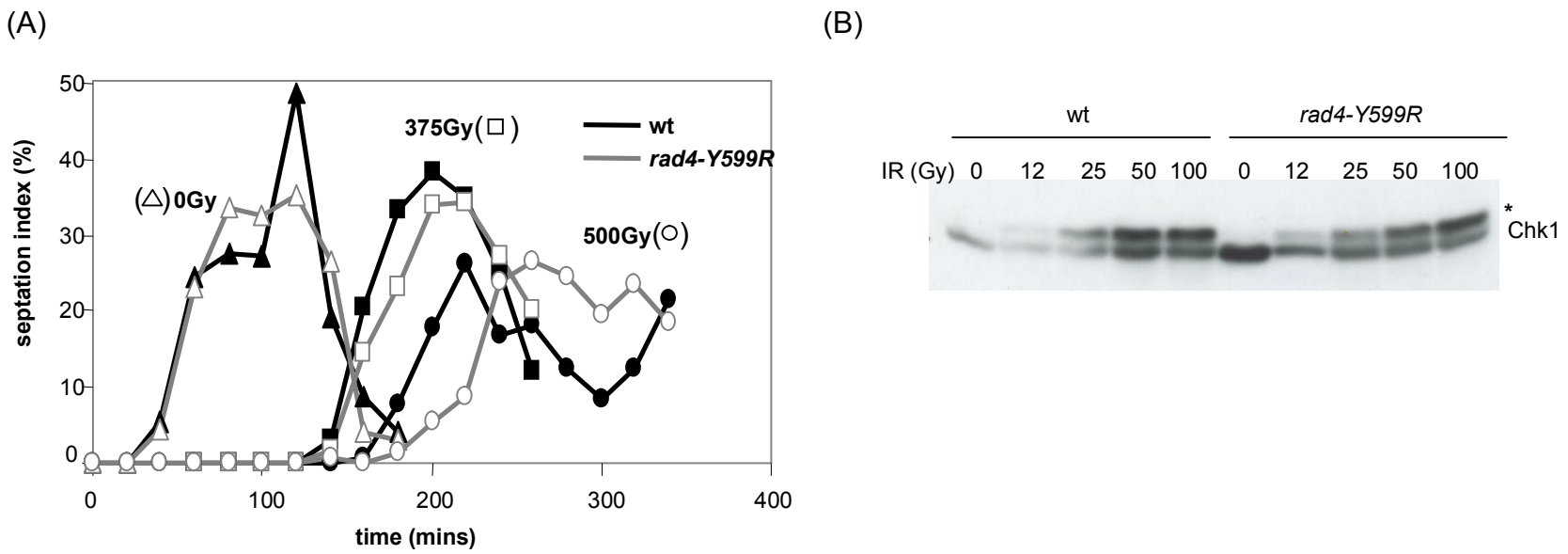

Figure 4-6- Analysis of checkpoint function in the *rad4-Y599R* mutant in response to IR
(A) Cells were synchronized in G2 phase by lactose gradient, and irradiated with γ -rays. Samples were collected every 20 minutes, fixed with methanol and stained with DAPI and calcofluor. Septation was scored under a fluorescence microscope. Triangles: non-irradiated control; squares: 375Gy; circles: 500Gy. (B) Chk1 phosphorylation is not defective in *rad4-Y599R* in response to IR. *rad4-Y599R* and wild type cells were untreated or irradiated with 12, 25, 50, or 100 Gy. The proteins were extracted immediately after irradiation and Chk1 phosphorylation was analyzed by western blot. * represents the phosphorylation form of Chk1.

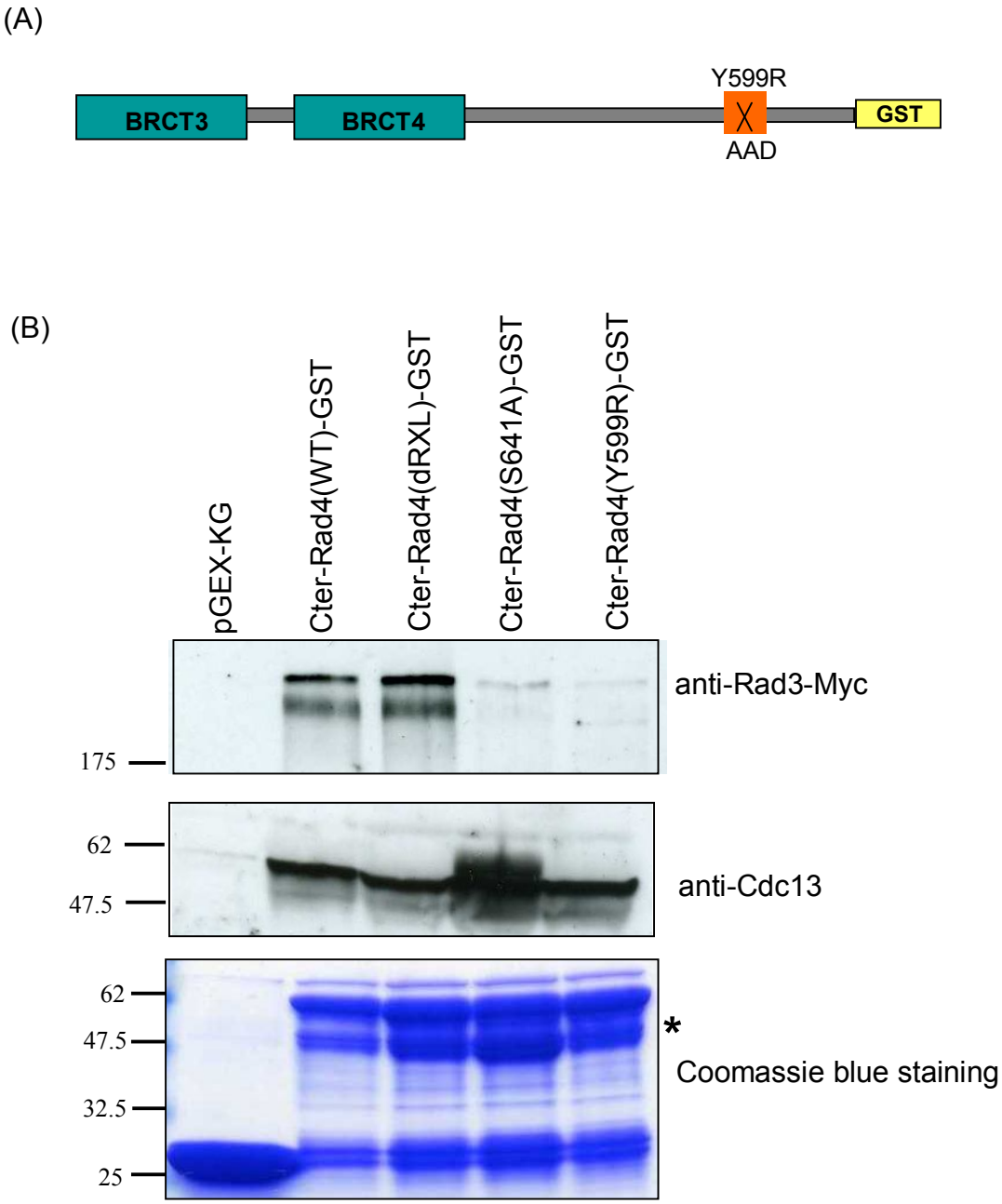

Figure 4-7- Rad3 and Rad4 C-terminal moiety interaction *in vitro*
(A) Schematic representation of the recombinant C-terminal Rad4 protein. The Rad4 C-terminal moiety includes the 3rd and 4th BRCT domains and C-terminal tail of Rad4. (B) GST pull down. GST alone (first lane), *rad4* wild-type, *rad4-dRXL rad4-S641A*, and *rad4-Y599R* mutants were expressed in *E.coli*. The fusion proteins were purified on glutathione sepharose beads and incubated with wild-type yeast cell extract expressing Myc-tagged Rad3. The samples were analyzed on SDS-PAGE followed by immunoblotting for Myc-tagged Rad3 (upper panel) and Cdc13 (middle panel). Equivalent loading was ensured by coomassie blue staining (lower panel). *represents a proteolysed form of Rad4.

Chapter 3) fused to a GST-tag were expressed in *Escherichia coli*, purified and subsequently incubated with *S. pombe* proteins extracts prepared from cells expressing a Myc-tagged version of Rad3. After GST pull-down and western blot, the membrane was probed with an anti-Myc antibody in order to detect the Rad3 protein (Fig.4-7B upper panel). An anti-Cdc13 antibody was used to detect Cdc13, a known interacting partner of Rad4 (Valerie Garcia, personal communication) for a positive control (Fig.4-7B middle panel). As a negative control, GST alone does not pull down Rad3 or Cdc13. Rad3 and Cdc13 are pulled-down with the wild-type form of the C-terminal Rad4-GST fragment. However, the amount of Rad3 pulled-down with recombinant Rad4-Y599R-GST fragment is significantly reduced compared to the wild-type, while the interaction with Cdc13 is not affected (Fig.4-7B).This significant reduction in the interaction between Rad3 and the Rad4 AAD mutant was reproduced in two independent experiments. These results indicate that Rad4 C-terminal moiety physically interacts with Rad3 *in vitro*, and this interaction is dependent on the AAD.

4.1.8 Chk1 phosphorylation maintenance defect in *rad4 AAD* mutant

In chapter 5, the role of the AAD is thoroughly investigated in the context of a LacI/LacO artificial checkpoint induction system. In this artificial system, the AAD plays an important role which in our interpretation reflects specifically the amplification step of checkpoint signaling; therefore, it was interesting to study the dynamics of Chk1 phosphorylation at different time after exposure to DNA damage. This is reported below.

(A) In response to IR

Asynchronous wild type and *rad4-Y599R* cells were irradiated with 100 Gy (or mock irradiated as a control) and proteins were extracted immediately after irradiation or 30,

60, 90, 120, and 180 minutes after irradiation. Cells were continuously grown at 30°C during the time course after IR. Chk1 is not phosphorylated in the absence of irradiation in both wild-type and *rad4-Y599R* cells (Fig. 4-8A). In wild-type and *rad4-Y599R* cells Chk1 phosphorylation occurs immediately after IR. While Chk1 phosphorylation is maintained up to 180 minutes after IR in wild-type cells, it decreases in *rad4-Y599R* 90 minutes after IR (Fig. 4-8A). A simple interpretation would be that *rad4-Y599R* is capable of activating Rad3-mediated Chk1 phosphorylation, but is defective in the maintenance of Chk1 phosphorylation in response to IR. Another alternative interpretation is perhaps that the fraction of cells that were in S-phase (~10%) in the asynchronous culture at the time of IR are defective in activating Chk1 phosphorylation when entering G2/M phase. Whether or not this precocious Chk1 de-phosphorylation is associated with an early release from checkpoint arrest has not been addressed in this particular experiment and needs to be further clarified.

In order to distinguish whether the early decrease in Chk1 phosphorylation in *rad4-Y599R* after IR reflects the population of irradiated G2-phase cells (~70% in asynchronous culture) being unable to maintain Chk1 phosphorylation, or the population of irradiated S-phase cells (~10% in asynchronous culture) being unable to activate Chk1, wild-type and *rad4-Y599R* cells were synchronized in G2-phase and G2 synchronous cells challenged with 50 Gy of IR. Cells were synchronized in G2-phase using a *cdc25-22* mutant (a thermo-sensitive strain) temperature shift to 36.5°C. Cells were subsequently released into the cell cycle at 25°C. Chk1 phosphorylation is observed in both *cdc25-22* and *cdc25-22 rad4-Y599R* cells up to 90 minutes after irradiation in G2-phase (Fig. 4-8B), after which phosphorylation decreases. This suggests that the reduced Chk1 phosphorylation between 90 and 180 minutes observed after the irradiation of an asynchronous population of *rad4-Y599R* cells, when

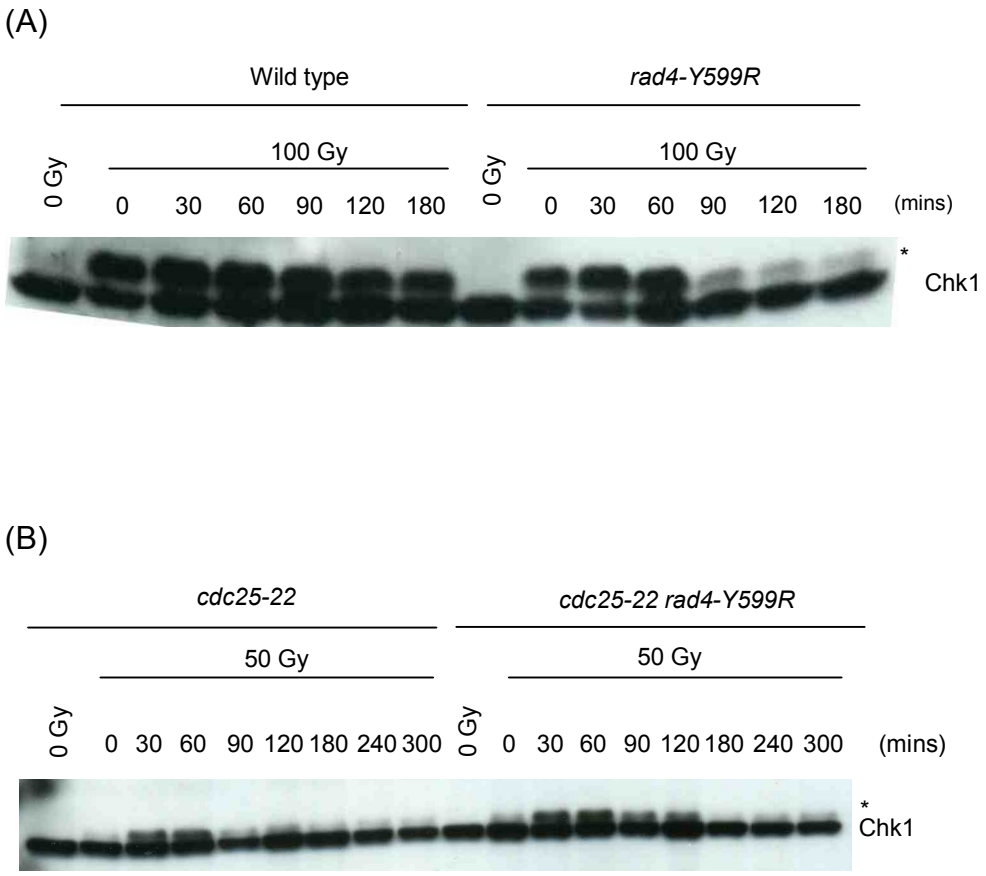

Figure 4-8- The maintenance of Chk1 phosphorylation in response to IR in *rad4-Y599R*

Chk1 phosphorylation in response to IR in (A) asynchronous wild-type and *rad4-Y599R* cells and (B) G2 synchronized *cdc25-22* and *cdc25-22 rad4-Y599R.* Cells were synchronized by temperature shift. Cells from (A) and (B) were irradiated with IR using the indicated dose and protein extracted were prepared at different time points after irradiation. Chk1 phosphorylation was analyzed by western blot. * represents the phosphorylation form of Chk1.

compared to wild-type (Fig. 4-8A), is due to the population of cells irradiated while in S-phase.

To explore further the hypothesis that the *rad4-Y599R* Chk1 phosphorylation defect at later time points in response to IR is an S-phase specific effect, irradiation was performed cells synchronized in S-phase. *cdc25-22* and *cdc25-22 rad4-Y599R* cells were synchronized in G2-phase by a temperature shift at 36.5°C and then released into the cell cycle at 25°C. The cell cycle progression was followed by FACS. Cells were irradiated with 50 Gy at 80 minutes after release when cells were in S-phase as indicated by FACS (Fig. 4-9A). Irradiated *cdc25-22* or *cdc25-22 rad4-Y599R* cells have an identical cell-cycle profile by FACS when comparing to un-irradiated cells (Fig. 4-9A). A minor reduction of Chk1 phosphorylation is observed in *rad4-Y599R* cells immediately after IR (at 90 and 120 minutes after release) compared to control cells, but Chk1 phosphorylation in *rad4-Y599R* and control cells then become similar at later time points, corresponding to cells entering G2-phase (Fig. 4-9B, upper panel). Interestingly, H2A phosphorylation is significantly reduced in *rad4-Y599R* compared to control cells (Fig. 4-9B, middle panel). Therefore, while Chk1 phosphorylation is only slightly decreased in *rad4-Y599R*, H2A phosphorylation appears to be more severely compromised. This particular experiment indicates it might be worth following further time points after IR in order to determine whether wild-type cells in *cdc25-22* background have an S/M checkpoint arrest after IR and whether *rad4-Y599R* cells behave as wild-type cells.

Taken together, our data suggest that *rad4-Y599R* cells have a defect in Chk1 phosphorylation at later time points after IR and this defect is specifically due to the cells irradiated while in S-phase at the time of IR. These appear to be defective in Chk1

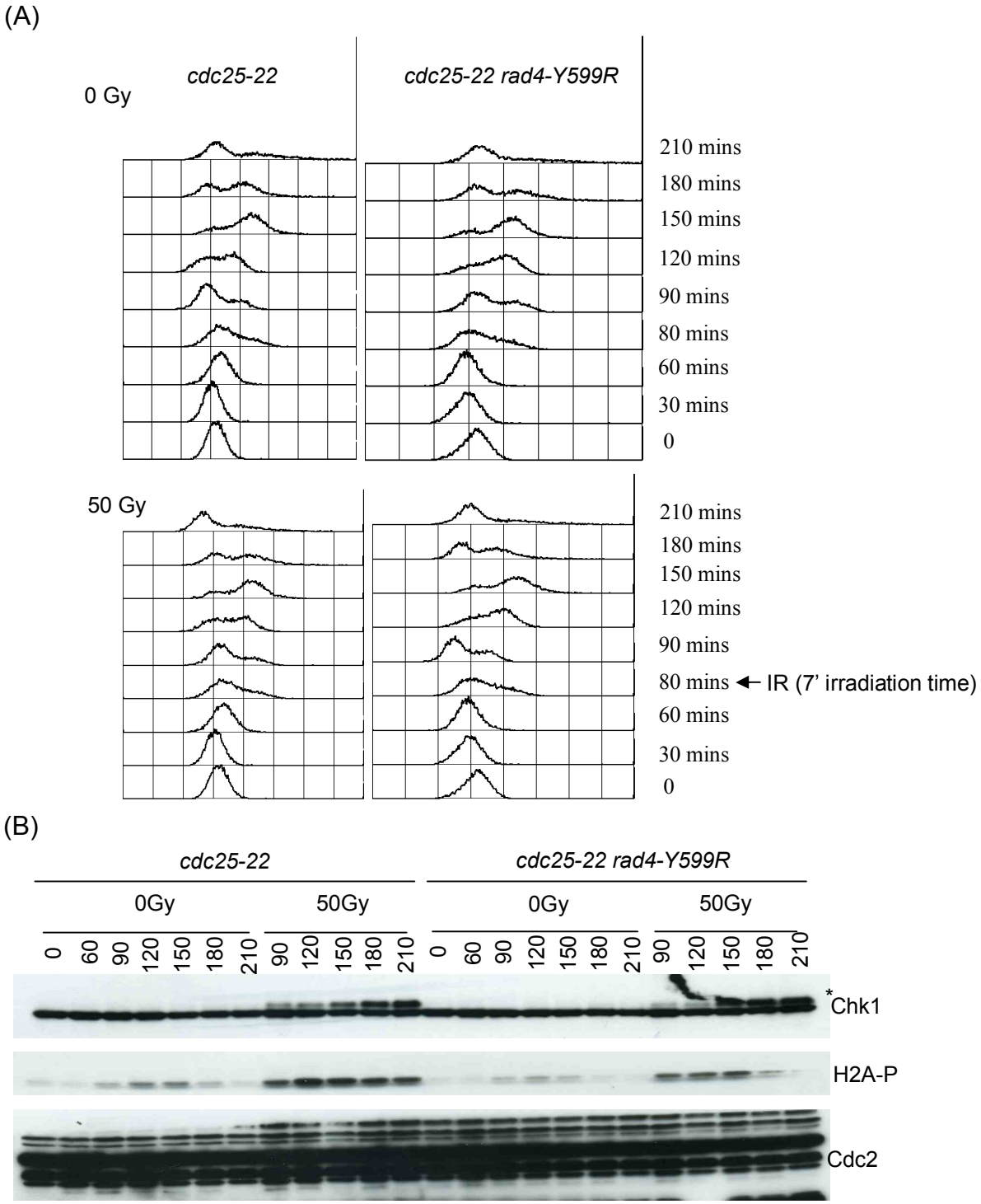

Figure 4-9- Chk1 and H2A phosphorylation in response to IR performed during S-phase

(A) *cdc25-22* and *cdc25-22 rad4-Y599R* cells were blocked by temperature shift, released into G2 phase and cells were irradiated with 50 Gy (mock IR as a control) 80 minutes after release. Cell cycle progression was followed by FACS analysis. (B) Proteins were extracted at different time points after irradiation or mock irradiation. Chk1 and H2A phosphorylation were analyzed by western blot. * represents the phosphorylation form of Chk1. Cdc2 was used as a loading control.

phosphorylation when entering G2/M phase. However, IR delivered in S-phase to synchronous *rad4-Y599R* cells causes a defect in H2A phosphorylation rather than Chk1 phosphorylation. H2A phosphorylation is important for prolonged checkpoint arrest in response to IR (Nakamura et al., 2004). Therefore, this suggests that *rad4-Y599R* cells are indeed compromised in checkpoint maintenance.

(B) In response to UV-irradiation

At the time of starting the experiment of UV-irradiation with different doses in asynchronous wild-type and *rad4-Y599R* cells (Fig. 4-5C), the concept of checkpoint maintenance had not been considered. Therefore, when I performed this experiment (see Chapter 2 Material and Methods 2.3.4 (B) for detail) there was a delay approximately 15~20 minutes between each sample before harvesting cells after UV-irradiation. In order to investigate the role of the AAD in checkpoint maintenance in response to UV, asynchronous cells were evenly spread on the YEA plates, exposed to 100 J/m^2 of UV-irradiation, and Chk1 phosphorylation was followed at different time points after UV-irradiation. When I performed the experiment to study the function of *rad4-Y599R* cells in checkpoint maintenance after UV, the timing of collecting each sample was done precisely. Chk1 phosphorylation occurs approximately at same time, 20 minutes after damage, in both wild-type and *rad4-Y599R* cells and is very similar in wild-type and *rad4-Y599R* cells 20 and 30 minutes after UV (Fig. 4-10A). In a similar experiment studying later time points after UV-irradiation, while Chk1 phosphorylation occurred at the same time for both wild-type and *rad4-Y599R* cells, Chk1 phosphorylation decreased earlier in the *rad4-Y599R* mutant (Fig. 4-10B). However, when repeating this experiment, this significant difference in Chk1 phosphorylation between wild-type and *rad4-Y599R* mutant was not detected.

Figure 4-10- The maintenance of Chk1 phosphorylation in response to UV-irradiation in *rad4-Y599R*
(A)(B) Asynchronous wild-type and *rad4-Y599R* cells were irradiated with 100 J/m^2 of UV and the proteins were extracted at different time points after irradiation. (A) and (B) are two independent experiments. (C) *cdc25-22* and *cdc25-22 rad4-Y599R* cells were synchronized in G2-phase by block and release and immediately irradiated with 10 J/m^2 of UV or mock irradiated. Cell cycle progression was followed by FACS analysis and the proteins were extracted at different time points after irradiation. Chk1 phosphorylation was analyzed by western blot. * represents the phosphorylation form of Chk1.

(A)

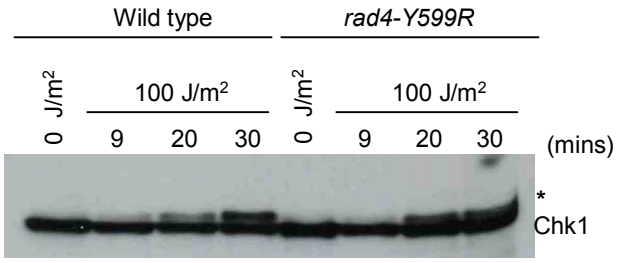
Wild type
rad4-Y599R
0 J/m2
100 J/m2
0 J/m2
100 J/m2
0 9 20 30 0 9 20 30 (mins)
*
Chk1

(B)

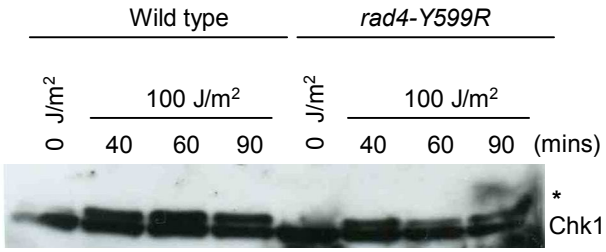
Wild type
rad4-Y599R
0 J/m2
100 J/m2
0 J/m2
100 J/m2
0 40 60 90 0 40 60 90 (mins)
*
Chk1

(C)

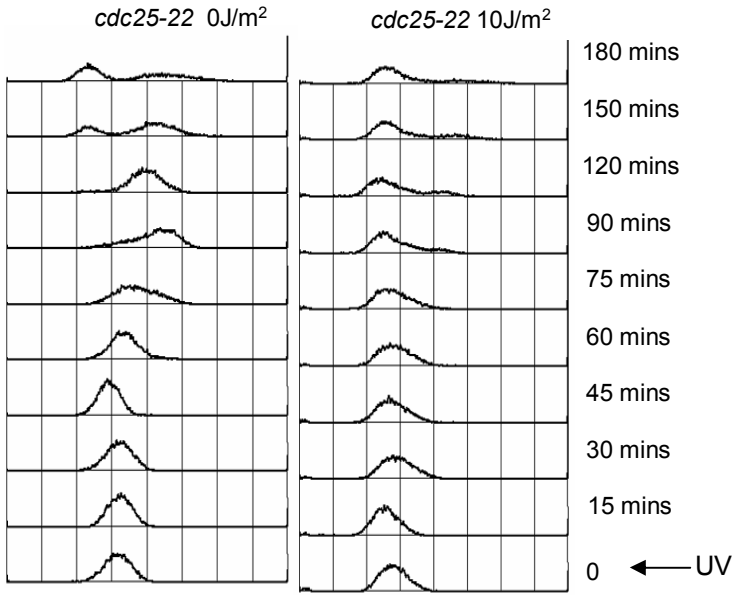
cdc25-22 0J/m2
cdc25-22 10J/m2
180 mins
150 mins
120 mins
90 mins
75 mins
60 mins
45 mins
30 mins
15 mins
0
UV

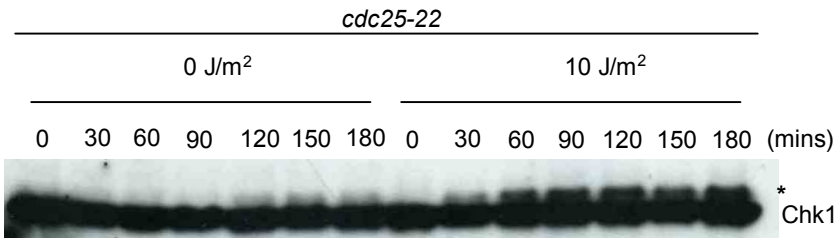
cdc25-22
0 J/m2
10 J/m2
0 30 60 90 120 150 180 0 30 60 90 120 150 180 (mins)
*
Chk1

In order to distinguish whether Chk1 phosphorylation after UV-irradiation in *rad4-Y599R* was due to the population of G2-phase cells or S-phase cells at the time of irradiation, G2-phase cells synchronized by *cdc25-22* mutant temperature shift were irradiated with 50 J/m^2 of UV. Chk1 phosphorylation in wild-type cells persisted for three hours after exposure to UV (data not shown). This meant we could not interpret the experiment. Therefore, a similar experiment using wild-type (*rad4*$^+$) cells exposed to a lower dose of UV-irradiation (10 J/m^2) was performed to establish how long Chk1 phosphorylation would persist. Unexpectedly, Chk1 phosphorylation in wild-type cells persists for three hours after UV damage, similar to the situation with a high dose of UV-irradiation. As we know from a previous result (Fig. 4-3), wild-type cells recover from checkpoint arrest at 120 minutes after 50J/m^2 of UV-irradiation. In contrary to the data presented here, it might be due to the fact that I spread cells on the Hybond™-ECL™ nitrocellulose membrane instead of a PVDF membrane filter or YEA plates to irradiate with UV when I performed this particular experiment (see Chapter 2 Material and Methods 2.3.4 (C) for detail). This technique might affect the cell sensitivity to UV-irradiation. Thus, we could not conclude that *rad4-Y599R* mutant is compromised for maintenance of Chk1 phosphorylation in response to UV-irradiation.

4.1.9 *rad4 AAD* mutant is sensitive to DNA damage occurring in S phase

In response to UV, HU, and CPT, but not IR, H2A phosphorylation is significantly reduced in asynchronous *rad4-Y599R* cells when compared to wild type (Valerie Garcia, personal communication). This suggests that the *rad4 AAD* mutant is defective in dealing with DNA damage generated specifically in S phase. Furthermore, H2A phosphorylation is reduced in *rad4-Y599R* cells when compared to wild-type cells in response to both UV- and ionizing-irradiation when cells are synchronized in S phase with HU. This reduction was not observed when *rad4-Y599R* cells synchronized in G2

phase. These experiments support the hypothesis that *rad4-Y599R* cells have a defect in dealing with DNA damage occurring specifically in S-phase but not in G2-phase cells.

As shown before, asynchronous *rad4-Y599R* cells are not significantly sensitive to IR (Fig.4-2C) and when IR is performed on G2 cells, no Chk1 phosphorylation defect and no checkpoint defect are detected (Fig. 4-6A.B). In order to determine whether the sensitivity of *rad4-Y599R* cells to DNA damage is specific to the population of S-phase cells, cell survival was measured after cells were challenged with IR during S-phase. Firstly, *cdc25-22* or *cdc25-22 rad4-Y599R* cells were blocked in G2 at 36.5°C, released at 25°C and the cell cycle progression was monitored by FACS analysis. The FACS profile shows that both *cdc25-22* and *cdc25-22 rad4-Y599R* cells are synchronized in G2-phase and progress into the cell cycle with an almost identical profile (Fig. 4-11A). The majority of *cdc25-22* and *cdc25-22 rad4-Y599R* cells progressed into S-phase 60 minutes after release and S-phase is completed within 30 minutes. Cells were collected and irradiated with 100 Gy of IR at 60 (early S-phase) and 75 minutes (middle of S-phase) after release according to FACS analysis. Cells were plated on YEA plates and cell survival was scored after incubating cells at 30°C for 3 days. Interestingly, both *cdc25* and *cdc25-22 rad4-Y599R* were highly sensitive when IR was delivered 60 minutes after release. *cdc25-22* cells show 7.1% of cell viability and *cdc25-22 rad4-Y599R* cells show 2.4% of cell viability (Fig. 4-11B). When IR was delivered 75 minutes after release, *rad4-Y599R* survival is significantly reduced (18.6%) compared to wild-type cells (57.2%) (Fig. 4-11B). This demonstrates that, although the *rad4 AAD* mutant exhibits a very mild sensitivity to IR when irradiated as asynchronous cells (70% cells in G2) (Fig. 4-2C), the *rad4 AAD* mutant exhibits a significant sensitivity when IR is performed during S-phase. These suggests that the Rad4 AAD is most important for cells while they are in S-phase for resistance to DNA damage, and that

(A)

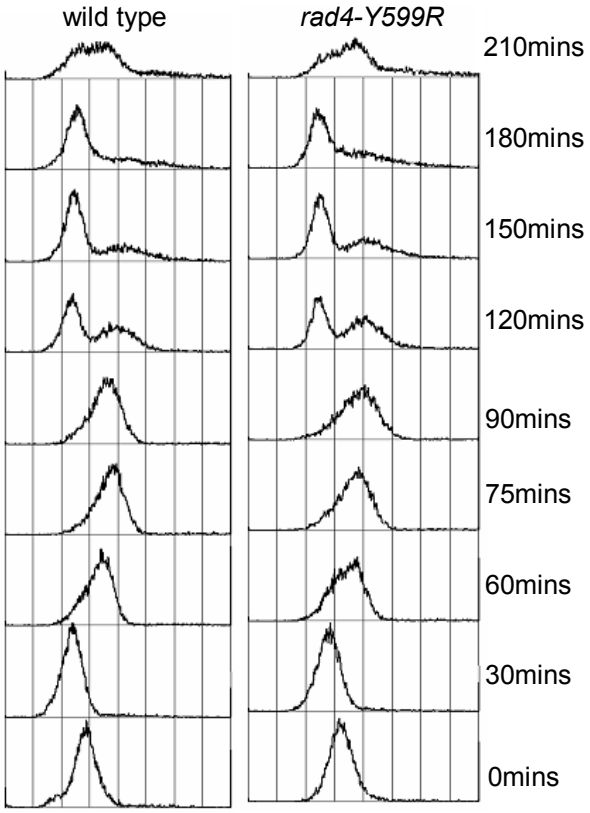

(B)

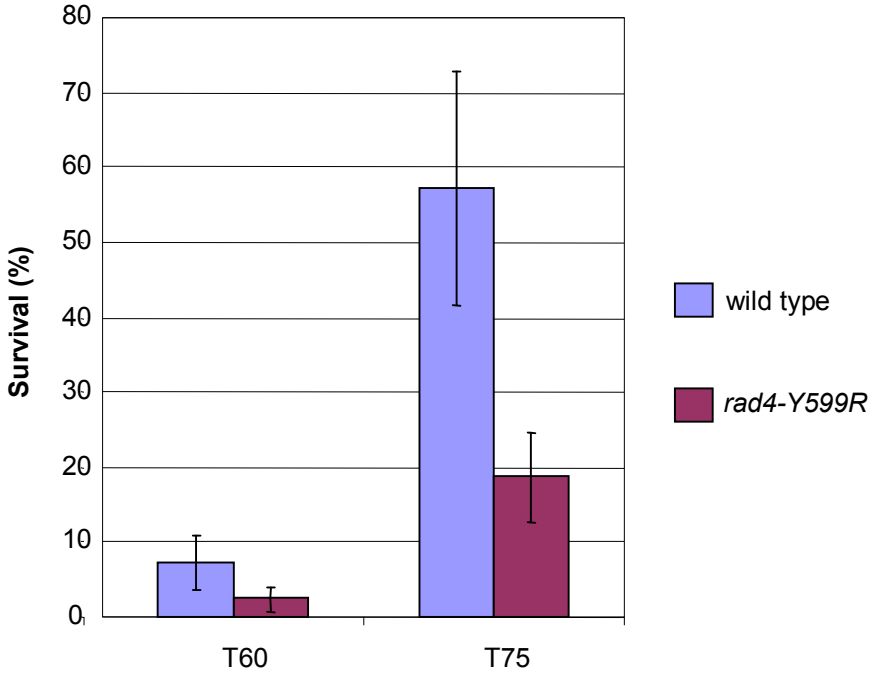

Figure 4-11- Survival of *cdc25-22 rad4-Y599R* cells in response to IR performed during S phase
(A) *cdc25-22* and *cdc25-22 rad4-Y599R* cells were blocked by temperature shift at 36.5˚C and then released in G2 phase at 25˚C, and cell cycle progression was followed by FACS analysis. (B) *cdc25-22* and *cdc25-22 rad4-Y599R* cells were irradiated in S phase with 100 Gy at two time points (60 and 75 minutes after release) and plated onto YEA. Cell survival was calculated relative to non-irradiated cells by counting the resulting colonies after 3 days at 30˚C. The data shown is representative of an average of two individual experiments.

this might link to an important role of the Rad4 AAD in H2A phosphorylation when DNA damage occurs in S-phase.

4.2 Functional characterization of Rad4 C-terminal non-BRCT tail

4.2.1 Rad4 C-terminal truncation mutants are slightly sensitive to DNA damage

Most of the Cdc2 phosphorylation sites, the RXL motif (detailed in Chapter 3), as well as the AAD are located on the unstructured C-terminal tail of Rad4 (Fig. 4-2A). To further understand the function of this C-terminal tail, we performed a series of truncations (Fig. 4-12A). The $Rad4^{1-487}$ protein is truncated right after the fourth BRCT domains (so the whole unstructured C-terminal tail is deleted); $Rad4^{1-580}$ is truncated just before the AAD and $Rad4^{1-610}$ is truncated after the AAD. These constructs were integrated into the genome using the RMCE system (described in Chapter 2), and therefore the truncated Rad4 proteins are expressed from the endogenous *rad4* promoter. Two groups have previously shown that the C-terminus of Rad4 is not essential for cell survival (Fenech et al., 1991; Saka and Yanagida, 1993). Consistently with these observations, none of our three truncations affect cell viability (Fig. 4-12B). Next, we investigated whether the expression of the three different C-terminal truncated proteins conferred sensitivity to DNA damaging agents. All C-terminal truncations confer a mild sensitivity to the DNA damaging agents, but are not sensitive to IR. This suggest that the C-terminus of Rad4 is only partially required for DNA damage responses. This phenotype in response to genotoxic agents is similar to *rad4 AAD* mutant. However, the extent of the truncation does not affect cells sensitivity to DNA damage, and whether or not the truncation including the AAD makes no differences. This is probably because that these truncations disrupt the Rad4 interaction with Rad3 by altering the folding of

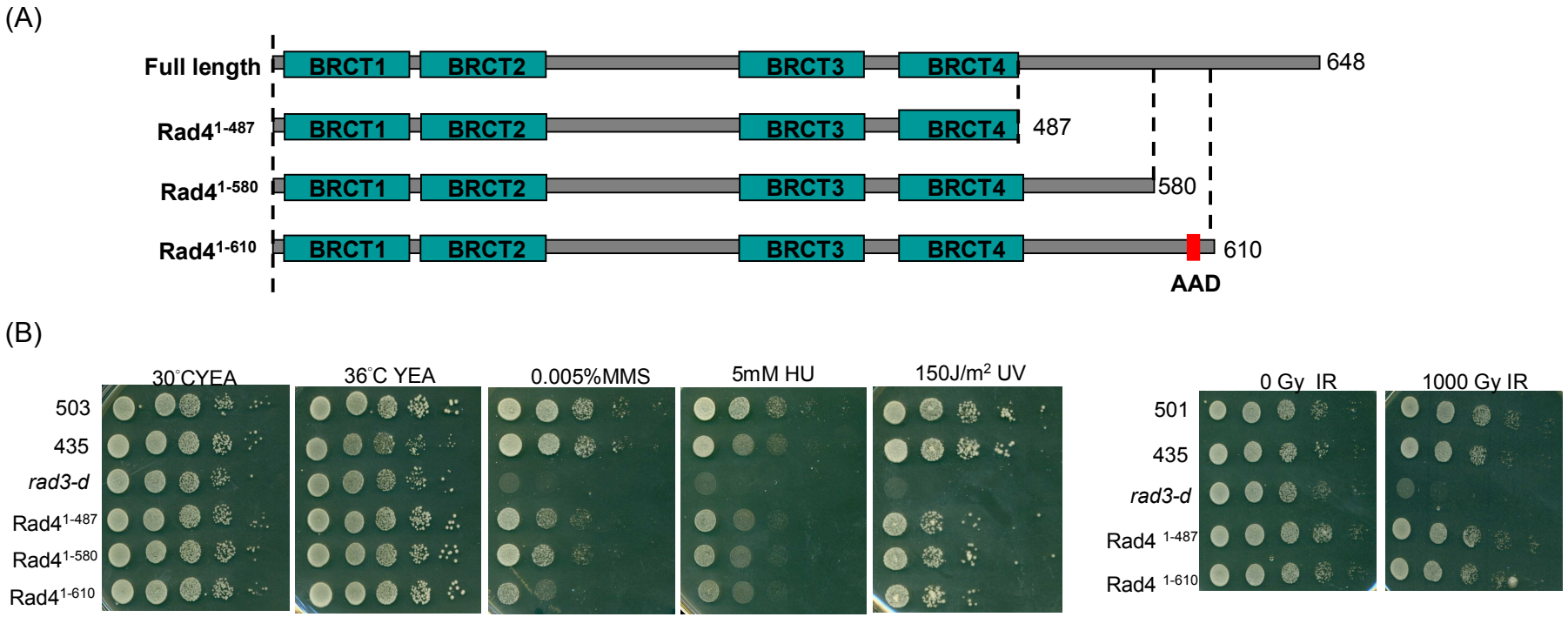

Figure 4-12- Functional analysis of the Rad4 C-terminal truncations
(A) Schematic representation of full length Rad4 protein and three C-terminal truncations, Rad4$^{1-487}$, Rad4$^{1-580}$, and Rad4$^{1-610}$.
(B) Spot tests of the cells expressing the Rad4 C-terminal truncations. 10-fold serial dilutions starting from 1x10^{7}cells/ml were spotted onto YEA plates and exposed to UV or to different genotoxic agents with the indicated doses. The plates were incubated at 30°C for 3 days or 36°C. “501” and “435” are *rad4*$^{+}$ and *rad4*$^{+}$ (RMCE) controls, respectively.

the AAD.

4.2.2 Overexpression of Rad4 C-terminus does not affect cell viability

The overexpression of the Rad4 C-terminus(Rad4$^{491-648}$), was previously found to severely inhibit cell growth (Saka et al., 1994). They suggested that this might be caused by that RKLRRR sequences at Rad4 C-terminal tail might serve as NLS (nuclear localization signal) binding to the chromatin, a function requiring a putative NLS. To further understand the function of the C-terminal phosphorylation sites and the AAD, we overexpressed the unstructured C-terminal tail of Rad4, wild type or mutated at the sites or domains mentioned above, in *S. pombe* cells. We hypothesize that because overexpression of Rad4 C-terminal fragment inhibits cell growth, we could assess the function of different sites or domain by studying their effect on survival, *i.e.* an abolishment or a reduction of the dominant negative phenotype of the wild type fragment. The C-terminal part of Rad4 (Rad4$^{488-648}$), starting right after the fourth BRCT domain up to the stop codon, was amplified by PCR (Fig. 4-13A). The PCR fragment was cloned into a pREP41 vector in fusion with the NLS and a TAP tag, and the resulting plasmid was introduced into wild-type yeast cells. C-terminal Rad4 expression was under the control of the thiamine-repressible *nmt41* promoter. Surprisingly, cells overexpressing Rad4 C-terminal fragment grow normally upon spot test (Fig. 4-13B) and the cell morphology is normal (Fig. 4-13C), similar to the control cells transformed with an empty vector. C-terminal Rad4 overexpression was confirmed by western blot in order to rule out the possibility of defective expression. As a depicted in Fig. 4-13D, the C-terminus of Rad4 was expressed (5th and 6th lanes correspond to the cells transformed with C-terminal of Rad4) while no Rad4-TAP is detected in cells transformed with an empty vector (1st and 2nd lanes). The discrepancy between our result and those from Saka et al. could have been explained by their use of a pREP1

Figure 4-13- Functional analysis of the C-terminal Rad4 overexpression (A) Schematic representation of Rad4 protein. Rad4$^{488-648}$ (yellow) was overexpressed in *S. pombe*. (B) Spot tests of the cells overexpressing C-terminal Rad4 to analyze the sensitivity to DNA damage and the DNA replication inhibitor HU. Wild-type cells were transformed with the empty vector (pREP41 with NLS-TAP) or the plasmid carrying C-terminal Rad4 (pREP41 with C-Rad4-NLS-TAP) . Two transformants for each transformation were spotted on the plates in the absence thiamine for overexpression and exposed to UV or different genotoxic agents. The plates were incubated at 30°C for 5 days. (C) The cells were fixed in 100% methanol, stained with DAPI and calcofluor after induction and the images were taken under a fluorescence microscope. (D) Overexpression of C-terminal Rad4 in the pREP41 vector with a TAP tag and NLS (about 42 KDa) was verified by western blot. Extracts were from cells transformed with C-terminus Rad4 (lane 5,6,7,8) or the empty vector used as a negative control (lane 1,2,3,4) or a strain carrying a Rad4-TAP tag in the genome as a positive control (lane 9). (E) Wild-type cells transformed with vector only (pREP1) or a vector carrying C-terminal Rad4 grew in the absence or presence of thiamine at 30°C. Cell morphology was observed under fluorescence microscope.

(A)

(B)

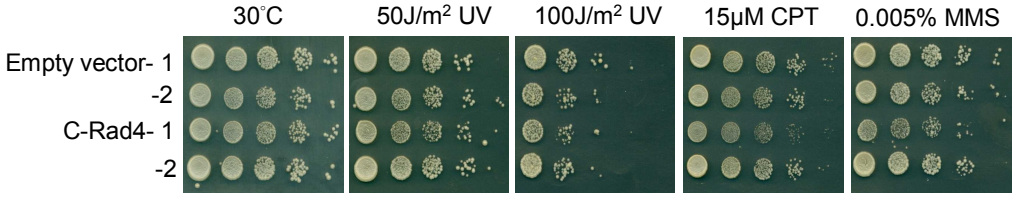

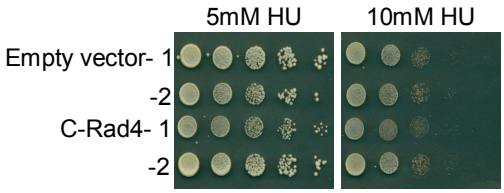

(C)

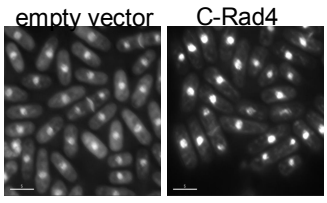

pREP41-NLS-TAP

(D)

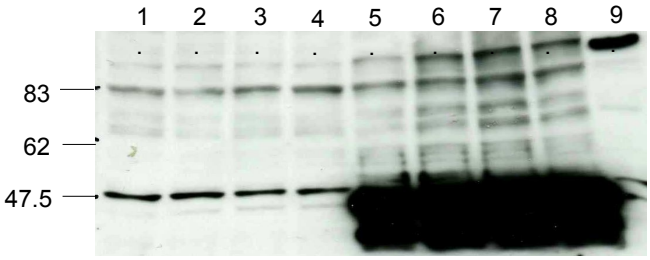

Lane 1.2.3.4 : Empty vector (pREP41)

Lane 5.6.7.8 : pREP41-C-Rad4

Lane 9. : control (Rad4-TAP)

(E)

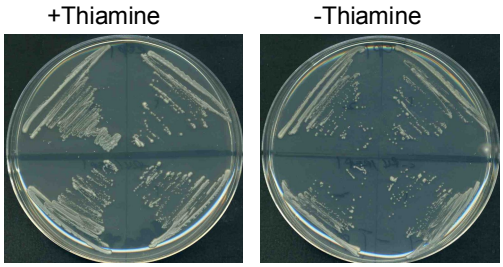

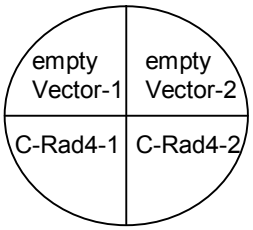

pPREP1

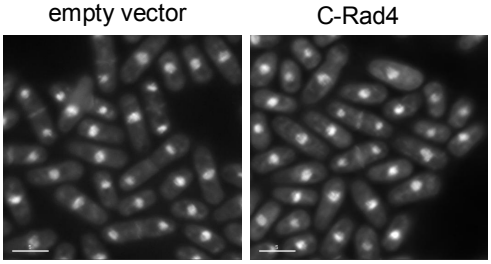

pREP1

vector, in which C-terminal Rad4 expression is controlled under the *nmt1* promoter, allowing a higher expression level of C-terminal Rad4. Furthermore, the absence of additional of the NLS was performed in their experiment, *i.e.*, the cytotoxicity being elicited by an increased level of Rad4 C-terminal in the cytoplasm. To address this possibility, Rad4 C-terminal fragment was overexpressed in a pREP1 vector (under the control of a *nmt1* promoter) without an addition of the NLS, as described in the Saka et al. Cells overexpressing the Rad4 C-terminus under the control of the *nmt1* showed no cell growth defect compared to control cells transformed with the empty vector (Fig. 4-13E, upper panel). Again, cell morphology observed under microscopy was similar to wild-type cells (Fig. 4-13E, lower panel). Since the expression of Rad4 C-terminal fragment did not affect cell growth, we were unable to study the function of specific domains or residues in the unstructured C-terminal part of Rad4.

4.3 Conclusion

In this chapter, the function of Rad4 AAD is characterized in *S. pombe* cells. *S. pombe* strains mutated in the AAD (*rad4-Y599R* and *rad4-AAD*) are slight sensitive to UV, MMS and HU. Both mutants do not completely prevent Rad3-mediated G2/M checkpoint activation after DNA damage. However, the sensitivity to DNA damage increases in the *rad4-Y599R* mutant when DNA damage occurs in S-phase. In addition, the *rad4-Y599R* mutant is significantly compromised for H2A phosphorylation when DNA damage occurs in S-phase. We also show that *in vitro* Rad4 physically associates with Rad3 in a Rad4 AAD-dependent manner. Interestingly, *S. pombe* cells expressing the Rad4 C-terminal truncations, whether the AAD is retained or not, show similar effects for sensitivity to DNA damage as the *rad4-Y599R* mutant.

Chapter 5 Role of Rad4^{TopBP1} ATR-activating domain in a LacI/LacO artificial checkpoint induction system

5.1 Introduction

The tethering of both Ddc2 and Ddc1 to Lac operator (LacO) repeats integrated in the genome is sufficient to cause Rad53 and Rad9 phosphorylation and maintain a G2/M arrest in the absence of exogenous DNA damage in *S. cerevisiae* (Bonilla et al., 2008). In mammalian cells, Soutoglou and Misteli have also successfully established a system to activate the DDR signaling (*i.e.*, H2AX phosphorylation) by targeting proteins involved in DSBs signaling or repair, (*i.e.*, Mre11, Nbs1, ATM, and MDC1) to LacO repeats integrated in a chromosome in mouse cells (Soutoglou and Misteli, 2008). These two pieces of work suggest that the physical interaction of DNA damage checkpoint proteins or DNA repair proteins with chromatin is a key step in activation of the DDR. In essence, this strategy mimics the accumulation of checkpoint or repair proteins triggered by DNA lesions. However, neither the groups have tested the role of mammalian TopBP1 or *S. cerevisiae* Dpb11, the homologues of *S. pombe* Rad4.

Therefore, we were interested in addressing the role of Rad4 in the artificial checkpoint induction system. We first tried to establish this artificial induction checkpoint system in the absence of exogenous DNA damage in *S. pombe* cells by targeting of engineered checkpoint proteins to LacO array integrated in a chromosome (Fig. 5-1). Checkpoint proteins (Rad3, Rad9 and Rad4) were engineered to fuse a GFP-LacI-NLS tag and expressed in a strain carrying the LacO array in the genome. If this artificial system successfully induces checkpoint activation, it suggests that this engineering of checkpoint proteins can bypass the requirement of exogenous DNA damage. Besides,

Figure 5-1- Schematic of the LacI/LacO artificial induction checkpoint system
Three vectors expressing Rad3 in fusion with GFP-LacI-NLS, Rad9 with GFP-LacI-NLS, and Rad4 with GFP-LacI-NLS were constructed. Fusion proteins were expressed in *S. pombe* cells harboring the 256 copies of LacO repeats integrated at the ura4 locus on chromosome III. In this study, we examine whether expression of a single checkpoint fusion protein GFP-LacI-Rad3, GFP-LacI-Rad9 or Rad4-GFP-LacI, or co-expression of GFP-LacI-NLS-Rad9 or Rad4-GFP-LacI-NLS in combination with GFP-LacI-NLS-Rad3 is able to induce checkpoint activation.

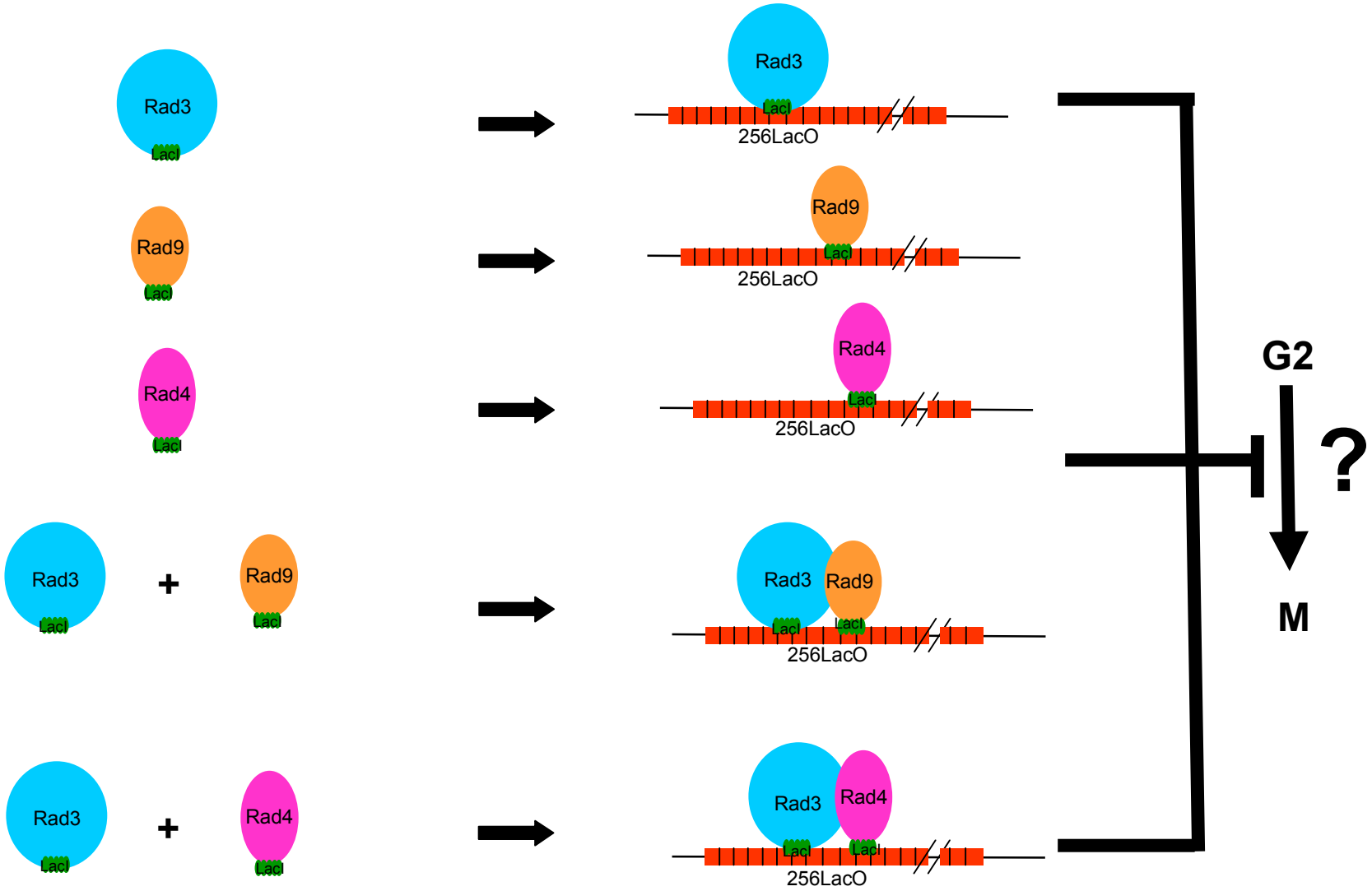
Rad3
LacI
Rad9
LacI
Rad4
LacI
Rad3
+
Rad9
LacI
LacI
Rad3
+
Rad4
LacI
LacI
Rad3
LacI
256LacO
Rad9
LacI
256LacO
Rad4
LacI
256LacO
Rad3
Rad9
LacI
LacI
256LacO
Rad3
Rad4
LacI
LacI
256LacO
G2
?
M

checkpoint activation in this system occurs in a ssDNA-RPA-independent manner (Bonilla et al., 2008), suggesting that checkpoint activation in the LacI/LacO tethering system is more focusing on a chromatin-mediated checkpoint maintenance/amplification step. Taken advantage of this system, we also studied a role of Rad4 AAD in this artificial checkpoint induction system.

5.2 Engineering of checkpoint proteins applied to an artificial checkpoint induction system

Plasmids for expression of Rad3, Rad3 kinase-dead (KD-D2249E), Rad9 or Rad4 each in fusion to the LacI-NLS-GFP tag have been constructed. N-terminal fusion of GFP-LacI-NLS to Rad3 and Rad9, and C-terminal fusion to Rad4 were designed because N-terminal tagged Rad3 and Rad9 and C-terminal tagged Rad4 previously made in the laboratory were shown to be functional (Valerie Garcia, personal communication).

5.2.1 N-terminal tagging of GFP-LacI-NLS to *rad3* cDNA

The plasmid pT572 carries the GFP-LacI-NLS cassette in which LacI has a 11 base pairs C-terminal deletion to prevent its tetra-merization (Straight et al., 1996). The *Nde*I restriction site present in the GFP was destroyed by site-directed mutagenesis choosing codons (using primers L5 and L6) so as not to change the translation of the amino acids. Then the GFP-LacI-NLS fragment was amplified by PCR using a 5' primer (L7) carrying a *Nde*I restriction site and a 3' primer (L8) carrying a *Nde*I restriction site and eliminating the stop codon present next to the NLS in the template. The PCR product was digested by *Nde*I, and then subsequently cloned into the *Nde*I site present in 5' of *rad3* cDNA in pREP41 (Tony Carr's plasmid collection # 570) (Fig.5-2). Alternatively,

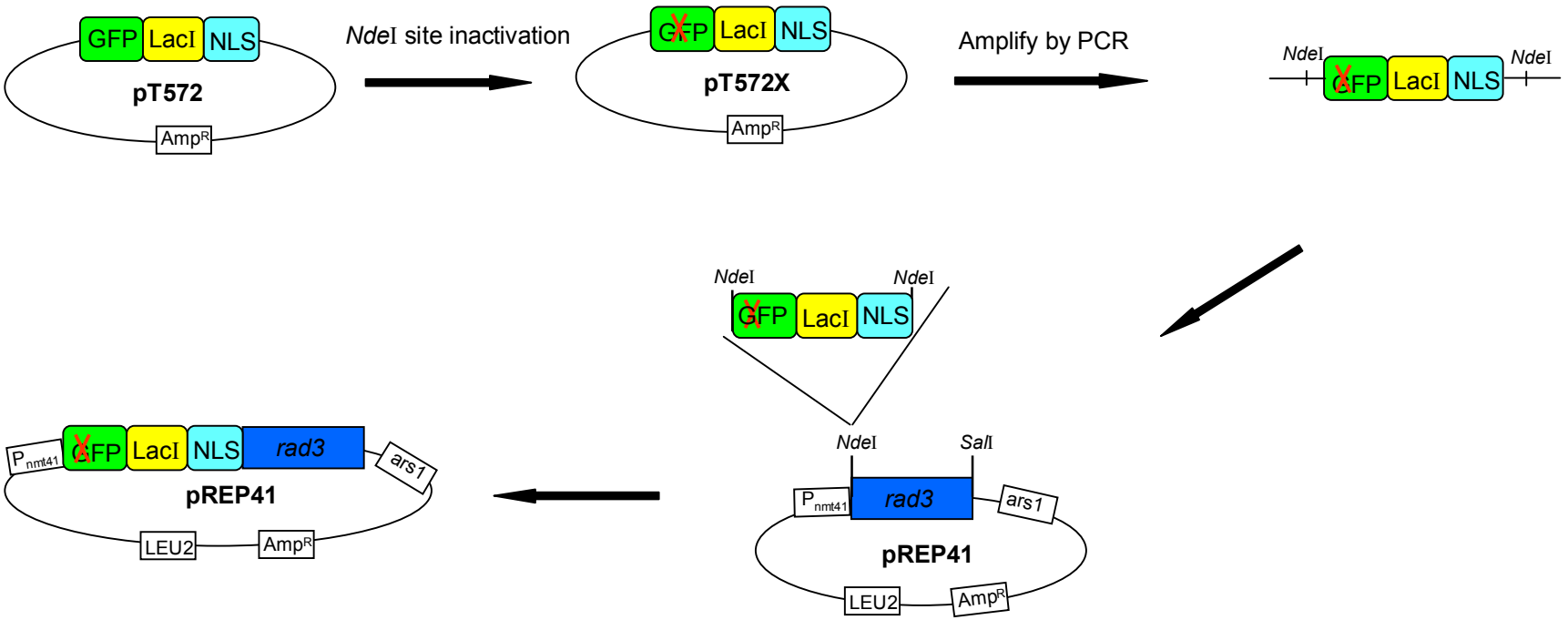

Figure 5-2- Construction of pSJ52 expressing GFP-LacI-NLS-Rad3
The *Nde*I site present in pT572 on the GFP ORF was destroyed by mutagenesis PCR (X). GFP-LacI-NLS was amplified by PCR from pT572X with primers carrying the *Nde*I restriction sites and eliminating the stop codon present in the NLS. GFP-LacI-NLS was cloned into pREP41-*rad3* (from Tony Carr's plasmid collection # 570) at the *Nde*I site located between the *nmt41* promoter and *rad3* open reading frame (ORF).

the GFP-LacI-NLS tag was cloned into 5' of *rad3-KD* cDNA in pREP41 (Tony Carr's plasmid collection # 572).

5.2.2 N-terminal tagging of GFP-LacI-NLS to *rad9* cDNA

The GFP-LacI-NLS fragment described above was cloned into the *Nde*I site of pREP42 (Tony Carr's plasmid collection # 8). Then, *rad9* cDNA (from *rad9* cDNA-GST in pREP41; Tony Carr's plasmid collection # 106) was amplified by PCR with primers (L9 and L10) each carrying a *Sal*I site using plasmid # 106 as a template. This PCR fragment was cloned at the *Sal*I site in 3' of GFP-LacI-NLS tag in pREP42 constructed above (Fig. 5-3).

5.2.3 C-terminal tagging of GFP-LacI-NLS to *rad4* cDNA

The *rad4* gene was amplified by PCR using a 5' primer (cut5-1) with a *Nde*I site and 3' primer (L11) eliminating the stop codon and carrying a *Sal*I site using plasmid # 85 (Valerie Garcia's plasmid collection) as a template, and cloned into the *Nde*I/*Sal*I sites in pREP42. Then the GFP-LacI-NLS PCR fragment was amplified by PCR with primers (L12 and L13) each carrying a *Sal*I restriction site using pT572 as a template. The PCR product was digested by *Sal*I, and then subsequently inserted at the *Sal*I site in 3' of *rad4* in pREP42 (Fig.5-4).

The orientation of all constructions was checked by DNA sequencing. While a Rad3 fusion construct was cloned into a pREP41 vector containing a LEU2 marker, Rad9 and Rad4 fusion proteins, respectively, were cloned into a pREP42 vector containing an ura4 marker. The two different markers are useful for co-selection of co-transformation. Both pREP41 and pREP42 carry the thiamine-inducible *nmt41* promoter.

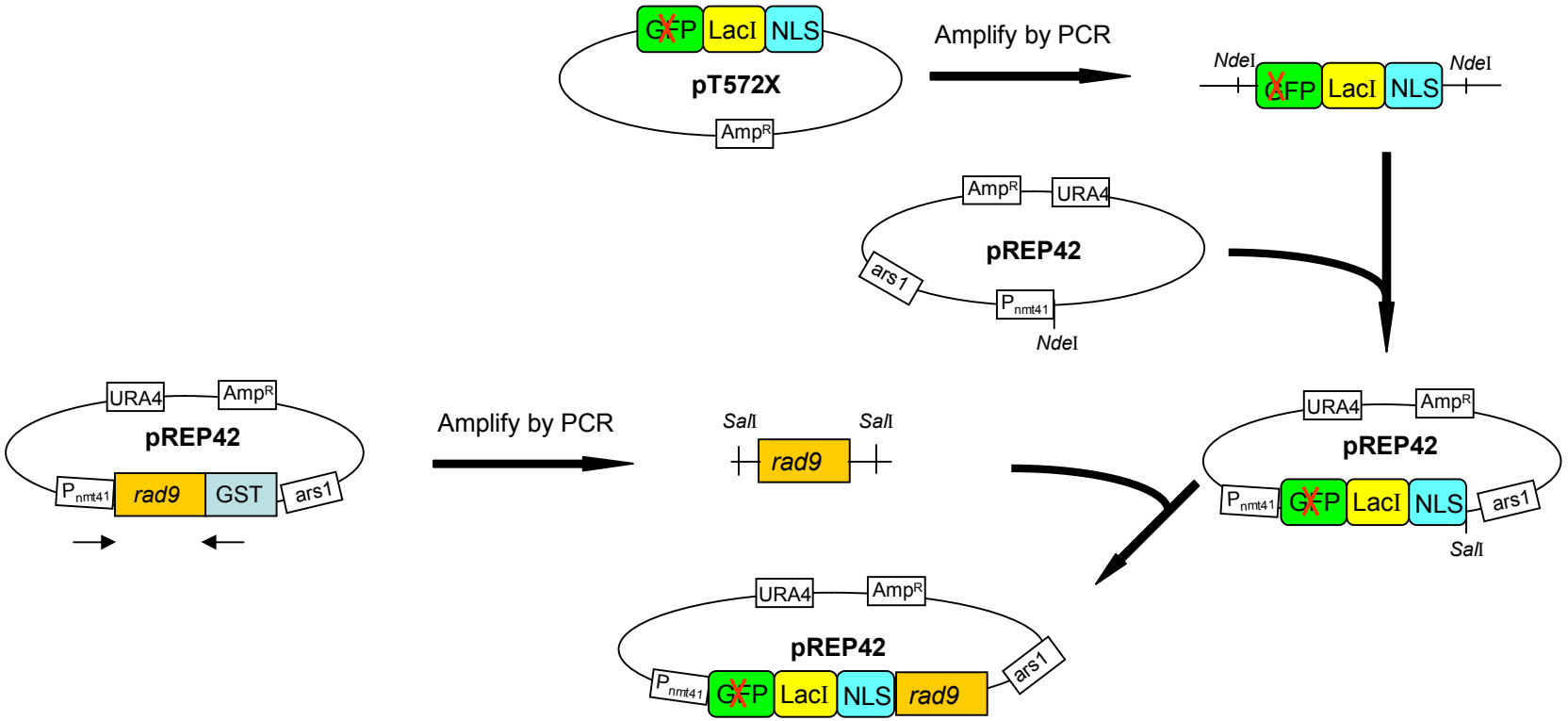

Figure 5-3- Construction of pSJ59 expressing GFP-LacI-NLS-Rad9
GFP-LacI-NLS was amplified by PCR from pT572X (see Fig. 5-2) with primers carrying the *Nde*I restriction sites and eliminating the stop codon present in the NLS. GFP-LacI-NLS was cloned into the *Nde*I site of pREP42 (Tony Carr's plasmid collection # 8). cDNA Rad9 fragment was subcloned into pREP42 containing GFP-LacI-NLS. *rad9* cDNA (from *rad9* cDNA-GST in pREP41; Tony Carr's plasmid collection # 106) was amplified by PCR with primers carrying *Sal*I sites using plasmid #106 as a template. This PCR fragment was cloned at the *Sal*I site in 3' of GFP-LacI-NLS tag in pREP42.

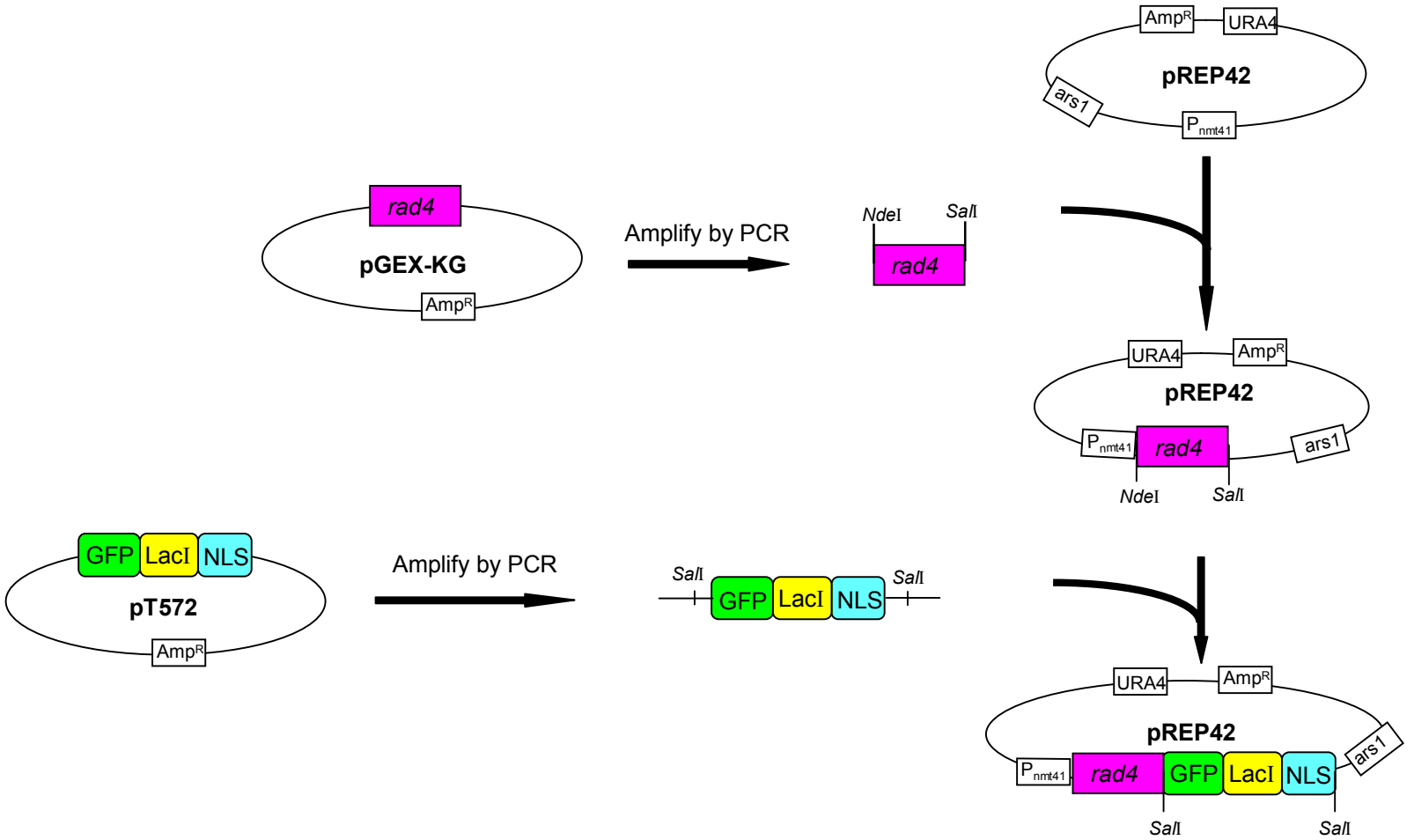

Figure 5-4- Construction of pSJ58 expressing Rad4-GFP-LacI-NLS
The *rad4* gene was amplified by PCR using a 5' primer with a *Nde*I site and 3' primer eliminating the stop codon and carrying a *Sal*I site using a plasmid # 85 (Valerie Garcia's plasmid collection) as a template. This PCR fragment was cloned into the *Nde*I/*Sal*I sites in 3' of the *nmt41* promoter in pREP42 (Tony Carr's plasmid collection # 8). The GFP-LacI-NLS PCR fragment was inserted at the *Sal*I site in 3' of *rad4* in pREP42.

5.3 Rad3, Rad9 or Rad4 in fusion with GFP-LacI-NLS is functional

Wild type cells and a *rad3*-deleted strain were transformed with either the empty vector pREP41 (Tony Carr's plasmid collection # 5) or plasmids for expression of Rad3 (pSJ52) or Rad3 KD (pSJ55) in fusion with GFP-LacI-NLS. Similarly, a wild-type strain and a *rad9*-deleted strain were transformed with either empty vector pREP42 or a plasmid for expression of Rad9 in fusion with GFP-LacI-NLS (pSJ59). For induction, a single transformant was grown in appropriate selective YNB medium (a construct based on pREP41/pREP42 vector: medium in the absence of leucine/uracil) in the absence of thiamine at 30°C for 16 hours. Transformants were spotted on the appropriate selective YNB plates without thiamine supplemented with HU. Alternatively, plates were irradiated with UV. Rad4 is an essential protein; therefore, we tested whether a plasmid for expression of Rad4 in fusion with GFP-LacI-NLS (pSJ58) is functional in a *rad4-116* thermo-sensitive strain. For induction, a single transformant was grown in YNB medium in the absence of uracil and thiamine at 25°C for 16 hours. Similarly, the sensitivity to UV and HU of transformants was tested. Cell growth was checked after incubation for 3~5 days at different temperatures *i*.e., 25°C, 30°C, and 36°C.

The growth of wild type cells expressing GFP-LacI-NLS-Rad3 is similar to wild type cells carrying an empty vector in response to UV, HU or in absence of treatment (control plates). GFP-LacI-NLS-Rad3 suppresses the hypersensitivity to UV and HU of *rad3-d* cells, showing that the fusion construct is functional. Expression of GFP-LacI-NLS-Rad3 KD in wild type cells causes an increasing of sensitivity to UV and HU, indicative of a dominant-negative effect (Fig.5-5A). The growth of wild type cells expressing GFP-LacI-NLS-Rad9 is similar to wild type cells carrying an empty vector in response to UV, HU, and in absence of treatment. GFP-LacI-NLS-Rad9 suppresses the hypersensitivity to UV and HU of *rad9-d* cells, showing that the fusion

Figure 5-5- Functional analysis of checkpoint proteins, Rad3, Rad9, and Rad4 in fusion with GFP-LacI-NLS
(A) pREP41 carrying wild-type Rad3 or Rad3 kinase dead (*rad3-KD*) in fusion with GFP-LacI-NLS was used to transform wild-type or *rad3-d* cells. Empty vector pREP41 was transformed in the cells as a control. The transformants were cultured in the appropriate selection medium in the absence of thiamine for 16 hours in order to allow expression of the fusion proteins, and 10-fold serial dilutions of $1x10^7$cells/ml were spotted on the plates in the absence of leucine and thiamine. To test the sensitivity to UV, the plate was irradiated with $50J/m^2$ UV. To test the sensitivity to HU, plates were supplemented with 5mM HU. Plates were incubated at 30˚C for 2~3 days.
(B) Similarly to (A), pREP42 carrying Rad9 in fusion with GFP-LacI-NLS was used to transform wild-type or *rad9-d* cells. Empty vector pREP42 was transformed in the cells as a control. The sensitivity to UV or HU of transformants was tested as in (A).
(C) Similarly to (A) and (B), pREP42 carrying full-length Rad4 in fusion with GFP-LacI-NLS was used to transform wild-type or thermo-sensitive *rad4-116* cells. Empty vector pREP42 was transformed into cells as a control. The transformants were cultured in the appropriate selection medium (absence of uracil) without thiamine for 16 hours at 25˚C. The sensitivity to UV or HU of transformants was tested. Plates were incubated under 25˚C, 30˚C, 36˚C.

For (A) and (B), two independent transformants were tested at the same time.

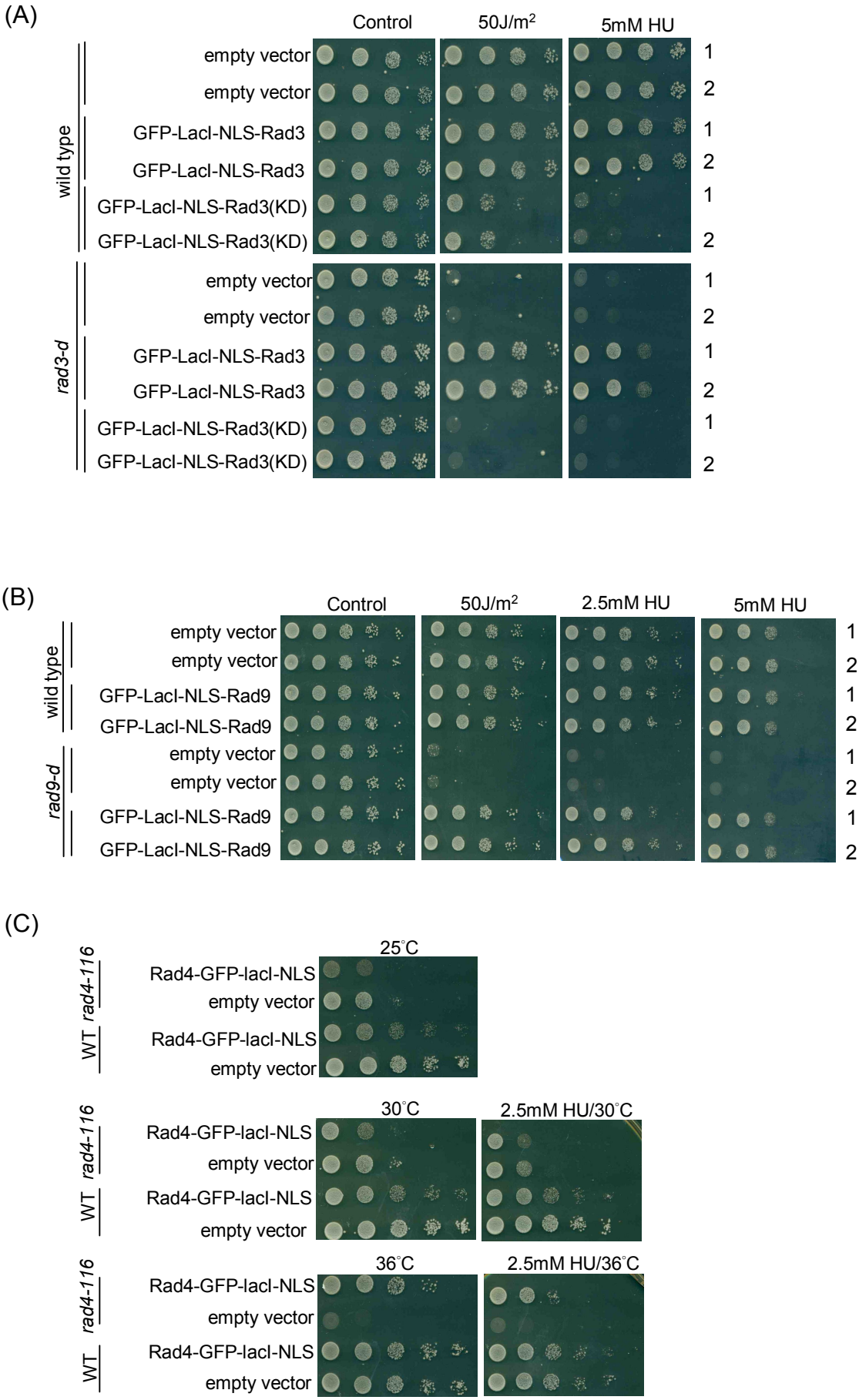
(A)
Control
50J/m2
5mM HU
wild type
rad3-d
empty vector
empty vector
GFP-LacI-NLS-Rad3
GFP-LacI-NLS-Rad3
GFP-LacI-NLS-Rad3(KD)
GFP-LacI-NLS-Rad3(KD)
1
2
(B)
Control
50J/m2
2.5mM HU
5mM HU
wild type
rad9-d
empty vector
GFP-LacI-NLS-Rad9
(C)
25˚C
30˚C
2.5mM HU/30˚C
36˚C
2.5mM HU/36˚C
WT
rad4-116
Rad4-GFP-lacI-NLS
empty vector

construct is functional (Fig.5-5B). Both wild type and *rad4-116* cells with Rad4-GFP-LacI-NLS grow slowly compared to the cells with an empty vector at 25°C and 30°C, suggesting that Rad4 in fusion with GFP-LacI-NLS has a dominant negative effect for cell growth. However, *rad4-116* cells with Rad4-GFP-LacI-NLS had a similar cell growth to wild type cells carrying an empty vector at 36°C, showing that Rad4-GFP-LacI-NLS is able to rescue the growth defect of *rad4-116* cells at 36°C (Fig.5-5C).

Altogether, Rad3, Rad9, and Rad4 in fusion with GFP-LacI-NLS are expressed in *S. pombe* cells, and the constructs are functional since their expressions are able to suppress the phenotypes of the corresponding mutant or deletion strains.

5.4 The tethering of a checkpoint protein fusion causes a cell elongation phenotype

Plasmids for expression of Rad3 (pSJ52), Rad9 (pSJ59), or Rad4 (pSJ58) in fusion with GFP-LacI-NLS were introduced into cells carrying 256 copies of LacO (approximately 10 kb). The LacO array, linked to a NAT resistance marker, was integrated at the *ura4* locus on chromosome III (generated by Takashi Morishita). Empty vectors pREP41 and pREP42 were also used for transformation as controls. A single transformant was grown in the appropriate selective medium in the presence or absence of thiamine for at least 16 hours. Cell morphology was observed under Delta Vision fluorescent microscope. In the absence of thiamine, when the protein fusions are expressed, foci are formed in cells expressing checkpoint protein in fusion with GFP-LacI-NLS (Fig.5-6A bottom panel, red arrow). No foci are formed in the cells carrying the empty vector pREP41 or pREP42 (Fig.5-6A bottom panel). In the presence of thiamine (15 μM), cells transformed with empty vector pREP41 or pREP42, GFP-LacI-NLS-Rad3,

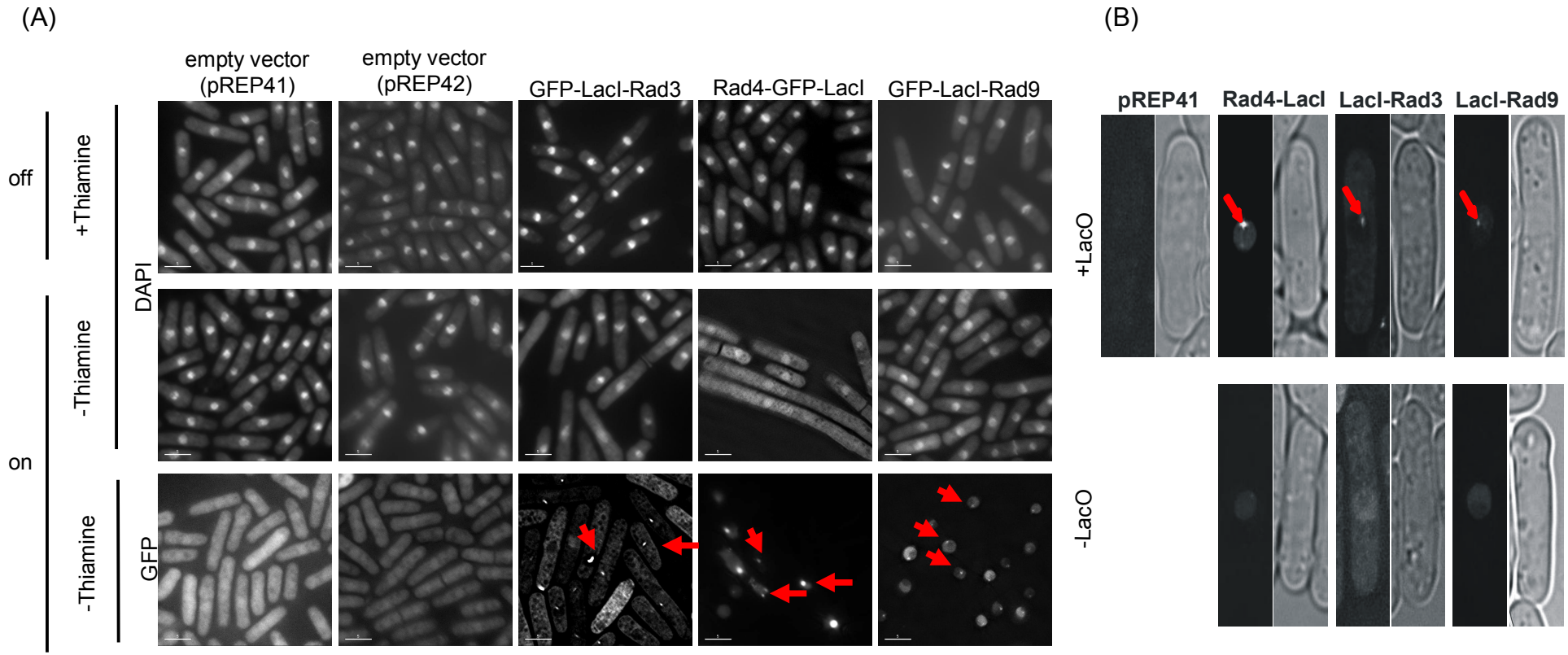

Figure 5-6- Checkpoint protein in fusion with GFP-LacI-NLS form foci in the cells carrying the LacO array
(A) Expression of GFP-LacI-NLS-Rad3, Rad4-GFP-LacI-NLS, or GFP-LacI-NLS-Rad9 was repressed in the appropriate selective medium in the presence of 15 μM thiamine (upper panel) or induced in the appropriate selective medium in the absence of thiamine (middle and lower panels). Empty vectors were used as a control. Cell morphology and nuclear DNA were visualized by staining with DAPI and calcoflour using the DAPI filter (upper and middle panels) and GFP foci formation (red arrow) was observed using the FITC filter (lower panel) under the Delta Vision fluorescent microscope. (B) GFP-LacI-NLS-Rad3, Rad4-GFP-LacI-NLS, or GFP-LacI-NLS-Rad9 was expressed in the cells with (upper panel) or without the LacO array (lower panel). Empty vectors were used as a control. GFP foci was observed using the FITC filter (left panel) and interference contrast microscope (DIC) images of cell morphology is presented at right panel.

Rad4-GFP-LacI-NLS or GFP-LacI-NLS-Rad9 all have normal morphology (Fig.5-6A top panel). In the absence of thiamine, cells transformed with either GFP-LacI-NLS-Rad3 or Rad4-GFP-LacI-NLS show a cell elongation phenotype, a hallmark of checkpoint activation. A cell elongation phenotype was not observed in cells transformed with GFP-LacI-NLS-Rad9 (Fig.5-6A middle panel). Furthermore, a control experiment showed that when GFP-LacI-NLS-Rad3, Rad4-GFP-LacI-NLS or GFP-LacI-NLS-Rad9 was expressed in the cells with or without the LacO array, the foci formation was observed in cells harboring the LacO array (Fig. 5-6B, upper panel) but not in cells without the LacO array (Fig. 5-6B, lower panel). Altogether, these data suggest that expression of a single checkpoint protein (Rad3 or Rad4) is sufficient to arrest cell cycle progression. Bonilla, Melo et al., showed co-localization of Ddc2 and Ddc1 to chromatin is necessary to activate the checkpoint response in *S. cerevisiae*, but this seems not to be the case in *S. pombe* cells.

rad3 and *rad9* (each in fusion with GFP-LacI-NLS), *rad3* and *rad4* (each in fusion with GFP-LacI-NLS), or empty vectors pREP41 and pREP42 were used to co-transform the strain harboring 256 copies of LacO using the *LEU2* and *ura4* markers for co-selection. The transformants were grown in the appropriate selective medium in the presence or absence of thiamine (for the repressed or induced condition, respectively). In the absence of thiamine, co-expression of both GFP-LacI-Rad3 and GFP-LacI-Rad9 or both GFP-LacI-Rad3 and Rad4-GFP-LacI in the cells harboring the LacO array causes a cell elongation phenotype (Fig.5-7 middle panel) and these cells show foci under the microscope (Fig.5-7 right panel, red arrow). In the presence of thiamine, neither elongation nor foci were observed (Fig.5-7 left panel). This suggests that targeting of the checkpoint proteins onto chromatin can successfully induce a robust DNA damage checkpoint response in the absence of exogenous DNA damage.

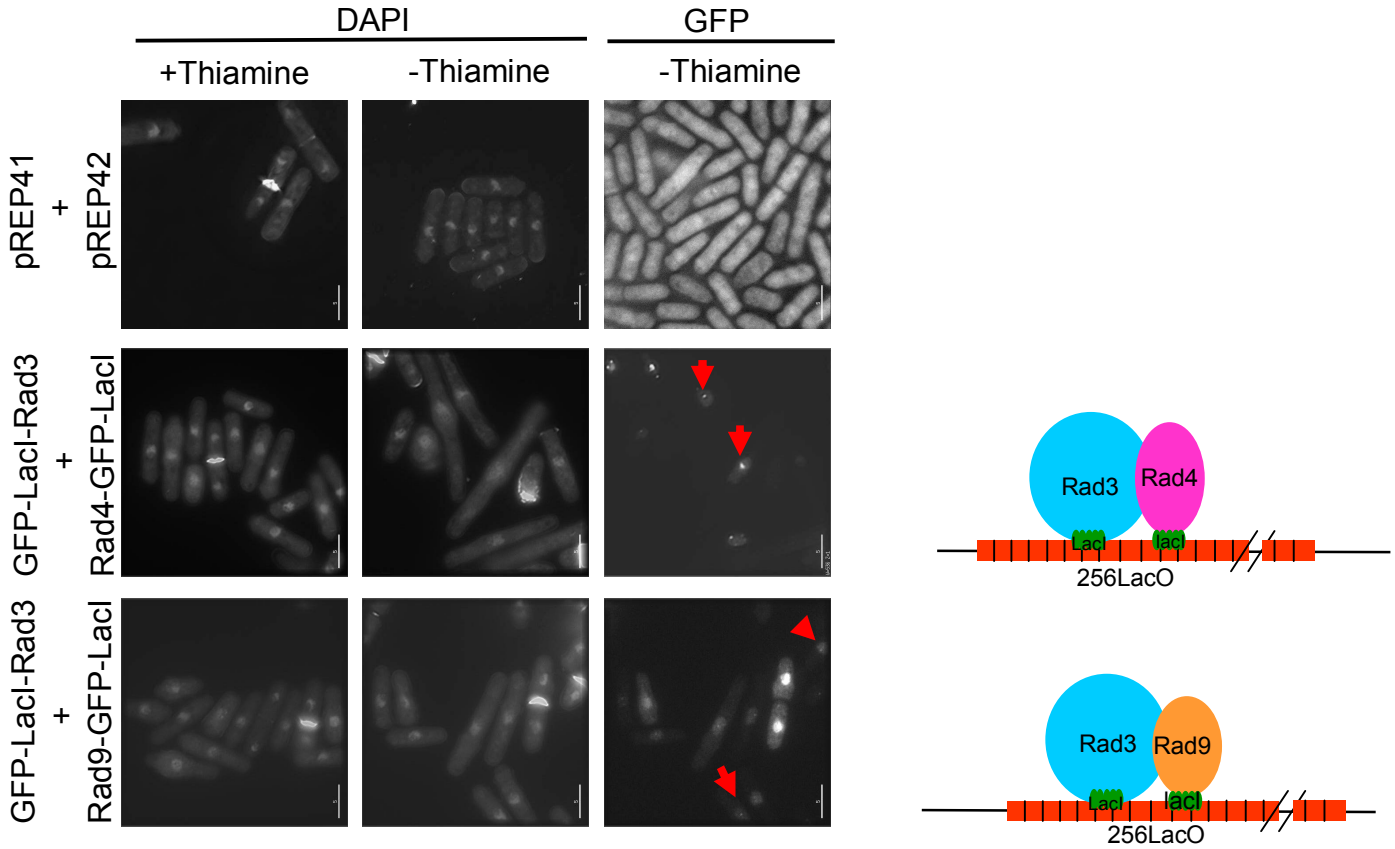

Figure 5-7- Co-expression of two checkpoint proteins in fusion with GFP-LacI-NLS form foci in the cells carrying the LacO array GFP-LacI-NLS-Rad3 and Rad4-GFP-LacI-NLS, or GFP-LacI-NLS-Rad3 and GFP-LacI-NLS-Rad9 were co-repressed in the appropriate selective medium in the presence of 15 μM thiamine (left panel) or co-induced in the appropriate selective medium in the absence of thiamine (middle and right panels). Empty vectors were used as a control. Cell morphology and nuclear DNA was visualized by staining with DAPI and calcoflour using the DAPI filter (left and middle panels) and GFP foci formation was observed using the FITC filter (right panel) under the Delta Vision fluorescent microscope.

5.5 Checkpoint protein tethering to a LacO array induces Chk1 phosphorylation

5.5.1 Single checkpoint protein tethering causes Chk1 phosphorylation

Chk1 phosphorylation was used as a marker of DNA damage checkpoint activation when tethering checkpoint proteins to LacO array integrated in the chromatin. GFP-LacI-NLS alone was first expressed in the cells carrying the LacO array in order to verify that targeting of GFP-LacI-NLS (rather of the checkpoint proteins) does not induce Chk1 phosphorylation. The expression vector pREP41 carrying GFP-LacI-NLS cassette under the control of *nmt41* promoter was introduced into two different strains expressing Chk1-HA with or without the LacO array. The transformants were grown in the appropriate selective medium in the presence of thiamine overnight. The cells were then released in the appropriate selective medium in the absence of thiamine. Cells were collected 20, 22, and 24 hours after induction and before induction (time=0). Protein extracts were analyzed on SDS-PAGE and Chk1 phosphorylation was detected using an anti-HA antibody. The cells carrying the LacO array have a slight elevated level of Chk1 phosphorylation compared to a strain without LacO array in the absence of induction (Fig.5-8A). However, Chk1 phosphorylation does not increase when GFP-LacI-NLS is expressed (20, 22, and 24 hours after induction) (Fig.5-8A). The slight basal level of Chk1 phosphorylation observed in the presence of thiamine might be caused by the instability of the LacO repeats and/or the passage of replication fork through the LacO repeats. However, Chk1 phosphorylation observed after induction is not caused by tethering of GFP-LacI-NLS itself. Altogether, these data suggest that targeting GFP-LacI-NLS to LacO array does not significantly induce Chk1 phosphorylation.

To determine whether cells expressing either GFP-LacI-NLS-Rad3, Rad4-GFP-LacI-NLS or GFP-LacI-NLS-Rad9 induce checkpoint activation,

Figure 5-8- Chk1 phosphorylation upon expression of single a checkpoint protein in fusion with LacI
(A) GFP-LacI-NLS was expressed in cells with or without the LacO array in the appropriate selective medium. Cells were collected and proteins were extracted before induction and 20, 22, and 24 hours after induction. (B) GFP-LacI-NLS-Rad3, GFP-LacI-NLS-Rad9, or Rad4-GFP-LacI-NLS were individually expressed in cells with or without the LacO array in the appropriate selective medium in the absence of thiamine. Cells were collected and proteins were extracted at 14, 16, 18, 20 hours after induction. (C) GFP-LacI-NLS-Rad3 was expressed in cells carrying the LacO array either wild type or *hta1-S129A hta2-S128A* background in the appropriate selective medium. Cells were collected and proteins were extracted before induction and at 18, 20, and 22 hours after induction. Chk1 phosphorylation was analyzed by western blot and detected using an anti-HA antibody (upper panel). Cdc2 was used as a loading control (lower panel). * represents the phosphorylation form of Chk1.

(A)

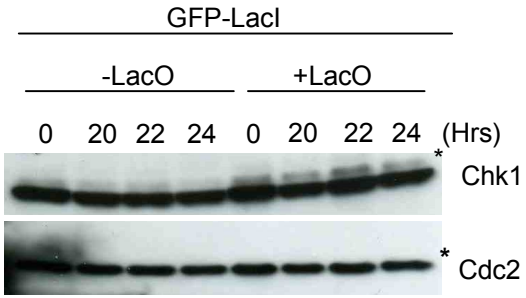
GFP-LacI
-LacO
+LacO
0 20 22 24 0 20 22 24 (Hrs)
*
Chk1
*
Cdc2

(C)

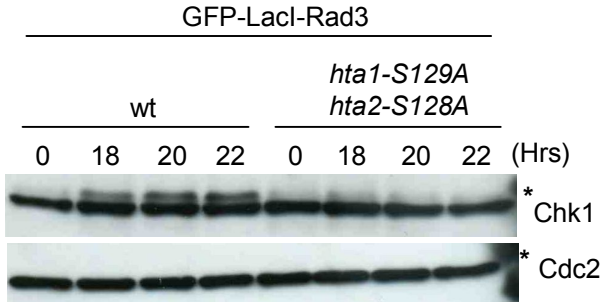
GFP-LacI-Rad3
wt
hta1-S129A
hta2-S128A
0 18 20 22 0 18 20 22 (Hrs)
*
Chk1
*
Cdc2

(B)

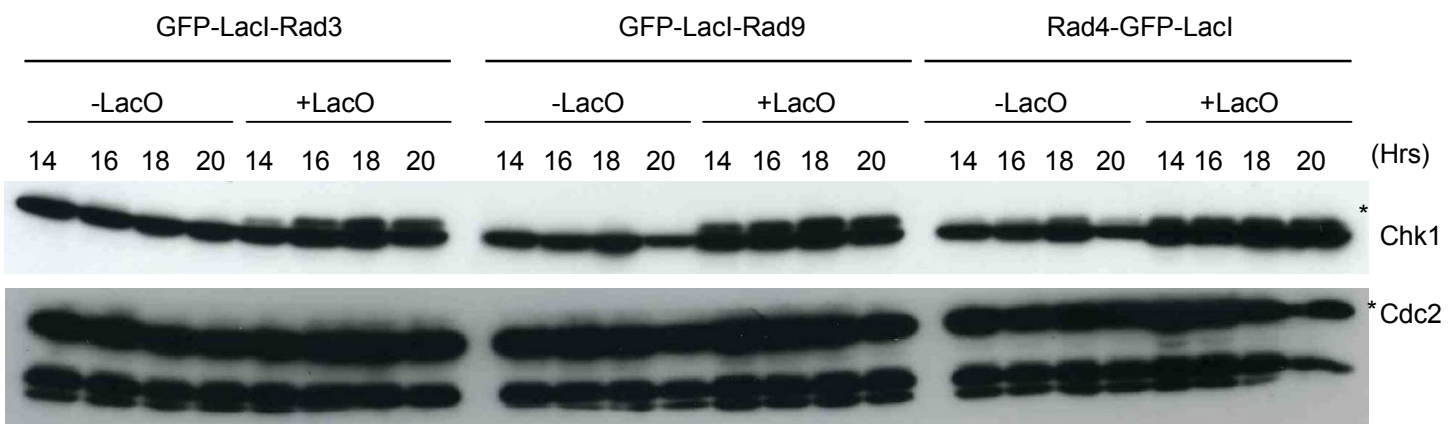
GFP-LacI-Rad3
GFP-LacI-Rad9
Rad4-GFP-LacI
-LacO
+LacO
-LacO
+LacO
-LacO
+LacO
14 16 18 20 14 16 18 20 14 16 18 20 14 16 18 20 14 16 18 20 14 16 18 20 (Hrs)
*
Chk1
*
Cdc2

GFP-LacI-NLS-Rad3, Rad4-GFP-LacI-NLS, or GFP-LacI-NLS-Rad9 was introduced into the two different strain cells expressing Chk1-HA with or without LacO array. The transformants were firstly grown in the appropriate selective medium in the presence of thiamine overnight, and then cells were released in the appropriate selective medium in the absence of thiamine. Cells were collected 14, 16, 18, 20 hours after induction and protein were extracted. As we expected, Chk1 phosphorylation is not detectable in the cells lacking the LacO array and expressing GFP-LacI-NLS-Rad3 or GFP-LacI-NLS-Rad9. However, Chk1 phosphorylation is detected when these fusion proteins are expressed in the cells harboring the LacO array in the genome. This indicates that expression of GFP-LacI-NLS-Rad3 or GFP-LacI-NLS-Rad9 in the cells harboring the LacO array induces checkpoint signaling.

A slight Chk1 phosphorylation is caused by expressing Rad4-GFP-LacI-NLS in the cells lacking LacO array. Rad4 is known to be essential for initiation of DNA replication and to be involved in checkpoint responses. Therefore, cells overexpressing Rad4-GFP-LacI-NLS might generate spontaneous endogenous damage, leading cells to activate the DNA replication and/or DNA damage checkpoint. This might explain why Chk1 is phosphorylated even in the cells lacking LacO array and why a multiple septum is often observed in a single cell overexpressing Rad4. However, a much higher level of Chk1 phosphorylation is induced by expressing Rad4-GFP-LacI-NLS in the cells harboring the LacO array (Fig.5-8B). These results indicate that targeting of GFP-LacI-NLS-Rad3, GFP-LacI-NLS-Rad9 or Rad4-GFP-LacI-NLS to the LacO array is able to activate Rad3-dependent checkpoint signaling in the absence of exogenous DNA damage and importantly, the Chk1 phosphorylation is not due to overexpression of checkpoint proteins.

5.5.2 Checkpoint activation induced by Rad3 tethering is dependent on H2A phosphorylation

DSBs cause histone H2A phosphorylation surrounding ~50 kb bp (*S. cerevisiae*) or 1 megabase (mammalian cells) away on the each side of DSB in a ATR/Mec1/Rad3-dependent manner (Downs et al., 2000; Nakamura et al., 2004; Ward and Chen, 2001). To assess if the checkpoint response induced by Rad3 tethering to LacO repeats requires histone H2A phosphorylation, a H2A phosphorylation site mutant (*hta1-S129A hta2-S128A*, a kind gift from Paul Russell (Nakamura et al., 2004)) carrying LacO array was generated. GFP-LacI-NLS-Rad3 was introduced in wild-type or a H2A phosphorylation mutant strain. The transformants were grown in the appropriate selective medium with thiamine, and then cells were released in the appropriate selective medium in the absence of thiamine. Cells were collected before induction and 18, 20, and 22 hours after induction, and the protein extracts were analyzed for Chk1 phosphorylation by western blotting. Chk1 phosphorylation is induced by expression of GFP-LacI-NLS-Rad3 in wild type but not in the H2A phosphorylation site mutants carrying the LacO array (Fig.5-8C), suggesting that Chk1 phosphorylation occurs in a H2A phosphorylation-dependent manner in this artificial system. In response to DNA damage, H2A phosphorylation is not required for Chk1 activation. Rather phosphorylation of H2A is presumed to play an important role in recruiting and maintaining checkpoint proteins or repair factors at sites of damage (Nakamura et al., 2004). Therefore, Chk1 phosphorylation in the LacI/LacO artificial induction checkpoint system may correspond to chromatin-mediated, ssDNA-RPA-independent checkpoint maintenance/amplification rather than the initiation of checkpoint activation.

5.5.3 Rad4 AAD mutant is defective in checkpoint activation

In Chapter 4, we have shown that *S. pombe* strains mutated in the AAD of *rad4* show a slight sensitivity to DNA damage and HU and have a defect in Chk1 phosphorylation in response to DNA damage. The question of whether the AAD plays a role in Chk1 activation was re-addressed using the LacI-LacO tethering system. When GFP-LacI-NLS-Rad3 was targeted to the LacO array in a *rad4-Y599R* genetic background, Chk1 phosphorylation is highly reduced when compared to wild type cells (Fig.5-9A.B.C). This shows that endogenous of the AAD is required for checkpoint activation-induced by Rad3 tethering to a LacO array.

Next, the Y599R mutation was introduced by mutagenesis PCR into pREP42-Rad4-GFP-LacI-NLS. Plasmids for expression of GFP-LacI-NLS-Rad9, Rad4-GFP-LacI-NLS or Rad4-Y599R-GFP-LacI-NLS (pSJ60) were introduced in cells harboring the LacO array either alone or in combination with GFP-LacI-NLS-Rad3. A single transformant was cultured in the appropriate selective medium in the presence of thiamine overnight and then released into thiamine-free medium. Expression of either of GFP-LacI-NLS-Rad3, GFP-LacI-NLS-Rad9, or Rad4-GFP-LacI-NLS in the cells with the LacO array induces Chk1 phosphorylation while Rad4-Y599R-GFP-LacI-NLS does not (Fig.5-9D). Co-expression of GFP-LacI-NLS-Rad3 and GFP-LacI-NLS-Rad9 induces Chk1 phosphorylation earlier and more prominently than when expressing only one or the other construct. Co-expression of GFP-LacI-NLS-Rad3 and Rad4-GFP-LacI-NLS also induces Chk1 phosphorylation earlier and more prominently than when expressing one or the other. (Fig.5-9D). Interestingly, when GFP-LacI-NLS-Rad3 and Rad4-Y599R-GFP-LacI-NLS are co-expressed in the cells with LacO array, Chk1 is not phosphorylated (Fig.5-9D). This indicates that Rad4 AAD mutant prevents Chk1 phosphorylation by exercising a dominant negative effect on

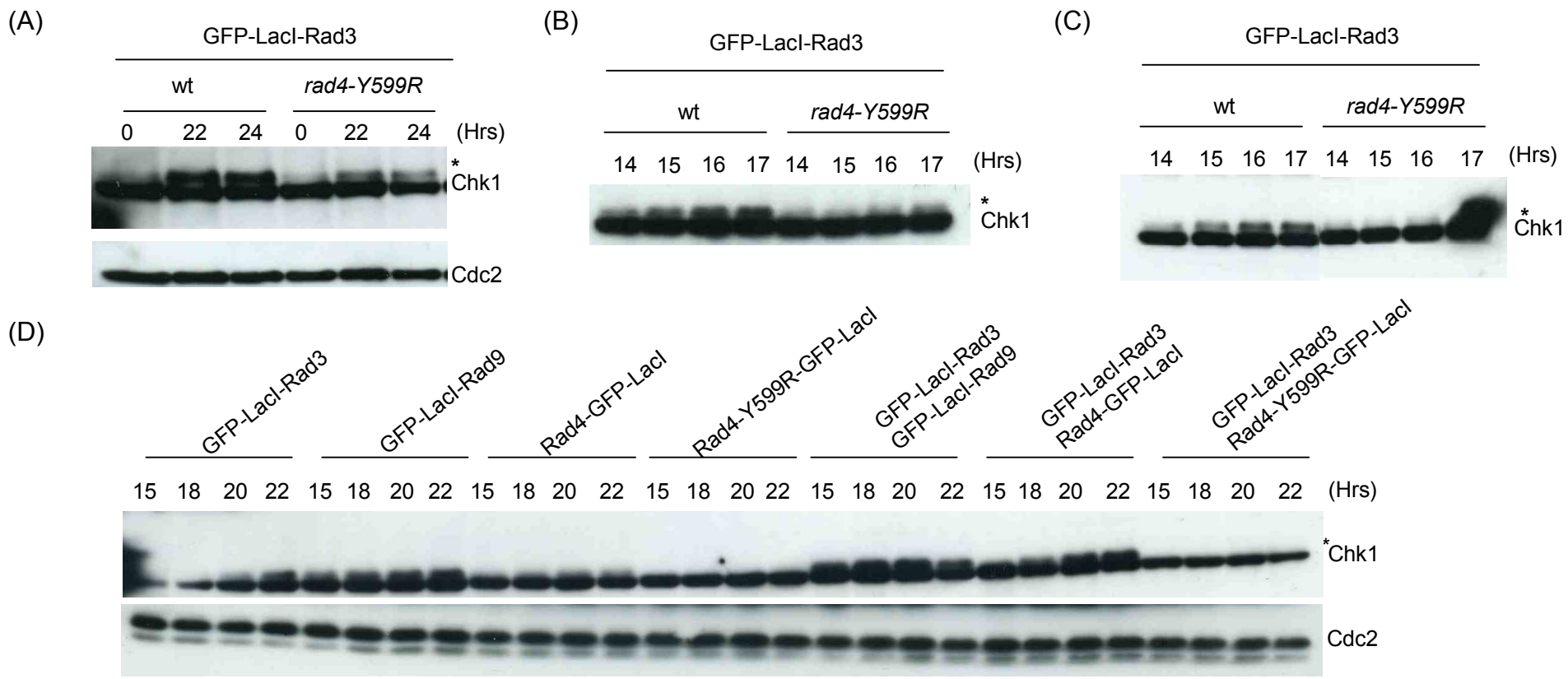

Figure 5-9- Role of Rad4 ATR-activating domain (AAD) in the LacI/LacO system
(A) GFP-LacI-NLS-Rad3 was expressed either in wild-type or *rad4-Y599R* cells carrying the LacO array. Chk1 phosphorylation was analyzed before induction and at 20, and 22 hours after induction by western blot and detected using an anti-HA antibody. (B) (C) are duplicated of (A) representing three entirely independent experiments. (D) Single or two checkpoint proteins in fusion with GFP-LacI-NLS were expressed in the cells harboring the LacO array. Chk1 phosphorylation was analyzed at 15, 18, 20, 22 hours after induction by western blot. Cdc2 was used as a loading control. * represents the phosphorylation form of Chk1.

Rad3-mediated checkpoint activation in this tethering system. Since this artificial system is believed to be ssDNA-RPA-independent, this suggests that the AAD of Rad4 plays a role in chromatin-mediated checkpoint maintenance/amplification.

5.6 Role of Rad4 Cdc2 phosphorylation sites in a LacI/LacO system

Previously, we have shown that *S. pombe* strains mutated at Rad4 Cdc2 phosphorylation sites are mildly sensitive to DNA damage or HU (Chapter 3). Similarly, strains mutated in Rad4 AAD have mild sensitivity to DNA damage and HU (Chapter 4). However, the *rad4 AAD* mutant causes a significant effect in a LacI/LacO system. In addition, we have shown that *in vivo* Rad4 phosphorylation on S592 (a SP/TP site) in response to IR or HU is dependent on Rad3. S592 is in proximity to the AAD, and we suspected that it might be implicated in regulating the function of the AAD. Therefore, it is interesting to investigate the role of Rad4 Cdc2 phosphorylation sites under a LacI/LacO system. Rad4 Cdc2 consensus sites T589 and S592 are present within one cluster thus I started to study these two Cdc2 consensus sites in a LacI/LacO system. T589A and S592A mutations (2A) were introduced by mutagenesis PCR in pREP42-Rad4-GFP-LacI-NLS. Plasmids for expression of GFP-LacI-NLS-Rad3, Rad4-GFP-LacI-NLS or Rad4-2A-GFP-LacI-NLS (pSJ72) were introduced in the cells harboring the LacO array either alone or co-expression of Rad4-GFP-LacI-NLS or Rad4-2A-GFP-LacI-NLS in combination with GFP-LacI-NLS-Rad3. A single transformant was cultured in the appropriate selective medium in the presence of thiamine overnight and then released into a thiamine-free medium. Expression of either GFP-LacI-NLS-Rad3 or Rad4-GFP-LacI-NLS in the cells with the LacO array induces Chk1 phosphorylation while Rad4-2A-GFP-LacI-NLS does not (Fig.5-10).

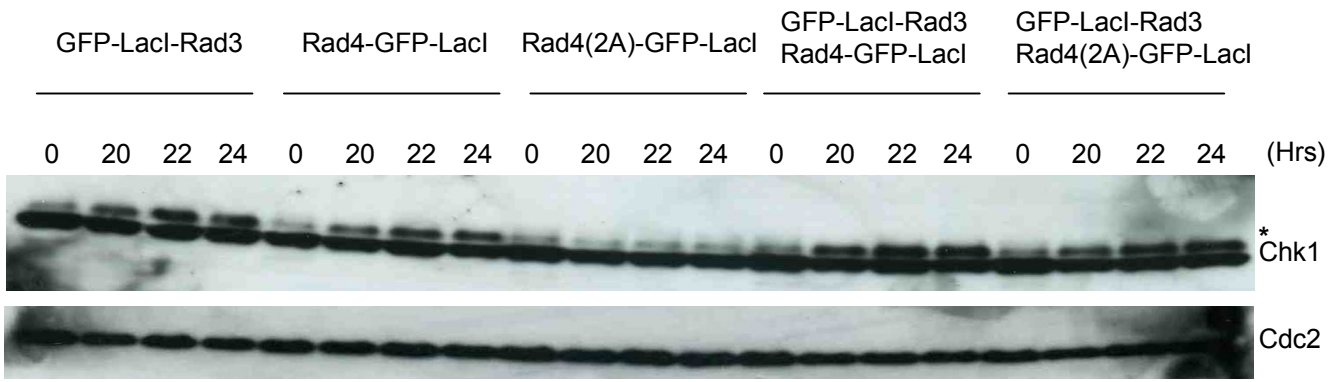

Figure 5-10- Role of Rad4 Cdc2 phosphorylation sites in the LacI/LacO system
GFP-LacI-NLS-Rad3, Rad4-GFP-LacI-NLS, or Rad4-T589A.S592A (2A)-GFP-LacI-NLS were expressed in the cells harboring the LacO array. GFP-LacI-NLS-Rad3 and Rad4-GFP-LacI-NLS or GFP-LacI-NLS-Rad3 and Rad4-T589A.S592A (2A)-GFP-LacI-NLS were co-expressed in the cells harboring the LacO array. Chk1 phosphorylation was analyzed before induction and at 20, 22 and 24 hours after induction by western blot, and detected using an anti-HA antibody. Cdc2 was used as a loading control. * represents the phosphorylation form of Chk1.

Co-expression of GFP-LacI-NLS-Rad3 and Rad4-GFP-LacI-NLS in the cells harboring the LacO array induces Chk1 phosphorylation (see Fig. 5-9D) and this occurs similarly when GFP-LacI-NLS-Rad3 and Rad4-2A-GFP-LacI-NLS are co-expressed (Fig.5-10). This experiment has been done only once and therefore, this result remains to be confirmed. However, if this observation is correct, it suggests that Rad4 phosphorylation at T589 and/or S592 is potentially responsible for recruitment of Rad3 to LacO array (sites of DNA damage) when Rad4 is expressed alone in this system. And that this maybe a prerequisite for AAD functions in checkpoint maintenance/amplification.

5.7 Rad4 tethering bypasses the requirement for Rad9 C-terminus phosphorylation on T412 in the Chk1 activation pathway

In response to DNA damage, it is known that Rad3 phosphorylates the Rad9 C-terminus on residues T412/S423 and that T412 phosphorylation is required for Rad4 interaction with both Rad9 and Rad3 (Furuya et al., 2004). To analyze the role of this Rad9 C-terminal phosphorylation in the tethering system, pREP41-GFP-LacI-NLS-Rad3 and empty vector pREP42 were co-introduced into the cells carrying the LacO array either in a wild type or in a *rad9-T412A* background. A single transformant was cultured in the appropriate selective medium in the presence of thiamine overnight and then released into a thiamine-free medium. Cells were collected before and after induction. Expression of GFP-LacI-NLS-Rad3 induces Chk1 phosphorylation in wild-type cells with the LacO array and Chk1 phosphorylation-induced by Rad3-tethering to chromatin is abolished in *rad9-T412A* cells, suggesting that Rad9 phosphorylation on T412 is required for the checkpoint response in this system. Interestingly, Chk1 phosphorylation occurs in the *rad9-T412A* cells when expressing both GFP-LacI-NLS-Rad3 and

Rad4-GFP-LacI-NLS to LacO array, indicating that Rad4 targeting bypasses the requirement for Rad9 phosphorylation on T412 (Fig.5-11). Therefore, this confirms Furuya's model where the Rad9 C-terminal phosphorylation is required for Rad4 recruitment and the formation of an active checkpoint complex.

5.8 The tethering of the Rad4 C-terminal moiety is not sufficient to activate the checkpoint response

When expressed at high level, AAD is sufficient to stimulate ATR kinase activity *in vitro* (Kumagai et al., 2006). As shown above, expression of Rad4-GFP-LacI-NLS in cells carrying the LacO array induced Chk1 phosphorylation. In order to examine whether the tethering of the C-terminus of Rad4 (amino acid 488-648 containing the AAD) in fusion with GFP-LacI-NLS to chromatin is sufficient to induce checkpoint activation, full-length Rad4 (Rad4-GFP-LacI-NLS) or the C-terminus of Rad4 (C-Rad4-GFP-LacI-NLS) were expressed in the cells carrying the LacO array. While the full-length Rad4-GFP-LacI-NLS could induce Chk1 phosphorylation at both 20 and 22 hours after induction, C-Rad4-GFP-LacI-NLS could not (Fig.5-12A). This suggests that even though Rad4 C-terminus contains the AAD, it is not sufficient to activate Rad3 in this system. Rad3-dependent Chk1 phosphorylation may require the Rad4 N-terminus to interact with Rad3. Co-expression of GFP-LacI-NLS-Rad3 and C-Rad4-GFP-LacI-NLS also does not cause Chk1 phosphorylation in a *rad4-Y599R* background (Fig.5-12B). While co-expression of Rad3 and Rad4 in fusion with GFP-LacI in a *rad4-Y599R* background has not been tested, we expect that full-length Rad4 is able to bypass the *rad4-Y599R* defect. Altogether, these results suggest that the C-terminus of Rad4 containing the AAD is not sufficient to activate Rad3 in this system, and that a Rad4 N-terminal moiety is necessary to induce checkpoint activation. Perhaps

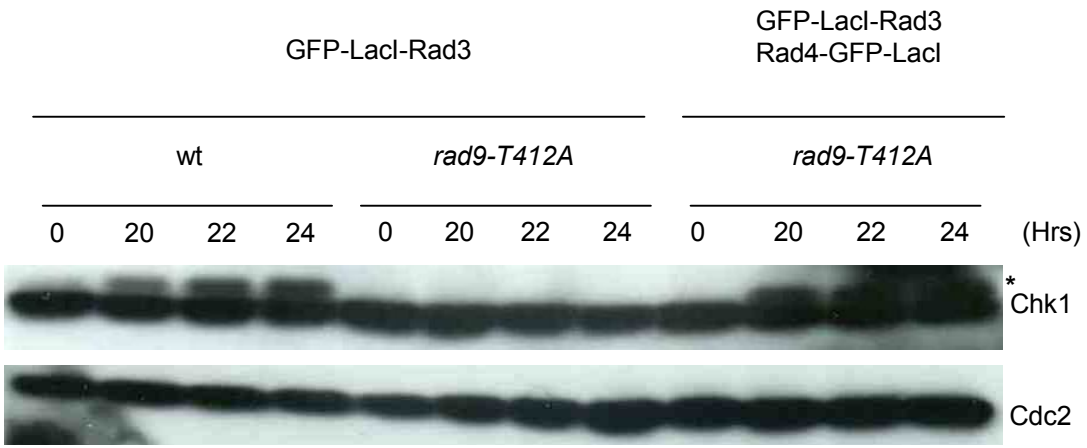

Figure 5-11- Rad4 bypasses the requirement for C-terminus Rad9 phosphorylation at T412
GFP-LacI-NLS-Rad3 was expressed either in wild-type or *rad9-T412A* cells harboring the LacO array. GFP-LacI-NLS-Rad3 and Rad4-GFP-LacI-NLS were co-expressed in *rad9-T412A* cells harboring the LacO array. Chk1 phosphorylation was analyzed before induction and at 20, 22 and 24 hours after induction by western blot. Cdc2 was used as a loading control.
* represents the phosphorylation form of Chk1.

(A)

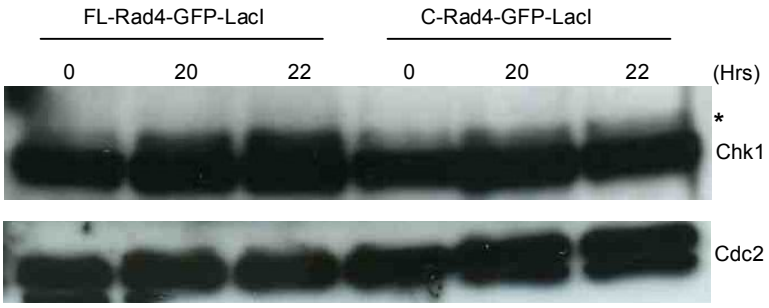

(B)

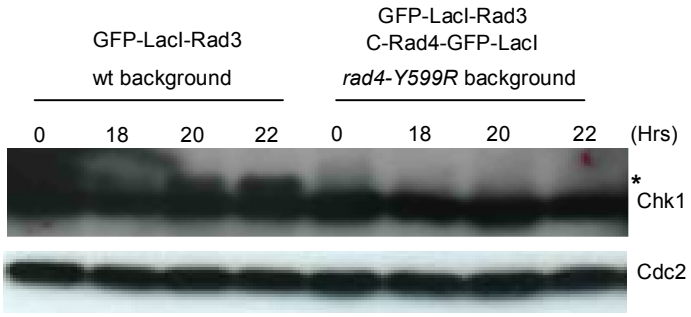

Figure 5-12- Role of C-terminal Rad4 in the LacI/LacO system
(A) Full length Rad4 and C-terminal Rad4 (from amino acid 488 to stop codon, containing the AAD) were expressed in the cells carrying the LacO array. Chk1 phosphorylation was analyzed before induction and at 20, 22 hours after induction by western blot, and was detected using an anti-HA antibody. (B) GFP-LacI-Rad3 was expressed in the cells carrying the LacO array and in parallel, GFP-LacI-Rad3 and C-terminal of Rad4-GFP-LacI were co-expressed in *rad4-Y599R* cells carrying the LacO array. Chk1 phosphorylation was analyzed before induction and at 18, 20, and 22 hours after induction by western blot. Cdc2 was used as a loading control. * represents the phosphorylation form of Chk1.

the Rad4 N-terminal moiety is required for interaction with other checkpoint factors, *i.e.*, Crb2 to be enable to initiate of a checkpoint response (Saka et al., 1997) because this system does not bypass the requirement for other checkpoint components for the initiation of the checkpoint pathway.

5.9 Instability of the LacO array in the cells

The 10 kb LacO array is known to be unstable due to the recombination within LacO repeats (Takashi Morishita, personal communication). The LacO array is linked to a NAT^R marker and is integrated at the *ura4* locus on chromosome III (Fig.5-13A). In this study, cells harboring the LacO array were crossed with several different strains in order to generate the cells expressing *chk1* tagged with HA in different genetic backgrounds. In order to check the length of LacO repeats, we performed southern blot analysis. Yeast genomic DNA was digested with *Hind*III, separated on 0.7% agarose gel, and probed by LacO sequences. Apparently, both *chk1:HA* LacO::NAT and *rad4-Y599R chk1:HA* LacO::NAT have lost LacO repeats. Since the LacO array integrated in a chromosome originally is 10 kb, cells expressing *chk1:HA* LacO::NAT in wild type or *rad4-Y599R* background were shown to carry 3 kb or 6 kb of LacO repeats (Fig.5-13B). Two bands were observed on the southern blot *i.e.* 3 kb and 6 kb of LacO repeats were carried in the cells expressing *chk1:HA* LacO::NAT. This could be explained by one population of cells having lost more LacO repeats than the other population of cells. Strains of *rad9-T412A chk1:HA* LacO::NAT and *hta1-S129A hta2-S128A chk1:HA* LacO::NAT carried ~6kb or ~4.5 kb of LacO repeats (Fig.5-13B). It seems that the version of LacO repeats we used was not stable but Chk1 was still able to be phosphorylated when a LacI fusion protein was expressed in the cells harboring 3kb of LacO repearts. David J. Sherratt's group has devised a version of 240 copies of LacO which contains tandem

(A)

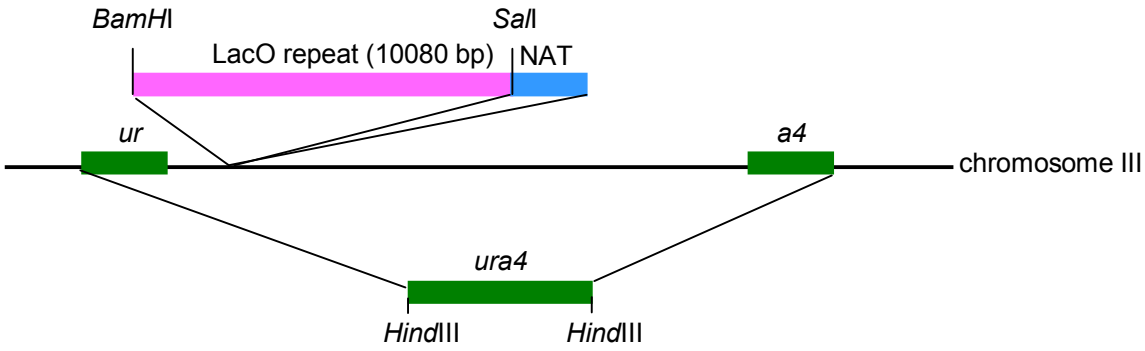

(B)

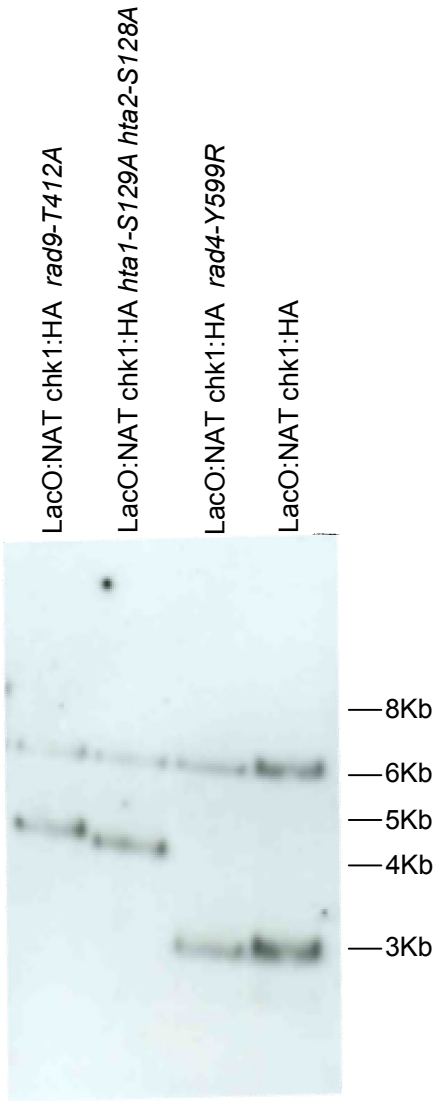

Figure 5-13- Detection of LacO repeats by southern blot
(A) Diagrammatic representation of LacO repeats linked to a NAT^R marker integrated at *ura4* locus on chromosome III (generated by Takashi Morishita). (B) Genomic DNA was extracted from chk1:HA of wild-type, *rad4-Y599R*, *hta1-S129A hta2-S128A*, or *rad9-T412A* cells harboring the LacO repeats. DNA was digested with *Hind*III, separated on 0.7% agarose gel, transferred and hybridized with a probe for LacO repeats (see Chapter 2 Material and Method).

repeated LacO flanked by 10 bp of different random sequences, and this has a substantial effect on reducing the occurrence of recombination and thus stabilizes the LacO repeats (Lau et al., 2003). This version of LacO repeats has been integrated in the *S. pombe* genome successfully and it seems relatively stable in the cells (Takashi Morishita, personal communication). It can be useful for further study.

5.10 Conclusion

An artificial checkpoint induction system in the absence of exogenous lesions was successfully established in *S. pombe* cells. The checkpoint activation in this LacI/LacO artificial system is ssDNA-independent and H2A phosphorylation-dependent. In response to DNA damage, H2A phosphorylation is not required for Chk1 activation; H2A phosphorylation is a platform for recruitment of checkpoint factors such as Crb2 and is implicated in checkpoint maintenance (Nakamura et al., 2004). Therefore, the LacI/LacO system can be used to study checkpoint activation focusing on chromatin-mediated checkpoint maintenance/amplification. The Rad4 AAD is required for checkpoint activation in this artificial system but not in response to DNA damage (Chapter 4), indicating that Rad4 AAD is implicated in chromatin-mediated checkpoint maintenance/amplification. Interestingly, the tethering of the Rad4 C-terminus to the LacO array is not sufficient to induce Chk1 phosphorylation, suggesting that N-terminus of Rad4 is required for Rad3 activation in this system. Besides, Rad4 targeting to LacO array bypasses the requirement for Rad9 phosphorylation on T412. This confirms Furuya's model where the Rad9 C-terminus phosphorylation is required for Rad4 recruitment and the formation of an active checkpoint complex (Rad9-Rad4, Rad9-Rad3) in response to IR or HU.

Chapter 6 Screen for separation-of-function *rad4* alleles by hydroxylamine random mutagenesis using the RMCE system

6.1 Introduction

Even though site-directed mutagenesis of chosen residues or domains is an excellent method for targeting mutation and identifying their specific domain functions, our knowledge of the Rad4 protein structure is limited. This approach therefore is not useful to identify novel functional motifs. To overcome this limitation, a random mutagenesis screen was initiated for identifying novel and informative mutants. To utilize the new RMCE system (Watson et al., 2008), the plasmid containing the loxP-*rad4*-loxM3 was subjected to a random mutagenesis by exposure to hydroxylamine hydrochloride which is a highly specific mutagenic chemical agent. It reacts with cytosine and causes the specific replacement of a guanine by an adenine, thus causing only the GC to AT transition (Hong and Ames, 1971). The RMCE system was used to create a library of *S. pombe* strains in which the wild-type *rad4* sequence had been replaced by a randomly mutagenized one. The resulting library was screened for specific phenotypes *i.e.*, sensitivity to DNA damaging agents or to replication inhibitor, HU.

Interestingly, the N-terminus of Xcut5 in *Xenopus* ensures the essential replicative function of Cut5, whereas the checkpoint activation function resides in the C-terminus (Hashimoto et al., 2006; Yan et al., 2006). In *S. pombe*, a thermo-sensitive *rad4-116* mutant is sensitive to UV and IR but the replicative function and replication checkpoint are proficient at 26°C. When the temperature increases to 32°C, *rad4-116* mutant cells

have normal cell-growth during S-phase but the checkpoint does not be activated in the presence of HU. The *rad4-116* mutant thus seems to be a separation of function mutant: the replicative function is present but S/M checkpoint function is lost by shifting the temperature. Therefore, we were particularly interested in identifying separation of function mutants affected specifically in Rad4 checkpoint activity. Because the role of Rad4 in replication is essential, mutants affecting replication should not be recovered from this screen unless they are hypomorphic. These will be identified by their slow-growth or thermo-sensitivity. For potentially interesting mutants, the *rad4* gene will be sequenced to localize the mutation site. We anticipate identifying several specific Rad4 mutants via this screen, which will be characterized genetically and biochemically using the methods and reagents discussed in previous chapters, and further methods available in the laboratory as appropriate.

6.2 Optimization of hydroxylamine concentration for random mutagenesis screening

We first examined the best concentration of hydroxylamine to be used to introduce random mutations efficiently in the plasmid containing loxP-*rad4*-loxM3 (pSJ25). Because Rad4 is an essential gene, increasing the dose of hydroxylamine for mutagenesis should decrease the number of transformants. 1, 2.5, 5, 10, and 50 M hydroxylamine solution have been tested (but 50 M of hydroxylamine solution was not soluble). The hydroxylamine hydrochloride was dissolved in 4.55 ml ice-cold sterile MQ water and 450 µl of 5 M NaOH, and pH value was adjusted to 6.7. The solution was kept on ice until use.

pSJ25 was incubated with 1, 2.5, 5, or 10 M hydroxylamine solution (detailed in 2.6).

Subsequently, DNA was recovered from the hydroxylamine mixture and was used to transform *S. pombe* cells using the RMCE system (detailed in 2.5). The transformants were selected on EMM+ade+thi plates at 25°C. The number of colonies was scored, and the relationship between the number of transformants and the concentration of hydroxylamine treatment was determined (Fig. 6-1). As expected, increasing the concentration of hydroxylamine decreases the number of transformants. Treatment with 5 M hydroxylamine solution decreased the number of the transformants down to about 50%. We subsequently used a 5 M hydroxylamine for the screen.

6.3 Screening of transformants

A screening protocol was established and is summarized in Fig 6-2. 10 μg of the plasmid pSJ25 was incubated in 5 M hydroxylamine solution at 37°C for 20 hours. DNA was purified from the hydroxylamine solution and the recovered DNA was used to transform in *S. pombe* ("435" base-strain). Transformants were selected on EMM+ade+thi plates by incubation at 25°C. Transformants on EMM+ade+thi plates were re-streaked to fresh EMM+ade+thi plates and incubated at 25°C for 2~3 days. The fresh cells were replicated on YEA plates and grown at 25°C for 2 days in order to lose the plasmid. Transformants were then replicated on 5-FOA plates to select for cells which have lost the *ura4* marker (expected to have replaced *rad4* open reading frame by the randomly mutagenised *rad4*). The 5-FOA resistant strains were inoculated in 1 ml YE in 96-well square plates (Thermo Fisher) and cells were incubated at 25°C for 2 days. In parallel, wild-type, the *rad3-d* and *rad4-116* (temperature-sensitive strain) cells were inoculated in the 96-well plates as controls. The libraries were stored in 50% glycerol at -80°C for further analysis.

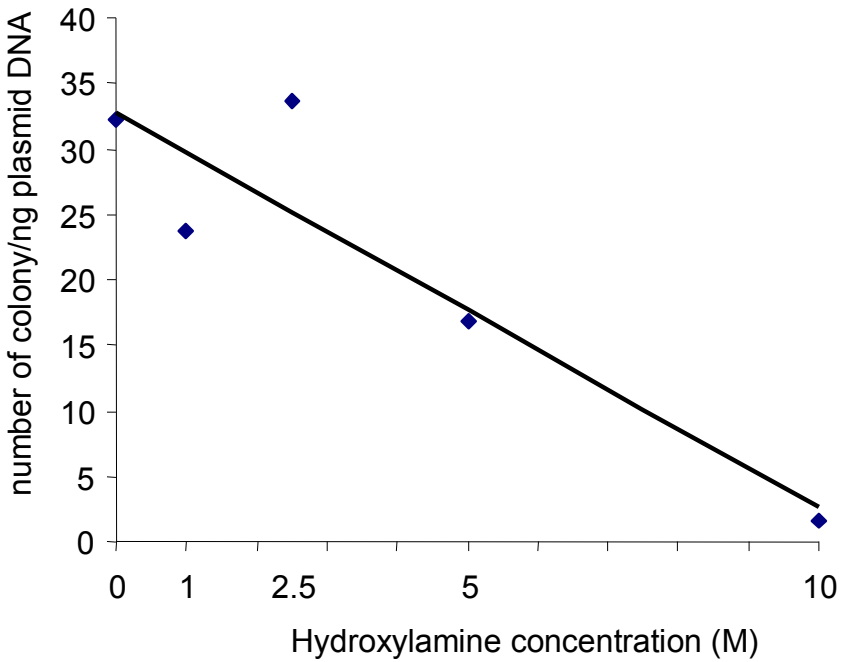

Figure 6-1- Effect of the concentration of hydroxylamine on the number of transformants
10 µg plasmid (pSJ25) carrying a wild-type *rad4* was incubated with increasing doses of hydroxylamine. DNA was recovered from the hydroxylamine mixture and the recovered DNA was used to transform *S. pombe* cells. The number of colonies was scored, and the relationship between the number of transformants and the concentration of hydroxylamine treatment was determined.

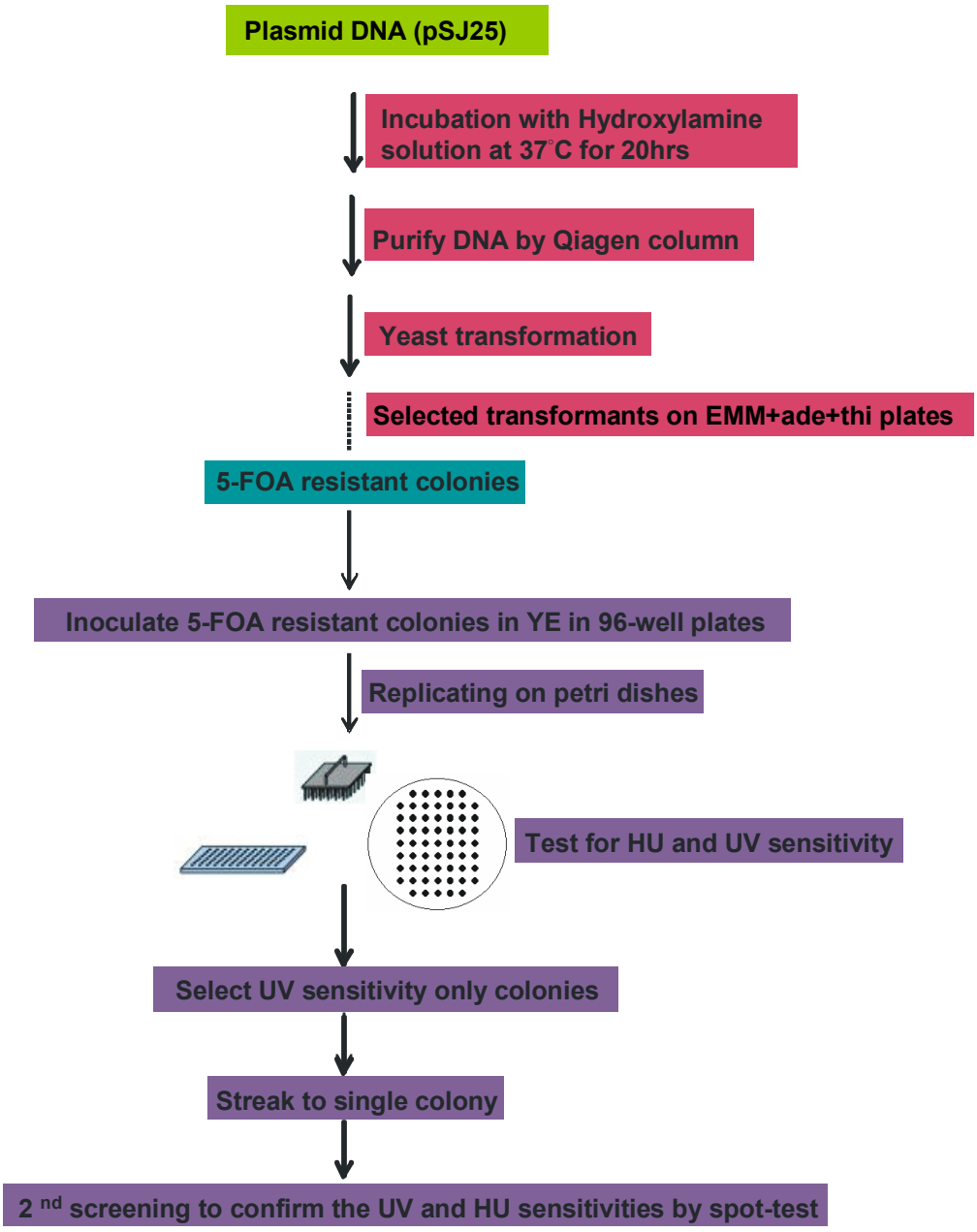

Figure 6-2- Procedure for generation and screening of the Rad4^{TopBP1} library created by hydroxylamine mutagenesis.

The details are in the text.

In the first step of the screen, the "48-pin device (frogger)" was used to replicate cells from a 96-well plate onto petri dishes with YEA plus 5 μg/ml phloxin B (Gurr Certistain®). Phloxin B is used to determine cells viability, *i.e.*, dead cells showed a dark red color while viable cells are light pink. To assess HU and UV sensitivity, cells were replicated on YEA plates in the presence of HU or replica plates were irradiated with UV light. The plates were incubated at 25°C. To test the thermo-sensitivity, cells were transferred to plates and were incubated at 36°C. HU is used for screening mutants defective in the DNA replication checkpoint response and UV is used for screening mutants defective in both DNA damage and DNA replication checkpoint. We were particularly interested in isolating mutants which showed sensitivity to UV only because cell sensitivity to UV only might suggest that cells are defective in DNA damage checkpoint but not in DNA replication checkpoint. Colonies exhibiting sensitivity to UV only at the first screening, and were picked up from the 96-well plates and streaked on YEA plates to give rise to single colony. Cells from a single colony were used for the second screening in order to confirm the sensitivity to UV (HU was also tested) by spot-test. Wild-type, *rad3-d* and *rad4-116* were used as control cells. It is noted that it was difficult to detect the UV-sensitivity because too many cells were transferred using the "frogger" in the first screen. We isolated 45 putative mutants exhibiting sensitivity to UV only in the first screen.

In the second step of the screen, these 45 potential candidates were tested by spot-test. Most of strains only sensitive to UV isolated from the first stage turned to be sensitive to HU only (such as 116, 133, 235, 277, and 2M-3…*etc*) (Fig. 6-3). 11 strains appeared to be sensitive to UV (117, 304, 2M-4, 1-9, 1-47, 1-64, 1-223, 2-94, 2-259, 2-434, and 2-442) but all of them also appeared to be sensitive to HU-treatment (Fig. 6-3). Unfortunately, no strain was sensitive to UV only. 4037 colonies in total have been

Figure 6-3- Functional analysis of Rad4 mutants generated from the hydroxylamine random mutagenesis
Stains exhibiting UV sensitivity at the first step of screen were tested by spot test for their sensitivity (or not) to DNA damaging agents or the replication inhibitor HU. 10-fold serial dilutions of $1x10^6$ cells/ml were spotted onto YEA plates without or exposive to UV or to different genotoxic agents at the indicated doses. Plates were incubated at 25°C, and/or 36°C. “501” and “435” are *rad4*$^+$ and *rad4*$^+$ (RMCE) controls, respectively. *rad4-116* is a thermo-sensitive strain, and *rad3-d* is a negative control strain. Only strains showing sensitivity to UV and/or HU are named.

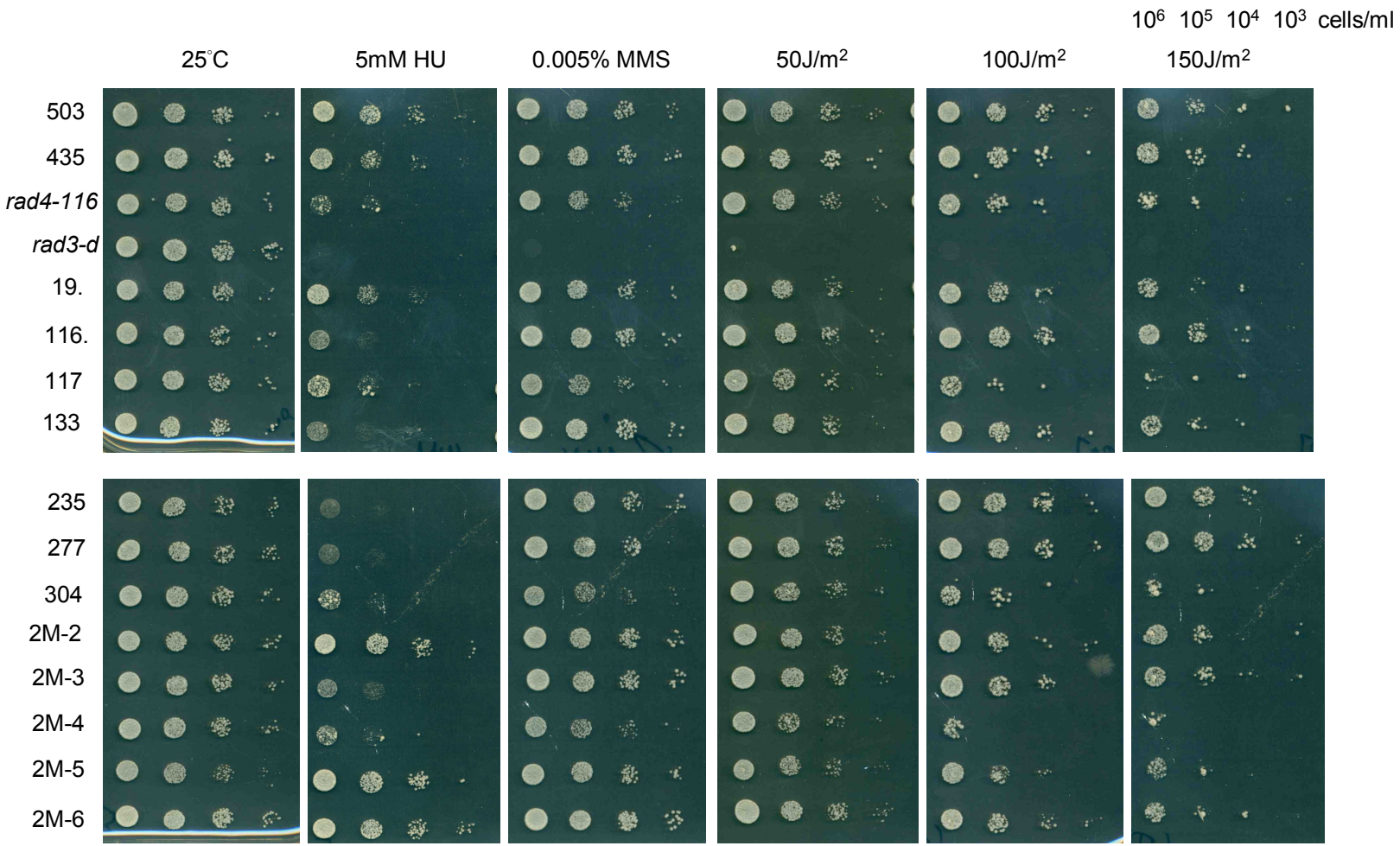
10^6 10^5 10^4 10^3 cells/ml
25°C
5mM HU
0.005% MMS
50J/m^2
100J/m^2
150J/m^2
503
435
rad4-116
rad3-d
19.
116.
117
133
235
277
304
2M-2
2M-3
2M-4
2M-5
2M-6

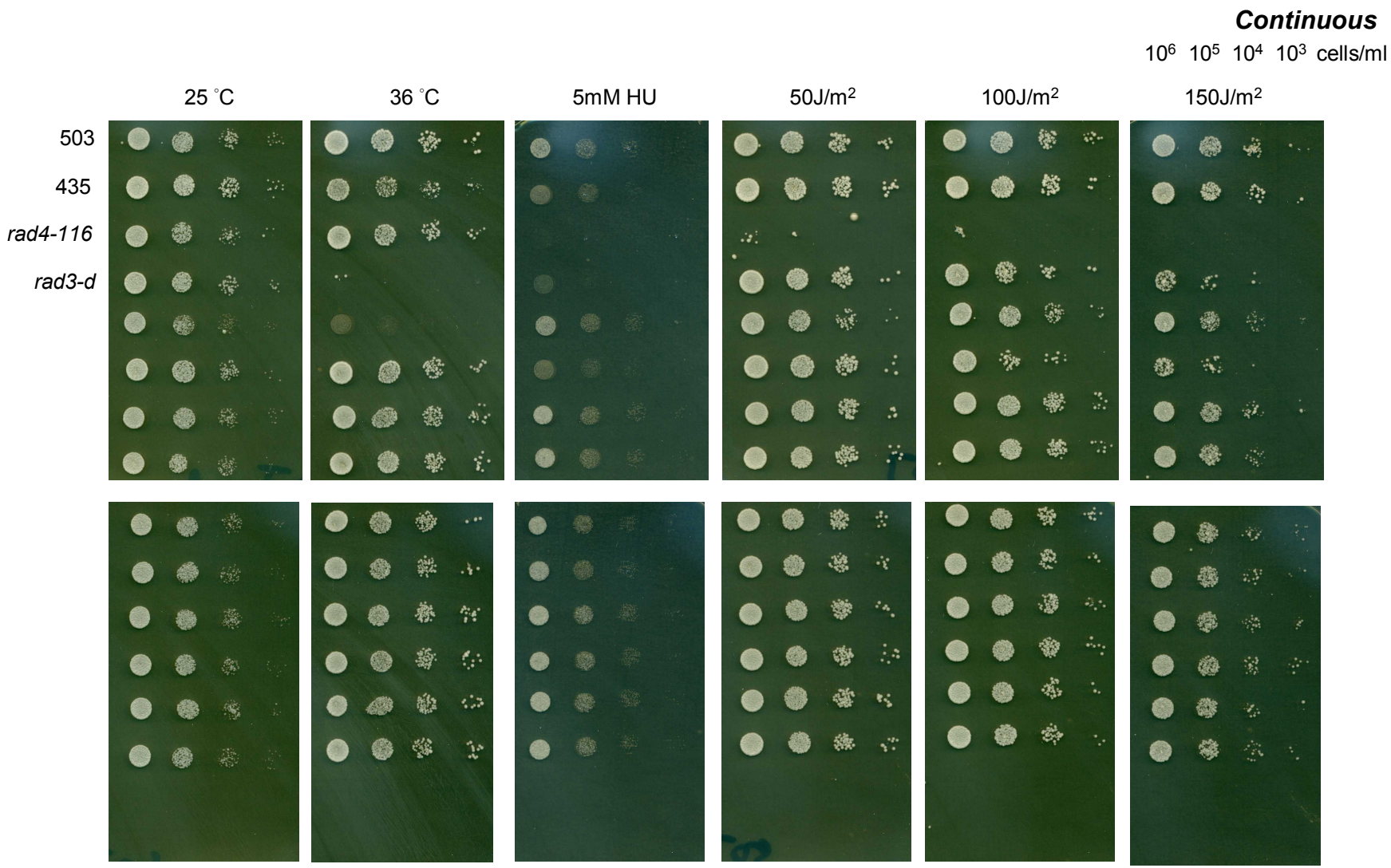
Continuous
10^6 10^5 10^4 10^3 cells/ml
25 ˚C
36 ˚C
5mM HU
50J/m2
100J/m2
150J/m2
503
435
rad4-116
rad3-d

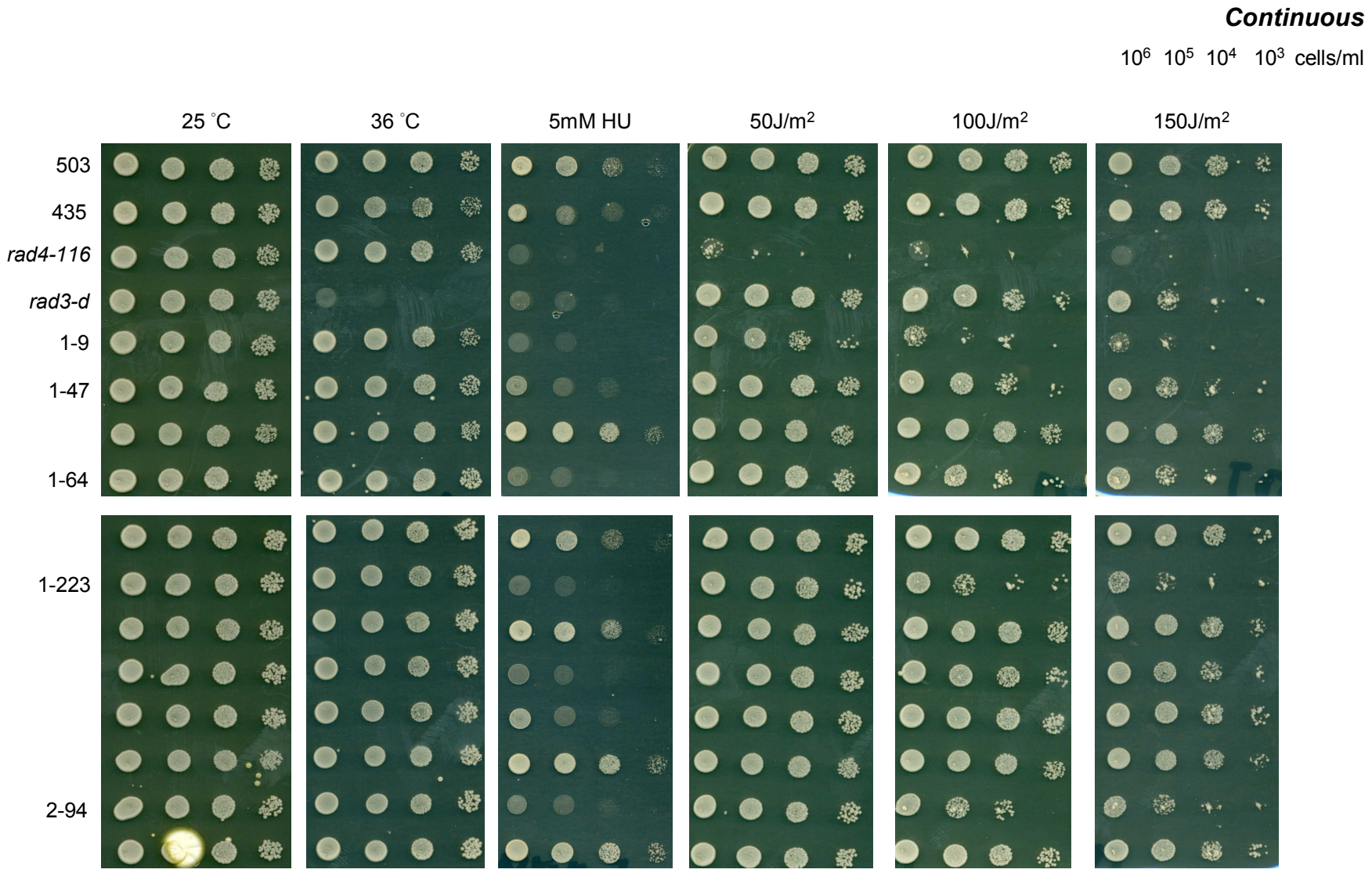
Continuous
10^6 10^5 10^4 10^3 cells/ml
25 ˚C
36 ˚C
5mM HU
50J/m2
100J/m2
150J/m2
503
435
rad4-116
rad3-d
1-9
1-47
1-64
1-223
2-94

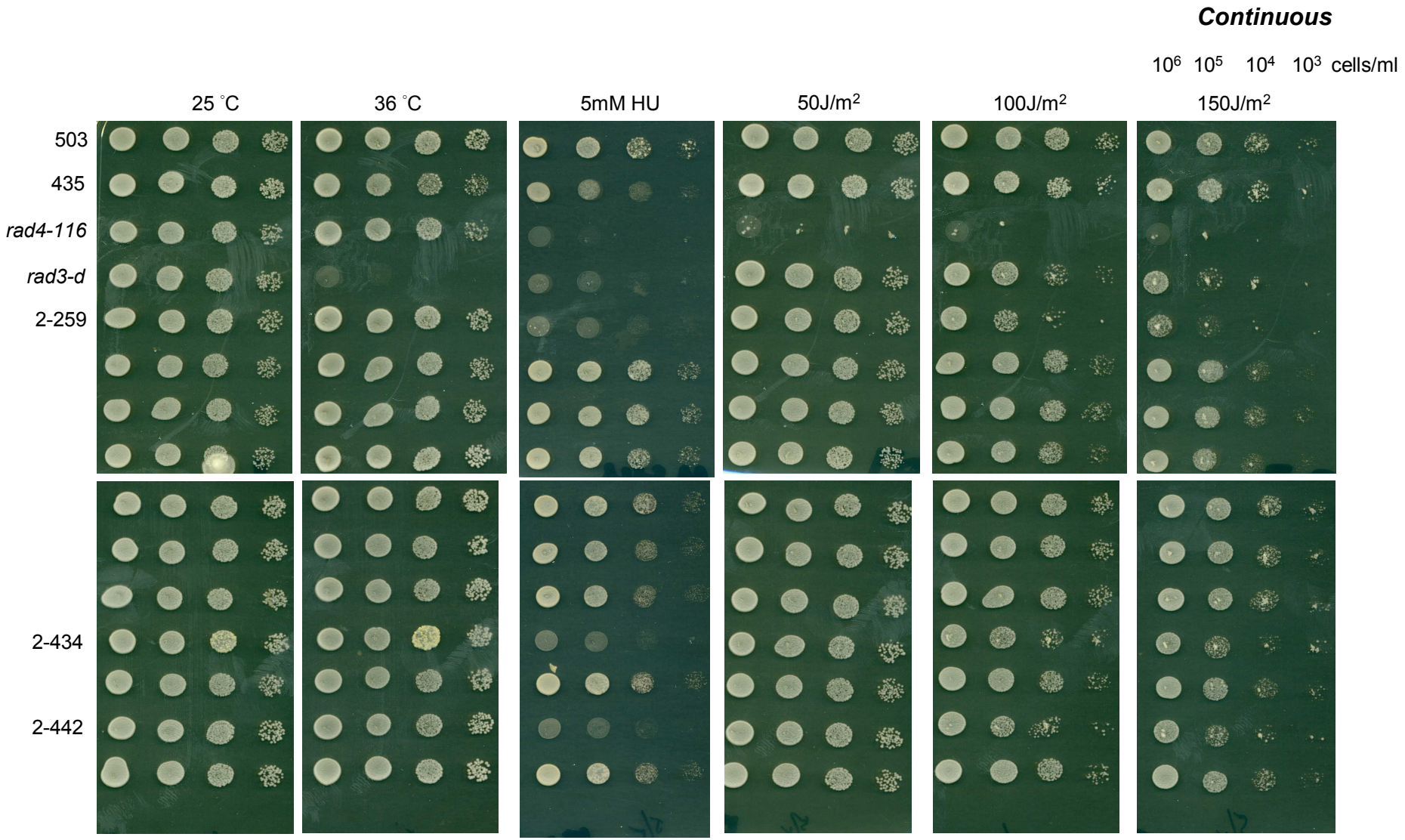
Continuous
10^6 10^5 10^4 10^3 cells/ml
25 ˚C
36 ˚C
5mM HU
50J/m2
100J/m2
150J/m2
503
435
rad4-116
rad3-d
2-259
2-434
2-442

analyzed and the mutant strains obtained in this library can be classified into six classes (table 6-4). Three classes have defect in both replication and checkpoint, and they are: 7 strains, slow-growth at 25°C and sensitive to both UV and HU (class I); 4 strains are sensitive at 36°C and to HU (class III); 1 strain is sensitive at 36°C and to HU and UV (class VI). Class II: 25 strains are sensitive at 36°C (temperature-sensitive strain), suggesting theses mutants might be candidates for separation replicative function from checkpoint functions in Rad4. This remains to be confirmed because they have been tested only in the first step of the screen. Class IV: 468 strains are sensitive to HU only, suggesting they are defective in the replication checkpoint. Class V: 11 strains are sensitive to both HU and UV, suggesting that they might separate of function between replicative function and checkpoint function.

We did not isolate separation-of-function mutant defective in the DNA damage checkpoint but proficient in the replication checkpoint (UV^S but not HU^S). However, we identified 11 mutants are sensitive to HU and UV but without a slow-growth phenotype or thermo-sensitivity, suggesting separation between checkpoint and replication function. The *rad4* gene was sequenced to localize the mutations in three different strains sensitive to both UV and HU identified in this library. Interestingly, these three mutant strains all contain a mutation localized in the C-terminal non-BRCT tail of Rad4. Two of them carry a premature stop codon in the Rad4 C-terminus, *i.e.*, glutamine 516 (CAA) was mutated to a stop codon (TAA) in strain "304", glutamine 605 (CAA) was mutated to a stop codon (TAA) in strain "2M-4". The third strain ("117") has lysine 611 (CTT) mutated to phenylalanine (TTT). Their mild sensitivity to DNA damaging agents or HU was very similar to Rad4 C-terminal truncations (described in Chapter 4) which were sensitive to high dose of DNA damaging agents or HU. Since the sensitivity to both HU and UV was very mild and because we have no knowledge of the Rad4

	Class I	Class II	Class III	Class IV	Class V	Class VI
Number of strains	7	25	4	468	11	1
25°C	X					
36°C		X	X			X
5mM HU	X		X	X	X	X
100 J/m^2 UV	X				X	X

Table 6-4- Class of mutant strains obtained in the hydroxylamine random mutagenesis library
"X" presents the strain exhibiting slow-growth at 25°C, thermo-sensitive (36°C), or sensitive to HU or UV.

C-terminal function in checkpoint maintenance/amplification at this time, we did not further analyze the mutants generated from this library genetically and/or biochemically.

6.4 Discussion

Rad4 has an essential function in the initiation of DNA replication and also functions in the DNA damage and DNA replication checkpoints. The DNA replication machinery is a prerequisite for the checkpoint machinery to activate the replication checkpoint (Garcia et al., 2005). Therefore, mutations affecting the DNA replicative function of Rad4 are likely to affect its checkpoint function. The *S. pombe* thermo-sensitive *rad4-116* mutant has a mutation (T45M) located in the first BRCT domain. *rad4-116* mutant is sensitive to UV and IR but retains its DNA replication function and has an intact replication checkpoint function at 26°C (McFarlane et al., 1997; Saka and Yanagida, 1993). The *rad4-116* mutant displayed normal growth during S-phase at 32°C but the replication checkpoint was abolished in the presence of HU. Therefore, checkpoint function appears to be separated from the replication function in this mutant at the temperature of 32°C.

When initiating this screen, we were interested in identifying new Rad4 mutants having only a checkpoint defect. 11 mutants showing sensitivity to both UV and HU were isolated, which might be involved in regulating both the DNA damage checkpoint and the replication checkpoint. Interestingly, 3 of these 11 mutants (the only ones we have sequenced) have a mutation localized in the C-terminal tail of Rad4. This suggests that the Rad4 C-terminus is responsible for interaction with proteins implicated in the DNA checkpoint pathway. The Rad4 C-terminus does not seem to be required for DNA

replication since these 3 mutants grew as well as control cells at 25°C and 36°C. This is consistent with our later data showing that Rad4 C-terminal truncation does not effect cell growth (detailed in Chapter 4). In other words, the replication function in Rad4 can be separated from some of the checkpoint function. However, the sensitivity to UV and HU of these C-terminal mutants is mild comparing to *rad4-116* cells. Based on our study, the unstructured C-terminal tail of Rad4 seems to play a role in checkpoint maintenance/amplification that is independent of DNA replication function (detailed in Chapter 4, 5, and 7). The *rad4-Y599R* mutant defective in checkpoint maintenance/amplification shows slight sensitivity to DNA damage and HU and has a subtle DNA damage checkpoint deficiency. Therefore, these three C-terminal Rad4 mutants are possibly deficient in checkpoint maintenance/amplification but remains proficient in initiation of checkpoint activation according to their mild phenotype in sensitivity to UV and HU. The fact that it seems impossible to separate checkpoint activation function and replicative function of Rad4 is likely due to the BRCT domain of Rad4 interacting with DNA replication proteins (Noguchi et al., 2002) and with checkpoint proteins (Saka et al., 1997) (see figure 1-11). Therefore, mutation in theses domains will affect both functions.

Chapter 7 Final discussion

To characterize the structural function of fission yeast Rad4^{TopBP1}, we have been investigating the role of Rad4^{TopBP1} Cdc2 consensus phosphorylation sites, a putative RXL motif, and a putative ATR-activating domain (AAD). We also performed a hydroxylamine random mutagenesis genetic screen in order to obtain separation of function mutants of Rad4 (Chapter 6). Unfortunately, we were not able to separate a checkpoint activation function from replicative function.

Characterization of Rad4 Cdc2 phosphorylation sites and a putative RXL motif

In addition to the roles of CDK in regulating the initiation of DNA replication (Zegerman and Diffley, 2007), CDK is also known to regulate the DNA damage checkpoint (Bonilla et al., 2008) and homologous recombination repair pathways (Caspari et al., 2002; Ira et al., 2004).

- **Role of Rad4 Cdc2 phosphorylation sites**

In vivo, Rad4 is phosphorylated in response to DNA damage or replication inhibition (HU) and this phosphorylation occurs in a Cdc2 and Rad3-dependent manner: Rad4 bandshift induced by IR was shown to be dependent on both Cdc2 and Rad3 (see Fig. 3-5A). Rad4 is phosphorylated by Cdc2 *in vitro*, and the phosphorylation sites were identified by mass spectroscopy. Following up these observations (Valerie Garcia, personal communication), I have constructed several mutants carrying either single or various combination of alanine substitution of these Cdc2 phosphorylation sites. The mutant carrying seven substitutions (serine/threonine to alanine) of Cdc2

phosphorylation sites (*rad4-7A*) displays a slight sensitivity to HU and DNA damaging agents (Fig.3-1C), but does not show a cell-cycle defect in the absence of DNA damage. Considering the multiple functions of Rad4, we postulated that these Cdc2 phosphorylation sites might be involved in the control of re-replication. However, even in a strain overexpressing Cdc18, no re-replication defect could be attributed to *rad4-7A*, suggesting that Rad4 Cdc2-dependent phosphorylation does not play a role in the control of DNA re-replication (Fig.3-3, 3-4).

Considering that no evidence was obtained for a role of Rad4 phosphorylation in the control of DNA replication initiation, it may be conceivable that Rad4 phosphorylation by Cdc2 is involved in the DNA damage or DNA replication checkpoint control. This assumption is supported by the fact that Rad4 bandshift that is dependent on Cdc2 is also dependent on Rad3 (Fig. 3-5A.B). Interestingly, Rad4 phosphorylation on S592 as well as Rad4 bandshift are highly reduced in a *rad3-d* strain following IR or HU-treatment compared to wild-type cells (Fig. 3-5A.B). However, testing Rad4 phosphorylation on S592 in a *cdc2* analog sensitive mutant in response to IR or HU would be required to establish if Rad4 S592 is phosphorylated directly by Cdc2. Altogether, these observations lead us to propose three possible mechanisms for Rad4 phosphorylation by Cdc2. First, (but unlikely) Rad4 is directly phosphorylated at Cdc2 consensus sites by Rad3 following DNA damage. Second, Rad3 phosphorylates Rad4 on other residues than Cdc2 consensus phosphorylation sites (but Rad4 does not contain consensus SQ/TQ sites for Rad3 or Tel1-dependent phosphorylation) and this is a prerequisite for Rad4 phosphorylation on consensus sites by Cdc2 following DNA damage. Third, Rad3 phosphorylates a Rad4-interacting partner which subsequently allows Rad4 phosphorylation on consensus sites by Cdc2 following DNA damage.

CDK activity has been suggested to be important for checkpoint maintenance. In *S. cerevisiae*, Cdc28 plays a role in Rad53 phosphorylation induced by tethering of Ddc2-GFP-LacI and Ddc1-GFP-LacI to LacO array in a LacI/LacO system (Bonilla et al., 2008). This system in *S. cerevisiae* (and our work presented in Chapter 5) suggests that checkpoint activation which occurs in an ssDNA-independent manner recapitulates a step of chromatin-mediated checkpoint maintenance/amplification.

- **Role of Rad4 RXL motif and S641**

Rad4 was found to interact with Cdc13 (cyclin B) *in vivo* in the laboratory (Valerie Garcia, personal communication) and *in vitro* (Fig. 4-7B). Besides, the RXL motif serve as a docking site for the binding of the CyclinA-CDK kinase complex onto its substrate (K. Fukuchi et al., 2003), and the RXL motif is often necessary for CDK-phosphorylation of substrates containing RXL motifs (Loog and Morgan, 2005; Schulman et al., 1998). S641 has been identified to be highly phosphorylated by Cdc2 *in vitro* by mass spectrometry and it is in close proximity to the RXL motif. Therefore, we hypothesized that a Rad4 interaction with Cdc13 is required for Rad4 phosphorylation by Cdc2, and that this might be dependent on the RXL motif and S641. Rad4 CDK phosphorylation mutants are not strongly sensitive to DNA damaging agents or HU (Fig. 3-1C). Therefore, even if the RXL motif and S641 were required for Rad4 phosphorylation by Cdc2, it is not surprising that *rad4-dRXL* and *rad4-S641A* do not exhibit highly sensitivity to DNA damage and HU (Fig. 3-6B). However, the recombinant C-terminus Rad4 where the RXL motif is deleted or S641 is mutated to alanine does not affect Rad4 interaction with Cdc13 *in vitro* (Fig. 4-7B). This suggests that a RXL motif and S641 in Rad4 do not play a role in interaction with Cdc13. Intriguingly, the interaction of recombinant C-terminus Rad4 mutated on S641A with Rad3 is highly reduced in a GST-pull down assay (Fig. 4-7B). However, the S641A

mutant is not sensitive to DNA damage *in vivo* (Fig. 3-6B). This suggests that Rad4 interaction with Rad3 may not rely on S641 *in vivo*, but instead relies on N-terminus of Rad4 and/or tyrosine 599 in Rad4 (within C-terminus of Rad4) (detail in Chapter 4 and below).

Characterization of a putative AAD in Rad4

TopBP1/Dpb11/Rad4 is known to have an essential role in the initiation of DNA replication and the checkpoint response (Garcia et al., 2005). These diverse functions are conserved between Rad4 homologous in different eukaryotes but the molecular mechanisms underlying these distinct functions are unclear. The TopBP1 AAD in *Xenopus* and mammalian cells was found to interact with, and stimulate, ATR kinase activity (Kumagai et al., 2006). After we initiated our study of the AAD in *S. pombe*, two groups have independently shown that Dpb11 in *S. cerevisiae* has the ability to activate Mec1-Ddc2 complex, while Dpb11 lacking its C-terminus beyond the fourth BRCT tail is unable to activate Mec1 kinase activity (Mordes et al., 2008b; Navadgi-Patil and Burgers, 2008). This suggests that the C-terminus tail of Dpb11, displaying no significant homology with the AAD in higher eukaryotes, performs the same function in Mec1 activation as TopBP1 AAD.

- **The AAD is conserved in yeasts**

The AAD was first reported to not be conserved in yeast (Kumagai et al., 2006). However an alignment of the core of the AAD between yeast species and the hTopBP1 AAD was provided by Charly Chahwan (Fig. 4-1). In all the fungi species used for the alignment, the conserved tryptophan present in higher eukaryotes (W1138 in Xcut5 or W1145 in hTopBP1) is replaced with another aromatic amino acid, a tyrosine (Y) (see

Fig. 4-1). Interestingly, there is a SQ/TQ present within the AAD in mammals (S1138) and *Xenopus* (S1131), whereas it is replaced by a Cdc2 phosphorylation consensus TP/SP motif (S592) in *S. pombe* (Fig. 7-1).

- **Role of Rad4 AAD in response to DNA damage**

We have identified a short sequence of (21 amino-acids) in the unstructured C-terminal tail of *S. pombe* Rad4 sharing homology with the AAD of TopBP1. In order to study the role of a putative AAD in stimulating ATR kinase activity in *S. pombe*, *S. pombe* strains expressing Rad4 with either a deletion of the conserved core of the AAD (*rad4-AAD*, deleted for a small region 595-601 (EHVSYID)) or a substitution of the key aromatic amino acid localized within the AAD (*rad4-Y599R*) were constructed. Both *rad4 AAD* mutants (*rad4-Y599R* and *rad4-AAD*) show a higher sensitivity than wild-type cells to high doses of DNA damaging agents *i.e.* UV, MMS and HU (Fig. 4-2B). However, *rad4 AAD* mutants are less sensitive than a *rad3-d* strain in response to genotoxic agents, suggesting that these mutants reduce, but do not completely prevent, Rad3-mediated checkpoint activation. In addition, *rad4-AAD* (null) and *rad4-Y599R* could not maintain the G2 checkpoint arrest after UV-irradiation (Fig. 4-3), resulting in a subtle G2/M checkpoint defect. Also, Chk1 phosphorylation (Fig. 4-5C) and activation of Cds1 kinase (Fig. 4-5A.B) are compromised in the *rad4 AAD* mutant after UV-irradiation. Consistently, a series of C-terminal truncations expressed in *S. pombe* cells under the endogenous *rad4* promoter show sensitivity to DNA damages and HU but are less sensitive compared to a *rad3-d* strain (Fig. 4-12B). Unexpectedly, the sensitivity of a strain expressing Rad4 deleted for its whole C-terminal tail is almost identical to the sensitivity of a strain expressing a C-terminal truncation of Rad4 but retaining the AAD (Fig. 4-12B). These observations suggest that these truncations disrupt the Rad4 interaction with Rad3, possibly by altering the folding of the AAD; in turn the

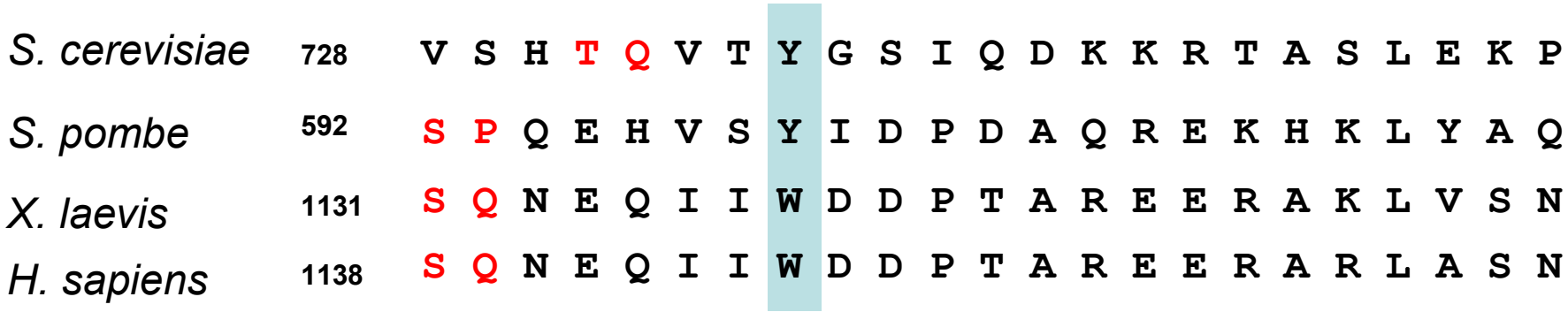

Figure 7-1- Alignment of the core of TopBP1 AAD with yeasts
A conserved SQ/TQ site (in red) resides within the region of the AAD in *Xenopus* and human. The SQ/TO motif is replaced by a SP/TP Cdc2 consensus phosphorylation sites (in red) in *S. pombe*. The key aromatic residue are black characters on a blue background.

checkpoint response is compromised.

- **Role of the AAD in Rad4 association with Rad3**

Our *in vitro* biochemical study shows that a physical interaction between Rad3 and the Rad4 C-terminal moiety is highly reduced but not completely abolished in Rad4 with a mutation Y599R in the AAD (Fig. 4-7B, upper panel), suggesting that Rad4 physically associates with Rad3 in a AAD-dependent manner. Because the *rad4 AAD* mutants have a subtle checkpoint defect, our results imply that, although the Rad4 C-terminal moiety with an intact AAD is required for the interaction with Rad3 *in vitro*, it is not the only mechanism implicated in Rad3-mediated checkpoint activation and plays a minor role in response to DNA damage in asynchronous cells or G2-phase cells. Our data also indicate that either the N-terminal part of Rad4 or other regions of the C-terminus used in the experiment is required for interaction/activation of Rad3.

Kumagai et al., demonstrate that TopBP1 plays an important role as an ATR activator. They have addressed the detail of this mechanism by showing that Xcut5 stimulates Xatr kinase activity and interacts with Xatr in a Xatrip-dependent manner (Kumagai et al., 2006). Similarly, Mordes et al., (Ball et al., 2007; Mordes et al., 2008a; Mordes et al., 2008b) have shown *in vitro* that the ATR-TopBP1 interaction and TopBP1-dependent ATR kinase activation both occur in an ATRIP/Ddc2-dependent manner in mammals and *S. cerevisiae*. Furthermore, *in vivo*, the association of ATRIP with TopBP1 is essential for TopBP1-dependent ATR activation in damage checkpoint signaling in mammals and *S. cerevisiae*. This evidence from mammals and *S. cerevisiae*, lead us to hypothesize that the existence of a weak association between Rad3 and the Rad4 C-terminus moiety with a mutation in the AAD that we see in our GST-pull down experiment is perhaps due to the fact that the Rad4 C-terminus moiety binds to the

surface of Rad26, a homologue of ATRIP. So far, we have only analyzed the interaction between Rad4 and Rad3. In further experiments it will be interesting to investigate how Rad26 is involved in the stimulation of Rad3 kinase activity by the Rad4 AAD.

- **Role of Rad4 AAD in response to DNA damage specifically in S-phase**

The *rad4-Y599R* mutant does not display a G2/M checkpoint defect when IR occurs during G2-phase (Fig. 4-6) and it is not sensitive to IR (Fig. 4-2C), but shows a significant sensitivity when IR occurs in S-phase (Fig. 4-11). This indicates that *rad4-Y599R* sensitivity to IR is specifically in S-phase but not G2-phase cells. In accordance with this idea, the *rad4-Y599R* mutant (asynchronous cells) is sensitive to UV, MMS, CPT (S-phase specific DNA damage agents). However, this is unclear because when cells are irradiated in S-phase, there is no difference in Chk1 phosphorylation detected between wild-type and *rad4-Y599R* cells (Fig. 4-9). Interestingly, we observed that H2A phosphorylation is significantly compromised in *rad4-Y599R* mutant cells when IR was delivered in S-phase (Fig. 4-9). In contrast, H2A phosphorylation in *rad4-Y599R* and wild-type cells is similar when irradiation is performed in G2 synchronous cells (Valerie Garcia, personal communication). Asynchronous *rad4-Y599R* cells also show a reduction in H2A phosphorylation in response to UV, HU, and CPT, but not to IR (Valerie Garcia, personal communication). Therefore, *rad4-Y599R* cells have a clear defect in H2A phosphorylation (rather than Chk1 phosphorylation) in response to DNA damage specific for S-phase. Taken together, these data suggest that the AAD plays a role in chromatin-mediated checkpoint maintenance/amplification restricted to S phase. Chk1 phosphorylation is known to be required for G2/M checkpoint activation (Walworth and Bernards, 1996); Cds1 kinase activity is required for S/M checkpoint activation and preventing replication forks collapse when replication is stressed or DNA damage occurs during S-phase (Lambert

and Carr, 2005; Lindsay et al., 1998). Chk1 phosphorylation might be not a good indicator of checkpoint activation when damage is performed in S-phase, therefore, studying Cds1 kinase activity might be helpful to delineate the precise the role of the Rad4 AAD in S phase.

Characterization of Rad4 AAD in a LacI/LacO artificial system

- **Characterization of a LacI/LacO system in *S. pombe* cells**

We successfully established an artificial checkpoint induction system in the absence of exogenous DNA damage in *S. pombe* cells by targeting checkpoint proteins onto chromatin via LacI-LacO interaction. Similarly in *S. cerevisiae* (Bonilla et al., 2008) and mouse cells (Soutoglou and Misteli, 2008), checkpoint proteins in fusion with LacI artificially tethered to a LacO array-integrated into a chromosome induces Chk1 (or Rad53) phosphorylation, a hallmark of checkpoint activation, in the absence of exogenous DNA lesions. Therefore, this tethering system provides a useful platform for studying mechanisms of the Rad3-mediated DNA damage checkpoint pathway in *S. pombe*.

The checkpoint response can be simply divided into two steps: the initiation of checkpoint activation, which occurs in a ssDNA-RPA-dependent manner (Zou and Elledge, 2003); and checkpoint maintenance/amplification, which occurs in a ssDNA-RPA-independent but H2A phosphorylation-dependent manner (discussed later).

LacI-Rad3 tethering to a LacO array causes Chk1 phosphorylation. Chk1

phosphorylation does not occur when LacI-Rad3 is expressed in the cells lacking the LacO array (Fig.5-8B). However, Chk1 phosphorylation could be due to the replication fork collapsing in the system. When DNA replication origins are firing in the artificial tethering system, the progressing replication forks are possibly hindered by LacI-LacO binding. If so, the Cds1 kinase will be require to stabilize the replication fork. In the absence of Cds1, the replication fork will collapse and ssDNA-RPA will be generated, leading to Chk1 phosphorylation. However, expressing GFP-LacI in cells carrying the LacO array does not appear to increase Chk1 phosphorylation (Fig.5-8A), implying that ssDNA-RPA is not generated upon GFP-LacI interaction with LacO. Thus, our tethering system allows us to bypass the generation of ssDNA-RPA and can be used to study checkpoint activation focusing on checkpoint maintenance/amplification.

Consistent with this, Bonilla et al., observed only rarely spontaneous Rad52 focus occurring when Ddc1-GFP-LacI and Ddc2-GFP-LacI are co-localized to LacO arrays, suggesting such tethering experiment did not induce spontaneous DNA damage (Bonilla et al., 2008). It was observed that, in the mammalian system, neither resected DNA nor the ssDNA binding factor RPA were detected upon tethering of any of the LacI fusion proteins (Soutoglou and Misteli, 2008). As mentioned before, Cds1 activation has not been tested in our artificial checkpoint system. But, it would help to understand whether the replication fork is stalled and stabilized upon LacI interaction with LacO. In fact, there is an increased level of background of Chk1 phosphorylation when expressing GFP-LacI in the cells harboring the LacO array compared to cells without the LacO array (Fig.5-8A). Therefore, we can not exclude the possibility of that Chk1 phosphorylation is due to the presence of LacO repeats in the cells. In our *S. pombe* LacI/LacO system, up to 16 hours are required to express a LacI fusion protein in the cells under the *nmt* promoter. During the induction, the LacI-LacO interaction might become

a barrier when a DNA replication fork is progressing through the LacO array. Therefore, the replication checkpoint complex might load around LacO array. Unlike the *S. pombe* system, galactose induction is conducted in a *S. cerevisiae* LacI/LacO system and a LacI fusion protein can be expressed an hour after induction. In addition, G2-arrested cells can be (and often are) used to perform experiments in the system of Bonilla, Melo et al. Thus, the checkpoint activation in their artificial induction system is independent of replication checkpoint. This might be a reason why co-localization of two checkpoint proteins to the chromatin is not necessary in our *S. pombe* system, but it is necessary in *S. cerevisiae* system. But, this remains to be established.

The role of chromatin modification (histone H2A C-terminal phosphorylation and H4-K20 methylation) in checkpoint signaling is important for accumulation mediator proteins such as mammalian 53BP1, *S. pombe* Crb2 and *S. cerevisiae* Rad9 at sites of DNA damage (Du et al., 2006; Huyen et al., 2004). However, Crb2 phosphorylation at T215 is sufficient to accumulate Crb2 in the absence of H2A phosphorylation and methylation (Du et al., 2006). Surprisingly, Chk1 is phosphorylated when Rad3 is targeted to LacO array in wild-type but not in a H2A phosphorylation mutant (Fig.5-8C). This demonstrates that Chk1 phosphorylation induced by Rad3 tethering in the LacI/LacO artificial system is dependent on chromatin modification. These data support the contention that the LacI/LacO system corresponds to chromatin-mediated checkpoint maintenance/amplification.

Bonilla et al., show that Rad53 is phosphorylated only when Ddc2-GFP-LacI and Ddc1-GFP-LacI are simultaneously targeted to the LacO array in *S. cerevisiae*, and that targeting either Ddc2-GFP-LacI or Ddc1-GFP-LacI is not sufficient to induce Rad53 phosphorylation (Bonilla et al., 2008). However, Soutoglou and Misteli show

checkpoint signaling (H2A phosphorylation) is elicited by recruitment of any one of Nbs1, Mre11, MDC1 or ATM to LacO array in mouse cells, and tethering any of these proteins to chromatin is sufficient to recruit protein partners expressed endogenously (Soutoglou and Misteli, 2008). Similarly to mammals, in *S. pombe* the tethering of single checkpoint proteins LacI-Rad3, LacI-Rad9 or Rad4-LacI to a LacO array is sufficient to induce checkpoint activation. Presumably, the checkpoint proteins tethered to the LacO array are able to recruit other endogenous checkpoint proteins in order to induce checkpoint activation in *S. pombe*, as is the case in mammalian cells. The dependency on endogenous protein is confirmed by the fact that when, expressing LacI-Rad3 in *rad4-Y599R* (Fig.5-9A.B.C) or *rad9-T412A* (Fig.5-11) mutant cells carrying the LacO array, Rad3-mediated Chk1 phosphorylation are compromised. It remains possible that a DNA replication fork is stalled (discussed before), and the checkpoint complex expressed endogenously is pre-formed. Thus, whether a complex pre-exists or is formed subsequently after tethering is unknown.

- **Role of Rad4 AAD in a LacI/LacO system**

To understand the role of Rad4 AAD in checkpoint activation, Rad4 mutated in the AAD in fusion with LacI was expressed in the artificial LacI/LacO system. While Chk1 is phosphorylated when Rad4-LacI is tethered to chromatin, it is not when Rad4-Y599R-LacI is expressed (Fig.5-9D), implying that the AAD is necessary for Rad4-induced checkpoint activation in this system. Moreover, co-expressing LacI-Rad3 and Rad4-LacI in cells carrying the LacO array elicits Chk1 phosphorylation whereas co-expressing LacI-Rad3 and Rad4-Y599R-LacI could not (Fig.5-9D). The overexpression of Rad4-Y599R-LacI in the cells harboring the LacO array apparently has a dominant negative effect, preventing Rad3-induced Chk1 phosphorylation even in the presence of endogenous wild-type Rad4. Altogether, this suggests that AAD plays

an important role in checkpoint signaling, independently of ssDNA formation and likely mediated by chromatin (H2A phosphorylation). Compared to the case in wild-type cells, targeting of GFP-LacI-NLS-Rad3 to LacO array in *rad4-Y599R* cells causes a significantly reduced Chk1 phosphorylation (Fig.5-9A.B.C). Because checkpoint activation in the artificial LacI/LacO induction system likely occurs in an ssDNA-RPA-independent manner and a H2A phosphorylation-dependent manner, it indicates that Rad4 AAD plays an important role in chromatin-mediated checkpoint maintenance/amplification.

- **Rad4 C-terminus is not sufficient to activate checkpoint in a LacI/LacO system**

We have shown that the tethering of a C-terminus fragment of Rad4 carrying AAD does not induce Chk1 phosphorylation (Fig.5-12A). In addition, Chk1 phosphorylation is highly reduced when targeting of LacI-Rad3 to LacO array in *rad4-Y599R* cells, but additional targeting of the C-terminus Rad4 does not have ability to rescue the Chk1 phosphorylation defect (Fig.5-12B). This suggests that Rad4 N-terminus moiety may be required for interaction with other checkpoint proteins, such as endogenously expressed Crb2, to be able to initiate the checkpoint activation (Saka et al., 1997) because this system does not bypass the requirement for other checkpoint components for the initiation of the checkpoint pathway. This is consistent with the hypothesis mentioned above. This idea was also recently demonstrated by Choi et al. that both N terminal and C-terminal of TopBP1 were required for recruitment to ssDNA-RPA via interaction with ATRIP to form a stable complex, leading to activate ATR kinase (Choi et al.).

- **Role of Rad4 Cdc2 phosphorylation sites in a LacI/LacO system**

A conserved SQ/TQ motif localizes within the AAD which are S1131 in *Xenopus* and

S1138 in human cells (Fig. 7-1). S1131 in Xcut5 is shown to be phosphorylated by Xatm and thereby enhances Xcut5 association with Xatr-Xatrip complex and stimulates Xatr kinase activity in response to DSBs (Yoo et al., 2007). In *S. cerevisiae*, Dpb11 phosphorylation on T731 (a SQ/TQ site) by Mec1 stimulates Mec1-Ddc2 complex kinase activity (Mordes et al., 2008b).

The SQ/TQ motifs in Xcut5 and Dpb11 thus seem to play a conserved function in Xatr/Mec1 kinase activation. Even though the *S. pombe* Rad4 AAD does not contain an SQ/TQ motif, Rad4 T589 and S592 (SP/TP sites) are found in proximity to the AAD and S592 phosphorylation is shown to be dependent on Rad3 *in vivo* (detailed in Chapter 3). Interestingly, our preliminary observation shows that, unlike Rad4-LacI tethering, Rad4-T589A.S592A(2A)-LacI targeting to LacO array does not induce Chk1 phosphorylation. However, targeting of LacI-Rad3 and Rad4-2A-LacI to LacO array induces Chk1 phosphorylation to the extent as targeting LacI-Rad3 and Rad4-LacI (Fig.5-10). This suggests that the Rad4 phosphorylation on T589 and S592 is required for increasing the local concentration of Rad3 at sites of damaged chromatin in order to enforce checkpoint signaling. Rad4 phosphorylation on T589 and S592 is thus a prerequisite for Rad3 activity by Rad4 AAD. Consistently, Rad4 Cdc2 phosphorylation mutant has a very mild sensitivity to DNA damage agents and HU (Fig.3-1).

- **Other checkpoint proteins addressed in a LacI/LacO system**

Rad9 C-terminal phosphorylation at T412 by Rad3 is required for recruiting Rad4 and promotes Chk1 activation (Furuya et al., 2004). Therefore, we used our tethering system to dissect out the role of Rad9 in DNA damage checkpoint activation. Chk1 is not phosphorylated when LacI-Rad3 is targeted to LacO array in *rad9-T412A* cells (Fig.5-11). This indicates that Rad3-induced Chk1 activation is largely dependent on the

endogenous Rad9 C-terminus phosphorylation on T412. We also show that the reduction of Chk1 phosphorylation in *rad9-T412A* cells is rescued by co-expression of LacI-Rad3 and Rad4-LacI, indicating that Rad4-LacI tethering bypasses the requirement for Rad9 phosphorylation on T412 in the tethering LacI/LacO system. Thus, these observations are consistent with Furuya et al's model where the Rad9 C-terminal phosphorylation on T412 promotes formation of Rad9-Rad4 complex in order to activate Rad3.

The clamp loader Rad17 is required to recruit the 9-1-1 complex to sites of damage (Zou et al., 2002). It remains to be tested whether Rad17 has any additional roles during checkpoint activation. If it is its only function, Rad17 is predicted to be not required when Rad9 is tethered to chromatin. When Ddc1-GFP-LacI and Ddc2-GFP-LacI are targeted to LacO array in *S. cerevisiae*, Rad53 phosphorylation is still elicited in cells with deletion of *mec3* and *rad17*, suggesting that the formation of clamp is not required in *S. cerevisiae* checkpoint pathway (Bonilla et al., 2008). In order to understand the role of Rad17 and 9-1-1 during checkpoint pathway, further experiments are being carried out by Chris Wardlaw, a PhD student in the laboratory. Chk1 phosphorylation is not elicited by Rad3 tethering to LacO array in *rad1-d*, *rad9-d*, or *rad17-d* cells. This suggests that Rad9 conformation with Rad1 and Hus1 is essential for checkpoint activation in this system. But, importantly, whether Rad17 is necessary when Rad9 is tethered to chromatin in the system is still unknown.

- **A predicted model**

Taken together, our findings in the LacI/LacO tethering system lead us to draw a model focusing on the step of checkpoint maintenance/amplification because checkpoint activation occurs in this artificial system in an ssDNA-RPA-independent manner and a

H2A phosphorylation-dependent manner (Fig.7-2). In response to DNA damage, H2A phosphorylation by Rad3 occurs quickly once checkpoint activation is initiated (ssDNA-RPA-dependent) and spreads both sides of LacO array. γ-H2A recruits Crb2 (Du et al., 2003; Nakamura et al., 2004) and Crb2 phosphorylation at T215 (a SP/TP site) is critical for association with Rad4 (Du et al., 2006; Saka et al., 1997). The Rad4-associated chromatin may recruit Rad3 via Rad4 C-terminus phosphorylation on T589 and S592 (Rad3 dependent), and Rad4 activates Rad3 in an AAD-dependent manner. Rad4 AAD may provide a positive feedback for the checkpoint amplification in order to keep propagating and maintaining checkpoint signaling until the damaged DNA is repaired. The activated Rad3 phosphorylates H2A and the signal is spread (amplification). In our predicted model, more Rad3 is recruited to LacO array and this interacts with Rad4 via the AAD. Rad3 has been shown to be required for Chk1-dependent damage checkpoint activation but is dispensable for its maintenance (Martinho et al., 1998); however, Rad3 was shown to be required for both Cds1-dependent S-phase checkpoint activation and maintenance. If our model is correct, this indicates that ssDNA-independent LacI/LacO system in *S. pombe* mimics checkpoint activation in response to replication stress or DNA damage occurring in S-phase. This supports the findings that *rad4-Y599R* cells have defect in dealing DNA damage specifically during S-phase (detail in Chapter 4). Recent reports show that when HU-arrest cells are challenged with IR, Rad52 focus formation is inhibited, suggesting replication stress or DNA damage in S-phase causes the limitation of ssDNA-PRA formation processing from DSBs (Barlow and Rothstein, 2009). Interestingly, TopBP1-dependent ATR activation was reported to occur independently of RPA (Ball et al., 2007). Altogether, these experiments reveal that Rad4 AAD is essential for chromatin-mediated checkpoint maintenance/amplification and that it plays an important role in S-phase when ssDNA-RPA formation is limited (detail in Chapter 4

Figure 7-2- Model of Rad4 ATR-activating domain required for checkpoint maintenance/amplification

(A) **initiation of checkpoint activation**: The 9-1-1 complex is recruited to damaged chromatin by Rad17 independently of the Rad3-Rad26 complex in response to DNA damage (ssDNA-RPA-dependent). Phosphorylation of Rad9 by Rad3 promotes association Rad9 with Rad4 and Rad3 with Rad4. Subsequently, the Rad3-mediated Chk1 pathway is activated and H2A is phosphorylated surrounding both sides of damaged chromatin in a Rad3-dependent manner. Phosphorylated H2A recruits Crb2 and Crb2 brings additional Rad4.

(B) **maintenance/amplification of checkpoint activation**: The Rad4-associated chromatin may recruit Rad3 via Rad4 C-terminal phosphorylation on T589 and S592 (Rad3-dependent), and Rad4 interacts and activates Rad3 in an AAD-dependent manner. Rad4 AAD may provide a positive feedback for the checkpoint amplification in order to keep propagating and maintaining checkpoint signaling until the damaged DNA is repaired. The activated Rad3 phosphorylates further H2A and the signal spread (amplification). An additional protein (?) might interact with phosphorylated H2A and the candidate (?) possible is Brc1.

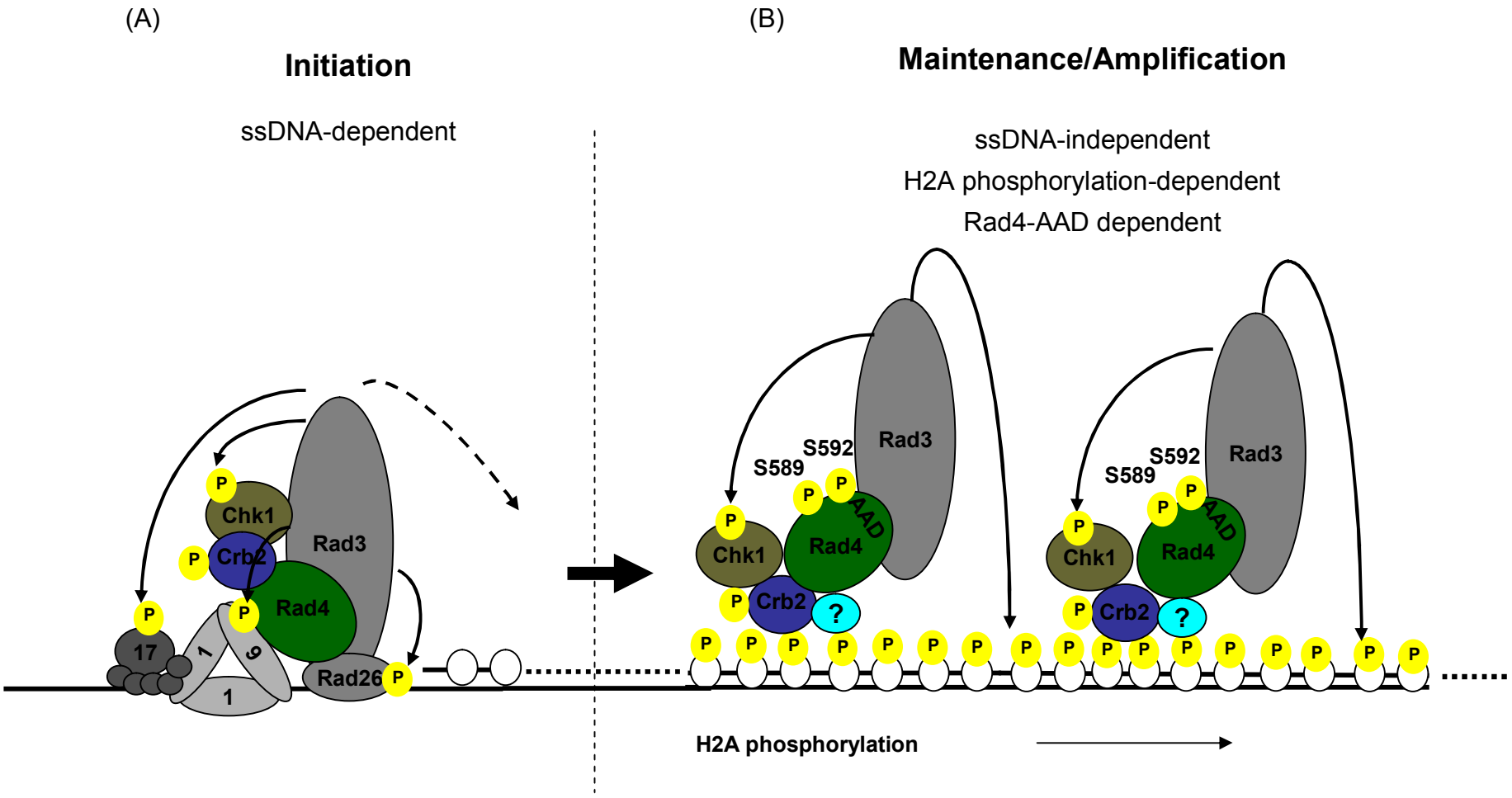
(A)
Initiation
ssDNA-dependent
(B)
Maintenance/Amplification
ssDNA-independent
H2A phosphorylation-dependent
Rad4-AAD dependent
Chk1
Crb2
Rad3
Rad4
Rad26
17
1
9
1
S589
S592
AAD
?
H2A phosphorylation

and 5).

- **Further studies (carried out by Chris Wardlaw, a phD student)**

Based on our predicted model, Rad4 AAD is implicated in the chromatin-mediated checkpoint maintenance/amplification via H2A phosphorylation. A future study of whether checkpoint maintenance/amplification in a LacI/LacO system is dependent on phosphorylated H2A association with Crb2 would help greatly to understand our predicted model. *crb2-K619E* and *crb2-K617E* are mutants disrupting Crb2 binding to γ-H2A (Kilkenny et al., 2008). Interestingly, reduced but not completely abolished Chk1 phosphorylation is observed when Rad3 is tethered to LacO array in a *crb2-K617E* or a *crb2-K619E* mutant (Chris Wardlaw, personal communication), suggesting that checkpoint maintenance is at least partially dependent on the interaction of Crb2 with γ-H2A.

Recently, Brc1, a six BRCT-domain protein, has been shown to bind with γ-H2A and to be critical for recovery from replication-associated DNA damage in *S. pombe* (Williams et al.). In addition, foci formation of Crb2 and Brc1 co-localize in response to CPT or IR (Williams et al.). This leads us to make a presumption that the remaining Rad3 tethering-induced Chk1 phosphorylation in the *crb2* mutants (*crb2-K617E* or *crb2-K619E*) may be due to an additional protein interaction with γ-H2A and that a candidate might be Brc1.

Conclusion

At present, evidence shows that mammalian TopBP1 AAD/*S. cerevisiae* Dpb11 C-terminus function as an activator of ATR/Mec1 kinase when TopBP1/Dpb11 is

overexpressed. We identified a potential AAD in the C-terminal tail of *S. pombe* Rad4. We have shown that Rad3 association with Rad4 occurs in an AAD-dependent manner. *S. pombe* strains mutated in AAD show a slight sensitivity to DNA damage and HU. The *rad4 AAD* mutants does not completely prevent Rad3-mediated G2/M checkpoint activation after DNA damage. The sensitivity in a *rad4-Y599R* mutant increases when damage occurs in S-phase, and H2A phosphorylation is compromised in *rad4-Y599R* cells when damage is delivered in S-phase. Importantly, Rad4 AAD is suggested to be playing an important role of in chromatin-mediated checkpoint maintenance/amplification in an artificial checkpoint induction system. Although the homology of Rad4 AAD in *S. pombe* with higher eukaryotes is limited, Rad4 AAD does play an important role in Rad3-mediated checkpoint activation. Taken together, we propose a model whereby the AAD of Rad4 is required for maintenance/amplification of the checkpoint signal in an ssDNA-independent manner. This pathway plays an important role specifically in S-phase, when resection is limited (ssDNA-independent).

References

Alcasabas, A. A., Osborn, A. J., Bachant, J., Hu, F., Werler, P. J., Bousset, K., Furuya, K., Diffley, J. F., Carr, A. M., and Elledge, S. J. (2001). Mrc1 transduces signals of DNA replication stress to activate Rad53. Nat Cell Biol *3*, 958-965.

Aparicio, O. M., Weinstein, D. M., and Bell, S. P. (1997). Components and dynamics of DNA replication complexes in *S. cerevisiae*: redistribution of MCM proteins and Cdc45p during S phase. Cell *91*, 59-69.

Araki, H., Leem, S. H., Phongdara, A., and Sugino, A. (1995). Dpb11, which interacts with DNA polymerase II (epsilon) in *Saccharomyces cerevisiae*, has a dual role in S-phase progression and at a cell cycle checkpoint. Proc Natl Acad Sci U S A *92*, 11791-11795.

Ball, H. L., and Cortez, D. (2005). ATRIP oligomerization is required for ATR-dependent checkpoint signaling. J Biol Chem *280*, 31390-31396.

Ball, H. L., Ehrhardt, M. R., Mordes, D. A., Glick, G. G., Chazin, W. J., and Cortez, D. (2007). Function of a conserved checkpoint recruitment domain in ATRIP proteins. Mol Cell Biol *27*, 3367-3377.

Ball, H. L., Myers, J. S., and Cortez, D. (2005). ATRIP binding to replication protein A-single-stranded DNA promotes ATR-ATRIP localization but is dispensable for Chk1 phosphorylation. Mol Biol Cell *16*, 2372-2381.

Barlow, J. H., and Rothstein, R. (2009). Rad52 recruitment is DNA replication independent and regulated by Cdc28 and the Mec1 kinase. Embo J *28*, 1121-1130.

Bell, S. P., and Dutta, A. (2002). DNA replication in eukaryotic cells. Annu Rev Biochem *71*, 333-374.

Blankley, R. T., and Lydall, D. (2004). A domain of Rad9 specifically required for activation of Chk1 in budding yeast. J Cell Sci *117*, 601-608.

Boddy, M. N., Furnari, B., Mondesert, O., and Russell, P. (1998). Replication checkpoint enforced by kinases Cds1 and Chk1. Science *280*, 909-912.

Bonilla, C. Y., Melo, J. A., and Toczyski, D. P. (2008). Colocalization of sensors is sufficient to activate the DNA damage checkpoint in the absence of damage. Mol Cell *30*, 267-276.

Booher, R. N., Alfa, C. E., Hyams, J. S., and Beach, D. H. (1989). The fission yeast cdc2/cdc13/suc1 protein kinase: regulation of catalytic activity and nuclear localization. Cell *58*, 485-497.

Brondello, J. M., Boddy, M. N., Furnari, B., and Russell, P. (1999). Basis for the checkpoint signal specificity that regulates Chk1 and Cds1 protein kinases. Mol Cell Biol *19*, 4262-4269.

Brown, N. R., Lowe, E. D., Petri, E., Skamnaki, V., Antrobus, R., and Johnson, L. N. (2007). Cyclin B and cyclin A confer different substrate recognition properties on CDK2. Cell Cycle *6*, 1350-1359.

Brown, N. R., Noble, M. E., Endicott, J. A., and Johnson, L. N. (1999). The structural basis for specificity of substrate and recruitment peptides for cyclin-dependent kinases. Nat Cell Biol *1*, 438-443.

Calonge, T. M., and O'Connell, M. J. (2008). Turning off the G2 DNA damage checkpoint. DNA Repair (Amst) *7*, 136-140.

Carr, A. M. (2002). DNA structure dependent checkpoints as regulators of DNA repair. DNA Repair (Amst) *1*, 983-994.

Caspari, T., Dahlen, M., Kanter-Smoler, G., Lindsay, H. D., Hofmann, K., Papadimitriou, K., Sunnerhagen, P., and Carr, A. M. (2000). Characterization of *Schizosaccharomyces pombe* Hus1: a PCNA-related protein that associates with Rad1 and Rad9. Mol Cell Biol *20*, 1254-1262.

Caspari, T., Murray, J. M., and Carr, A. M. (2002). Cdc2-cyclin B kinase activity links Crb2 and Rqh1-topoisomerase III. Genes Dev *16*, 1195-1208.

Chen, S., de Vries, M. A., and Bell, S. P. (2007a). Orc6 is required for dynamic recruitment of Cdt1 during repeated Mcm2-7 loading. Genes Dev *21*, 2897-2907.

Chen, X., Zhao, R., Glick, G. G., and Cortez, D. (2007b). Function of the ATR N-terminal domain revealed by an ATM/ATR chimera. Exp Cell Res *313*, 1667-1674.

Choi, J. H., Lindsey-Boltz, L. A., Kemp, M., Mason, A. C., Wold, M. S., and Sancar, A. Reconstitution of RPA-covered single-stranded DNA-activated ATR-Chk1 signaling. Proc Natl Acad Sci U S A *107*, 13660-13665.

Choi, J. H., Lindsey-Boltz, L. A., and Sancar, A. (2007). Reconstitution of a human ATR-mediated checkpoint response to damaged DNA. Proc Natl Acad Sci U S A *104*, 13301-13306.

Choi, J. H., Lindsey-Boltz, L. A., and Sancar, A. (2009). Cooperative activation of the ATR checkpoint kinase by TopBP1 and damaged DNA. Nucleic Acids Res.

Cimprich, K. A., and Cortez, D. (2008). ATR: an essential regulator of genome integrity. Nat Rev Mol Cell Biol *9*, 616-627.

Cortez, D., Guntuku, S., Qin, J., and Elledge, S. J. (2001). ATR and ATRIP: partners in checkpoint signaling. Science *294*, 1713-1716.

Czornak, K., Chughtai, S., and Chrzanowska, K. H. (2008). Mystery of DNA repair: the role of the MRN complex and ATM kinase in DNA damage repair. J Appl Genet *49*, 383-396.

de Jager, M., van Noort, J., van Gent, D. C., Dekker, C., Kanaar, R., and Wyman, C. (2001). Human Rad50/Mre11 is a flexible complex that can tether DNA ends. Mol Cell *8*, 1129-1135.

Delacroix, S., Wagner, J. M., Kobayashi, M., Yamamoto, K., and Karnitz, L. M. (2007). The Rad9-Hus1-Rad1 (9-1-1) clamp activates checkpoint signaling via TopBP1. Genes Dev *21*, 1472-1477.

den Elzen, N., Kosoy, A., Christopoulos, H., and O'Connell, M. J. (2004). Resisting arrest: recovery from checkpoint arrest through dephosphorylation of Chk1 by PP1. Cell Cycle *3*, 529-533.

den Elzen, N. R., and O'Connell, M. J. (2004). Recovery from DNA damage checkpoint arrest by PP1-mediated inhibition of Chk1. Embo J *23*, 908-918.

Dischinger, S., Krapp, A., Xie, L., Paulson, J. R., and Simanis, V. (2008). Chemical genetic analysis of the regulatory role of Cdc2p in the *S. pombe* septation initiation network. J Cell Sci *121*, 843-853.

Doe, C. L., Dixon, J., Osman, F., and Whitby, M. C. (2000). Partial suppression of the fission yeast rqh1 (-) phenotype by expression of a bacterial Holliday junction resolvase. Embo J *19*, 2751-2762.

Dolan, W. P., Sherman, D. A., and Forsburg, S. L. (2004). *Schizosaccharomyces pombe* replication protein Cdc45/Sna41 requires Hsk1/Cdc7 and Rad4/Cut5 for chromatin binding. Chromosoma *113*, 145-156.

Downs, J. A., Lowndes, N. F., and Jackson, S. P. (2000). A role for *Saccharomyces cerevisiae* histone H2A in DNA repair. Nature *408*, 1001-1004.

Du, L. L., Nakamura, T. M., Moser, B. A., and Russell, P. (2003). Retention but not recruitment of Crb2 at double-strand breaks requires Rad1 and Rad3 complexes. Mol Cell Biol *23*, 6150-6158.

Du, L. L., Nakamura, T. M., and Russell, P. (2006). Histone modification-dependent and -independent pathways for recruitment of checkpoint protein Crb2 to double-strand breaks. Genes Dev *20*, 1583-1596.

Duck, P., Nasim, A., and James, A. P. (1976). Temperature-sensitive mutant of *Schizosaccharomyces pombe* exhibiting enhanced radiation sensitivity. J Bacteriol *128*, 536-539.

Duncker, B. P., Chesnokov, I. N., and McConkey, B. J. (2009). The origin recognition complex protein family. Genome Biol *10*, 214.

Durkacz, B., Carr, A., and Nurse, P. (1986). Transcription of the cdc2 cell cycle control gene of the fission yeast *Schizosaccharomyces pombe*. EMBO J *5*, 369-373.

Edwards, R. J., Bentley, N. J., and Carr, A. M. (1999). A Rad3-Rad26 complex responds to DNA damage independently of other checkpoint proteins. Nat Cell Biol *1*, 393-398.

Emili, A. (1998). MEC1-dependent phosphorylation of Rad9p in response to DNA damage. Mol Cell *2*, 183-189.

Esashi, F., and Yanagida, M. (1999). Cdc2 phosphorylation of Crb2 is required for reestablishing cell cycle progression after the damage checkpoint. Mol Cell *4*, 167-174.

Falck, J., Coates, J., and Jackson, S. P. (2005). Conserved modes of recruitment of ATM,

ATR and DNA-PKcs to sites of DNA damage. Nature *434*, 605-611.

Fenech, M., Carr, A. M., Murray, J., Watts, F. Z., and Lehmann, A. R. (1991). Cloning and characterization of the *rad4* gene of *Schizosaccharomyces pombe*; a gene showing short regions of sequence similarity to the human *XRCC1* gene. Nucleic Acids Res *19*, 6737-6741.

Forsburg, S. L. (2003). Overview of *Schizosaccharomyces pombe*. Curr Protoc Mol Biol *Chapter 13*, Unit 13 14.

Forsburg, S. L., and Nurse, P. (1991). Cell cycle regulation in the yeasts *Saccharomyces cerevisiae* and *Schizosaccharomyces pombe*. Annu Rev Cell Biol *7*, 227-256.

Furnari, B., Blasina, A., Boddy, M. N., McGowan, C. H., and Russell, P. (1999). Cdc25 inhibited in vivo and in vitro by checkpoint kinases Cds1 and Chk1. Mol Biol Cell *10*, 833-845.

Furuya, K., Poitelea, M., Guo, L., Caspari, T., and Carr, A. M. (2004). Chk1 activation requires Rad9 S/TQ-site phosphorylation to promote association with C-terminal BRCT domains of Rad4TOPBP1. Genes Dev *18*, 1154-1164.

Gambus, A., Jones, R. C., Sanchez-Diaz, A., Kanemaki, M., van Deursen, F., Edmondson, R. D., and Labib, K. (2006). GINS maintains association of Cdc45 with MCM in replisome progression complexes at eukaryotic DNA replication forks. Nat Cell Biol *8*, 358-366.

Garcia, V., Furuya, K., and Carr, A. M. (2005). Identification and functional analysis of TopBP1 and its homologs. DNA Repair (Amst) *4*, 1227-1239.

Giannattasio, M., Lazzaro, F., Plevani, P., and Muzi-Falconi, M. (2005). The DNA damage checkpoint response requires histone H2B ubiquitination by Rad6-Bre1 and H3 methylation by Dot1. J Biol Chem *280*, 9879-9886.

Gopalakrishnan, V., Simancek, P., Houchens, C., Snaith, H. A., Frattini, M. G., Sazer, S., and Kelly, T. J. (2001). Redundant control of rereplication in fission yeast. Proc Natl Acad Sci U S A *98*, 13114-13119.

Gottlieb, T. M., and Jackson, S. P. (1993). The DNA-dependent protein kinase: requirement for DNA ends and association with Ku antigen. Cell *72*, 131-142.

Guo, Z., Kumagai, A., Wang, S. X., and Dunphy, W. G. (2000). Requirement for Atr in phosphorylation of Chk1 and cell cycle regulation in response to DNA replication blocks and UV-damaged DNA in *Xenopus* egg extracts. Genes Dev *14*, 2745-2756.

Hammet, A., Magill, C., Heierhorst, J., and Jackson, S. P. (2007). Rad9 BRCT domain interaction with phosphorylated H2AX regulates the G1 checkpoint in budding yeast. EMBO Rep *8*, 851-857.

Hanada, K., Budzowska, M., Davies, S. L., van Drunen, E., Onizawa, H., Beverloo, H. B., Maas, A., Essers, J., Hickson, I. D., and Kanaar, R. (2007). The structure-specific endonuclease Mus81 contributes to replication restart by generating double-strand DNA breaks. Nat Struct Mol Biol *14*, 1096-1104.

Harrison, J. C., and Haber, J. E. (2006). Surviving the breakup: the DNA damage checkpoint. Annu Rev Genet *40*, 209-235.

Hashimoto, Y., and Takisawa, H. (2003). *Xenopus* Cut5 is essential for a CDK-dependent process in the initiation of DNA replication. Embo J *22*, 2526-2535.

Hashimoto, Y., Tsujimura, T., Sugino, A., and Takisawa, H. (2006). The phosphorylated C-terminal domain of *Xenopus* Cut5 directly mediates ATR-dependent activation of Chk1. Genes Cells *11*, 993-1007.

Heyer, W. D., Li, X., Rolfsmeier, M., and Zhang, X. P. (2006). Rad54: the Swiss Army knife of homologous recombination? Nucleic Acids Res *34*, 4115-4125.

Hirano, T., Funahashi, S. I., Uemura, T., and Yanagida, M. (1986). Isolation and characterization of *Schizosaccharomyces pombe* cutmutants that block nuclear division but not cytokinesis. Embo J *5*, 2973-2979.

Hong, J. S., and Ames, B. N. (1971). Localized mutagenesis of any specific small region of the bacterial chromosome. Proc Natl Acad Sci U S A *68*, 3158-3162.

Huertas, P., Cortes-Ledesma, F., Sartori, A. A., Aguilera, A., and Jackson, S. P. (2008). CDK targets Sae2 to control DNA-end resection and homologous recombination. Nature.

Huertas, P., and Jackson, S. P. (2009). Human CtIP mediates cell cycle control of DNA end resection and double strand break repair. J Biol Chem *284*, 9558-9565.

Humpal, S. E., Robinson, D. A., and Krebs, J. E. (2009). Marks to stop the clock: histone modifications and checkpoint regulation in the DNA damage response. Biochem Cell Biol *87*, 243-253.

Huyen, Y., Zgheib, O., Ditullio, R. A., Jr., Gorgoulis, V. G., Zacharatos, P., Petty, T. J., Sheston, E. A., Mellert, H. S., Stavridi, E. S., and Halazonetis, T. D. (2004). Methylated lysine 79 of histone H3 targets 53BP1 to DNA double-strand breaks. Nature *432*, 406-411.

Ira, G., Pellicioli, A., Balijja, A., Wang, X., Fiorani, S., Carotenuto, W., Liberi, G., Bressan, D., Wan, L., Hollingsworth, N. M.*, et al.* (2004). DNA end resection, homologous recombination and DNA damage checkpoint activation require CDK1. Nature *431*, 1011-1017.

Ishimi, Y., Komamura-Kohno, Y., You, Z., Omori, A., and Kitagawa, M. (2000). Inhibition of Mcm4,6,7 helicase activity by phosphorylation with cyclin A/Cdk2. J Biol Chem *275*, 16235-16241.

Jallepalli, P. V., Brown, G. W., Muzi-Falconi, M., Tien, D., and Kelly, T. J. (1997). Regulation of the replication initiator protein p65cdc18 by CDK phosphorylation. Genes Dev *11*, 2767-2779.

Jazayeri, A., Falck, J., Lukas, C., Bartek, J., Smith, G. C., Lukas, J., and Jackson, S. P. (2006). ATM- and cell cycle-dependent regulation of ATR in response to DNA double-strand breaks. Nat Cell Biol *8*, 37-45.

Jiang, X., Sun, Y., Chen, S., Roy, K., and Price, B. D. (2006). The FATC domains of PIKK proteins are functionally equivalent and participate in the Tip60-dependent activation of DNA-PKcs and ATM. J Biol Chem *281*, 15741-15746.

Kamimura, Y., Masumoto, H., Sugino, A., and Araki, H. (1998). Sld2, which interacts with Dpb11 in *Saccharomyces cerevisiae*, is required for chromosomal DNA replication. Mol Cell Biol *18*, 6102-6109.

Kastan, M. B., and Bartek, J. (2004). Cell-cycle checkpoints and cancer. Nature *432*, 316-323.

Keogh, M. C., Kim, J. A., Downey, M., Fillingham, J., Chowdhury, D., Harrison, J. C., Onishi, M., Datta, N., Galicia, S., Emili, A.*, et al.* (2006). A phosphatase complex that

dephosphorylates gammaH2AX regulates DNA damage checkpoint recovery. Nature *439*, 497-501.

Khanna, K. K., and Jackson, S. P. (2001). DNA double-strand breaks: signaling, repair and the cancer connection. Nat Genet *27*, 247-254.

Kilkenny, M. L., Dore, A. S., Roe, S. M., Nestoras, K., Ho, J. C., Watts, F. Z., and Pearl, L. H. (2008). Structural and functional analysis of the Crb2-BRCT2 domain reveals distinct roles in checkpoint signaling and DNA damage repair. Genes Dev *22*, 2034-2047.

Kumagai, A., and Dunphy, W. G. (2000). Claspin, a novel protein required for the activation of Chk1 during a DNA replication checkpoint response in *Xenopus* egg extracts. Mol Cell *6*, 839-849.

Kumagai, A., Lee, J., Yoo, H. Y., and Dunphy, W. G. (2006). TopBP1 activates the ATR-ATRIP complex. Cell *124*, 943-955.

Labib, K., and Gambus, A. (2007). A key role for the GINS complex at DNA replication forks. Trends Cell Biol *17*, 271-278.

Lambert, S., and Carr, A. M. (2005). Checkpoint responses to replication fork barriers. Biochimie *87*, 591-602.

Lau, I. F., Filipe, S. R., Soballe, B., Okstad, O. A., Barre, F. X., and Sherratt, D. J. (2003). Spatial and temporal organization of replicating *Escherichia coli* chromosomes. Mol Microbiol *49*, 731-743.

Lavin, M. F., and Shiloh, Y. (1997). The genetic defect in ataxia-telangiectasia. Annu Rev Immunol *15*, 177-202.

Lee, J., Kumagai, A., and Dunphy, W. G. (2007). The Rad9-Hus1-Rad1 checkpoint clamp regulates interaction of TopBP1 with ATR. J Biol Chem *282*, 28036-28044.

Lee, J. K., and Hurwitz, J. (2001). Processive DNA helicase activity of the minichromosome maintenance proteins 4, 6, and 7 complex requires forked DNA structures. Proc Natl Acad Sci U S A *98*, 54-59.

Lee, S. E., Moore, J. K., Holmes, A., Umezu, K., Kolodner, R. D., and Haber, J. E.

(1998). Saccharomyces Ku70, mre11/rad50 and RPA proteins regulate adaptation to G2/M arrest after DNA damage. Cell *94*, 399-409.

Leroy, C., Lee, S. E., Vaze, M. B., Ochsenbien, F., Guerois, R., Haber, J. E., and Marsolier-Kergoat, M. C. (2003). PP2C phosphatases Ptc2 and Ptc3 are required for DNA checkpoint inactivation after a double-strand break. Mol Cell *11*, 827-835.

Limbo, O., Chahwan, C., Yamada, Y., de Bruin, R. A., Wittenberg, C., and Russell, P. (2007). Ctp1 is a cell-cycle-regulated protein that functions with Mre11 complex to control double-strand break repair by homologous recombination. Mol Cell *28*, 134-146.

Lindsay, H. D., Griffiths, D. J., Edwards, R. J., Christensen, P. U., Murray, J. M., Osman, F., Walworth, N., and Carr, A. M. (1998). S-phase-specific activation of Cds1 kinase defines a subpathway of the checkpoint response in *Schizosaccharomyces pombe*. Genes Dev *12*, 382-395.

Liu, E., Li, X., Yan, F., Zhao, Q., and Wu, X. (2004). Cyclin-dependent kinases phosphorylate human Cdt1 and induce its degradation. J Biol Chem *279*, 17283-17288.

Liu, K., Lin, F. T., Ruppert, J. M., and Lin, W. C. (2003). Regulation of E2F1 by BRCT domain-containing protein TopBP1. Mol Cell Biol *23*, 3287-3304.

Lobachev, K., Vitriol, E., Stemple, J., Resnick, M. A., and Bloom, K. (2004). Chromosome fragmentation after induction of a double-strand break is an active process prevented by the RMX repair complex. Curr Biol *14*, 2107-2112.

Loog, M., and Morgan, D. O. (2005). Cyclin specificity in the phosphorylation of cyclin-dependent kinase substrates. Nature *434*, 104-108.

Lopez-Girona, A., Furnari, B., Mondesert, O., and Russell, P. (1999). Nuclear localization of Cdc25 is regulated by DNA damage and a 14-3-3 protein. Nature *397*, 172-175.

Lou, Z., Minter-Dykhouse, K., Franco, S., Gostissa, M., Rivera, M. A., Celeste, A., Manis, J. P., van Deursen, J., Nussenzweig, A., Paull, T. T.*, et al.* (2006). MDC1 maintains genomic stability by participating in the amplification of ATM-dependent DNA damage signals. Mol Cell *21*, 187-200.

Majka, J., Binz, S. K., Wold, M. S., and Burgers, P. M. (2006a). Replication protein A directs loading of the DNA damage checkpoint clamp to 5'-DNA junctions. J Biol Chem *281*, 27855-27861.

Majka, J., Niedziela-Majka, A., and Burgers, P. M. (2006b). The checkpoint clamp activates Mec1 kinase during initiation of the DNA damage checkpoint. Mol Cell *24*, 891-901.

Makiniemi, M., Hillukkala, T., Tuusa, J., Reini, K., Vaara, M., Huang, D., Pospiech, H., Majuri, I., Westerling, T., Makela, T. P., and Syvaoja, J. E. (2001). BRCT domain-containing protein TopBP1 functions in DNA replication and damage response. J Biol Chem *276*, 30399-30406.

Manolis, K. G., Nimmo, E. R., Hartsuiker, E., Carr, A. M., Jeggo, P. A., and Allshire, R. C. (2001). Novel functional requirements for non-homologous DNA end joining in *Schizosaccharomyces pombe*. Embo J *20*, 210-221.

Martinho, R. G., Lindsay, H. D., Flaggs, G., DeMaggio, A. J., Hoekstra, M. F., Carr, A. M., and Bentley, N. J. (1998). Analysis of Rad3 and Chk1 protein kinases defines different checkpoint responses. Embo J *17*, 7239-7249.

Masai, H., Taniyama, C., Ogino, K., Matsui, E., Kakusho, N., Matsumoto, S., Kim, J. M., Ishii, A., Tanaka, T., Kobayashi, T.*, et al.* (2006). Phosphorylation of MCM4 by Cdc7 kinase facilitates its interaction with Cdc45 on the chromatin. J Biol Chem *281*, 39249-39261.

Masumoto, H., Muramatsu, S., Kamimura, Y., and Araki, H. (2002). S-Cdk-dependent phosphorylation of Sld2 essential for chromosomal DNA replication in budding yeast. Nature *415*, 651-655.

McCready, S. J., Osman, F., and Yasui, A. (2000). Repair of UV damage in the fission yeast *Schizosaccharomyces pombe*. Mutat Res *451*, 197-210.

McFarlane, R. J., Carr, A. M., and Price, C. (1997). Characterisation of the *Schizosaccharomyces pombe rad4*/*cut5* mutant phenotypes: dissection of DNA replication and G2 checkpoint control function. Mol Gen Genet *255*, 332-340.

Melo, J., and Toczyski, D. (2002). A unified view of the DNA-damage checkpoint. Curr Opin Cell Biol *14*, 237-245.

Melo, J. A., Cohen, J., and Toczyski, D. P. (2001). Two checkpoint complexes are independently recruited to sites of DNA damage in vivo. Genes Dev *15*, 2809-2821.

Mochida, S., Esashi, F., Aono, N., Tamai, K., O'Connell, M. J., and Yanagida, M. (2004). Regulation of checkpoint kinases through dynamic interaction with Crb2. EMBO J *23*, 418-428.

Mondesert, O., McGowan, C. H., and Russell, P. (1996). Cig2, a B-type cyclin, promotes the onset of S in *Schizosaccharomyces pombe*. Mol Cell Biol *16*, 1527-1533.
Mordes, D. A., Glick, G. G., Zhao, R., and Cortez, D. (2008a). TopBP1 activates ATR through ATRIP and a PIKK regulatory domain. Genes Dev *22*, 1478-1489.

Mordes, D. A., Nam, E. A., and Cortez, D. (2008b). Dpb11 activates the Mec1-Ddc2 complex. Proc Natl Acad Sci U S A.

Morishima, K., Sakamoto, S., Kobayashi, J., Izumi, H., Suda, T., Matsumoto, Y., Tauchi, H., Ide, H., Komatsu, K., and Matsuura, S. (2007). TopBP1 associates with NBS1 and is involved in homologous recombination repair. Biochem Biophys Res Commun *362*, 872-879.

Moser, B. A., and Russell, P. (2000). Cell cycle regulation in *Schizosaccharomyces pombe*. Curr Opin Microbiol *3*, 631-636.

Nakamura, T. M., Du, L. L., Redon, C., and Russell, P. (2004). Histone H2A phosphorylation controls Crb2 recruitment at DNA breaks, maintains checkpoint arrest, and influences DNA repair in fission yeast. Mol Cell Biol *24*, 6215-6230.

Navadgi-Patil, V. M., and Burgers, P. M. (2008). Yeast DNA replication protein Dpb11 activates the Mec1/ATR checkpoint kinase. J Biol Chem.

Navadgi-Patil, V. M., and Burgers, P. M. (2009). The unstructured C-terminal tail of the 9-1-1 clamp subunit Ddc1 activates Mec1/ATR via two distinct mechanisms. Mol Cell *36*, 743-753.

Newlon, C. S. (1997). Putting it all together: building a prereplicative complex. Cell *91*, 717-720.

Nguyen, V. Q., Co, C., and Li, J. J. (2001). Cyclin-dependent kinases prevent DNA re-replication through multiple mechanisms. Nature *411*, 1068-1073.

Nishitani, H., Lygerou, Z., Nishimoto, T., and Nurse, P. (2000). The Cdt1 protein is required to license DNA for replication in fission yeast. Nature *404*, 625-628.

Noguchi, E., Shanahan, P., Noguchi, C., and Russell, P. (2002). CDK phosphorylation of Drc1 regulates DNA replication in fission yeast. Curr Biol *12*, 599-605.

O'Connell, M. J., Raleigh, J. M., Verkade, H. M., and Nurse, P. (1997). Chk1 is a wee1 kinase in the G2 DNA damage checkpoint inhibiting cdc2 by Y15 phosphorylation. Embo J *16*, 545-554.

O'Connell, M. J., Walworth, N. C., and Carr, A. M. (2000). The G2-phase DNA-damage checkpoint. Trends Cell Biol *10*, 296-303.

Ogiwara, H., Ui, A., Onoda, F., Tada, S., Enomoto, T., and Seki, M. (2006). Dpb11, the budding yeast homolog of TopBP1, functions with the checkpoint clamp in recombination repair. Nucleic Acids Res *34*, 3389-3398.

Ohuchi, T., Seki, M., Branzei, D., Maeda, D., Ui, A., Ogiwara, H., Tada, S., and Enomoto, T. (2008). Rad52 sumoylation and its involvement in the efficient induction of homologous recombination. DNA Repair (Amst) *7*, 879-889.

Ohuchi, T., Seki, M., Kugou, K., Tada, S., Ohta, K., and Enomoto, T. (2009). Accumulation of sumoylated Rad52 in checkpoint mutants perturbed in DNA replication. DNA Repair (Amst) *8*, 690-696.

Oliva, A., Rosebrock, A., Ferrezuelo, F., Pyne, S., Chen, H., Skiena, S., Futcher, B., and Leatherwood, J. (2005). The cell cycle-regulated genes of *Schizosaccharomyces pombe*. PLoS Biol *3*, e225.

Osman, F., Dixon, J., Doe, C. L., and Whitby, M. C. (2003). Generating crossovers by resolution of nicked Holliday junctions: a role for Mus81-Eme1 in meiosis. Mol Cell *12*, 761-774.

Paciotti, V., Clerici, M., Lucchini, G., and Longhese, M. P. (2000). The checkpoint protein Ddc2, functionally related to *S. pombe* Rad26, interacts with Mec1 and is regulated by Mec1-dependent phosphorylation in budding yeast. Genes Dev *14*, 2046-2059.

Pardo, B., Gomez-Gonzalez, B., and Aguilera, A. (2009). DNA repair in mammalian

cells: DNA double-strand break repair: how to fix a broken relationship. Cell Mol Life Sci *66*, 1039-1056.

Paull, T. T., and Lee, J. H. (2005). The Mre11/Rad50/Nbs1 complex and its role as a DNA double-strand break sensor for ATM. Cell Cycle *4*, 737-740.

Paull, T. T., Rogakou, E. P., Yamazaki, V., Kirchgessner, C. U., Gellert, M., and Bonner, W. M. (2000). A critical role for histone H2AX in recruitment of repair factors to nuclear foci after DNA damage. Curr Biol *10*, 886-895.

Paulsen, R. D., and Cimprich, K. A. (2007). The ATR pathway: fine-tuning the fork. DNA Repair (Amst) *6*, 953-966.

Petermann, E., and Caldecott, K. W. (2006). Evidence that the ATR/Chk1 pathway maintains normal replication fork progression during unperturbed S phase. Cell Cycle *5*, 2203-2209.

Puddu, F., Granata, M., Di Nola, L., Balestrini, A., Piergiovanni, G., Lazzaro, F., Giannattasio, M., Plevani, P., and Muzi-Falconi, M. (2008). Phosphorylation of the budding yeast 9-1-1 complex is required for Dpb11 function in the full activation of the UV-induced DNA damage checkpoint. Mol Cell Biol.

Raji, H., and Hartsuiker, E. (2006). Double-strand break repair and homologous recombination in *Schizosaccharomyces pombe*. Yeast *23*, 963-976.

Ren, B., Cam, H., Takahashi, Y., Volkert, T., Terragni, J., Young, R. A., and Dynlacht, B. D. (2002). E2F integrates cell cycle progression with DNA repair, replication, and G(2)/M checkpoints. Genes Dev *16*, 245-256.

Rhind, N., and Russell, P. (2000). Chk1 and Cds1: linchpins of the DNA damage and replication checkpoint pathways. J Cell Sci *113 (Pt 22)*, 3889-3896.

Rios-Doria, J., Fay, A., Velkova, A., and Monteiro, A. N. (2006). DNA damage response: determining the fate of phosphorylated histone H2AX. Cancer Biol Ther *5*, 142-144.

Robinett, C. C., Straight, A., Li, G., Willhelm, C., Sudlow, G., Murray, A., and Belmont, A. S. (1996). In vivo localization of DNA sequences and visualization of large-scale chromatin organization using *lac* operator/repressor recognition. J Cell Biol *135*, 1685-1700.

Rodriguez, M., Yu, X., Chen, J., and Songyang, Z. (2003). Phosphopeptide binding specificities of BRCA1 COOH-terminal (BRCT) domains. J Biol Chem *278*, 52914-52918.

Rogakou, E. P., Pilch, D. R., Orr, A. H., Ivanova, V. S., and Bonner, W. M. (1998). DNA double-stranded breaks induce histone H2AX phosphorylation on serine 139. J Biol Chem *273*, 5858-5868.

Roos-Mattjus, P., Hopkins, K. M., Oestreich, A. J., Vroman, B. T., Johnson, K. L., Naylor, S., Lieberman, H. B., and Karnitz, L. M. (2003). Phosphorylation of human Rad9 is required for genotoxin-activated checkpoint signaling. J Biol Chem *278*, 24428-24437.

Russell, P., and Nurse, P. (1986). *Schizosaccharomyces pombe* and *Saccharomyces cerevisiae*: a look at yeasts divided. Cell *45*, 781-782.

Saka, Y., Esashi, F., Matsusaka, T., Mochida, S., and Yanagida, M. (1997). Damage and replication checkpoint control in fission yeast is ensured by interactions of Crb2, a protein with BRCT motif, with Cut5 and Chk1. Genes Dev *11*, 3387-3400.

Saka, Y., Fantes, P., Sutani, T., McInerny, C., Creanor, J., and Yanagida, M. (1994). Fission yeast *cut5* links nuclear chromatin and M phase regulator in the replication checkpoint control. Embo J *13*, 5319-5329.

Saka, Y., and Yanagida, M. (1993). Fission yeast *cut5*+, required for S phase onset and M phase restraint, is identical to the radiation-damage repair gene *rad4*+. Cell *74*, 383-393.

Sanders, S. L., Portoso, M., Mata, J., Bahler, J., Allshire, R. C., and Kouzarides, T. (2004). Methylation of histone H4 lysine 20 controls recruitment of Crb2 to sites of DNA damage. Cell *119*, 603-614.

Schulman, B. A., Lindstrom, D. L., and Harlow, E. (1998). Substrate recruitment to cyclin-dependent kinase 2 by a multipurpose docking site on cyclin A. Proc Natl Acad Sci U S A *95*, 10453-10458.

Schwartz, M. F., Duong, J. K., Sun, Z., Morrow, J. S., Pradhan, D., and Stern, D. F. (2002). Rad9 phosphorylation sites couple Rad53 to the *Saccharomyces cerevisiae* DNA damage checkpoint. Mol Cell *9*, 1055-1065.

Seki, M., Nakagawa, T., Seki, T., Kato, G., Tada, S., Takahashi, Y., Yoshimura, A., Kobayashi, T., Aoki, A., Otsuki, M., *et al.* (2006). Bloom helicase and DNA topoisomerase III alpha are involved in the dissolution of sister chromatids. Mol Cell Biol *26*, 6299-6307.

Seki, T., and Diffley, J. F. (2000). Stepwise assembly of initiation proteins at budding yeast replication origins in vitro. Proc Natl Acad Sci U S A *97*, 14115-14120.

Sheu, Y. J., and Stillman, B. (2006). Cdc7-Dbf4 phosphorylates MCM proteins via a docking site-mediated mechanism to promote S phase progression. Mol Cell *24*, 101-113.

Shiotani, B., and Zou, L. (2009). ATR signaling at a glance. J Cell Sci *122*, 301-304.
Shroff, R., Arbel-Eden, A., Pilch, D., Ira, G., Bonner, W. M., Petrini, J. H., Haber, J. E., and Lichten, M. (2004). Distribution and dynamics of chromatin modification induced by a defined DNA double-strand break. Curr Biol *14*, 1703-1711.

Song, B., and Sung, P. (2000). Functional interactions among yeast Rad51 recombinase, Rad52 mediator, and replication protein A in DNA strand exchange. J Biol Chem *275*, 15895-15904.

Soutoglou, E., and Misteli, T. (2008). Activation of the cellular DNA damage response in the absence of DNA lesions. Science *320*, 1507-1510.

Srivastava, N., Gochhait, S., de Boer, P., and Bamezai, R. N. (2008). Role of H2AX in DNA damage response and human cancers. Mutat Res.

St Onge, R. P., Besley, B. D., Pelley, J. L., and Davey, S. (2003). A role for the phosphorylation of hRad9 in checkpoint signaling. J Biol Chem *278*, 26620-26628.

Stevens, C., and La Thangue, N. B. (2004). The emerging role of E2F-1 in the DNA damage response and checkpoint control. DNA Repair (Amst) *3*, 1071-1079.

Stiff, T., Reis, C., Alderton, G. K., Woodbine, L., O'Driscoll, M., and Jeggo, P. A. (2005). Nbs1 is required for ATR-dependent phosphorylation events. Embo J *24*, 199-208.

Stiff, T., Walker, S. A., Cerosaletti, K., Goodarzi, A. A., Petermann, E., Concannon, P., O'Driscoll, M., and Jeggo, P. A. (2006). ATR-dependent phosphorylation and activation of ATM in response to UV treatment or replication fork stalling. Embo J *25*, 5775-5782.

Straight, A. F., Belmont, A. S., Robinett, C. C., and Murray, A. W. (1996). GFP tagging of budding yeast chromosomes reveals that protein-protein interactions can mediate sister chromatid cohesion. Curr Biol *6*, 1599-1608.

Stucki, M., Clapperton, J. A., Mohammad, D., Yaffe, M. B., Smerdon, S. J., and Jackson, S. P. (2005). MDC1 directly binds phosphorylated histone H2AX to regulate cellular responses to DNA double-strand breaks. Cell *123*, 1213-1226.

Sun, Y., Xu, Y., Roy, K., and Price, B. D. (2007). DNA damage-induced acetylation of lysine 3016 of ATM activates ATM kinase activity. Mol Cell Biol *27*, 8502-8509.

Sung, P. (1997a). Function of yeast Rad52 protein as a mediator between replication protein A and the Rad51 recombinase. J Biol Chem *272*, 28194-28197.

Sung, P. (1997b). Yeast Rad55 and Rad57 proteins form a heterodimer that functions with replication protein A to promote DNA strand exchange by Rad51 recombinase. Genes Dev *11*, 1111-1121.

Sweeney, F. D., Yang, F., Chi, A., Shabanowitz, J., Hunt, D. F., and Durocher, D. (2005). *Saccharomyces cerevisiae* Rad9 acts as a Mec1 adaptor to allow Rad53 activation. Curr Biol *15*, 1364-1375.

Szostak, J. W., Orr-Weaver, T. L., Rothstein, R. J., and Stahl, F. W. (1983). The double-strand-break repair model for recombination. Cell *33*, 25-35.

Tak, Y. S., Tanaka, Y., Endo, S., Kamimura, Y., and Araki, H. (2006). A CDK-catalysed regulatory phosphorylation for formation of the DNA replication complex Sld2-Dpb11. Embo J *25*, 1987-1996.

Tanaka, K., and Russell, P. (2001). Mrc1 channels the DNA replication arrest signal to checkpoint kinase Cds1. Nat Cell Biol *3*, 966-972.

Tanaka, K., and Russell, P. (2004). Cds1 phosphorylation by Rad3-Rad26 kinase is mediated by forkhead-associated domain interaction with Mrc1. J Biol Chem *279*, 32079-32086.

Tanaka, S., Tak, Y. S., and Araki, H. (2007). The role of CDK in the initiation step of DNA replication in eukaryotes. Cell Div *2*, 16.

Toh, G. W., O'Shaughnessy, A. M., Jimeno, S., Dobbie, I. M., Grenon, M., Maffini, S., O'Rorke, A., and Lowndes, N. F. (2006). Histone H2A phosphorylation and H3 methylation are required for a novel Rad9 DSB repair function following checkpoint activation. DNA Repair (Amst) *5*, 693-703.

Uematsu, N., Weterings, E., Yano, K., Morotomi-Yano, K., Jakob, B., Taucher-Scholz, G., Mari, P. O., van Gent, D. C., Chen, B. P., and Chen, D. J. (2007). Autophosphorylation of DNA-PKCS regulates its dynamics at DNA double-strand breaks. J Cell Biol *177*, 219-229.

van Attikum, H., and Gasser, S. M. (2009). Crosstalk between histone modifications during the DNA damage response. Trends Cell Biol *19*, 207-217.

Vas, A., Mok, W., and Leatherwood, J. (2001). Control of DNA rereplication via Cdc2 phosphorylation sites in the origin recognition complex. Mol Cell Biol *21*, 5767-5777.
Vialard, J. E., Gilbert, C. S., Green, C. M., and Lowndes, N. F. (1998). The budding yeast Rad9 checkpoint protein is subjected to Mec1/Tel1-dependent hyperphosphorylation and interacts with Rad53 after DNA damage. Embo J *17*, 5679-5688.

Walker, J. R., Corpina, R. A., and Goldberg, J. (2001). Structure of the Ku heterodimer bound to DNA and its implications for double-strand break repair. Nature *412*, 607-614.

Walworth, N. C., and Bernards, R. (1996). rad-dependent response of the *chk1*-encoded protein kinase at the DNA damage checkpoint. Science *271*, 353-356.

Wan, S., Capasso, H., and Walworth, N. C. (1999). The topoisomerase I poison camptothecin generates a Chk1-dependent DNA damage checkpoint signal in fission yeast. Yeast *15*, 821-828.

Wang, H., and Elledge, S. J. (2002). Genetic and physical interactions between DPB11 and DDC1 in the yeast DNA damage response pathway. Genetics *160*, 1295-1304.

Wang, X. Q., Redpath, J. L., Fan, S. T., and Stanbridge, E. J. (2006). ATR dependent activation of Chk2. J Cell Physiol *208*, 613-619.

Ward, I. M., and Chen, J. (2001). Histone H2AX is phosphorylated in an ATR-dependent manner in response to replicational stress. J Biol Chem *276*, 47759-47762.

Watson, A. T., Garcia, V., Bone, N., Carr, A. M., and Armstrong, J. (2008). Gene tagging and gene replacement using recombinase-mediated cassette exchange in *Schizosaccharomyces pombe*. Gene *407*, 63-74.

Williams, J. S., Williams, R. S., Dovey, C. L., Guenther, G., Tainer, J. A., and Russell, P. gammaH2A binds Brc1 to maintain genome integrity during S-phase. Embo J *29*, 1136-1148.

Wilmes, G. M., Archambault, V., Austin, R. J., Jacobson, M. D., Bell, S. P., and Cross, F. R. (2004). Interaction of the S-phase cyclin Clb5 with an "RXL" docking sequence in the initiator protein Orc6 provides an origin-localized replication control switch. Genes Dev *18*, 981-991.

Wood, V., Gwilliam, R., Rajandream, M. A., Lyne, M., Lyne, R., Stewart, A., Sgouros, J., Peat, N., Hayles, J., Baker, S.*, et al.* (2002). The genome sequence of *Schizosaccharomyces pombe*. Nature *415*, 871-880.

Wu, L., and Hickson, I. D. (2003). The Bloom's syndrome helicase suppresses crossing over during homologous recombination. Nature *426*, 870-874.

Wuarin, J., and Nurse, P. (1996). Regulating S phase: CDKs, licensing and proteolysis. Cell *85*, 785-787.

Wysocki, R., Javaheri, A., Allard, S., Sha, F., Cote, J., and Kron, S. J. (2005). Role of Dot1-dependent histone H3 methylation in G1 and S phase DNA damage checkpoint functions of Rad9. Mol Cell Biol *25*, 8430-8443.

Yabuuchi, H., Yamada, Y., Uchida, T., Sunathvanichkul, T., Nakagawa, T., and Masukata, H. (2006). Ordered assembly of Sld3, GINS and Cdc45 is distinctly regulated by DDK and CDK for activation of replication origins. Embo J *25*, 4663-4674.

Yan, S., Lindsay, H. D., and Michael, W. M. (2006). Direct requirement for Xmus101 in ATR-mediated phosphorylation of Claspin bound Chk1 during checkpoint signaling. J Cell Biol *173*, 181-186.

Yang, X. H., and Zou, L. (2006). Recruitment of ATR-ATRIP, Rad17, and 9-1-1 complexes to DNA damage. Methods Enzymol *409*, 118-131.

Yanow, S. K., Lygerou, Z., and Nurse, P. (2001). Expression of Cdc18/Cdc6 and Cdt1 during G2 phase induces initiation of DNA replication. EMBO J *20*, 4648-4656.

Yoo, H. Y., Kumagai, A., Shevchenko, A., Shevchenko, A., and Dunphy, W. G. (2007). Ataxia-telangiectasia mutated (ATM)-dependent activation of ATR occurs through phosphorylation of TopBP1 by ATM. J Biol Chem *282*, 17501-17506.

Yu, X., Chini, C. C., He, M., Mer, G., and Chen, J. (2003). The BRCT domain is a phospho-protein binding domain. Science *302*, 639-642.

Zegerman, P., and Diffley, J. F. (2007). Phosphorylation of Sld2 and Sld3 by cyclin-dependent kinases promotes DNA replication in budding yeast. Nature *445*, 281-285.

Zeng, Y., Forbes, K. C., Wu, Z., Moreno, S., Piwnica-Worms, H., and Enoch, T. (1998). Replication checkpoint requires phosphorylation of the phosphatase Cdc25 by Cds1 or Chk1. Nature *395*, 507-510.

Zeng, Y., and Piwnica-Worms, H. (1999). DNA damage and replication checkpoints in fission yeast require nuclear exclusion of the Cdc25 phosphatase via 14-3-3 binding. Mol Cell Biol *19*, 7410-7419.

Zou, L., Cortez, D., and Elledge, S. J. (2002). Regulation of ATR substrate selection by Rad17-dependent loading of Rad9 complexes onto chromatin. Genes Dev *16*, 198-208.

Zou, L., and Elledge, S. J. (2003). Sensing DNA damage through ATRIP recognition of RPA-ssDNA complexes. Science *300*, 1542-1548.

Zou, L., and Stillman, B. (2000). Assembly of a complex containing Cdc45p, replication protein A, and Mcm2p at replication origins controlled by S-phase cyclin-dependent kinases and Cdc7p-Dbf4p kinase. Mol Cell Biol *20*, 3086-3096.

Appendix A. List of primers

name of primers	sequence	purpose
cut5-1 (forward primer)	ATTCGGAATTCATATGGGTTCTTCTAAACCACTC	
cut5-13 (forward primer)	GCATCTTATAGCCGGCGATTTTGATGCTCCAAAATACAAGG	T54A
cut5-14 (reverse primer)	CCTTGTATTTTGGAGCATCAAAATCGCCGGCTATAAGATGC	T54A
cut5-54 (forward primer)	CAATAGGACATTCTGCGCCTCATAATTC	T528A
cut5-55 (reverse primer)	GAATTATGAGGCGCAGAATGTCCTATTG	T528A
cut5-56 (forward primer)	GCCTCATAATGCTCCTTCCTTATTATCGG	S532A
cut5-57 (reverse primer)	CCGATAATAAGGAAGGAGCATTATGAGGC	S532A
cut5-58 (forward primer)	GGACATTCTGCGCCTCATAATGCTCCTTCC	T528A and S532A
cut5-59 (reverse primer)	GGAAGGAGCATTATGAGGCGCAGAATGTCC	T528A and S532A
cut5-64 (forward primer)	GGACATTCTGAGCCTCATAATGAACCTTCCTTATTATCG	T528E and S532E
cut5-65 (reverse primer)	CGATAATAAGGAAGGTTCATTATGAGGCTCAGAATGTCC	T528E and S532E
cut5-66 (forward primer)	CTATTAATTACCGAGGCTCATCGAAAACTC	S641A
cut5-67 (reverse primer)	GAGTTTTCGATGAGCCTCGGTAATTAATAG	S641A
cut5-72 (forward primer)	CAAAACCAGAAGCTCCGACAGCTCCACAAG	T589A and S592A
cut5-73 (reverse primer)	CTTGTGGAGCTGTCGGAGCTTCTGGTTTTG	T589A and S592A
cut5-76 (forward primer)	GAGCATGTTTCACGTATAGATCCAGACGCTC	Y599R
cut5-77 (reverse primer)	GAGCGTCTGGATCTATACGTGAAACATGCTC	Y599R
cut5-78 (forward primer)	TACAAAACCAGAAACTCCGACATCTCCACAACCAGACGCTCAACGTGAGAAA	deletion of 595-601

	CATAAGCTTTATG	
cut5-79 (reverse primer)	CATAAAGCTTATGTTTCTCACGTTGAGCGTCTGGTTGTGGAGATGTCGGAGTTTCTGGTTTTGTA	deletion of 595-601
cut5-80 (forward primer)	GCTTCTATTAATTACCGAGAGTCAT CGTAGGCGTTGAAAACATTGTTTAT	deletion of 643-645
cut5-81 (reverse primer)	ATAAACAATGTTTTCAACGCCTACGATGACTCTCGGTAATTAATAGAAGC	deletion of 643-645
cut5-82 (forward primer)	CTACTGGATGATTTCGCTCCCGAAACTGTTC	T278A
cut5-83 (reverse primer)	GAACAGTTTCGGGAGCGAAATCATCCAGTAG	T278A
cut5-84 (forward primer)	ATTCATTGATCAAGTTGCTCCATGGGCTATC	S483A
cut5-85 (reverse primer)	GATAGCCCATGGAGCAACTTGATCAATGAAT	S483A
cut5-86 (forward primer)	GATTCAACTAAATGCTAATGCAAAAGATTCAAC	S556A and S558A
cut5-87 (reverse primer)	GTTGAATCTTTTGCATTAGCATTTAGTTGAATC	S556A and S558A
cut5-92 (forward primer)	ATTCGAGAGCTCCGAAAGTCGATTTTCTCTAA	for C-terminal truncation
cut5-96 (forward primer)	TTATGTGCTTGCTCATGGTGGTACA	K126A
cut5-97 (reverse primer)	TGTACCACCATGAGCAAGCACATAA	K126A
cut5-98 (forward primer)	CTTAATAATGGAGCTTTTGAATTTT	K260A
cut5-99 (reverse primer)	AAAATTCAAAAGCTCCATTATTAAG	K260A
cut5-100 (forward primer)	TTACTGGATTTGCTGGGGAAGAACT	K408A
cut5-101 (reverse primer)	AGTTCTTCCCCAGCAAATCCAGTAA	K408A
cut5-102 (reverse primer)	TCGAATACTAGTAACTATACATATAAATAAACAATGTTTCAGATAGCCCATGGAGAAACTTG	Amplify Rad4 1-487
cut5-103 (reverse primer)	TCGAATACTAGTAACTATACATATAAATAAACAATGTTTCACCAAACAGTATCAATCTTGTC	Amplify Rad4 1-580

cut5-104 (reverse primer)	TCGAATACTAGTAACTATACATATAAATAAACAATGTTTCACTTATGTTTCT CACGTTGAG	Amplify Rad4 1-610
cut5-115 (forward primer)	GTTACAAAACCAGAAGAGCCGACATCTCCACAAG	T589E
cut5-116 (reverse primer)	CTTGTGGAGATGTCGGCTCTTCTGGTTTTGTAAC	T589E
cut5-119 (forward primer)	CCAGAAGAGCCGACAGAGCCACAAGAGCATG	T589E and S592E
cut5-120 (reverse primer)	CATGCTCTTGTGGCTCTGTCGGCTCTTCTGG	T589E and S592E
L5 (forward primer)	TAGATACCCAGATCACATGAAACAACATG	Mutated *Nde*I site in pT572
L6 (reverse primer)	CATGTTGTTTCATGTGATCTGGGTATCTA	Mutated *Nde*I site in pT572
L7 (forward primer)	ATTCGACATATGATGAGTAAAGGAGAAGAA	Amplify GFP-LacI-NLS with *Nde*I/*Nde*I from pT572
L8 (reverse primer)	ATTCGACATATGGGCAACCTTTCTCTTC	Amplify GFP-LacI-NLS with *Nde*I/*Nde*I from pT572
L9 (forward primer)	ATTCGAGTCGACTATGGAATTCACTGTTTCA	Amplify cDNA *rad9*
L10 (reverse primer)	ATTCGAGTCGACTCTAGTCTTCCTGAGAGAA	Amplify cDNA *rad9*
L11 (reverse primer)	ATTCGAGTCGACACGCCTACGGAGTTTTCG	Amplify *rad4*
L12 (forward primer)	ATTCGAGTCGACATGAGTAAAGGAGAAGAA	Amplify GFP-LacI-NLS with *Sal*I/*Sal*I from pT572
L13 (reverse primer)	ATTCGAGTCGACTTAGGCAACCTTTCTCTTC	Amplify GFP-LacI-NLS with *Sal*I/*Sal*I from pT572

Appendix B. List of plasmids

	Plasmid	Bacterial marker	Yeast marker
pSJ25	pAW8-loxP-Rad4 (wild-type)-loxM	Amp	LEU2
Valerie Garcia (#84)	pGEX-KG-cter-Rad4 (wild-type)	Amp	
Valerie Garcia (#85)	pGEX-KG- full-length Rad4 (wild-type)	Amp	
pSJ38	pGEX-KG-cter-Rad4-Y599R	Amp	
Valerie Garcia (#109)	pGEX-KG-cter-Rad4-S641A	Amp	
pSJ23	pGEX-KG-cter-Rad4-d(RXL)	Amp	
	pREP41-NLS-TAP-Rad4-(1462-1947)	Amp	LEU2
	pREP1-Rad4-(1462-1947)	Amp	LEU2
pSJ52	pREP41-Rad3-GFP-LacI-NLS	Amp	LEU2
pSJ55	pREP41-Rad3(KD)-GFP-LacI-NLS	Amp	LEU2
pSJ59	pREP42-Rad9-GFP-LacI-NLS	Amp	ura4
pSJ58	pREP42-GFP-LacI-NLS-Rad4	Amp	ura4
pSJ60	pREP42-GFP-LacI-NLS-Rad4-Y599R	Amp	ura4
pSJ62	pREP42-GFP-LacI-NLS-Rad4-(1462-1947)	Amp	ura4
pSJ47	pREP41-GFP-LacI-NLS	Amp	LEU2
pSJ72	pREP42-GFP-LacI-NLS-Rad4-T589A. S592A	Amp	ura4

Appendix C. Strains table

Strains	Genotype	mating type	Source or reference
501	*ade6-704 ura4D-18 leu1-32*	h-	This Lab
503	*ade6-704 ura4D-18 leu1-32*	h+	This Lab
SJ1	*loxP-rad4-T528A.S532A.T589A.S592A.S641A-loxM3 ade6-704 ura4D-18 leu1-32*	h+	This study
SJ3	*loxP-rad4-dAAD-loxM3 ade6-704 ura4D-18 leu1-32*	h+	This study
SJ5	*loxP-rad4-Y599R-loxM3 ade6-704 ura4D-18 leu1-32*	h+	This study
SJ7	*loxP-rad4-T54A.T528A.S532A.T589A.S592A.S64A-loxM3 ade6-704 ura4D-18 leu1-32*	h+	This study
SJ8	*loxP-rad4-dRXL(d643-645)-loxM3 ade6-704 ura4D-18 leu1-32*	h+	This study
SJ9	*loxP-rad4-S556A.S558A-loxM3 ade6-704 ura4D-18 leu1-32*	h+	This study
SJ10	*loxP-rad4-T278A-loxM3 ade6-704 ura4D-18 leu1-32*	h+	This study
SJ11	*loxP-rad4-S641A-loxM3 ade6-704 ura4D-18 leu1-32*	h+	This study
SJ13	*loxP-rad4-T528A.S532A.T589A.S592A-loxM3 ade6-704 ura4D-18 leu1-32*	h+	This study
SJ14	*loxP-rad4-Y599R-loxM3 chk1::KanMX6 ade6-704 ura4D-18 leu1-32*	h+	This study
SJ16	*loxP-rad4-dAAD-loxM3 chk1::KanMX6 ade6-704 ura4D-18 leu1-32*	h+	This study
SJ19	*loxP-rad4-Y599R-loxM3 cds1::KanMX6 ade6-704 ura4D-18 leu1-32*	h+	This study
SJ20	*loxP-rad4-dAAD-loxM3 cds1::KanMX6 ade6-704 ura4D-18 leu1-32*	h+	This study
SJ35	*loxP-rad4-S483A-loxM3 ade6-704 ura4D-18 leu1-32*	h+	This study

Strains	Genotype	mating type	Source or reference
SJ37	*loxP-rad4*$^{+}$*-loxM3 chk1::KanMX6 ade6-704 ura4D-18 leu1-32*	h+	This study
SJ38	*loxP-rad4*$^{+}$*-loxM3 cds1::KanMX6 ade6-704 ura4D-18 leu1-32*	h+	This study
	chk1-HA ura4-D18	h+	This lab
SJ62	*loxP-rad4-Y599R-loxM3 chk1:HA ade6-704 ura4D-18 leu1-32*	h+	This study
SJ68	*loxP-rad4-Y599R-loxM3 cdc25-22 ade6-704 ura4D-18 leu1-32*	h+	This study
SJ71	*loxP-rad4-T54A.T278A.S483A.T528A.S532A.T58A.S592A-loxM3 ade6-704 ura4D-18 leu1-32*	h+	This study
SJ100	*loxP-rad4-1~487-loxM3 ade6-704 ura4D-18 leu1-32*	h+	This study
SJ101	*loxP-rad4-1~610-loxM3 ade6-704 ura4D-18 leu1-32*	h+	This study
SJ102	*loxP-rad4-1~580-loxM3 ade6-704 ura4D-18 leu1-32*	h+	This study
	loxP-rad4-T528A.S532A.T589A.S592A-loxM3 ade6-704 ura4D-18 leu1-32	h+	This Lab (VG544)
	ura4::LacO:NAT leu1-32	h+	This Lab (Takashi Morishita)
SJ195	*ura4::LacO:NAT chk1-HA ade6-704 ura4-D18 leu1-32*	h+	This study
SJ254	*ura4::LacO:NAT chk1:HA loxP-rad4-Y599R-loxM3 ura4-D18 leu1-32*	h+	This study
SJ295	*ura4::LacO:NAT chk1:HA rad9-T412A ura4-D18 leu1-32*	h+	This study
SJ302	*loxP-rad4-T528E.S532E.T589E-loxM3 ade6-704 ura4-D18 leu1-32*	h+	This study
SJ304	*loxP-rad4-T528E.S532E-loxM3 ade6-704 ura4-D18 leu1-32*	h+	This study
	hta1-S129A hta2-S128A	h+	Paul Russell
	loxP-rad4-Y599R-loxM3 hta1-S129A hta2-S128A ade6-704 ura4D-18 leu1-32	h+	This Lab (Valerie Garcia)
SJ307	*loxP-rad4-T528E.S532E.T589E.S592E-loxM3 ade6-704 ura4-D18 leu1-32*	h+	This study

Strains	Genotype	mating type	Source or reference
SJ309	*ura4::LacO:NAT chk1:HA hta1-S129A hta2-S128A ade6-704 ura4-D18 leu1-32*	h-	This study
SJ320	*loxP-rad4^{+}-loxM3 ade6-704 ura4-D18 leu1-32*	h+	This study
SJ324	*loxP-rad4^{+}-loxM3 chk1:HA ade6-704 ura4-D18 leu1-32*	h+	This study
SJ327	*loxP-rad4-Y599R-loxM3 cdc25-22 chk1:HA ade6-704 ura4-D18 leu1-32*		This study
SJ337	*loxP-rad4^{+}-loxM3, cdc25-22 chk1:HA*		This study
JLP511	*leu1-32 ura4-294::nmt-GST-cdc18^{+}*	h+	Janet Leatherwood
	loxP-rad4-T54A.T278A.S483A.T528A.S532A.T58A.S592A-loxM3 leu1-32 ura4-294::nmt-GST-cdc18^{+}		This study